

https://dspace.org/

Coordinating properties of more highly preorganised ligands

De Sousa, Alvaro Silva

2015-03-05
http://hdl.handle.net/10539/17153

Downloaded from a DSpace repository. https://dspace.org/

COORDINATING PROPERTIES OF MORE HIGHLY PREORGANISED LIGANDS

by

Alvaro Silva da Sousa

A thesis presented in the
University of the Witwatersrand, Johannesburg
for the degree of Doctor of Philosophy

May 1995

ABSTRACT

The effect of adding C-methyl groups on metal ion selectivity patterns for open-chain and macrocyclic ligands is investigated by determining the protonation and complex formation constants of ligand derivatives of ethylenediamine, propylene, diethylenetriamine, 18-aneN_2O_4 and 12-aneN_4. It is shown that the addition of C-alkyl groups to ligands tends to increase the selectivity of the ligand for small relative to large metal ions.

The selectivity patterns of the bulky hydroxycyclohexyl group is investigated by adding it as a pendant donor group to parent amines and comparing these to analogues differing in the degree of C-alkylation. It is a surprising result that the presence of cyclohexenyl groups alter the selectivity in favour of small metal ions. The extra rigidity of the cylohexenyl ring and its trans donor atoms might be expected to enhance the preference for large metal ions, however the selectivity pattern produced derives from the relief of steric crowding on the outer surface of the complex. The fact that the methyl groups are forced closer together on the outside of the complex of a large metal ion leads to greater van der Waals repulsion and therefore destabilisation.

DECLARATION

I hereby declare that the work presented in this thesis was carried out by myself under the supervision of Prof. R. D. Hancock. This thesis has never been submitted before for any degree or examination in any other university.

A. S. de Sousa

5 day of May, 1995

ACKNOWLEDGEMENTS

I would like to express my sincere gratitude to my supervisor, Prof. R. D. Hancock, for his friendship, encouragement, continuous support and precious advice throughout the duration of this study.

Special thanks to Dr. J. Riebenspies in the USA for his invaluable help in crystal structure determinations.

I wish also to acknowledge the following people for their contributions to this thesis :

Prof. J.C.A Boeyens for his advice on crystal structure refinement;

Miss. L. Cook for her constant patience and assistance with X-ray crystallographic studies at the University of the Witwatersrand;

Mr. Craig Tavener for his assistance with graphics packages in crystallography;

The University of the Witwatersrand and the Council for Scientific and Industrial Research, for financial support;

Finally, but by no means less important , my family for their love, support, encouragement and understanding .

AIM OF THIS STUDY

The principal aim of this study was to investigate the effect of the bulky hydroxycyclohexyl pendant moiety as a means to control metal ion selectivity in a series of ligands. The areas of that were considered to achieve this are :

1) Synthesis of open chain amines derivatives containing the cyclohexyl pendant group and investigation of their stability and selectivity patterns.

2) Synthesis of a novel mixed-donor macrocycle for further investigation into the effect of the hydroxycyclohexyl pendant group.

3) Synthesis of a novel monosubstituted tetraaza macrocyclic compound "Scorpiand"

4) Modelling of potentiometric data for the determination of stability constants.

5) Rationalisation of steric effects by Molecular mechanics calculations

6) Structural determination of complexes of novel ligands to determine mode of coordination.

TABLE OF CONTENTS

CHAPTER1
Introduction
Chelates in medicine 1
Selection of donor atoms 4
Strengths of oxygen and nitrogen donor atoms 6
Design of chelating ligands 15

CHAPTER2
Introduction 17
The chelate effect 20
The macrocyclic effect 25
The cryptate effect 30
Metal ion selectivity and chelate ring size 36
Strucutrally reinforced ligands and metal ions 44

CHAPTER3
Open chain polyamines
Addition of pendant arms containing neutral oxygen donors to ethylenediamine 47
Structure of $[Cu(THEEN)](ClO_4)_2$ 49
Addition of pendant arms containing neutral oxygen donors to DIEN 64
Increasing the rigidity of the open-chain ligands 70
Comparison of the protonation constants 80

CHAPTER4
Mixed donor macrocycles
Addition of pendant oxygen donors to mixed donor macrocycles 82
Increasing the rigidity of the pendant donors 94
Crystal structure of $[Sr(Cy_2\text{-}K22)H_2O](ClO_4)_2$ 98
Sterically and structurally more complex pendant donor groups with neutral oxygen donors 106
Balance between inductive and steric effects on the thermodynamic stability of complexes 113
Molecular Mechanics studies of Cy_2-K22 116

CHAPTER5
Pendant oxygen donors of open chain amines 121
Introduction of the trans-cyclohexyl moiety in the pendant donor groups of diamines 124
Strucutre of Cy_2-EN 134
Strucutre of TCA 140
Strucutre of $[Cu(TCA)](ClO_4)_2$ 146
Preorganisation 152

The lone pair on Pb^{2+} ion 157
Solution studies 164
Stability constants for Cu and Ni complexes of TCA 166
Model submitted for curve fitting by simplex method 180
Spectroscopic study of competition titrations 182
Introducing trans hydroxycyclohexyl groups on diethylenetriamine 198
Strucutre of $[Cu(Cy2\text{-}dien)](ClO_4)_2$ 201
Introduction of hydroxycyclohexyl pendant groups to tetraazamacrocycles 209
Structure of $[Cu(cy\text{-}12ane\ N_4](ClO_4)_2$ 213

CHAPTER6
Conclusion 226

CHAPTER7
Synthetic methods
Synthesis of macrocycles 228
Synthesis of monosubstituted macrocycles 231
Ligand and metal complex synthesis
Instrumentation 233
Synthesis 235
Potentiometry
Potentiometric determination of stability constants 245
Instrumentation 246
Standardisation and calibration 247
Method of determining the stability constants 248
Spectroscopy
Spectroscopic studies of metal complexes 250
Instrumentation 250
X-ray analysis of crystals 251
Crystal preparation 251
Data collection and reduction 252
Solution and refinement of structure 252
References 254
List of publicaitons 270
Appendix 271

INTRODUCTION

CHELATES IN MEDICINE

There are a number of fields that currently require specific ligand design for selective metal complexation. These fields encompass the design of ligands for treatment of metal intoxication (May et al 1983 & Bullman et al 1987) , the need of complexes to act as imaging agents in the body (Lauffer et al 1987 , Deutsch et al 1983 & Parker et al 1993) and the selective extraction of precious metals in hydrometallurgy (Green et al 1982).

Much attention is currently being given to the field of nuclear medicine and the design of radiopharmaceuticals (Jurisson et al 1993, Parker et al 1990). Radiopharmaceuticals have a diagnostic and/or therapeutic application and the radionuclides used are invariably metals.

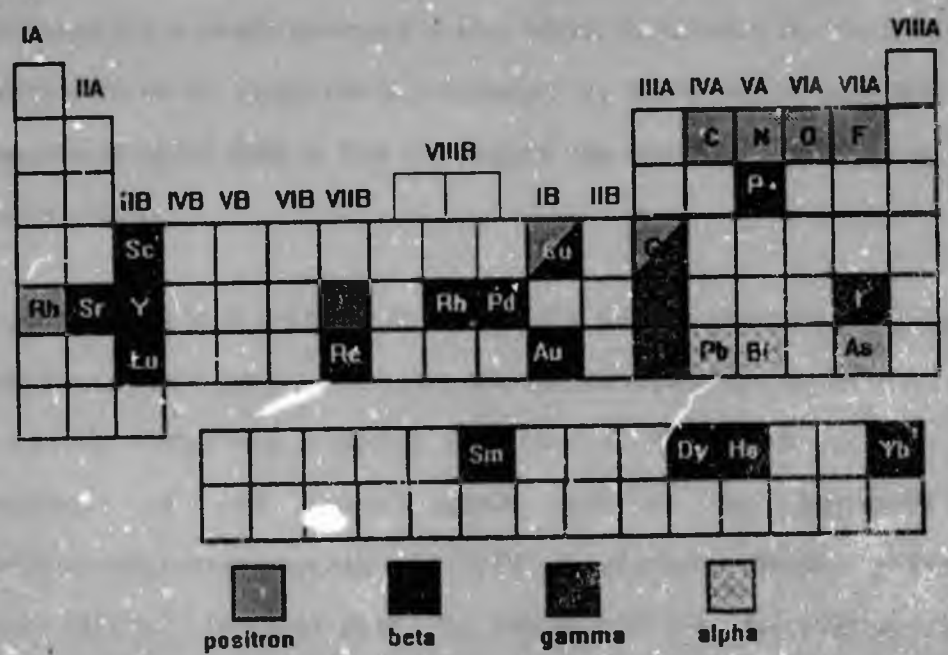


Figure 1 : medical radionuclides (Jurisson et al 1993)

The metal coordination sphere is an important factor in determining the stability of the radiolabelled complex in vivo (Hancock et al 1989). Of equal importance is the type of ligand used. Chelating ligands in medical applications must ideally form inert complexes and simultaneously impart desirable chemical and biological properties (Parker et al 1990).

Properties that are essential for medically useful chelating ligands include:

a) high water solubility

b) high relaxivity (for imaging of organs in the body)

c) inertness towards metal dissociation

The necessary relaxivity is achieved by incorporating coordinated water molecules that will be in rapid exchange with the bulk water (Lauffer et al 1987). Inertness to metal dissociation is of prime importance as the loss of the metal ion is poorly tolerated in vivo. Metal dissociation in vivo is largely irreversible as the metal ion is sequestered by the serum proteins and the complexing agent then is free to complex any one of the many abundant serum cations .

Success therefore depends on the design of a bifunctional complexing agent that has the dual purpose of being attached to a protein (antibiotic) and selectively complexing a chosen metal ion. Early work began with the complexes of well known ligands such as the derivatives of diethylenetriaminepentaacetic acid (DTPA) and ethylenediaminetetraacetic acid (EDTA) (Brechbiel et al 1986, Yeh et al 1979 & Meares et al 1984). The usefulness of these complexing agents was compromised by their complex

instability in vivo . They tended to lend themselves readily to metal dissociation promoted by acid or cation promoted pathways. Metal ions such as Ca^{2+} and Zn^{2+} are attracted by the anionic complexes of EDTA and DTPA resulting in the formation of mixed complex species. These species in turn promote the metal dissociation mechanism as they have reduced kinetic stability. An additional hinderance was the non-specificity in the binding of the metal ion to the protein, which must be minimised to avoid protein denaturation.

The problems of open chain complexing agents have to some degree been answered by Morphy et al 1988, Deshpande et al 1988 and Cox et al 1989 with the introduction of macrocyclic bifunctional complexing agents. The work of Parker et al 1983 and Chen et al 1988 showed that macrocyclic complexing agents display an inherent kinetic inertness at lower pH and are less sensitive to acid catalysed dissociation pathways. A significant amount of synthetic "architecture" is introduced in the preparation of these macrocyclic complexing agents so as to allow them the ability to form neutral or preferably cationic complexes. This produces the effect of drastically reducing electrostatic interactions with protons or cations. Possibly the most important contribution of the macrocycle can be summarised in the term "preorganisation", which implies a conformational restriction (Cram et al 1983). The conformation of the free ligand should closely resemble that which it adopts when in the metal complex. Unfavourable entropic and enthalpic contributions of complexation are reduced or eliminated in this fashion.

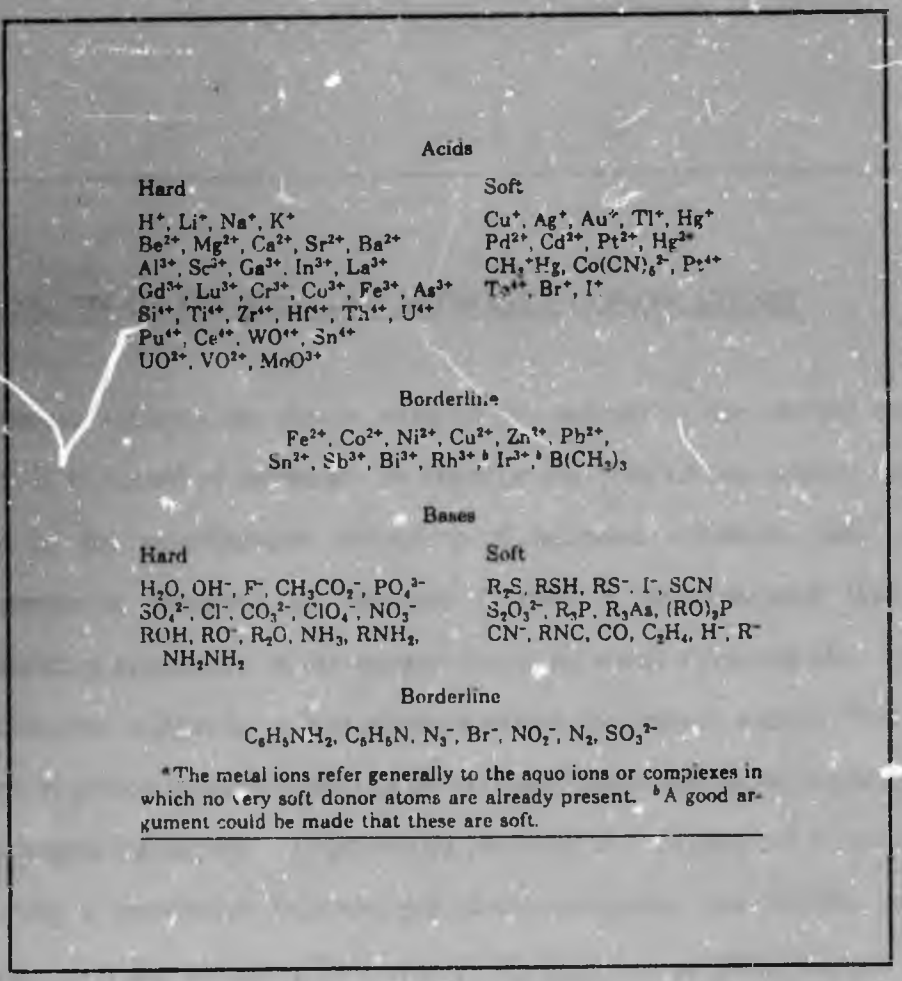
A number of macrocycles have been investigated for potential use in macrocyclic bifunctional complexing agents. The derivatives based on the 12-N_4 skeleton (1,4,7,10 tetraazacyclododecane) have attracted particular

interest (Riesen et al 1986a&b, Tweedle et al 1991 & Parker et al 1993). In most derivatives with the 12-N_4 backbone, functionalisation of three ring nitrogens by the introduction of carboxylate moieties is done to accommodate the charge at the metal centre. The fourth ring nitrogen is then accessible for further derivatisation. Phosphinic acid moieties have also been introduced as these tend to be bone directing and are more difficult to protonate (Parker et al 1993). Selective functionalisation of the fourth N-atom allows for variation of complex lipophilicity and minimisation of metal dissociation. Lipophilicity is a prerequisite for adequate clearance via the hepato-biliary pathway (Harrison et al 1993).

SELECTION OF DONOR ATOMS

A useful starting point for donor atom selection would be the established rule for the classification of acids and bases (Pearson 1963) : hard acids bind most strongly to hard bases and soft acids bind most strongly to soft bases. (HSAB theory)

This rule has served to explain a wide range of molecule - molecule and ion - molecule chemistry in terms of acid - base phenomena. With metal complexes the metal ions are Lewis acids, and therefore the donor atom strength is a measure of its intrinsic basicity (Hancock & Martell 1988). If a ligand is to be designed for a specific complexation of Fe^{3+} which the table classifies as hard, a hard donor should be employed such as a negative oxygen donor.



Acids

Hard	Soft
H^+, Li^+, Na^+, K^+	Cu^+, Ag^+, Au^+, Tl^+, Hg^+
Be^{2+}, Mg^{2+}, Ca^{2+}, Sr^{2+}, Ba^{2+}	Pd^{2+}, Cd^{2+}, Pt^{2+}, Hg^{2+}
Al^{3+}, Sc^{3+}, Ga^{3+}, In^{3+}, La^{3+}	CH_3^+Hg, $Co(CN)_5^{3-}$, Pt^{4+}
Gd^{3+}, Lu^{3+}, Cr^{3+}, Co^{3+}, Fe^{3+}, As^{3+}	Te^{4+}, Br^+, I^+
Si^{4+}, Ti^{4+}, Zr^{4+}, Hf^{4+}, Th^{4+}, U^{4+}	
Pu^{4+}, Ce^{4+}, WO^{4+}, Sn^{4+}	
UO^{2+}, VO^{2+}, MoO^{3+}	

Borderline

Fe^{2+}, Co^{2+}, Ni^{2+}, Cu^{2+}, Zn^{2+}, Pb^{2+},
Sn^{2+}, Sb^{3+}, Bi^{3+}, Rh^{3+},[b] Ir^{3+},[b] $B(CH_3)_3$

Bases

Hard	Soft
H_2O, OH^-, F^-, $CH_3CO_2^-$, PO_4^{3-}	R_2S, RSH, RS^-, I^-, SCN^-
SO_4^{2-}, Cl^-, CO_3^{2-}, ClO_4^-, NO_3^-	$S_2O_3^{2-}$, R_3P, R_3As, $(RO)_3P$
ROH, RO^-, R_2O, NH_3, RNH_2, NH_2NH_2	CN^-, RNC, CO, C_2H_4, H^-, R^-

Borderline

$C_6H_5NH_2$, C_5H_5N, N_3^-, Br^-, NO_2^-, N_2, SO_3^{2-}

[a] The metal ions refer generally to the aquo ions or complexes in which no very soft donor atoms are already present. [b] A good argument could be made that these are soft.

***Figure 2** Table of hard and soft acids and bases (Hancock & Martell 1988)*

A literature example is the ligand DFB (Desferriferrioxamine - B) that has negatively charged oxygen donors and consequently forms stable complexes of iron. Not all metal ions can be neatly classified as either soft or hard. Some display an intermediate behaviour and a choice of donor atoms becomes a more detailed consideration of a number of factors. Neutral oxygen donors ROH and R_2O are classified as hard, yet Fe^{3+} has little or no affinity for crown ethers with their hard oxygen donors. To have a global understanding

of the ambivalent behaviour of metal ions it is necessary to consider the properties of the donor atoms in the aqueous as well as the gaseous phases.

STRENGTHS OF OXYGEN AND NITROGEN DONOR ATOMS

In aqueous solution the donor atom of the solvent is the neutral oxygen donor. It is therefore necessary to examine the role of the neutral oxygen donor in the coordination chemistry of aqueous solutions. Gas phase measurements reported by Munson (1965) demonstrated that the coordinating properties of the oxygen donor in water were not identical to that observed in ligands such as alcohols, ethers, ketones or amides. From his studies of proton transfer reactions he proposed that continuous replacement of hydrogen by methyl groups would increase the basicity of a molecule exhibiting a correlation between gas phase energetics and relative proton affinities. Further studies (Taft et al 1978, Uppal et al 1982, Kappes et al 1982, Staley et al 1975) revealed the donor strength for sp^3 - hybridised oxygens as :

$$H_2O < ROH < R_2O$$

Figures that follow on the next page showing the gas phase binding energies of Li^+ to oxygen donor ligands substantiates the order of basicity to be $H_2O<CH_3OH<(CH_3)_2O$.

Inductive (electron releasing) effects of alkyl groups are observed in other

binding energy orders of Li^+ :

$$H_2C{=}O < CH_3HC{=}O < (CH_3)_2C{=}O$$

$$NH_3 < CH_3NH_2 < (CH_3)_3N$$

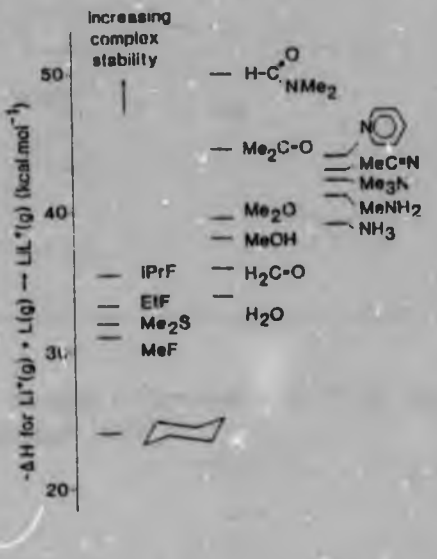


***Figure 3** : Enthalpies of formation of complexes of Li^+ in the gas phase (Data from Staley et al 1975)*

Such observations are not characteristic of Li^+ ion alone and similar inductive effect orders for alkyl substituents are observed for all metal ions in the gas phase. The formation free energies of Ni(I) bis - ligand complexes display the

same character as illustrated in the figure below.

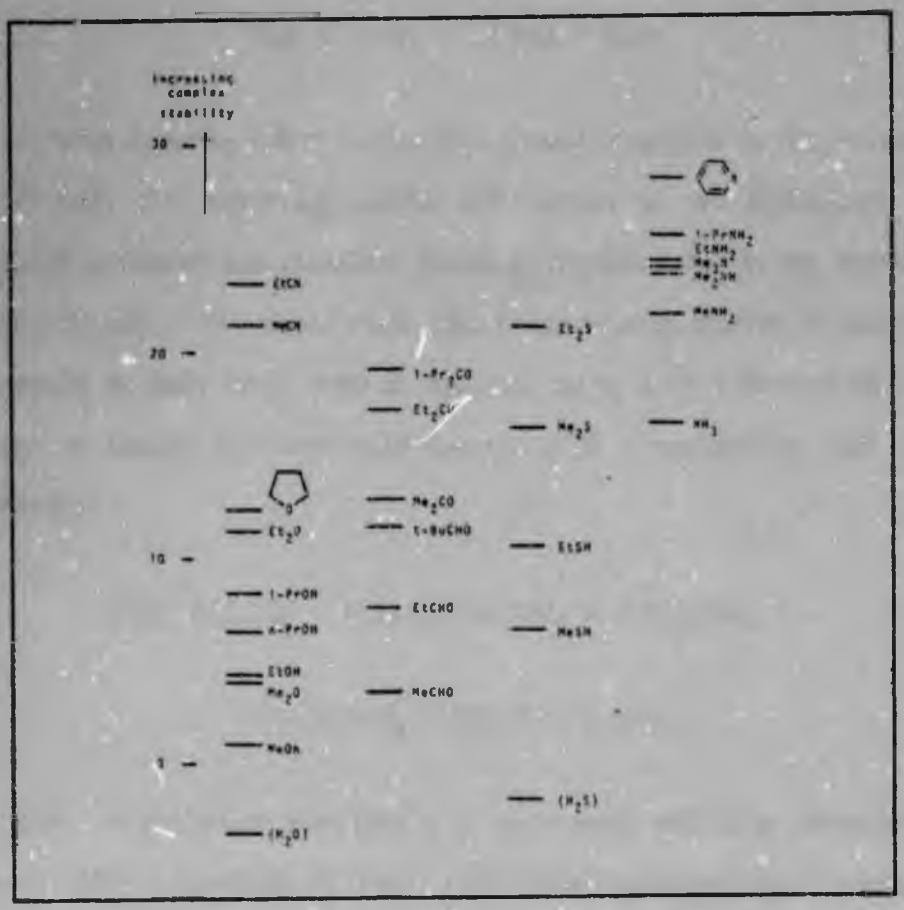


Figure 4 : Free energies of formation of Ni (I) bis - ligand complexes (Hancock & Martell 1989)

Coordination chemistry is flooded with examples of ligands having neutral saturated nitrogen donors. This can be assigned to the fact that the neutral nitrogen donor displays stronger coordinating properties with many metal ions than does the neutral oxygen donor. The nitrogen donor is also synthetically more convenient as it provides a locus for further chemistry to be introduced, such as the introduction of other chelating groups in the form of pendant moieties. As in the figures 3 and 4 the basicity towards metal ions in the gas

phase is :

$$NH_3 < RNH_2 < R_2NH < R_3N$$

The electron donating effect of the alkyl groups is evident in the increasing basicity with the increasing methyl substitution of the hydrogens. The ionization potential was therefore found to decrease due to the increased electron density at the donor atom. Gas phase basicity studies of amines (Brauman & Blair 1968, 1969 & Brauman et al 1971) showed that the basicity of amines increases with increased N - methylation and αC - methylation :

$$(CH_3CH_2)_2NH > (CH_3)_3CCH_2NH_2 > (CH_3)_3NH_2 >$$

$$CH_3CH_2NH_2 > CH_3NH_2 > NH_3$$

This order of gas phase basicities is in agreement with that proposed by Munson (1965). Brauman & Blair (1968, 1969) indicated that the basicity of diethylamine compared with water decreased in the following order :

$$(CH_3CH_2)_2NH > NH_3 > H_2O$$

The above order was later confirmed by Taft et al (1977). The effects of donor atom basicity on the complexes of ligands with saturated nitrogen donors is clearly visible when considering the enthalpies of complex formation and the energies of the d - d transition bands along the series of Cu^{2+} complexes. The increase of ΔH and ligand field strength along the series is caused by the greater donor strength as the zeroth nitrogens are replaced by primary and secondary nitrogens (Hancock & McDougall 1980).

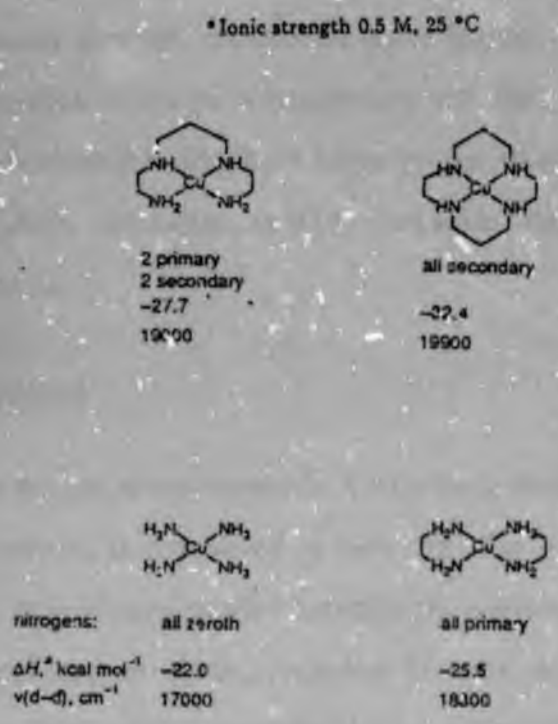


***Figure 5** : Increase in nitrogen donor basicity along the series of Cu^{2+} complexes (Hancock & Martell 1989)*

It is clear from the mentioned studies that the gas phase base strength for alcohols and amines obey the order :

TERTIARY > SECONDARY > PRIMARY

This general order seems to be a function of two variables; polarizibility effects and inductive effects arising from the alkyl substitution.

POLARIZIBILITY EFFECTS

The charge-induced dipole or polarizibility effects are primarily related to the size of the alkyl substituents. Polarization stabilises ions in the gas phase by

delocalisation of charge over the entire ion. Larger molecules have a greater number of atoms that will incorporate more bonds, and allow for a more facile delocalisation of charge in comparison with their smaller counterparts. The larger molecules therefore have larger proton affinities. The result of the favourable charge delocalisation with increasing alkyl substitution is an increase in basicity.

INDUCTIVE EFFECTS

These effects are not always apparent if pKa data, which are often the guide to inductive effects, is considered in isolation. The pKa values of primary amines show little change as alkyl substituents are changed from methyl, to ethyl, isopropyl and tert-butyl; implying that the substituents produce a uniform effect. Protonation constants along the series NH_3 through $N(CH_3)_3$ are NH_3, 9.2; NH_2CH_3, 10.6; $NH(CH_3)_2$, 10.8; $N(CH_3)_3$, 9.9 .

It appears that intrinsic basicity varies little in the series compared to the analogous phosphine series : PH_3, -14; PH_2CH_3, 0.0; $PH(CH_3)_2$, 3.9; $P(CH_3)_3$, 8.7 . Gas phase studies using mass and cyclotron resonance spectrometry (Munson 1965; Brauman et al 1971; Taagepera et al 1980; Taft et al 1978; Woodin & Beauchamp 1978,1975; Davidson & Kebarle 1976; Uppal & Staley 1982) prove this to be totally untrue and reveal the change in inductive effects with different alkyl substituents (Hancock et al 1983). Due to the concealed nature of these inductive effects Hancock et al (1983) suggested the term "hidden inductive effects". The macrocyclic effect in N - macrocycles is thought to have a large contribution from the inductive effects of the secondary nitrogens formed on cyclisation (Hancock & McDougall 1980); an example of hidden inductive effects since there is little or no difference in

pKa the values of primary and secondary amines.

These effects are based on the greater electron donating ability of the alkyl groups compared to hydrogen atoms. The more alkyl substituents are attached to the donor atom the more electron-rich it becomes and the greater the attraction will be for a positively charged metal ion. In the figure below is plotted the free energy of protonation in the gas phase for a series of bases involving methyl group substitution (Hancock & Martell 1988).

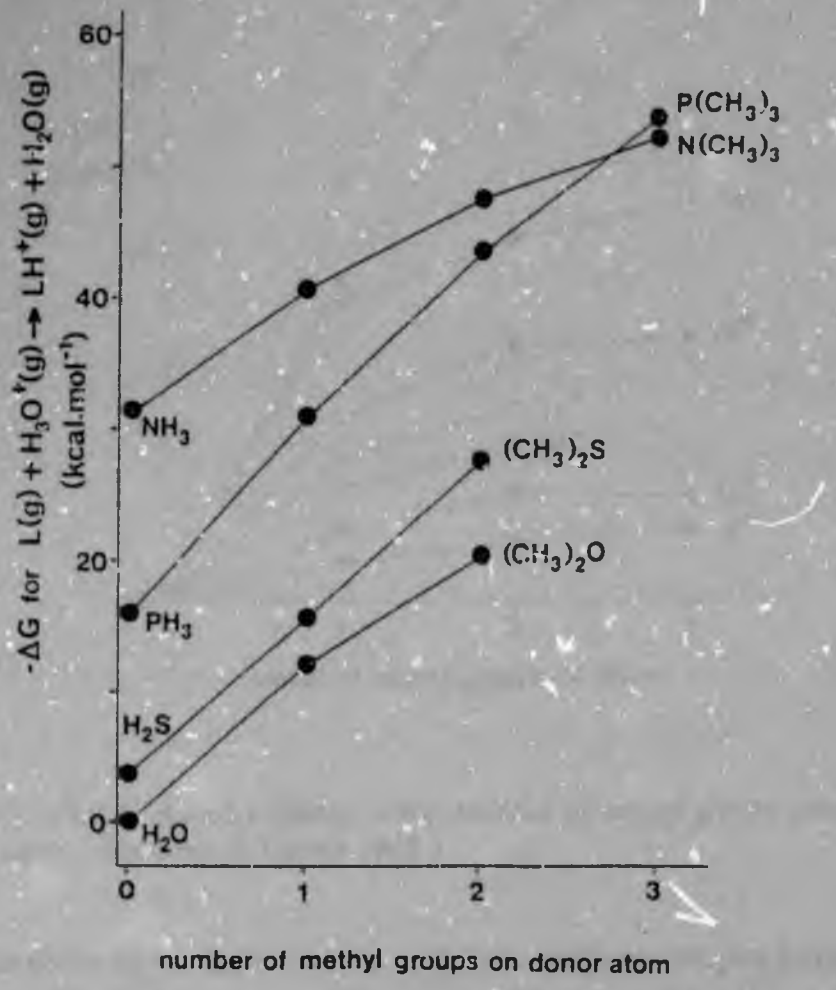


Figure 6 : Plot of Gibbs free energy versus number of methyl groups on donor atoms (Hancock & Martell 1988)

Similar trends are observed in the gas phase studies (Woodin & Beauchamp 1978; Kappes & Staley 1982) on the binding of amines to metal ions.

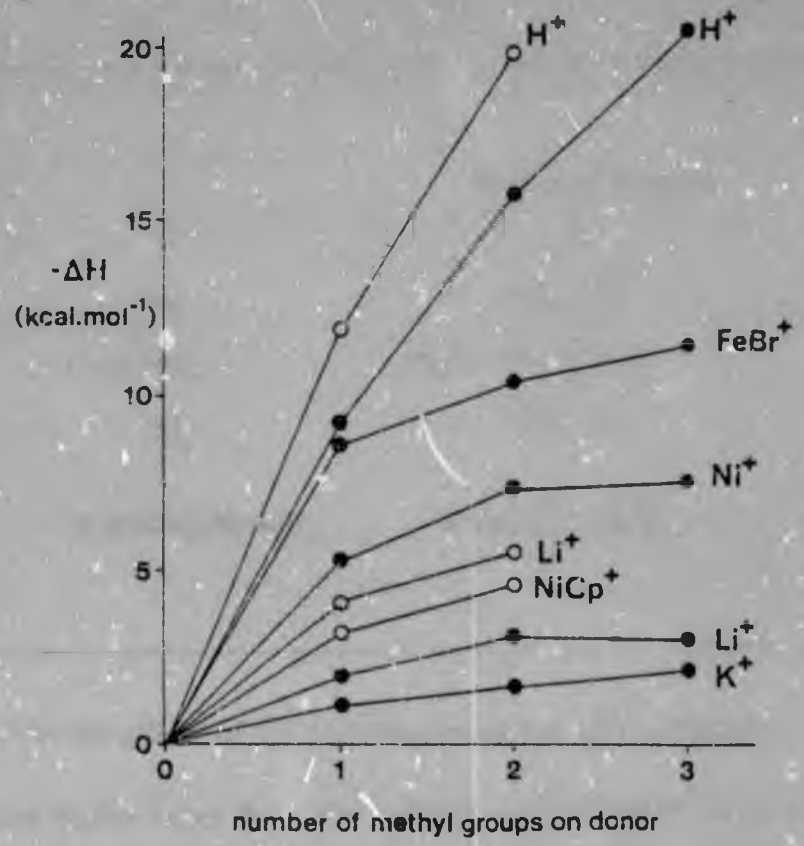


Figure 7 : Plot of enthalpy change versus number of methyl groups on the donor atom (Hancock & Martell 1988)

The figure above shows the increase in enthalpy change on complex formation in the gas phase, as hydrogen is replaced by methyl in the series from ammonia to triethylamine and in the series from water to dimethyl ether. The apparent inability of the amine series to adhere to its intrinsic basicity order

in aqueous solution is caused by two effects (Henderson & Speranl 1960; Jones & Arnett 1974). Solvation effects account in part for this anomaly . The poor basicity of $(CH_3)_3N$ is due to steric strain induced by the methyl groups on the bulky solvation sheath of the proton. In water the solvation sheath is sterically hindered by the methyl groups whereas in the gas phase the proton is bare and coordination to $N(CH_3)_3$ can occur with less strain.

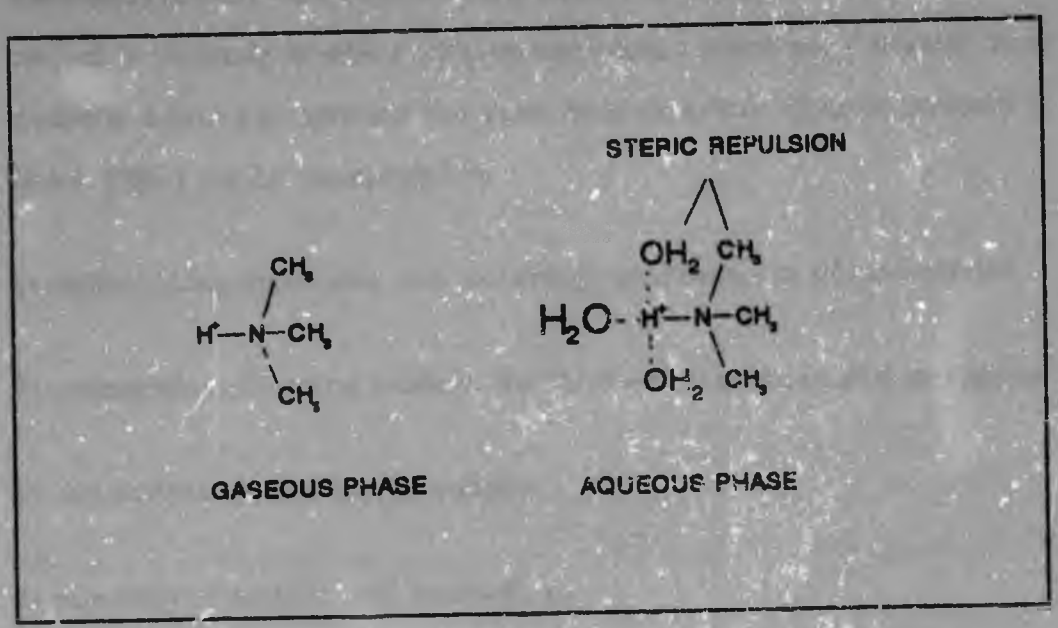


***Figure 8** : Proton affinity of $N(CH_3)_3$ in gaseous and aqueous media*

The second factor arises from the inability of $(CH_3)_3NH^+$ to disperse the positive charge to the solvent via hydrogen bonding (Hancock & Martell 1988; Trotman-Dickenson 1949).

DESIGN OF CHELATING LIGANDS

Alfred Werner in launching the field of coordination chemistry studied the first most fundamental examples of chelating ligands; ethylenediamine, carbonate and oxalate leading to two coordination sites on a metal ion. Rossotti & Rossotti (1961) defined a complex as : a species formed by the association of two or more species each capable of independent existence. The subject is currently involved with manipulating parameters (usually of a synthetic nature) to optimize this guest /host chemistry. Complementarity (Busch 1993) can be exemplified by :

1) studies fitting metal ions into low-energy conformations of macrocycles

2) optimization of binding forces by careful selection of hard/soft donor atoms

3) thermodynamic and kinetic stability

4) selectivity of metal-ligand interactions.

These points are to some degree affected by structural and electronic influences. Parameters of fundamental importance in ligand design where initially outlined by Lehn (1973) :

1) ligand topology

2) nature of binding sites

3) complexation environment.

The subject of "complementarity" as is recognised in studies on molecular

organisation can perhaps be best explained in the words of Lehn (1988); "complementarity is a congruence of shape and size factors and energetic or electronic compatibility between receptor and receptee, host and guest, or central atom and ligand ."

Busch (1990) outlined the following factors that underlie molecular organisation :

1) size

2) shape or geometry

3) topology or connectedness

4) rigidity.

Size and shape are almost subconsciously considered in complex formation; such is the fundamental importance of these factors. These two factors are more so involved with stereochemical complementarity. Rigidity and topology are involved in a more subtle manner. The modern chemist can think of *size and shape* as the *coarse adjustments* with *topological and rigidity factors* as the *fine tuning* for optimal complexation. In the words of Busch (1993) : "given a high level of complementarity (size and shape) an additional stereochemical contribution to the complexation affinity of receptor and receptee (for each other) is determined by topological and rigidity constraints."

Complementarity outlines the requirements for strong affinity which can then be arbitrarily enhanced by topological and rigidity constraints.

CHAPTER 2

INTRODUCTION

The chelate , macrocyclic and cryptate effects are the most important tools available to the coordination chemist that will allow the manipulation of complex stability and metal-ion selectivity. The "chelate effect" is associated with the improved stability of metal complexes containing chelate rings compared to the stability of a similar complex that contains none or fewer rings.

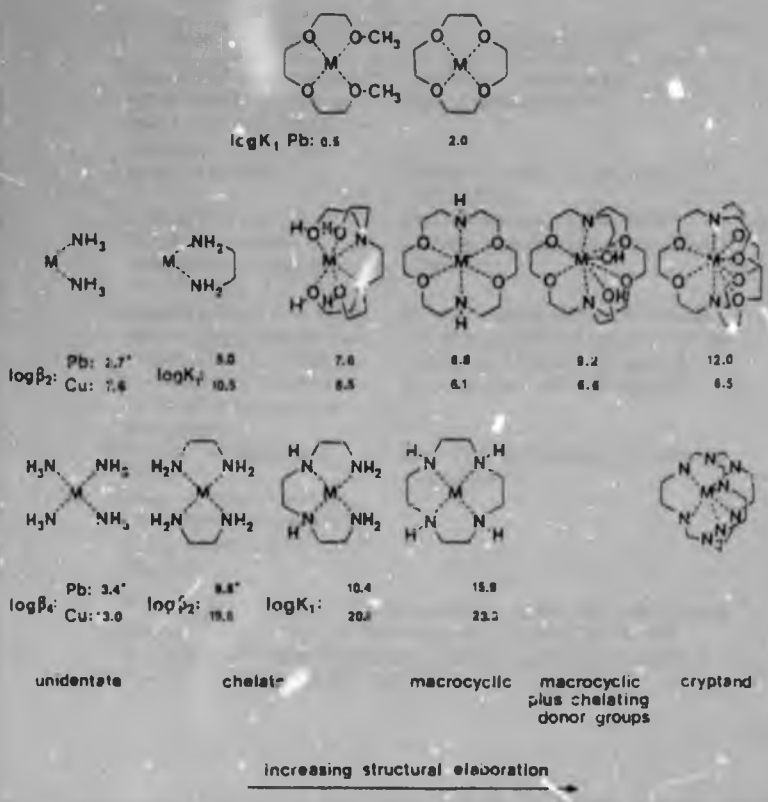


Figure 9 : complex stability of Cu^{2+} and Pb^{2+} for ligands increasing along the series unidentate, chelate, macrocyclic, and cryptate. (Hancock & Martell 1988)

As with all thermodynamic observations , enthalpic and entropic contributions are to be considered. It is common in many textbooks the conclusion that the chelate effect can be almost entirely attributed to an entropy effect. Enthalpy effects are regarded as less important since these do not always contribute in a positive manner. This approach differs from that expressed by Myers (1978) who concludes that both enthalpy and entropy factors contribute to the chelate effect.

Enthalpy effects	Entropy effects
Variation of bond strength[d] with electronegativities of metal ions and ligand donor atom	Number of chelate rings[b] Size of chelate ring[b,d]
Ligand field effects	Changes of solvation on complex[b,c] formation
Steric and electrostatic[b] repulsion between ligand donor groups in the complex	Arrangement of chelate rings[b] Entropy variations in uncoordinated ligands[d]
Enthalpy effects related to the conformation of the uncoordinated ligand	Effects resulting from differences in configurational entropies of the ligand in complex compounds
Other coulombic forces involved in chelate ring formation	*Entropy of solution of ligands*[d]
Enthalpy of solution of ligands[d]	*Entropy of solution of coordinated metal ions*[d]
Change of bond strength when ligand is changed (same donor and acceptor atom)[d]	

[a] Taken from Martell,[2] plus the addition of the last items in each column. [b] Considered an important contribution by Martell.
[c] Not applicable here, because no charged ligands are considered.
[d] Considered an important contribution by this author.

Figure 10 : Factors affecting the chelate effect (Myers 1978)

Just as controversial as the chelate effect is the macrocyclic effect that might also generally arise from either entropic or enthalpic contributions. The macrocyclic effect was initially proposed by Cabbiness & Margerum (1969) to rationalise the enhanced stability of macrocyclic metal complexes over their open chain analogues. To fully understand this effect the thermodynamic relationships of the Gibbs free energy term must be considered.

$$\Delta G^\circ = -RT \ln \beta$$

$$\Delta G^\circ = \Delta H^\circ - T\Delta S^\circ$$

The view as expressed by Cotton and Wilkinson (1980) is that the macrocyclic effect generally arises from the favourable entropy and enthalpy contributions simultaneously. This is in agreement with the work of Paoletti et al (1973) who suggested that although the entropy term appears to be dominant, both enthalpy and entropy terms contribute to the macrocyclic effect. The work of Jones et al (1975) on stabilities and kinetics of Cu^{2+} complexes of cyclic polythiaethers in 80% ethanol further substantiates the idea.

Cabbiness and Margerum (1969) proposed from their studies on Cu^{2+} complexes of Tet-A (c-meso-5,5,7,12,12,14-hexamethyl-1,4,8,11.tetraazacyclotetradecane) and 2,3,2,-Tet (1,4,8,11-tetraazaundecane) that the differences in configuration and solvation contributed to the observed macrocyclic effect. Hinz and Margerum (1974) studied the effect of ligand solvation using Ni^{2+} complex of cyclam and 2,3,2-Tet; the dominant factor for the macrocyclic effect was found to be the more favourable enthalpy.

THE CHELATE EFFECT

The model of the chelate effect as put forward by Schwarzenbach (1952) involves a displacement reaction (Martell et al 1994)

$ML_2(aq.,\ 1\ molal) + L^{\circ}\text{-}L^{\circ}(aq.,\ 1\ molal) \rightarrow ML^{\circ}_2(aq.,\ 1\ molal) + 2L(aq.,\ 1\ molal)$

He assumes in this model that for the above reaction $\Delta H^{\circ} = 0$...*ie.* the affinity of both ligands for the metal ion is equivalent.

$$\Delta H^{\circ} = H^{\circ}_{ML^{\circ}2} - H^{\circ}_{ML2} - H^{\circ}_{L\text{-}L^{\circ}} - 2H^{\circ}_{L}$$

$$\Delta S^{\circ} = S^{\circ}_{ML^{\circ}2} - S^{\circ}_{ML2} - S^{\circ}_{L\text{-}L^{\circ}} - 2S^{\circ}_{L}$$

If internal and solvation entropies remain constant then ΔS° is equal to the generated translational entropy of the solute. *ie.* the number of molecules that are displaced into solution with the introduction of the chelate. Entropy and enthalpy changes on complexation involved in the chelate effect may be difficult to interpret if these are solvation differences. Chelate complexes having less water of solvation will have a more favourable enthalpy of complexation as less water must be removed before the complex can be formed. However , the release of fewer water molecules produces an adverse effect to the entropy contribution.

Adamson (1954) showed that for the generation of one mole of solute at the standard state of 1.00 molal

$$\Delta S^{\circ} = R \ln 55.5 = 7.9 \text{ e.u}$$

$\Delta S^{\circ} = 7.9n$ e.u n = no. of chelate rings at 25°C

An increase of approximately 2 logK units is observed for each chelate ring formed. The arguments of Schwarzenbach and Adamson have been discussed by Martell (1964) . Essentially the model of Schwarzenbach considers the chelate effect to arise because of the restricted volume in which the second donor atom can move, once the first donor atom is coordinated. Adamson, however, relates the chelate effect to the way in which the standard reference state is defined and suggests that it will disappear if the formation constants are expressed in mole fractions. Hancock and Martell (1989) suggest that both approaches are comparable since both Schwarzenbach and Adamson set the translational entropy to zero by; forcing the second unidentate ligand to move in a restricted volume in the first instance, and by completely filling the space of the reference state with reactants when expressing the constants as mole fractions in the latter.

Munro (1977) invalidates Adamson's choice of standard reference state and describes a state of unit mole fraction for all constituents of an equilibrium as unreal. It is therefore incorrect to conclude from Adamson's results that the chelate effect does not exist. Rasmussen (1956) investigated the magnitude of the chelate effect by setting up empirical entropy equations for species in aqueous solution. The entropy change resulted from a difference in entropy between the unidentate and multidentate ligands due to the release of more unidentate ligand molecules in solution compared to the chelating ligand in a displacement reaction. Using Born-Haber type cycles (Myers 1978) to analyse the entropy and enthalpy of species in chelation reactions proved the enthalpy of solution of ligands to generally deviate from ideality which was not observed by Munro (1977). This may affect the equilibrium even more than the increase in translational entropy. Entropy of the species contributing to

ΔG° were also found to be non-ideal. Myers (1978) concluded that both entropy and enthalpy factors contribute to the chelate effect. Factors such as number and size of chelate rings, steric, electrostatic and ligand field effects , as well as the arrangement of the chelate rings were found to affect the enthalpy and entropy contributions (Martell 1966; Frausto da Silva 1983).

Martell et al (1994) illustrates a model calculation for a unidentate, MA_6, bidentate, MB_3, and a hexadentate ML ligand complexes assuming a six coordinate metal .

Table 1 : Comparison of dissociation of metal complexes and metal chelates in dilute solutions

Donor groups per ligand	Number of chelate rings	Equilibrium quotient	β	Total concentration of complex and metal ion					
				1.0 M		1.0×10^{-3} M		1.0×10^{-6} M	
				pM*	%Diss.	pM*	%Diss.	pM*	%Diss
1	0	$\frac{[MA_6]}{[M][A]^6}$	10^{12} M^{-6}	16.67	2.1×10^{-15}	3.75	18	6.00	100
2	3	$\frac{[MB_3]}{[M][B]^3}$	10^{18} M^{-3}	19.43	3.7×10^{-18}	13.43	3.7×10^{-9}	7.74	1.8
6	5	$\frac{[ML]}{[M][L]}$	10^{22} M^{-1}	22.00	1×10^{-28}	22.00	1×10^{-17}	22.00	1×10^{-14}

*For 100% excess ligand

Assuming a value of 10^{12} as the stability constant for MA_6, then MB_3 and ML

should have stability constants of 10^{18} and 10^{22} respectively with a chelate effect of approximately 2 log units per chelate ring. This model shows that dilution of the standard reference state contributes to a larger value of the chelate effect (Martell 1956, 1966). *ie.* chelates have and increased advantage in dilute solutions over their open chain analogues. Complex dissociation can be inhibited in very dilute solutions by having chelates with an greater number of chelate rings. A table from Martell et al (1994) contains thermodynamic data on the Ni^{2+} and Cu^{2+} complexes of ammonia and ethylenediamine.

	ΔG°	ΔH°	ΔS°	
Unidentate complex				
$[Ni(NH_3)_2(H_2O)_4]^{2+}$	−6.93	−7.8	−3	
$[Ni(NH_3)_4(H_2O)_2]^{2+}$	−11.07	−15.6	−15	
$[Ni(NH_3)_6]^{2+}$	−12.39	−24	−39	
$[Cu(NH_3)_2(H_2O)_4]^{2+}$	−10.68	−11.1	−1	
$[Cu(NH_3)_4(H_2O)_2]^{2+}$	−17.74	−22.0	−14	
Chelate analog				
$[Ni(En)(H_2O)_4]^{2+}$	−10.31	−9.0	4	
$[Ni(En)_2(H_2O)_2]^{2+}$	−19.09	−18.3	3	
$[Ni(En)_3]^{2+}$	−25.09	−28.0	−10	
$[Cu(En)(H_2O)_4]^{2+}$	−14.64	−13.1	5	
$[Cu(En)_2(H_2O)_2]^{2+}$	−27.54	−25.5	7	

	ΔG^*	ΔH^*	ΔS^*	$7.9n$
Chelate effect				
Ni(En)	−3.4	−1.2	7	7.9
$Ni(En)_2$	−8.0	−2.7	18	15.8
$Ni(En)_3$	−12.70	−4	29	23.7
Cu(En)	−4.0	−2.0	6	7.9
$Cu(En)_2$	−9.8	−3.5	21	15.8

***Figure 12** : Thermodynamic contributions to the chelate effect in Cu(II) and Ni(II) complexes of ethylenediamine (Martell et al 1994)*

The entropic contribution to the chelate effect is immediately apparent , and it is pointed out that it can be reasonably predicted with increments of 7.9 e.u as stated by Adamson. Although not as pronounced, an enthalpic contribution is also evident and this is mainly attributed to the fact that the polar groups that would be further apart in the complexes of ammonia are forced closer together by the ethylenediamine chelate.

Quoting from Martell et al (1994) "for metal ions which have considerable tendency for covalent coordinate bond formation (if their electronegativities are appreciable), the enthalpic contribution to the chelate formation can be important. This statement was further substantiated by reporting the enthalpy contribution of the chelate effect as a function of differing chelate ring size.

Thermodynamics of formation of metal chelates of EDTA homologs
$\mu = 0.10$ M and $T = 25.0°C$.

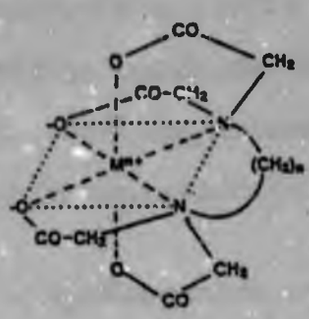
	n	Quantity	Metal ion					
			Mg^{2+}	Ca^{2+}	La^{3+}	Ni^{2+}	Cu^{2+}	Zn^{2+}
	2	log K	8.8	10.6	15.5	18.4	18.8	16.5
		ΔH^0	3.3	−6.1	−2.9	−7.4	−8.3	−4.6
		ΔS^0	52	28	61	59	58	60
	3	log K	6.3	7.3	11.3	18.1	18.8	15.2
		ΔH^0	9.1	−1.7	3.8	−6.7	−7.7	−2.3
		ΔS^0	59	27	64	60	60	62
	4	log K	6.3	5.6	9.2	17.3	17.2	15.0
		ΔH^0	8.5	−0.9	1.9	−7.0	−6.5	−3.5
		ΔS^0	57	23	48	56	57	57
	5	log K	5.2	4.5	9.0	13.8	16.1	12.6
		ΔH^0	–	–	–	−6.7	−10.9	−2.7
		ΔS^0	–	–	–	41	37	49

Figure 13 : Thermodynamic data as a function of chelate ring size (Martell et al 1994)

In the tabulated series of EDTA homologues a decrease in stability accompanies the increase in the chelate chain length that allows the iminodiacetate groups to be more separated. This decrease in stability is viewed as a consequence of changes in enthalpy rather than entropy. The explanation is that the longer the chelate chain the greater the coulombic repulsive forces that must be overcome in bringing the iminodiacetate groups closer together for complex formation.

THE MACROCYCLIC EFFECT

The ΔS and ΔH terms of the macrocyclic effect have been discussed in the literature as independent entities and hence the varying ideas of authors such as Arnaud-Neu et al (1978), Cabbiness and Margerum (1969), Hinz and Margerum (1974), Dei & Gori (197), Anichini et al (1977, 1978), Paoletti et al (1973), Jones et al (1975), Kodama & Kimura (1975, 1976) and Fabbrizzi et al (1976). This is so because of the need of the macrocyclic effect to explain the characteristic chemical properties associated with macrocyclic complexes such as the kinetic inertness and the stabilisation of the less frequent oxidation states of metal ions.

The significant difference between the macrocyclic and chelate effects is the expected absence of translational entropy effects , because there is the same number of particles in the equilibrium for the macrocycle as for the equilibrium of the open-chain ligand.

Hancock & Martell (1988) listed the following as important contributions regarding the macrocyclic effect :

1) preorganisation of the ligand

2) desolvation of donor atoms in the macrocyclic cavity

3) intrinsic basicities of donors

4) dipole-dipole repulsion in the cavity of the ligands

More recent publications (Hancock & Martell 1988, Hancock 1992, Martell et al 1994) have placed more emphasis on the contribution of enthalpy to the macrocyclic effect. Entropy may in some instances contribute to the macrocyclic effect but not as significantly as enthalpy. The favourable ΔH is illustrated in the next two tables.

		Na^+	K^+	Ba^{2+}
log K_1	18-crown-6	4.36	6.06	7.04
	pentaglyme	1.44	2.1	2.3
	log K (MAC)	2.92	3.96	4.74
ΔH	18-crown-6	−8.4	−13.4	−10.4
	pentaglyme	−4.0	−8.7	−5.6
	ΔH (MAC)	−4.4	−4.7	−4.8
ΔS	18-crown-6	−8	−17	−3
	pentaglyme	−7	−20	−8
	ΔS (MAC)	−1	3	5

Figure 14 : Thermodynamics of K^+, Na^+, and Ba^+ with 18-crown-6 and pentaglyme in 100% methanol (Martell et al 1994)

		Cu(II)	Ni(II)	Zn(II)
log K_1	cyclam	27.2	22.2	15.5
	2,3,2-tet	23.2	16.1	12.7
	log *K* (MAC)	4.0	6.1	2.8
ΔH	cyclam	−32.4	−24.1	−14.8
	2,3,2-tet	−26.5	−17.9	−11.6
	ΔH (MAC)	−5.9	−6.2	−3.2
ΔS	cyclam	12	21	21
	2,3,2-tet	16	15	19
	ΔS (MAC)	−4	6	2

***Figure 15** : Thermodynamics contributions of tetraazamacrocycles to the macrocyclic effect (**Martell et al 1994**)*

The origin of the favourable ΔH° seems to be mainly associated with the preorganisation of the ligand and the increased intrinsic basicities of its donor through alkylation. Preorganisation of the macrocyclic ligand involves the orientation of its donors that will overcome repulsive forces between polar groups. These same repulsive forces are only overcome in the open-chain ligand on complex formation , as donors that are far apart in the free ligand must be forced closer together on complexation.

INCREASE IN THE INTRINSIC BASICITY OF THE DONOR ATOM

As discussed in the section on inductive effects, trimethylamine is a poor donor for metal complex formation because of steric repulsion of the methyl groups and the inability to hydrogen bond in aqueous solution. The steric repulsion of methyl groups as well as their ability to inhibit solvation of the metal complex is minimised by the introduction of bridging between alkyl groups.

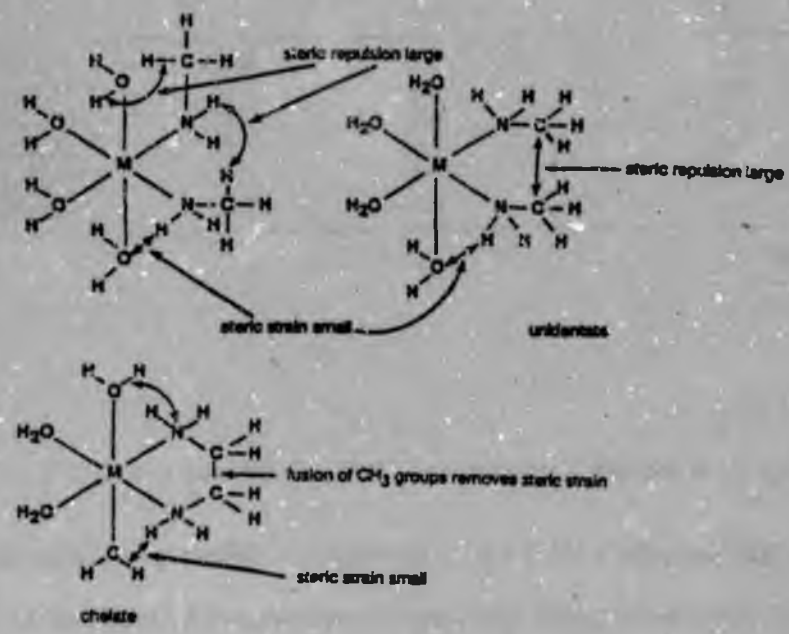
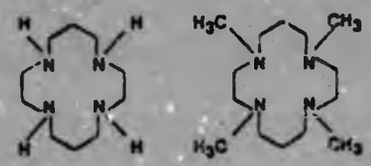


Figure 16 : Methyl group interactions in Aqueous solution

The resultant increase in the intrinsic basicity of the donor oxygen or nitrogen donor atoms produces an increase in the stability of the metal complexes due to the greater affinity of the donor atom for the metal ion. Increased alkylation does not necessarily enhance complex stability however, and steric

repulsions between methyl groups on repeated methylation may result in a decrease in complex stability (Hancock & Martell 1988).



	Cyclam	TMC	Δ log *K*	Ionic radius (Å)
log K_1 [Cu(II)]	27.2	18.3	8.9	0.65
log K_1 [Ni(II)]	22.2	8.6	13.6	0.69
log K_1 [Co(II)]	12.7	7.6	5.1	0.72
log K_1 [Zn(II)]	15.5	10.4	5.1	0.74
log K_1 [Cd(II)]	11.7	9.0	2.7	0.97
log K_1 [Pb(II)]	11.3	(~7.5)	(~3.8)	1.21

Figure 17 : Stability constants for TMC and cyclam (Martell et al 1994)

Molecular mechanics studies of Hancock et al (1988)indicated that the strain energies of tetramethyl cyclam are substantially higher than those of cyclam. This arises from steric repulsions between methyl groups and between methyl groups and the carbon backbone of the macrocycle. These increased strain energies have to be overcome for complex formation and this is reflected in the corresponding decrease in complex stability.

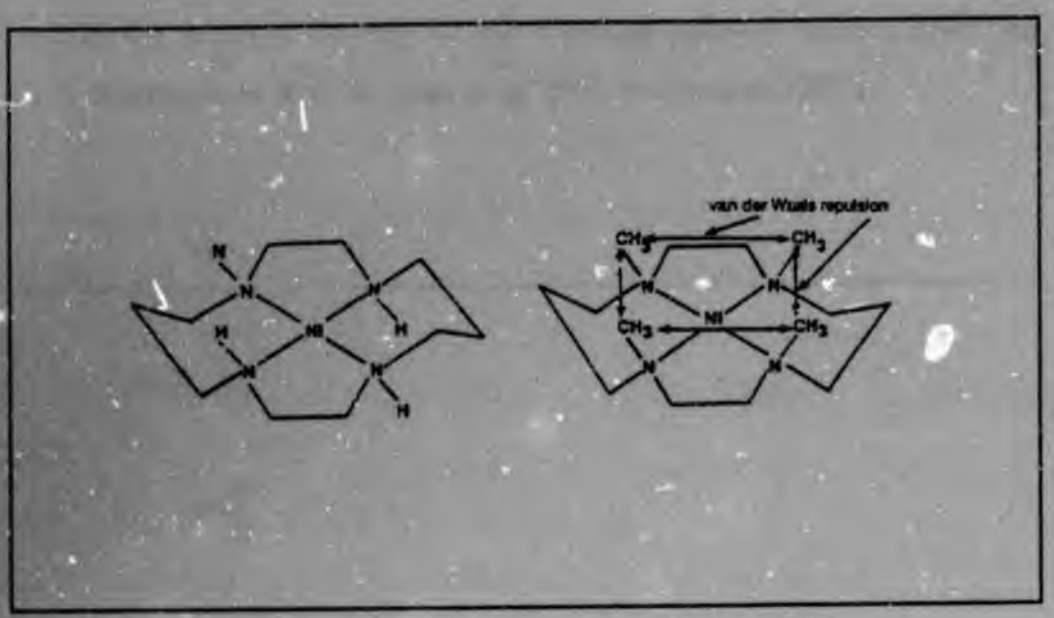


Figure 18 : Steric repulsive interactions on excessive alkylation

THE CRYPTATE EFFECT

The cryptate effect is often regarded as an appendage to the macrocyclic effect. As a result it is not as popular in the literature as its chelate and macrocyclic counterparts. The "cryptate effect" or "macrobicyclic effect" (Lehn & Sauvage 1975) serves to explain the enhanced complex stability observed for macrobicyclic ligands, that are synthesized by the addition of one or several linkages to an already existing macrocycle. The enhanced stabilities of macrobicyclic complexes relative to their open chain analogues are substantially larger than observed for the macrocyclic effect, and their chemical properties revolve around cavity size and number of coordinating donor sites.

Studies in the 70's and 80's have suggested that possibly the major or only

contributing factor to the cryptate effect is of an enthalpic origin (Anderegg 1975, Kauffman et al 1976, Spics et al 1980, Buschmann 1985).

THE MACROCYCLIC CAVITY AND THE METAL ION SIZE.

The concept of size-match selectivity in macrocyclic chemistry hinges itself on the idea that the macrocyclic ligands form complexes of increased stability with the metal ions that best match in size the rigid cavity at the centre of the ligand (Penderson et al 1967). This idea was contradicted by the stability patterns observed by Thom et al 1985a&b. This author showed that instead of the large macrocyclic cavities being able to accommodate large metal ions lying in the plane of the four nitrogens; the opposite was true.

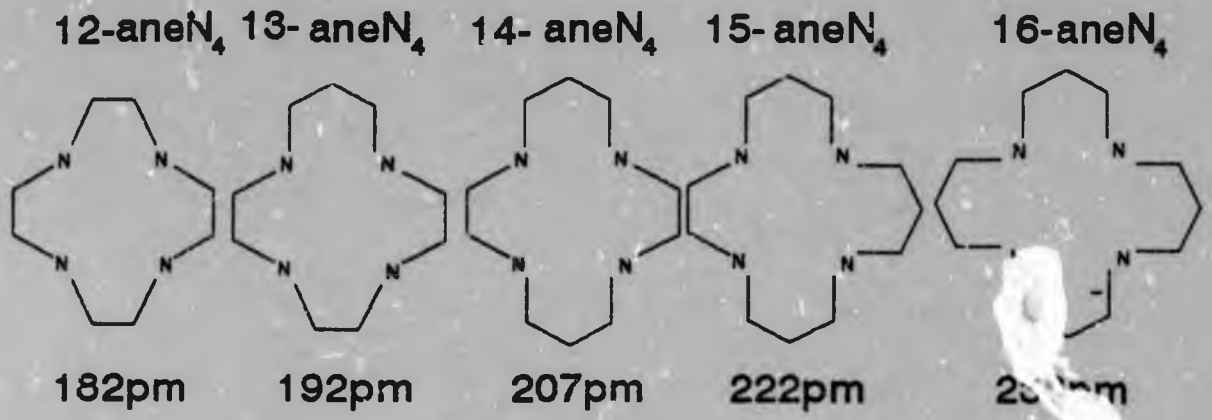


Figure 19 : Cavities sizes in the plane of the four N donors for macrocycles of increasing size(Hancock et al 1990 & Busch 1978)

Hole sizes in the diagram were calculated by molecular mechanics (Martin et al 1974 & Hancock et al 1980) for the metal ion in the plane of the Four N atoms in the ring.

The metal ions such as Pb^{2+} and Cd^{2+} that are relatively large, were found to form stable complexes with the 12-ane-N_4 possesing the smaller macrocyclic cavity. Inturn small metal ions were best complexed by the macrocycle with the largest macrocyclic cavity. Comparing 12-ane-N_4 with 13-ane-N_4 we notice that the stability of the Pb^{2+} complex decreases by 2.6 log units but that for the Cu^{2+}increases by 1.1 log units (Thom et al 1985b). Molecular mechanics calculations (Thom et al 1984) elucidated the ability of these macrocycles to adopt different conformers on complexation.

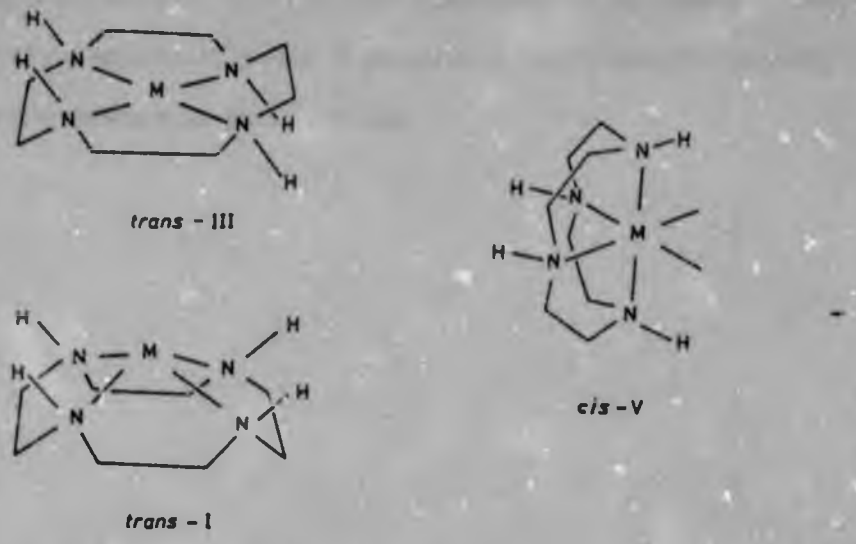


Figure 20 : Conformers on complexation (Thom et al 1984)

The large metal ions could escape being compressed in the small macrocyclic cavity by coordinating in an out-of-plane fashion as is illustrated by the trans-I conformer. The cis-V conformer becomes significant when the size of the

metal ion is sufficiently large to cause folding of the ligand.

The rigidity of the macrocyclic backbone is therefore not as dominating a factor as initially anticipated (Penderson et al 1967) and the factors that do govern the metal ion selectivity are those for open-chain ligands (Thom et al 1985 a&b). The selectivities of macrocyclic and open chain polyamines are related to the size of the chelate rings formed on complexation. In moving along the series from 12-ane-N_4 to 16-ane-N_4 there is an increase in the chelate ring sizes from five-membered to six-membered. The selectivity patterns observed can best be explained by the presence of six-membered rings as against five-membered chelate rings in the complex, instead of matching the metal ion size to the size of the macrocycle cavity (Thom et al 1985 a&b).

A study by Hancock and Ngwenya 1987 illustrates that increasing the chelate ring beyond six-membered results in an uniform drop of complex stability that shows no dependence on metal ion size.

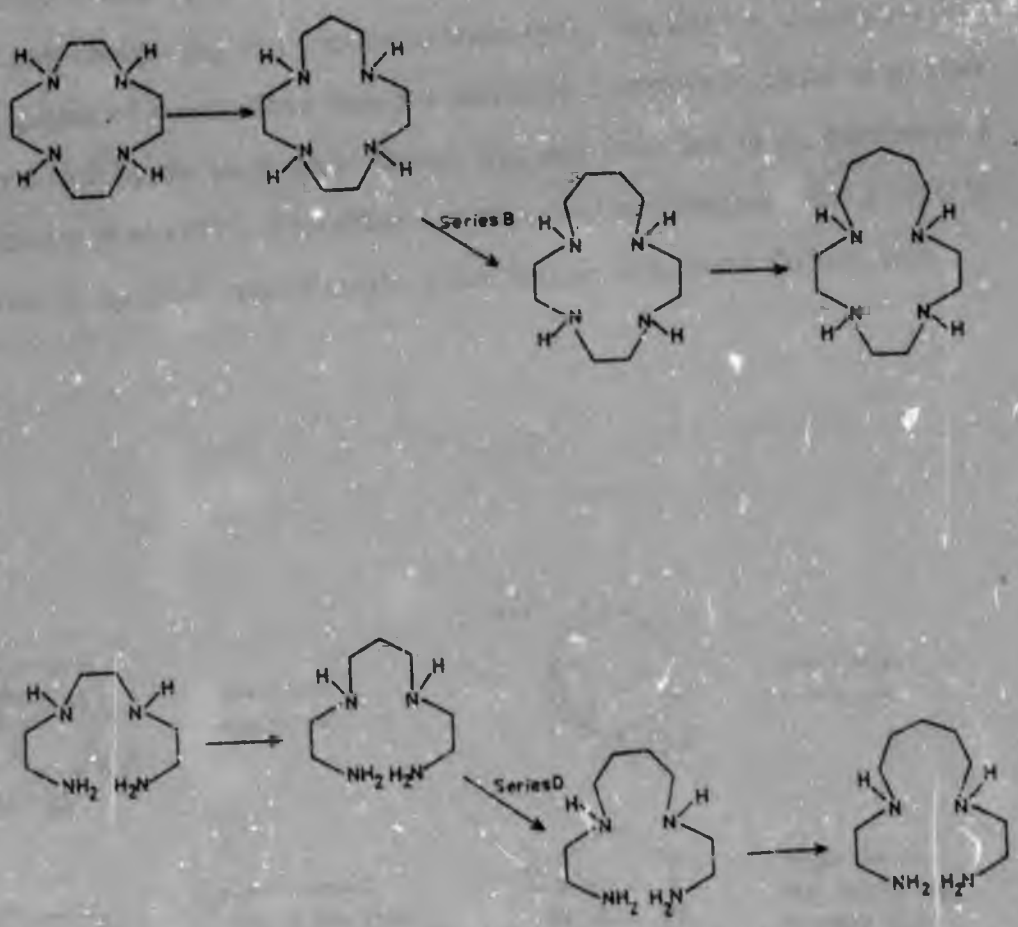


Figure 21 : Effect of increasing chelate ring size (Hancock & Ngwenya 1987)

METAL ION SELECTIVITY AND CHELATE RING SIZE

A more detailed inspection of the series 12-ane-N_4 to 16-ane-N_4 suggests that not only chelate ring size dominates macrocyclic ring size but in addition that complexes of larger metal ions are destabilised relative to those of smaller metal ions by the increase in chelate ring size from five to six membered (Hancock et al 1990). This effect was explained by Hancock 1989 & 1990 in terms of the steric requirements of five and six membered chelate rings.

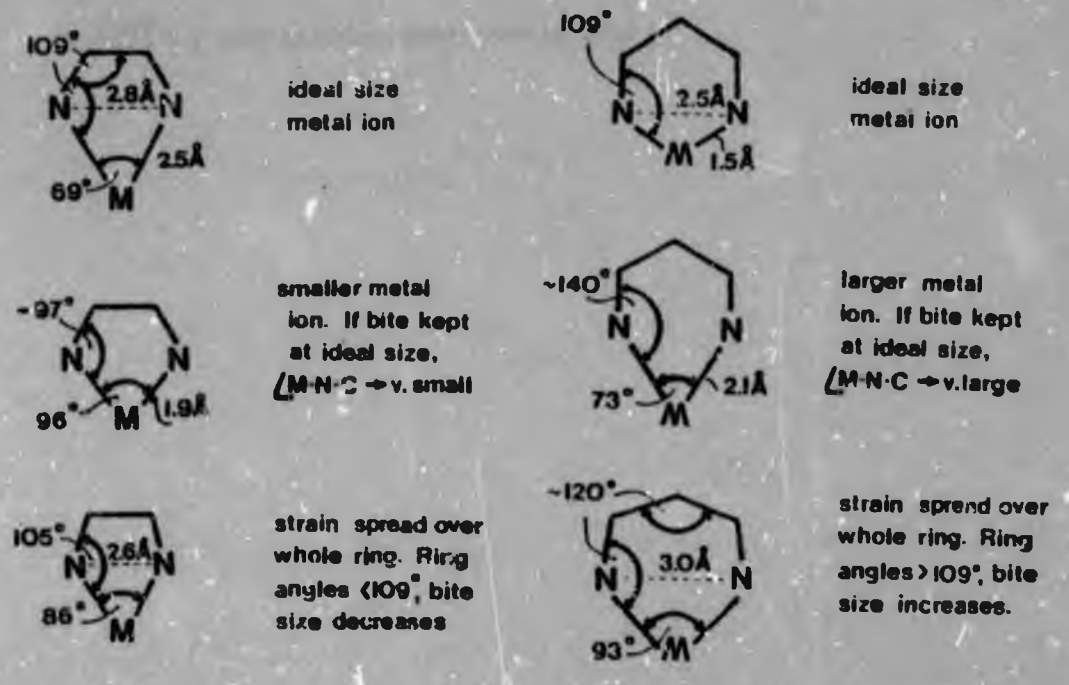


Figure 22 : Chelation geometry of five and six-membered chelate rings

Figure 22 shows the ideal M-N bond lengths and bond angles that produce minimum strain energy for five and six membered chelate rings as determined by molecular mechanics calculations (Hancock 1989). The ethylenediamine (EN) type of chelate ring directs the lone pairs of the saturated nitrogen donor to focus on a point 2.5 Å away forming a N-M-N bond angle of 69°. Such a bond length corresponds to a fairly large metal ion of radius approximately 1 Å , and the small N-M-N bond angle is consistent with high coordination number; i.e. larger coordination sphere. The six membered chelate ring comprised of propane-1,3-diamine (TN) exhibits minimum strain when the M-N bond length is 1.6 Å the corresponding N-M-N bond angle is 109.5°. This is in agreement with the smaller metal ions. This phenomenon can be graphically represented by the destabilisation of TMDTA (trimethylenediaminetetraacetic acid) complexes of large metal ions relative to EDTA (ethylenediaminetetraacetic acid).

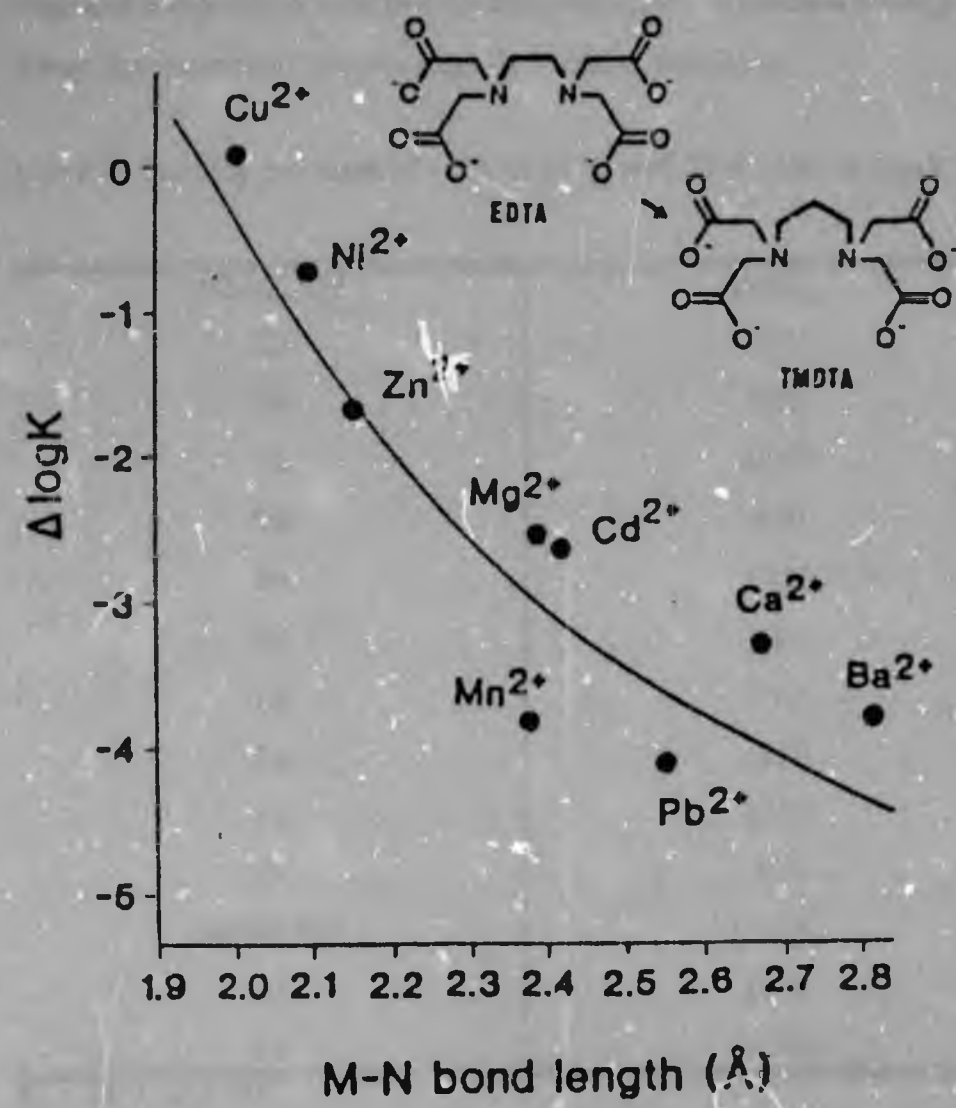


Figure 23 : plot of change in stability constant Δ log K vs bond length $r_{M\text{-}N}$

Hancock et al 1986 examined the role of polydentate ligands forming more than one chelate ring on complexation. Possibly a more accurate study of the selectivity effects of chelate ring size can be done on a ligand consisting of a single chelate ring. Having more than one chelate ring may impart some rigidity to the ligand which may result in a sharpening of the selectivity effect. Metal formation constants were determined for CTA (chromotropic acid; 4,5-dihydroxynaphthalene-2,7-disulfonate) which forms six membered chelate rings and compared to TIRON (4,5-dihydroxy-1,3-benzenedisulfonate) which forms five membered chelate rings on complex formation.

TABLE 2 : Stability constants of CTA at 25 °C and 0.1M ionic strength

METAL ION	LOGK$_1$
Cu	13.45
Ni	9.55
Zn	10.03
Cd	8.90
Pb	11.17
Be	16.3
La	9.82
In	16.04
Al	17.18
Fe	20.6
METAL ION	LOGK$_2$
Al	12.92
Fe	12.90

K_1 : $M + L = ML$

K_2 : $ML + L = ML_2$

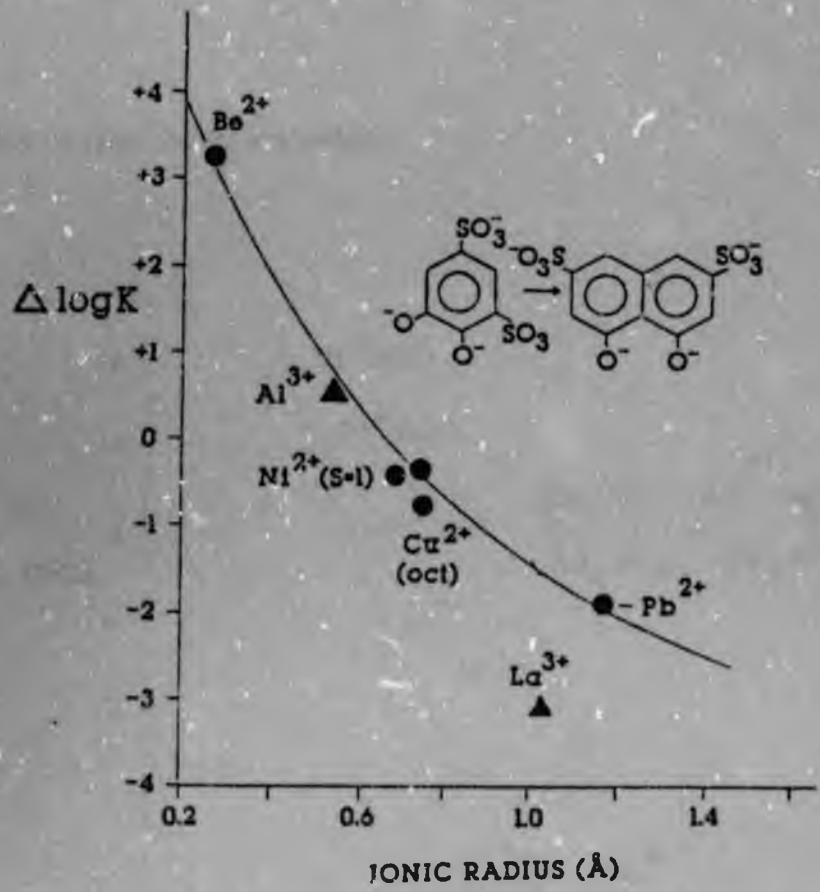


Figure 24 : plot of the change in the logarithm of the formation constant as a function of metal ionic radius for (Shanon et al) TIRON/CTA

From the data in TABLE 2 the change in the logarithm of the formation constant, Δ log K, accompanying the change in chelate ring size from the five in TIRON to six in CTA complexes, is plotted as a function of metal ionic radius in *Figure 24* above. All radii are octahedral except for Cu(II) that is square planar and Be(II) is tetrahedral since this is the dominant geometry of Be(II). There exists a similar relationship for 2,2,2 Tet versus 2,3,2 Tet.

The selectivity of six membered chelate rings against large metal ions such as Pb^{2+} is weakened for CTA when compared with the 2,2,2-Tet/2,3,2-Tet relationship since the slope of the TIRON/CTA relationship becomes less

steep at large metal ion radius.

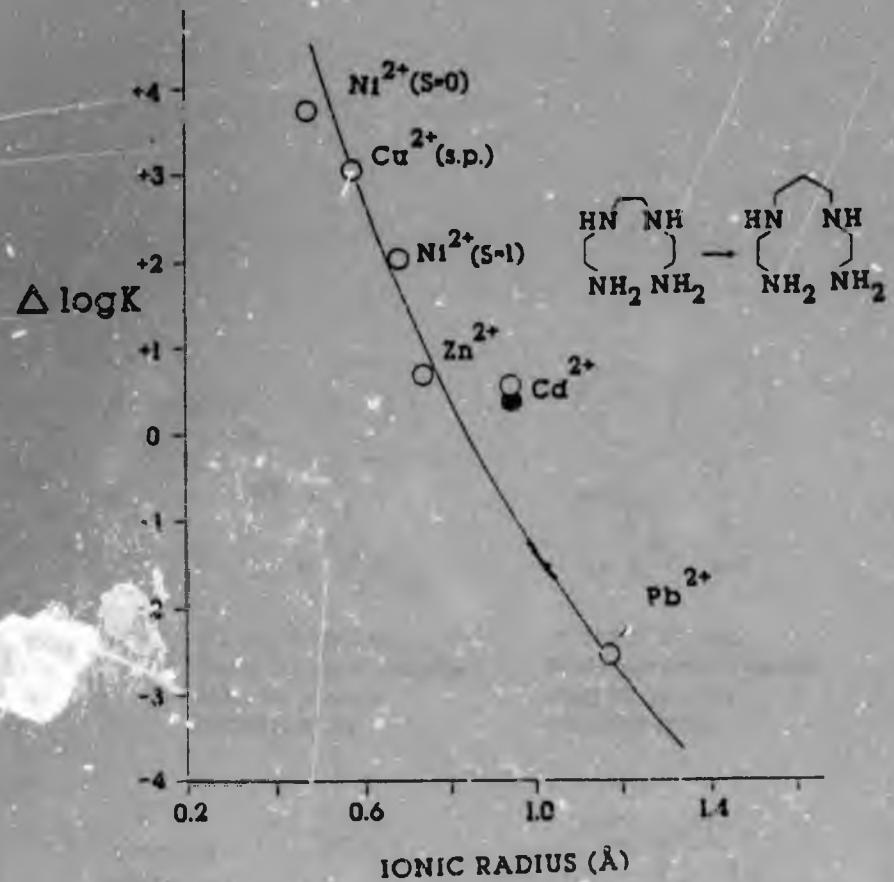


Figure 25 : plot of the change in logarithm of metal formation constant versus the metal ionic radius for 2,2,2-Tet/2,3,2-Tet (Shanon et al)

This might be explained by the metal ion coordinating with the CTA in a coplanar arrangement. The metal ion coordinates in a fashion so as to be above the plane of the donor atoms; this serves to minimise the steric strain that prevails for the larger metal ions. This is illustrated in figure 26.

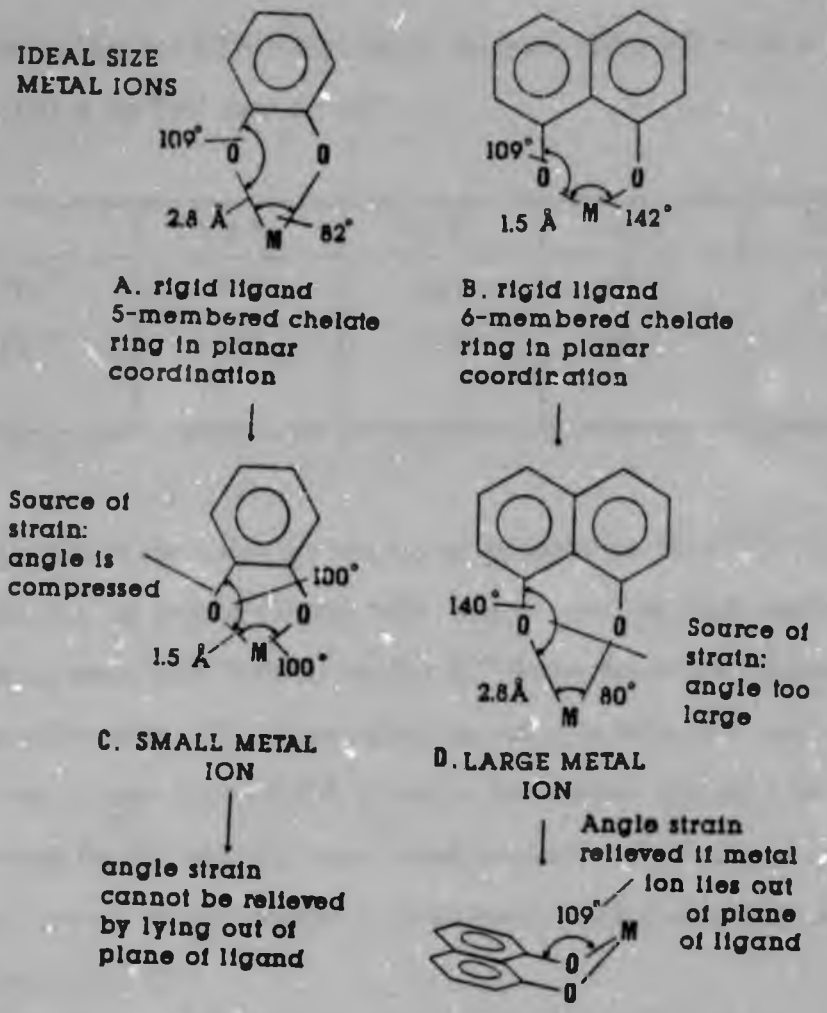


Figure 26 : Proposed bonding scheme for CTA for the metal ions of larger radius (Hancock et al 1990)

Figures 24 & 25 indicate that the chelate ring rigidity may promote size selectivity, since rigid six-membered chelate rings may act to promote selectivity for small metal ions of toxicological interest such as Al^{3+} relative to Fe^{3+} (Martell et al 1990). Gd^{3+} and In^{3+}, used as imaging agents (Lauffer et al 1987), are large and therefore six membered rings should be avoided in maximising selectivity for them. A suggestion can also be made from figure 24 that the introduction of fused aromatic rings to macrocycles can sharpen metal ion size selectivity as was investigated by Lindoy et al 1980.

Of interest for the CTA complexes is the more rapid fall off of $LogK_n$ with increasing n for Fe^{3+} than for Al^{3+}.

	$\log K_1$	$\log K_2$	$\log K_3$	$\text{Log } \beta_3$
Al^{3+}	17.2	12.9	(8.6)*	(39)
Fe^{3+}	19.2	12.9	(6.6)*	(39)

A suggestion is made that the bending of the metal ion out of the plane of the chelate ring , as proposed in figure 26 , may be more sterically demanding for the larger metal ions. With the smaller Al^{3+} (ionic radius 0.54 Å) coordinating in the plane of the CTA ligand steric crowding is reduced compared to the Fe^{3+} ion (ionic radius 0.65Å), where the chelate ring may be buckled. Selectivity for Al^{3+} over Fe^{3+} may be achieved with 1,8-dihydroxynaphthalene groups instead of catecholates in enterobactin analogues as investigated by Raymond et al 1984.

STRUCTURALLY REINFORCED LIGANDS AND METAL IONS.

The lack of rigidity in tetraazamacrocycles prevents the observation of a genuine size-match selectivity. The flexibility of the macrocycle that permits an out-of-plane coordination mode must be eliminated by the introduction of extra bridging between nitrogen donors on the macrocyclic ring if the size-match selectivity is to be observed (Wainwright 1980, Ramasubbu et al 1982, Hancock et al 1987 b and Hancock et al 1988). This makes the ligands more rigid and forces the metal ion to coordinate in the plane of the donor atoms.

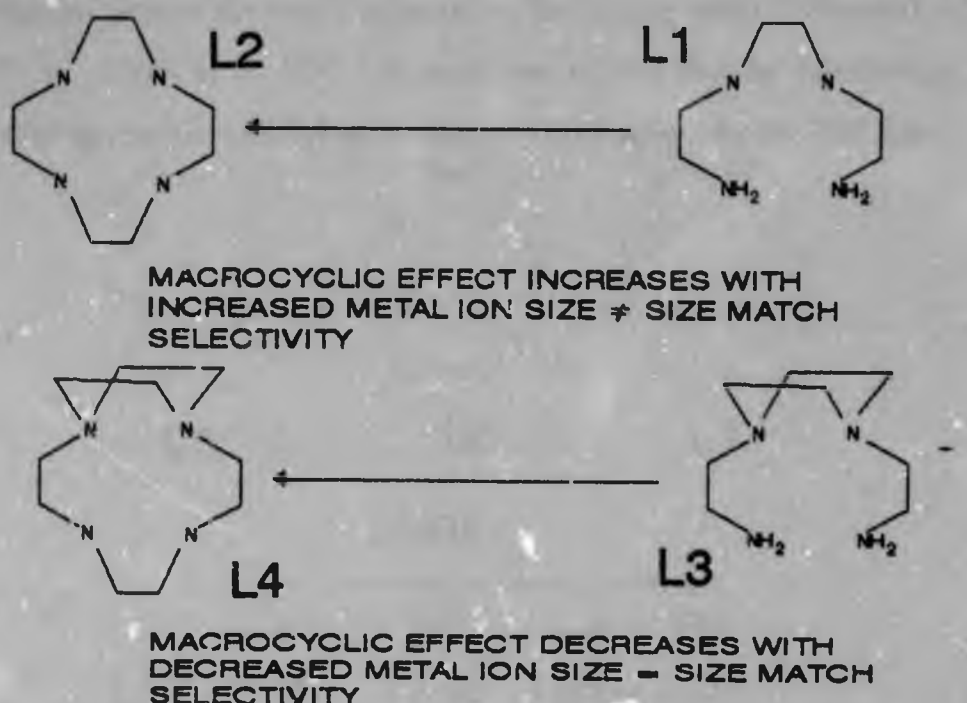
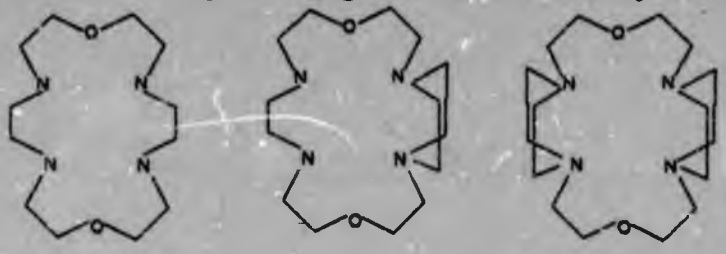


Figure 27 : increased rigidity causing selectivity behaviour to approximate genuine size-match selectivity (Hancock et al 1987)

In passing from L_2 to L_1 $logK_{mac}$ (thermodynamic manifestation of the macrocyclic effect) increases with increasing metal ion size, which is the direct opposite of that which is expected if size-match selectivity is observed. $LogK_{mac}$ however, is largest for small metal ions and decreases with increasing metal ion size when L_2 is compared to L_4. This behaviour is a closer approximation to genuine size-match selectivity (Hancock et al 1987b, 1988). The macrocycle L_5 complexes Cu^{2+} by adopting a folded conformation on complexation due to its relatively small size. No folding is necessary for the larger Cd^{2+} ion. As a result the copper complex of L_6 drops 13 log units in $logK_1$ while that for the cadmium experiences a drop of only 4 log units. The general drop in stability constants is assigned to the need for the double bridge to assume the boat conformation that is less stable (Hancock et al 1988). Wade et al 1990 has made use of this fact by introducing an increasing number of ethylene bridges to attain selectivity for Pb^{2+} ion.



L5 L6 L7

LOGK1

	Cu	Ni	Cd	Pb
L5	16.27	12.25	10.90	9.01
L6	7.04	<2	4.79	5.36
L7	—	—	—	4.73

Figure 28 : increasing rigidity of macrocycle by increasing number of ethylene bridges (Wade et al 1990)

The sharp decrease in $LogK_1$ data for L_3 is attributed to the fact there are two doubly-bridged ethylene units both of which must adopt the high energy boat conformers. Reinforcing tetraazamacrocycles results in bond stretching (Pattrick et al 1991). The reported Cu-N bond length of 2.09 Å is longer than either of the non-reinforced counterparts.

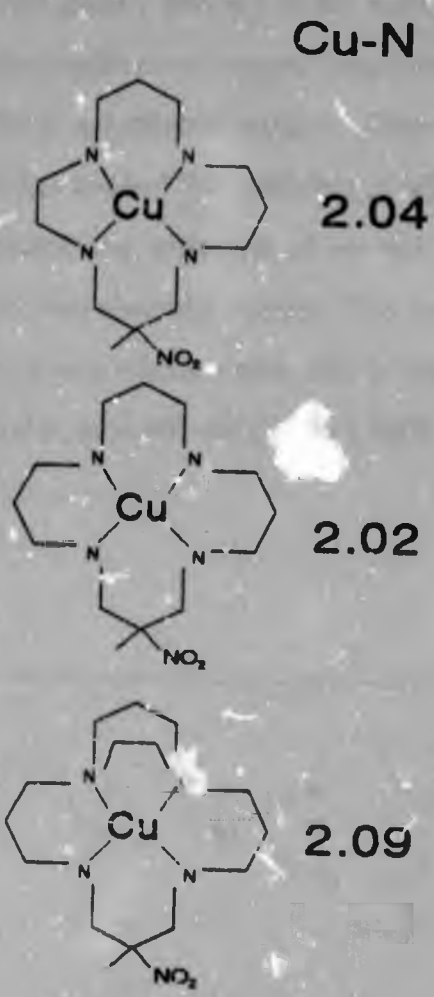


Figure 29 : bond stretching with reinforcement of tetraazamacrocycles (Pattrick et al 1991)

CHAPTER 3

OPEN CHAIN POLYAMINES

ADDITION OF PENDANT ARMS CONTAINING NEUTRAL OXYGEN DONORS TO ETHYLENEDIAMINE

The work of Hall and Dean (1960 a) on the study of DHEEN (N, N'- Bis-(2-hydroxyethyl)-ethylenediamine) copper complexes elucidated the nature of the chemistry behind substituted amines. Their spectrophotometric and conductometric studies showed the feasibility of ML and ML_2 complexes and furthermore postulated the existence of species arising from subsequent deprotonation of pendant alcoholic oxygens. The formation of ML_2 complexes was inhibited by increased substitution at the amine, and the tetrasubstituted derivatives produced strictly ML complexes (Hall & Dean 1960 b)

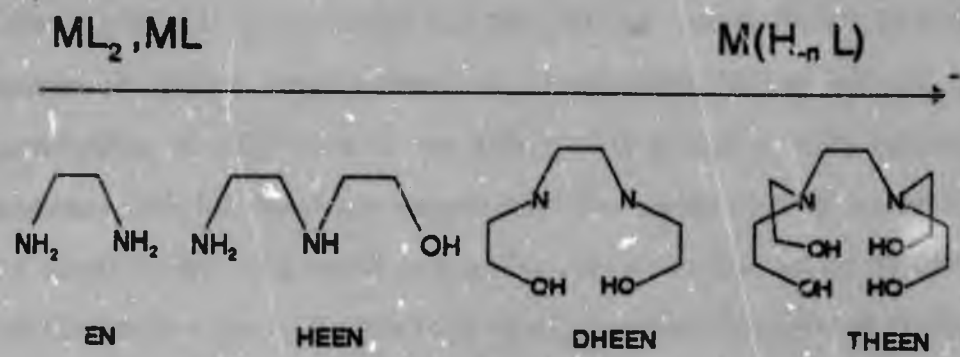


Figure 30 : Increased substitution of ethylenediamine and the postulated complexes that are present.

At the time this was viewed as evidence of the hydroxyl groups being involved in chelation forming a five membered ring. The data reported by Hall and Dean (1960 b) was obtained by solving the simultaneous equations of Bjerrum (1941) or calculated by the convergence method of Carlson et al (1945). A more detailed study of the tetrasubstituted amine THPED (N, N, N', N',-Tetrakis (2-hydroxypropyl) ethylenediamine) was done by Orama et al (1979) in which he showed that the main species formed were

$$ML^{2+},\ (MH_1L)^{+},\ (MH_2L)^{0}$$

with the metal ions Cu^{2+}, Zn^{2+}, Co^{2+}, and Pb^{2+}. The data by Orama was generated by postulating a feasible model and refining the data with a least squares computer program MINIQUAD75 (Gans et al 1976). A crystal structure of the copper complex of THPED showed that the ligand is hexadentate and consists of a dimer made up of two $(MH_1L)^{+}$ monomeric units held together by strong intermolecular hydrogen bonds (Orama & Orama 1979). It is noteworthy that the $(MH_1L)^{+}$ monomer has four five-membered chelate rings formed on complexation to the copper. The participation of only three of the hydroxyalkyl groups in each individual monomer with the metal may suggest a certain degree of steric crowding at the metal centre. This would substantiate the claim that as the degree of substitution increases so the feasibility of ML_n complexes becomes increasingly more unrealistic.

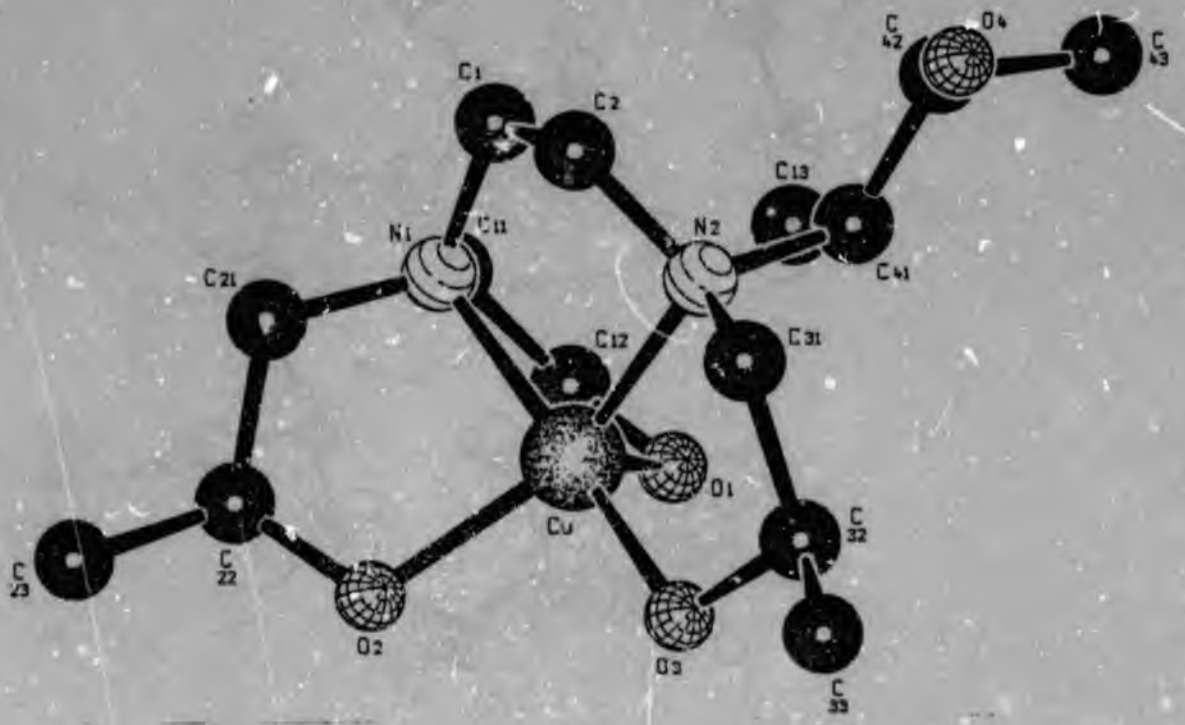


Figure 31 : Crystal structure of Copper complex of THPED (Orama & Orama 1979)

CRYSTAL STRUCTURE OF [Cu^{2+}(THEEN) $(ClO_4)_2$]

A crystal structure for the copper complex of THEEN also indicated a dimeric species comprising two $(MH_1L)^+$ monomers. There is however, no hydrogen bonding involved, but a formation of two M-O-M bridge that holds the two monomeric species together.

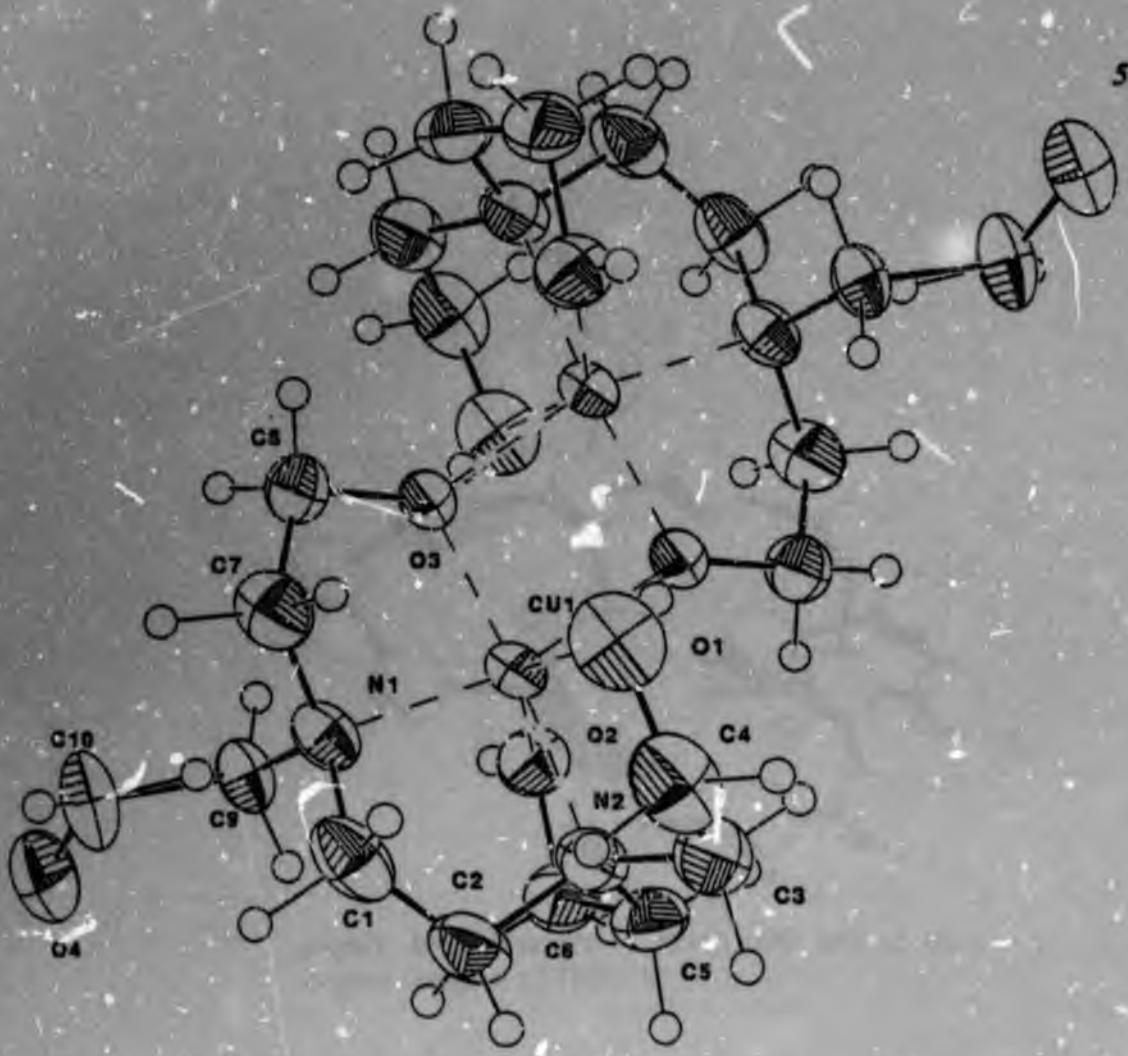


Figure 32 : Crystal structure of copper complex of THEEN (Hancock et al to be published)

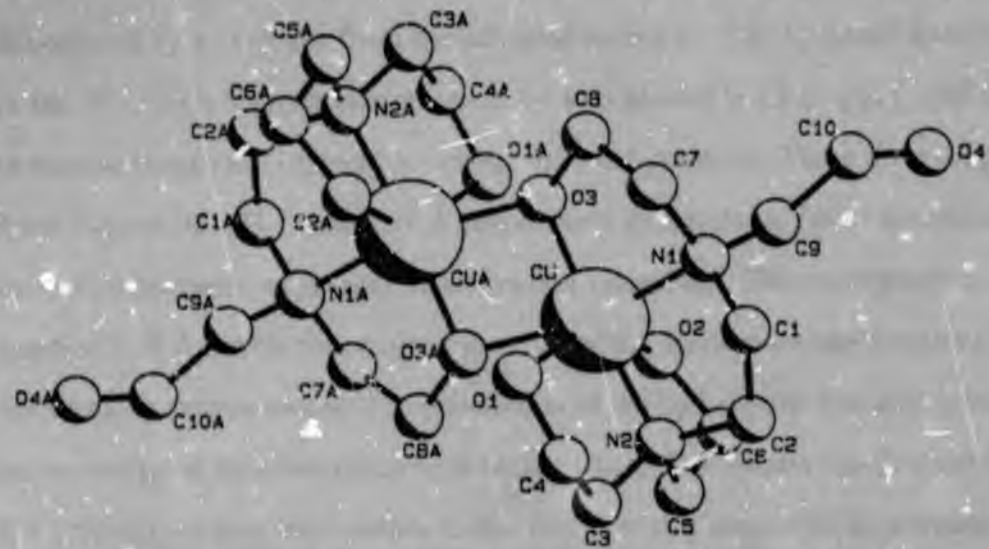


Figure 33 : Drawing of the coordination geometry around the two metal centres.

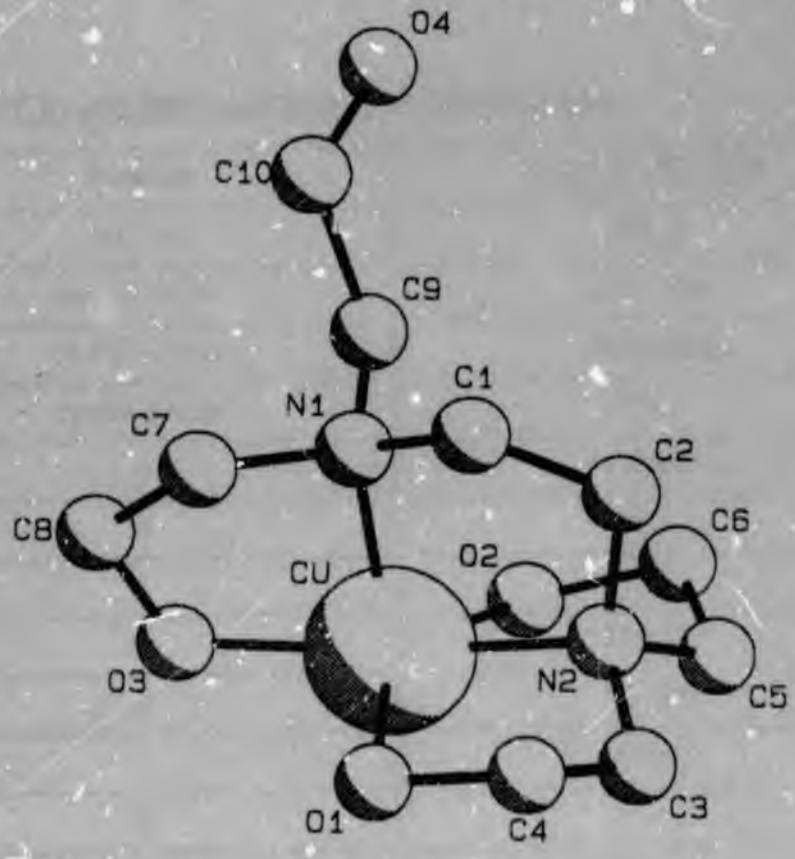


Figure 34 . Structure of monomeric unit of the copper complex of THEEN

The copper centre exhibits a distorted octahedron by coordination to 2 N-donors and 3 O-donors on one monomeric unit and the sixth coordination site is occupied by a O-donor from the adjacent monomer. The O-donor involved in the M-O-M bridges is characterised by a shortened bond length (1.93 Å) in comparison to the oxygens occupying the axial positions. These have longer bond lengths of 2.34 Å and 2.70 Å respectively due to Jahn Teller distortions as is characteristic of copper coordination chemistry. The excessively long bond of 2.70 Å can be rationalised in terms of the steric crowding imposed by the bridging oxygen atoms. The orientation of the hydroxyethyl moiety is such so as to suggest that coordination is taking place. The shorter Cu-O bond for the bridging oxygen, also points to the fact that this oxygen is deprotonated as was the case for THPED (Orama & Orama 1979).

TABLE OF CRYSTAL DATA AND STRUCTURE REFINEMENT

formula	$C_{10}H_{13}N_2O_8CLCu$
mol. wt	398.30
crystal colour	dark blue
crystal system	monoclinic
space group	$P2_{1/a}$
a	11.910(1)
b	8.102(1)
c	16.498(3)
α	90.03(1)
β	92.80(1)
γ	89.98(9)
z	4
V	1590.32
ρ	1.663 (calc)
	1.654 (measured)
abs. coeff	15.05
radiation	.71073
F(000)	820
scan mode	ω -2θ
scan speed	0.60-5.49
ω -scan angle	0.60+0.35tanθ
theta range	$11<\theta<20$
range h,k,l	30,10,21
crystal dimensions	0.38×0.31×0.43
reflections measured	3855
unique reflections	3247
used reflections	2768
parameters refined	216
final R	0.0486

TABLE OF ATOMIC COORDINATES [$\times 10^4$] AND EQUIVALENT ISOTROPIC DISPLACEMENT PARAMETERS [$(Å)^2 \times 10^3$]

	x	y	z	Ueq
Cu1	3882	732	83	34
N1	3567	2576	859	43
C1	2757	3684	397	55
C2	1889	2665	-66	59
N2	2402	1238	-526	48
C3	2574	1765	-1395	58
C4	3383	3175	-1488	68
O1	4438	2887	-1082	67
C5	1656	-183	-549	57
C6	1626	-1063	255	58
O2	2760	-1431	515	50
C7	4699	3321	968	55
C8	5552	2004	1168	56
O3	5308	572	690	38
C9	3094	1981	1614	44
C10	3050	3187	2326	61
O4	2260	2562	2884	68

TABLE OF BOND LENGTHS [Å] AND ANGLES [°]

N1-CU	2.016(4)	N2-CU-N1	88.0(2)
O1-CU	2.703(5)	O1-CU-N1	91.8(2)
O2-CU	2.338(4)	O1-CU-N2	75.1(2)
O3-CU	1.933(3)	O2-CU-N1	103.6(2)
C1-N1	1.498(7)	O2-CU-N2	79.7(2)
C7-N1	1.480(6)	O3-CU-N1	84.7(1)
C9-N1	1.491(6)	O3-CU-N2	171.0(2)
C2-C1	1.502(8)	O3-CU-O1	99.9(1)
N2-C2	1.497(7)	O3-CU-O2	107.0(1)
CU-N2	2.037(4)	C7-N1-C1	112.1(4)
C3-N2	1.507(6)	C9-N1-C1	112.3(4)
C5-N2	1.486(7)	C9-N1-C7	115.2(4)
C4-C3	1.508(9)	C2-C1-N1	109.8(4)
O1-C4	1.413(8)	N2-C2-C1	112.4(4)
C6-C5	1.507(8)	C3-N2-C2	111.7(4)
O2-C6	1.428(6)	C5-N2-C2	110.7(4)
C7-C8	1.499(7)	C5-N2-C3	107.0(4)
O3-C8	1.424(6)	C4-C3-N2	114.2(5)
C10-C9	1.564(7)	O1-C4-C3	112.6(5)
O4-C10	1.440(7)	C4-O1-CU	101.5(4)
		C6-C5-N2	113.5(4)
		O2-C6-C5	107.4(4)
		C6-O2-CU	107.4(3)
		C8-C7-N1	109.8(4)
		O3-C8-C7	109.9(4)
		C8-O3-CU	112.4(3)
		C10-C9-N1	114.8(4)
		O4-C10-C9	107.2(4)
		O2-CU-O1	149.9(1)

TABLE OF ANISOTROPIC DISPLACEMENT PARAMETERS

	u11	u22	u33	u23	u13	u12
Cu	33(3)	35(4)	39(2)	-1(7)	8(4)	0(2)
N1	49(2)	33(2)	50(4)	-0.0(8)	13(2)	0(5)
C1	77(1)	42(3)	57(4)	0(8)	20(0)	23(8)
C2	59(5)	53(3)	53(3)	0(8)	0(8)	30(3)
N2	43(6)	58(1)	42(8)	0(5)	0(7)	10(8)
C3	63(3)	84(5)	40(6)	12(5)	0(4)	16(3)
C4	92(7)	63(4)	56(0)	20(2)	18(8)	17(7)
O1	85(9)	50(5)	77(2)	10(3)	17(3)	0(3)
C5	35(5)	82(0)	55(6)	0(1)	0(1)	0(2)
C6	42(8)	76(7)	59(1)	0(0)	10(5)	-15(0)
O2	48(7)	62(2)	46(8)	10(1)	0(7)	-10(1)
C7	57(1)	37(7)	78(0)	-10(1)	0(8)	0(8)
C8	47(3)	53(5)	63(8)	63(8)	0(2)	0(6)
O3	37(4)	42(9)	39(8)	39(8)	0(5)	0(1)

TABLE OF HYDRC GEN COORDINATES AND ISOTROPIC DISPLACEMENT PARAMETERS

H	Xa	Yb	Zc	Ueq
1	2347	4480	816	71.7
2	3208	4425	-23	
3	1424	3454	-490	
4	1323	2147	358	
5	2892	702	-1705	
6	1770	2118	-1675	
7	3023	4278	-1242	
8	3508	3351	-2127	
9	813	208	-727	
10	1951	-1037	-993	
11	1148	-2191	185	
12	1247	-280	695	
13	4908	3932	413	
14	4704	4209	1456	
15	5528	1691	1804	
16	6379	2453	1043	
17	2250	1489	1466	
18	3610	893	1823	
19	3137	4494	2219	
20	3241	2514	1784	
21	4573	2112	-1169	
22	2721	-1743	882	
23	3191	2567	2996	

Martell et al (1959) alluded to the fact that these species can form dimers in solution over a certain pH range. This ability of aminoalcohols to form oxygen-bridged species was comprehensively documented by Bertrand and Eller (1975). the more acidic nature of aminoalcohols allow the subsequent coordinated aminoalkoxides to form additional bonds that may involve metal ions, as was the case for THEEN, or hydrogens of another coordinated alcohol group, as was the case for THPED.

In comparing the thermodynamic data for THPED and THEEN (Martell & Smith 1974-1989) a marked increase in stability of the THPED complexes is observed (Hall & Dean 1960 b).

TABLE 1 : Formation constants for complexes of THEEN, THPED and HETHPED (Hall & Dean 1960 b , Martell & Smith 1974-1989)

Metal	THEEN $\log K_1$	THPED $\log K_1$	HETHPED $\log K_1$
Co	5.4	6.33	5.96
Ni	6.5	7.65	7.25
Cu	8.49	9.75	9.36
Zn	4.74	6.09	5.67
Cd	7.04	7.80	7.73

Increasing the number of hydroxypropyl groups over hydroxyethyl groups results in an increased stability. Inductive effects of the additional electron releasing CH_3 groups makes the O-donor a better nucleophile and therefore more attractive to an electron poor metal.

Thom et al (1986) depicted an interesting relationship on the effect of adding oxygen donors in bridging units to ethylenediamine. the smaller metal ions, Cu^{2+}, and Zn^{2+}, show decreases in complex stability with an increasing number of O-donors, while the larger metal ions, Pb^{2+}, and Cd^{2+}, enjoy enhanced complex stability. A similar relationship is observed for an increased number of ethereal oxygen donors in bridging groups between two carboxylate groups for ligands such as oxalate (n=1) to TTDA (n=4) (triethylenetetraxoxydiacetate).

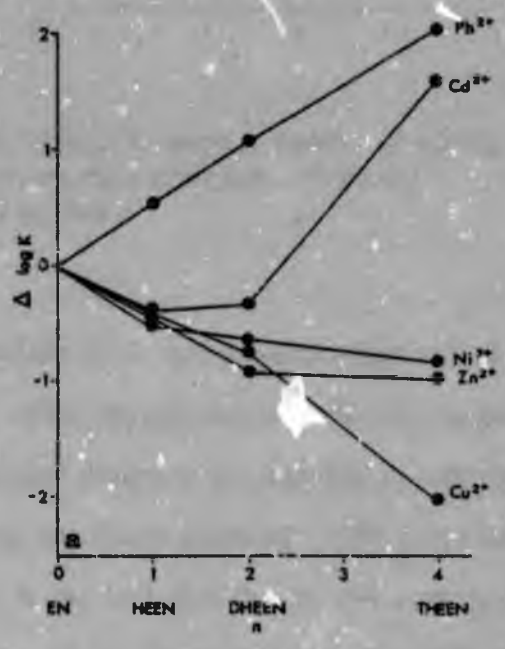


Figure 35 : Effect on complex stability of added hydroxyethyl groups
(Thom et al 1986)

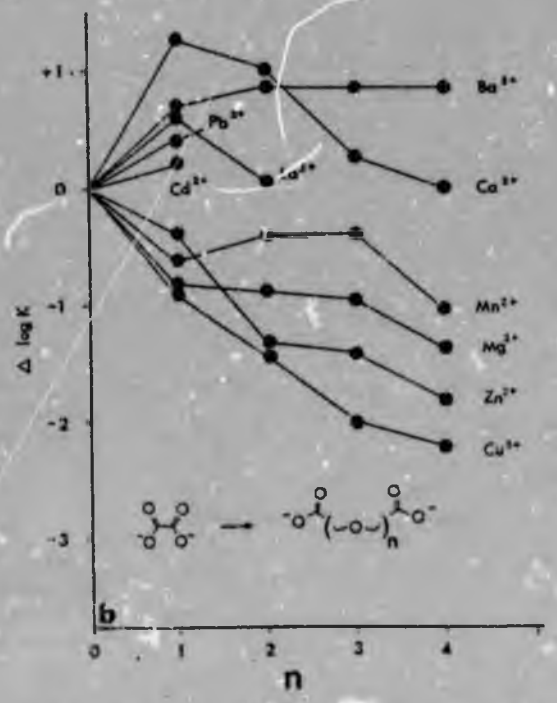


Figure 36 : Effect on complex stability of adding ethereal groups between the carboxylates of oxalate (Thom et al 1986)

Hancock (1986) initially attributed this size selectivity of the neutral oxygen donor as a property of the oxygen donor itself, and suggested that this is an additional rule for ligand design to be regarded in conjunction with the rule regarding chelate ring size. Later Hancock (1990) concluded that the effect relates more closely to the fact that the neutral oxygen donor is invariably coordinated as part of a five-membered chelate ring. The ligands triethanolamine and HPDE (bis (2-hydroxypropyl)ethanolamine) both have an equal number of oxygen donors that can only form five and six-membered rings respectively.

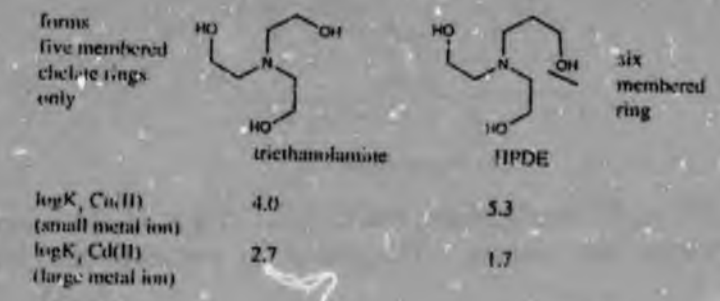


Figure 37 : Thermodynamic data for the Cu^{2+} and Cd^{2+} complexes of triethonolamine and HPDE

This is well illustrated by the change in complex stability, ΔLogK, plotted against metal ion ionic radius when altering EN to THEEN and oxalate to DETODA. The point is further reinforced by virtue of the fact that addition of ethereal donors to EN to give mixed donor macrocycles (18-ane N_2O_4) or cryptands (cryptand-2,2,2) does not alter the response in $LogK_1$. Large metal ions experience an appropriate increase in stability while the $logK_1$ for the small metal ion decreases.

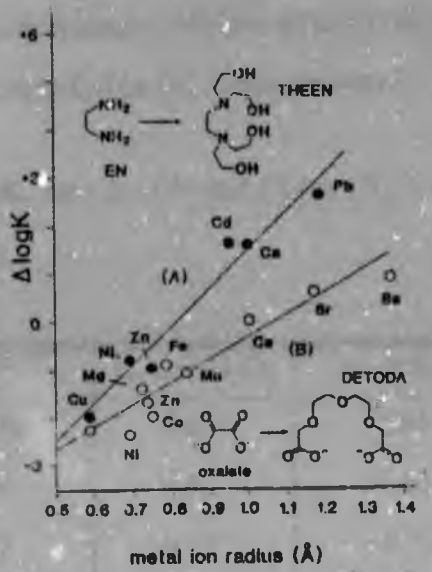


Figure 38 : change in $LogK_1$ when passing from EN to THEEN with the addition of hydroxyethyl groups and oxalate to DETCDA

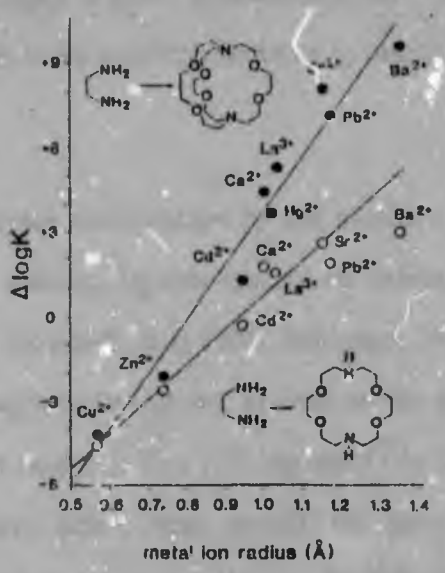


Figure 39 : change in $LogK_1$ when passing from EN to 18-ane-N_2O_4 and 2,2,2 cryptand by the addition of ethereal oxygens

In as much as THEEN and cryptand-2,2,2 can be regarded as being derivatives of EN brought about by subsequent additions of alcoholic or ethereal oxygens, so 12-ane-N_2O_2 can be regarded in the same manner.

TABLE 2 : Change in $LogK_1$ data for EN and 12-ane-N_2O_2 relating to metal ion size (Thom et al 1986).

Metal ion	EN	12-ane-N_2O_2	$\Delta LogK_1$ [c]	r^+
Cu	10.50	8.66[a]	-1.84	0.62
Ni	7.31	5.91[b]	-1.40	0.70
Zn	5.7	6.22[b]	+0.52	0.74
Cd	5.4	6.55[b]	+1.15	0.95
Pb	5.04	6.34[a]	+1.30	1.18

[a]data for 1,4-isomer [b]data for 1,7-isomer

[c] $\Delta LogK = LogK_1$ (12-ane-N_2O_2)-$LogK_1$ (EN)

As for the DHEEN analogue a good relationship for $\Delta LogK$ versus ionic radius is observed. $\Delta LogK$ increases with increasing metal ion size from EN to 12-ane-N_2O_2.

The phenomenon of complex stabilisation by the addition of groups having neutral oxygen donors to existing ligands cannot be rationalised in terms of the chelate effect alone (Hancock et al 1976, Adamson 1954), and requires consideration of the strength of the donor as well as the steric strain that is associated with complex formation. The 1.74 log units (ln 55.5) of additional stability from the chelate effect that would be associated with each hydroxyalkyl group should not be observed since by Adamson's definition of the standard reference state there would be 55.5 times as much water as any

other ligand in aqueous solution. Gas phase studies discussed in an earlier chapter show the order of basicity as $H_2O < ROH < R_2O$ towards protons and metal ions (Hancock et al 1983, Woodin et al 1978, Davidson et al 1976, Jones et al 1976).The order of basicity however implies an increase in stability for all metal ions. Small metal ions do not show an increase in complex stability. Complexes of small metal ions, having a more covalent nature suffer from increased steric strain at the metal centre. The stability that would be gained by replacing the water with the greater donor strength of a hydroxyalkyl chelating group is surpassed by the greater steric strain due to the distortion of the coordination polyhedron. This is not the case for the larger ionically bound metal ions. The trend observed can be summarised in the following scheme :

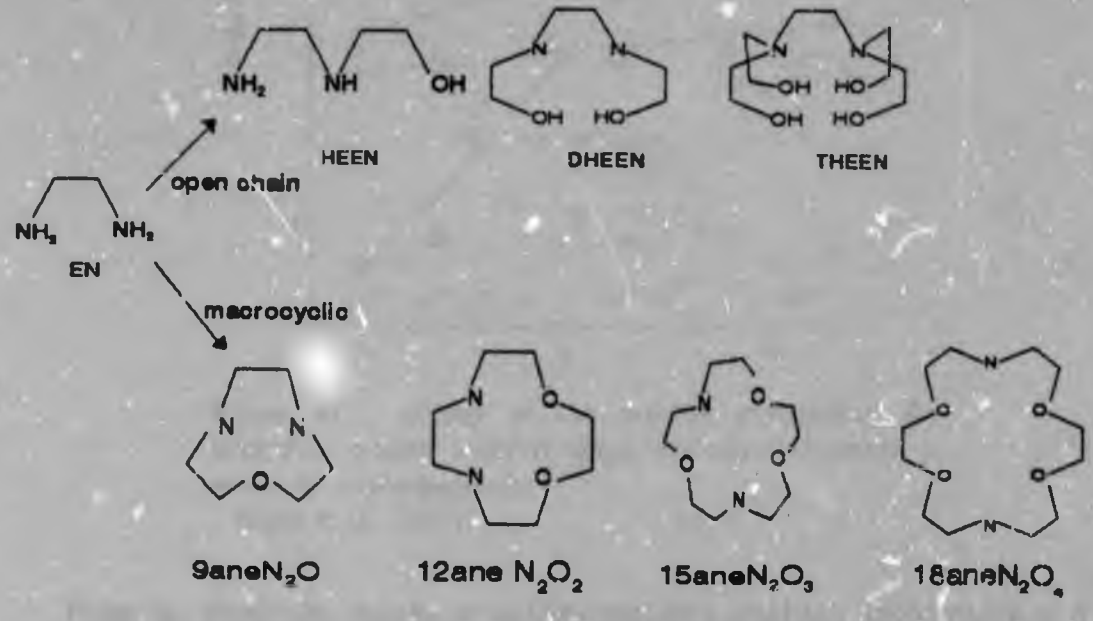


Figure 40 : Scheme showing the increase in number of oxygen donors corresponding to the increase in stability observed for the large metal ions

ADDITION OF PENDANT ARMS CONTAINING NEUTRAL OXYGEN DONORS TO DIEN

The addition of the neutral oxygen donor can be expressed in the simplest possible way when passing from EN to HEEN.

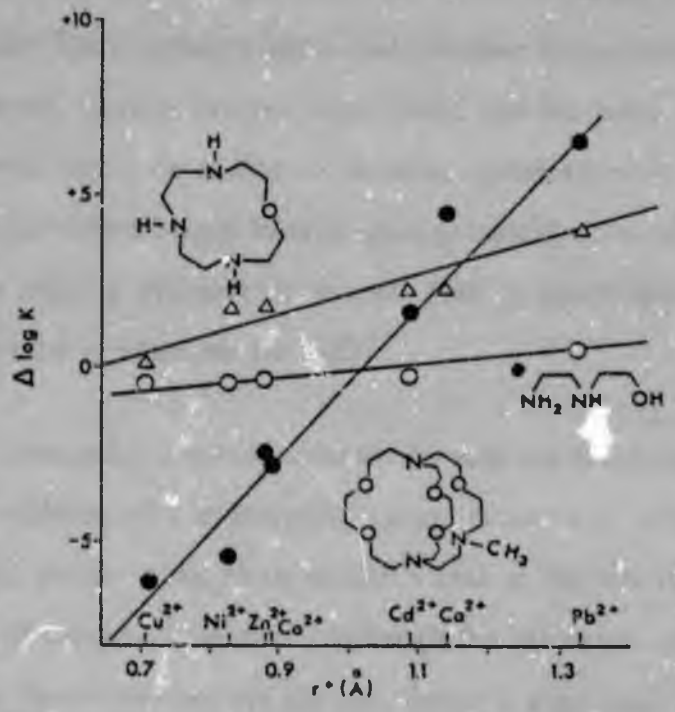


Figure 41 : change in the stability influencing the selectivity pattern when a single hydroxyalkyl group is added to ethylenediamine
(Wade et al 1987)

From the figure the change in stability resulting form the introductio.. of a single hydroxyethyl group is rather small as indicated by the flat slope of the relationship ΔLogK a function of ionic radius. The degree of flatness relates

to the fact that the addition of a single hydroxyethyl group to an amine is the least sterically demanding manner by which a neutral oxygen donor may be introduced (Wade et al 1987). The observation that large metal ions , unlike small metal ions , respond to added neutral oxygen donors with increased stability is brought to light by the crystal structure of $[Ni(HEEN)_2]$ (NO_3) by Wade et al (1987). The longer Ni-O bond length of 2.15 Å compared to 2.10 Å and 2.06 Å of $[Ni(EN)_2)$ $(H_2O)_2]^{2+}$ (Minacheva et al 1974) and $[Ni(H_2O)_6]^{2+}$ (Bigoli et al 1971) suggests steric problems are contributing to the decreased stabilisation of small metal ions. Molecular mechanics by Wade et al (1987) showed the origin of the Ni-O bond stretching to be accounted for by van der Waals repulsive interactions between hydrogens on the adjacent carbons on the ethylene bridges. Small metal ions are more affected by the induced steric strain on adding an alcoholic group which is less for larger metal ions that inturn benefit from the greater basicity of the alcoholic oxygen relative to water (Hancock & Martell 1988). McDougall et al (1978) reported similar interactions for DIEN.

The same relationship is not observed for the addition of an aminoethyl group as for the addition of a hydroxyethyl group. Hancock et al (1979) showed evidence for greater steric strain in DIEN than in the EN ring in terms of enthalpies of complex formation. Although the tabulated enthalpies imply comparable strain energies the nitrogen donor is a stronger donor than its oxygen counterpart, and its ability to bind much more strongly overcomes the unfavourable steric strain induced by adding the aminoethyl group.

TABLE 3 : Complex formation enthalpies of ethylenediamine and diethylenetriamine with Ni^{2+} (Hancock et al 1979).

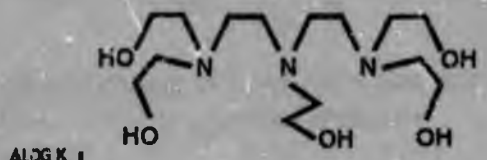
COMPLEX	LIGAND	ΔH kJ mol^{-1}
$[Ni(EN)_3]^{2+}$	EN	-117.2
$[Ni(DIEN)_2]^{2+}$	DIEN	-105.9

Alcoholic and ethereal oxygens are slightly better bases than the water with which they compete for coordination sites, while nitrogen donor are very much better donors than the water for most metal ions. Steric effects predominate over bond strength effects for O-donors, but for N-donors the larger free energy of M-N bond formation predominates over the steric effects.

The DIEN unit is itself a potential building block for more complex molecules by exploiting the primary and secondary amine moieties in its backbone. In much the same manner addition of hydroxyethyl groups to Dien producing PHEDIEN, results in a trend that is a replica of that observed for the EN study. The response of the change in $LogK_1$ is not as flat as for the EN analogue due to the complexity of the ligand. The greater the number of neutral oxygen donors that are added to an amine the more the complex stability of the large metal ions is favoured.

TABLE 4 : Stability constant data for DIEN, PHEDIEN

metal ion	Dien	Phedien	ΔlogK
pKa1	9.84	8.11	
pKa2	9.02	6.88	
pKa3	4.23	1.87	
Zn	8.8	12.03	+3.23
Pb	7.5	7.46	-0.04
Cd	8.05	12.65	-1.46
Cu	15.9	11.08	-4.82



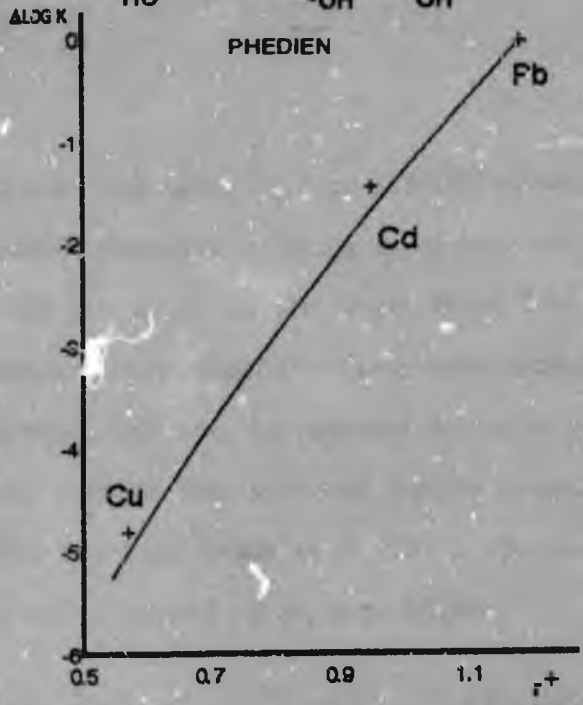


Figure 42 : plot of the change in LogK, as a function of metal ionic radius in passing from DIEN to PHEDIEN.

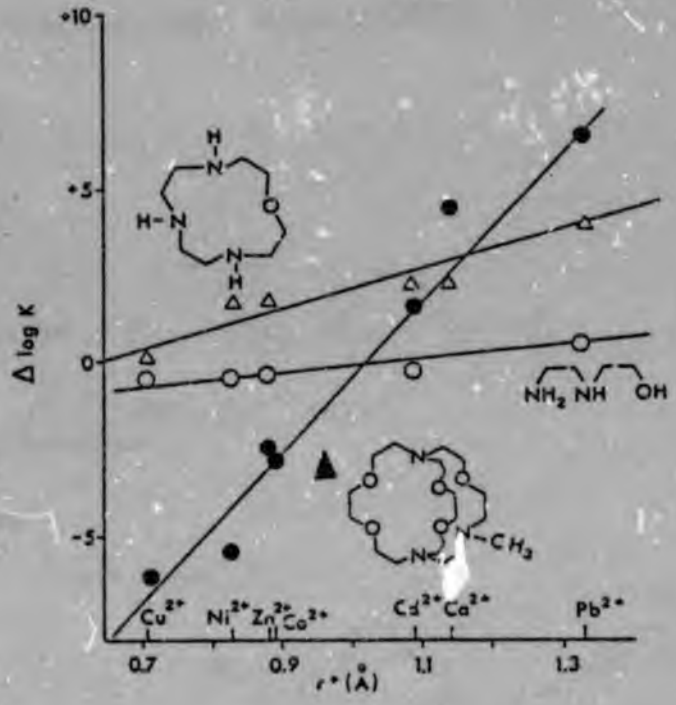


***Figure 43** : plot of change in $LogK_1$ as a function of metal ion radius in passing from DIEN to cryptand derivative*
(Wade et al 1987)

With addition of five hydroxyethyl groups to DIEN as compared to four in THEEN the steric implications for small metal ions are that much more highlighted as will the ability of the larger metal ions, with increased coordination numbers , to accommodate the greater number of donors. The relationship between DIEN and the cryptand derivative produces an even steeper slope and suggests that structural rigidity is another criteria for enhanced complex stability (Wade et al 1987). The order of enhanced complex stability with structural rigidity is as follows :

OPEN-CHAIN < MACROCYCLIC < MACROBICYCLIC

A similar scheme to that for EN derivatives can be set up as regards the addition of neutral oxygen donors to DIEN :

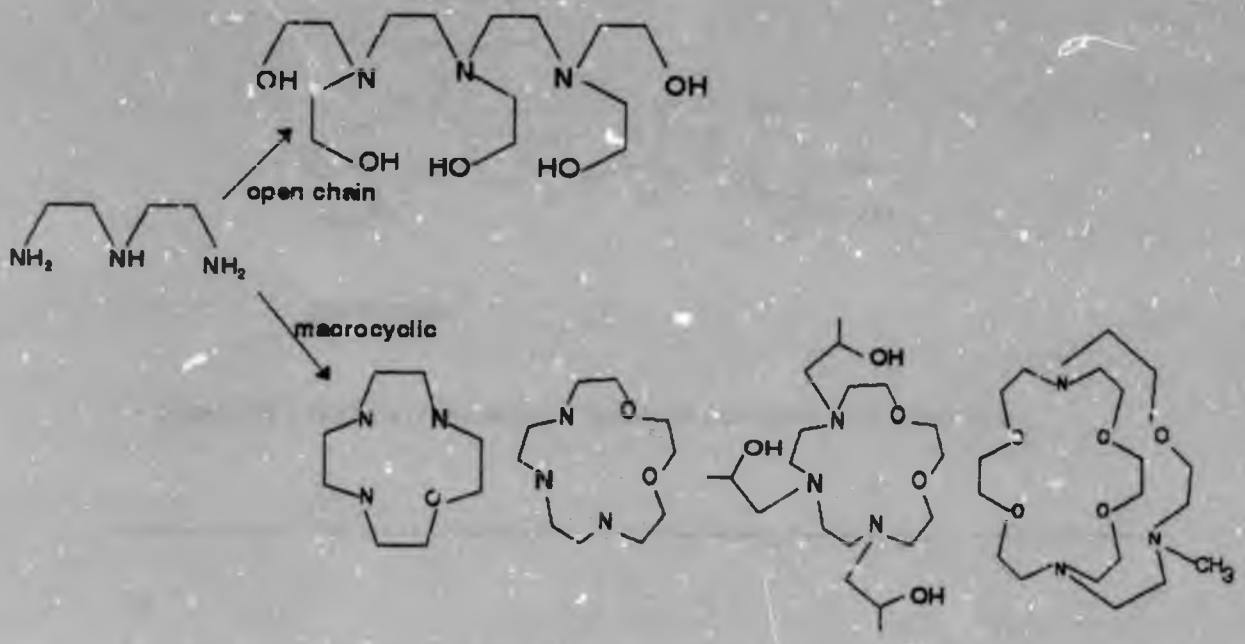
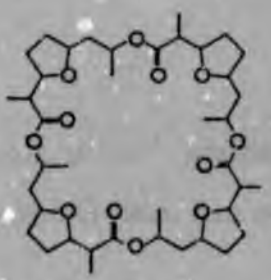
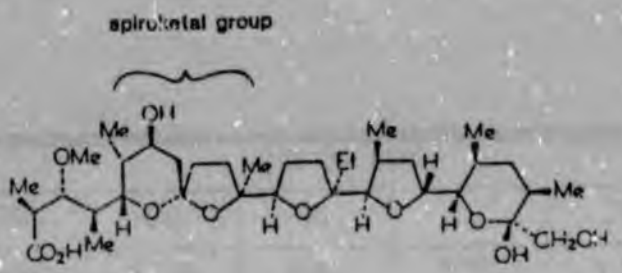


Figure 44 : Scheme for increasing number of oxygen donors addea to DIEN

This pattern of stabilisation (Hancock et al 1984) also manifests itself with other oxygen donor groups such as the tetrahydrofuran group (Hancock et al 1986, Wade et al 1987 & Tsukube 1984). The tetrahydrofuran group is of great significance (Westley 1977) because it is the moiety involved in naturally-occurring, metal-ion-binding antibiotics Nonactin and Monensin.



NONACTIN



monensin

Figure 45 : Naturally occurring antibiotics Nonactin and Monensin

---

INCREASING THE RIGIDITY OF THE OPEN-CHAIN LIGANDS

It seems from the studies of Hancock et al (1989) and Thom et al (1986) that addition of alcoholic or ethereal donors to amine ligands leads to changes in complex stability that are mainly controlled by the size of the metal ion. The predominant effect is that large metal ions show a more favourable change in complex stability than do the small metal ions when a neutral oxygen donor is added, and this effect is independent of whether the oxygen donor is part of a macrocyclic ring or of a pendant group attached to a parent amine to form a non-cyclic structure; i.e. the donor can either be ethereal or acoholic in nature. Not forgetting that alcoholic oxygens show a preference for

covalently bound metals such as Cu^{2+}, whereas the ethereal oxygen better accommodates the ionically bound metal ions such as Pb^{2+} (Thom et al 1986).

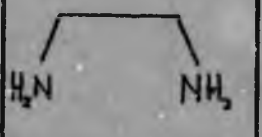
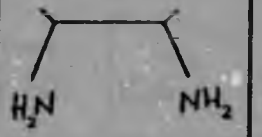
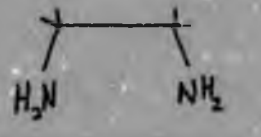
TABLE 5 : Thermodynamic data for HEEN and ODEN indicating the preference of ethereal oxygens for the ionically bound metal ions (Thom et al 1986).

	METAL ION				
PARAMETER	Cu	Ni	Cd	Zn	Pb
$LogK_1$ (HEEN)	10.09	6.82	5.28	5.28	5.58
$LogK_1$ (ODEN)	8.70	5.62	5.27	5.74	6.10
ΔLogK	-1.39	-1.20	-0.01	+0.46	+0.52

HEEN vs ODEN decreases : $Cu^{2+} > Ni^{2+} > Cd^{2+} > Zn^{2+} > Pb^{2+}$

The macrocyclic ring may serve to sharpen size selectivity, but this effect is not always easily distinguished in some structures due to the presence of macrocyclic cavities of intermediate size. From a synthetic point of view it is easier to introduce oxygen donors as pendant groups in a non-cyclic structure. The tailoring of metal ion selectivity may therefore be achieved in a more effective and facile manner by introduction of pendant moieties rather than using macrocyclic structures. The non-cyclic structure can be further tailored to manipulate metal selectivities. C-alkylation of ethylene bridges will impart greater rigidity to the structures. Inductive effects enhance the complex stabilities of metal ions by increasing the electron density on amine nitrogens allowing for better M-L bond formation due to increased overlap.

TABLE 5 : Thermodynamic stability constants of C-alkylated diamines (data from Martell & Smith 1974-1989)

PARAMETERS			
$\log\beta_2$ (Ni^{2+})	13.54	13.50	14.56
$\log\beta_2$ (Cu^{2+})	19.6	20.16	21.87

INCREASE IN INDUCTIVE EFFECTS →

ETHYLENEDIAMINE < DL-2,3-BUTYLENEDIAMINE < 1,1,2,2,-TETRAMETHYLETHYLENEDIAMINE

With N-alkylation the inductive effects of the additional electron releasing groups is overshadowed by the steric hinderance that they cause due to their crowding effect around the nitrogen donor. Looking at the data for EN and its derivatives with subsequent N-alkylation it is apparent that complex stability decreases with increased N-alkylation.

TABLE 7 : Thermodynamic stability constants of N-alkylated diamines (data from Martell & Smith 1974-1989)

PARAMETERS	H_2N NH_2	$MeNH$ NH_2	MeN NMe	Me_2N NMe_2
$\log K_1$ (Cu^{2+})	7.35	7.17	6.89	3.57
$\log K_1$ (Ni^{2+})	10.71	10.33	10.02	7.20

A feasible approach for enhanced metal selectivity appears to be the involvement of non-cyclic structures to which neutral oxygen donors have been added via pendant moeities; reinforced with C-alkylated bridges so as to exploit the subsequent inductive effects. It seems therefore that the introduction of cyclohexylene groups as bridging groups in place of ethylene bridges connecting two nitrogen donors will lead to substantial increases in complex stability. Schwarzenbach et al (1954) showed this to be true in their studies of *trans*-CDTA when compared to EDTA.

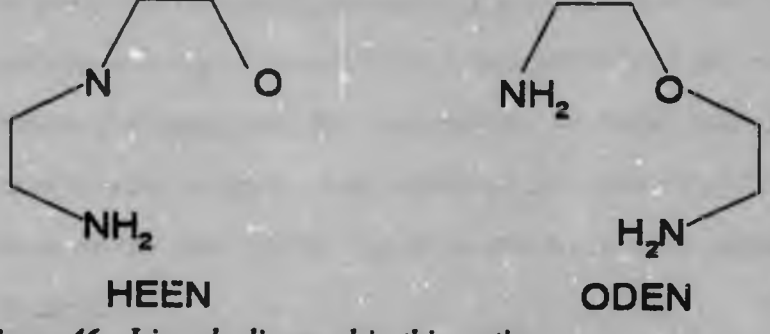


Figure 46 : Ligands discussed in this section

TABLE 8 : Formation constants for EN, EDTA, and *trans*-CDTA for comparison (de Sousa et al 1991)

Lewis acid	ionic radius	EN	EDTA	*trans*-CDTA
H^+		9.89	10.17	12.3
		7.08	6.11	6.12
Zn	0.74	5.7	16.44	19.35
Cu	0.75	10.54	18.70	21.92
Cd	0.95	5.45	16.36	19.84
Pb	1.18	5.04	17.88	20.24

Hancock & Martell (1988) interpreted the data for EDTA and trans-CDTA by using the concept of preorganisation (Cram et al 1985) in which the rigid cyclohexane ring of trans-CDTA is thought to hold the two nitrogens in the required arrangement for coordination to metal ions. It is thought that considerable energy must be expended in transforming the low-energy skew form of the free EDTA ligand to the trans form necessary for complex formation.

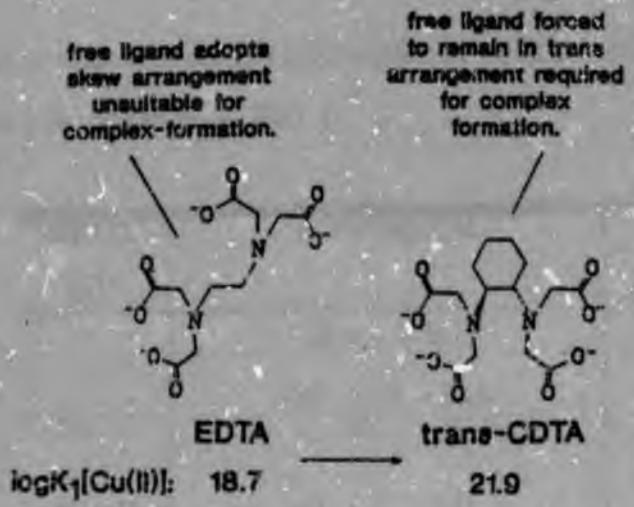


Figure 47 : skew and trans forms of EDTA and CDTA respectively (de Sousa et al 1991)

Introduction ot cyclohexylene groups as bridging groups should produce ligands of increased complex stability, and by analogy with CDTA, using trans-1,2-diaminocyclohexane instead of EN as the diamine to which two hydroxyethyl groups are added would give a more powerfully coordinating ligand than THEEN.

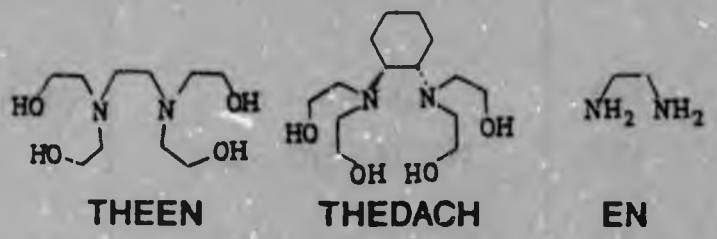


Figure 48 : Ligands THEEN, THEDACH and EN discussed from the tabulated data

TABLE 9 : Constants for complex formation of THEDACH with a selection of metal ions (de Sousa et al 1991)

METAL ION	EQUILIBRIUM	logK
	$H + L \rightleftharpoons HL$	10.06
	$HL + H \rightleftharpoons H_2L$	1.55
Cu(II)	$M + L \rightleftharpoons ML$	9.52
	$ML + OH \rightleftharpoons MLOH$	7.43
	$MLOH + OH \rightleftharpoons ML(OH)_2$	5.10
Zn(II)	$M + L \rightleftharpoons ML$	5.95
	$ML + OH \rightleftharpoons MLOH$	5.40
	$MLOH + OH \rightleftharpoons ML(OH)_2$	5.11
	$ML(OH)_2 + OH \rightleftharpoons ML(OH)_3$	2.96
Cd(II)	$M + L \rightleftharpoons ML$	7.61
	$ML + L \rightleftharpoons ML_2$	2.68
	$ML + OH \rightleftharpoons MLOH$	3.25
	$3M + 2L \rightleftharpoons M_3L_2$	22.06
Pb(II)	$M + L \rightleftharpoons ML$	6.49
	$ML + OH \rightleftharpoons MLOH$	5.55
Th(IV)	$M + L + OH \rightleftharpoons MLOH$	19.36
	$MLOH + OH \rightleftharpoons ML(OH)_2$	9.46

TABLE 10 : Formation constants for THEDACH, with literature values for THEEN, EN, EDTA, and *trans*-CDTA for comparison (de Sousa et al 1991)

		Log K				
Lewis acid	ionic radius	THEDACH	THEEN	EN	EDTA	*trans*-CDTA
H^+		10.06	8.38	9.89	10.17	12.3
		1.55	4.37	7.08	6.11	6.12
Zn	0.74	5.95	4.74	5.7	16.44	19.35
Cu	0.75	9.52	8.49	10.54	18.70	21.92
Cd	0.95	7.61	7.04	5.45	16.36	19.84
Pb	1.18	6.49	7.6	5.04	17.88	20.24

The tabulated comparison reflects the increases of $\log K_1$ in going from EDTA to trans-CDTA to be larger than those observed in going from THEEN to THEDACH. This partly relates to the presence of charged acetate groups on EDTA that stabilise the skew relative to the Trans conformer by electrostatic repulsion. In trans-CDTA the cyclohexylene bridge holds the ligand in the trans configuration and the electrostatic contribution stabilising the skew conformer is overcome. In THEEN and THEDACH the hydroxyethyl groups do not repel each other electrostatically and the effect on complex stability of stabilising the trans conformer is not as pronounced.

Schwarzenbach et al (1954) observed that the effect of the cyclohexylene bridge on the stability of trans-CDTA relative to EDTA complexes appeared to depend on the size of the metal ion.

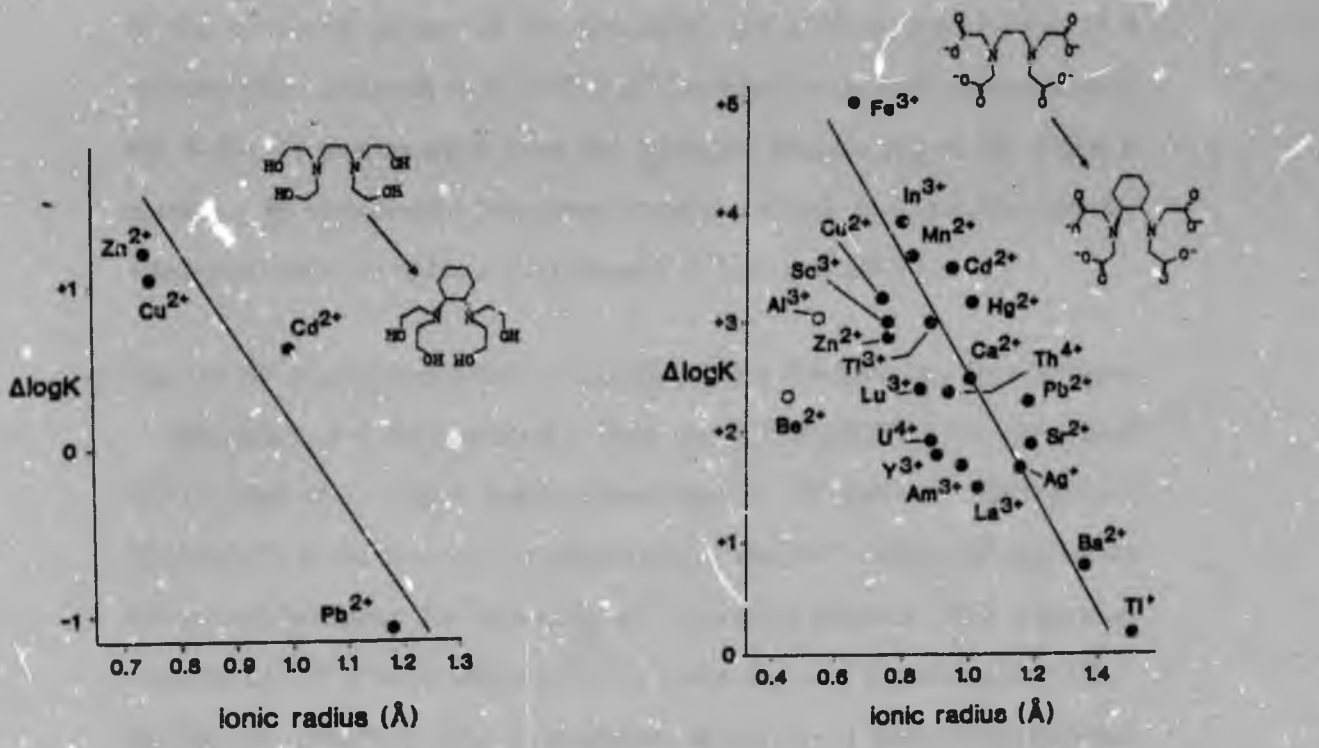


***Figure 49** : change in stability constant $LogK_1$ versus metal ionic radius (de Sousa et al 1991)*

The smallest metal ions show the strongest increase in $logK_1$ when changing the bridging ethylene groups to cyclohexylene bridges. This result seems to be contradicting the view (Hancock 1990, Hancock 1989, Hancock & Martell 1989) that five-membered chelate rings promote complex stability for large metal ions relative to small metal ions. The geometry arguements for five and six membered chelate rigs discussed in an earlier section illustrate how five

membered chelate rings focus the lone pairs of the donor atoms some distance away in the minimum strain arrangement, minimum steric strain can therefore only be achieved with coordination to large metal ions. Fusing a cyclohexane group to the bridge of the chelate ring should logically sharpen this effect due to the increased rigidity of the five-membered chelate ring. Fusion to a cyclohexylene ring such as in THEDACH makes it more difficult to decrease the N-C-C-N torsion angle from the minimum strain-value of 60° which is necessary to accomodate complexes of smaller metal ions as is the case for ethylenediamine complexes (McDougall & Hancock 1980).

High levels of preorganisation in ligands is often characterised by slow rates of metalation and demetalation (Hancock & Martell 1989) as for trans-CDTA and other highly preorganised ligands. Of particular interest for THEDACH is the slow rate of complexation with Ni^{2+} which will require an out-of-cell technique for measuring the formation constant. The formation constant of THEDACH with Th(IV) indicates that only deprotonated MH_1L species are observed. The coordination chemistry of perhydroxyalkylated polyamines is characterised by the existence of such species, and these ligands are capable of stabilising metal ions such as Fe(III) or Pu(IV) in solution up to pH values as high as 13, while still forming stable ML complexes at low pH. Metal ions such as In(III) Ga(III), Th(IV) or Bi(III) that traditionally show no affinity for neutral saturated nitrogen donor ligands may become important with ligands displaying the abovementioned complexing properties.

COMPARISON OF THE PROTONATION CONSTANTS

TABLE 11 : Protonation constants of THEDACH, THEEN, EN, EDTA and *trans*-CDTA

	THEDACH	THEEN	EN	EDTA	*trans*-CDTA
pKa_1 $H + L \rightleftharpoons HL$	10.06	8.38	9.89	10.17	12.3[a]
pKa_2 $HL + L \rightleftharpoons H_2L$	1.55	4.37	7.08	6.11	6.12

[a]This higher prtonation constant is observed with K^+ or tetramethylammonium salts as background electrolyte but is only 9.9 with the complexing Na^+ ion.

The formation constants reported in table 11 were measured using $NaNO_3$ as the background electrolyte. To eliminate the possibility that THEDACH is binding to Na^+ present in solution, the protonation constants were redetermined with 0.1M tetramethylammonium nitrate as the electrolyte. The protonation constants remained essentially unchanged from those obtained in 0.1M $NaNO_3$ proving conclusively that THEDACH has little or no affinity for the Na^+ ion. This could possibly have been anticipated when one considers the size of the Na^+ ion and the lower affinity of cyclohexylene bridged ligands for larger metal ions. The increase in protonation constant observed for trans-CDTA relative to EDTA is also observed for THEDACH relative to THEEN. This may be due to a mild "Proton Sponge" effect with the two nitrogens on THEDACH and trans-CDTA being held in positions that are closer to each other and therefore allow for cooperative hydrogen bonding. The fact that the subsequent protonation constants are substantially lower than for the ethylene-

bridged analogues, strongly supports the idea that cooperative hydrogen bonding must be broken if a second proton is to be added to the nitrogen donors.

CHAPTER 4

MIXED DONOR MACROCYCLES

ADDITION OF PENDANT OXYGEN DONORS TO MIXED DONOR MACROCYCLES

One of the first examples of macrocyclic ligands containing neutral oxygen donors is BHE-K22 reported by Kulstad & Malmsten (1980) and Gandour et al (1986). This class of ligands more than any other most profoundly validates the ligand design rule proposed for neutral oxygen donor groups :

The addition of neutral oxygen donor containing groups to a ligand will increase the selectivity of the ligand for the large metal ions relative to the small metal ions.

The class of mixed donor macrocycles containing N-donors and O-donors, ethereal in nature, show that further increase of neutral oxygen donors, whether they are alcoholic or ethereal and whether they form part of a pendant moiety or macrocyclic ring, inevitably obey the proposed rule for the addition of neutral oxygen donors. Hancock et al (1986) originally suggested that the enhanced selectivity for he larger metal ions could be rationalised by the tolerance of the larger metal ions towards the steric crowding produced by addition of neutral oxygen donors.

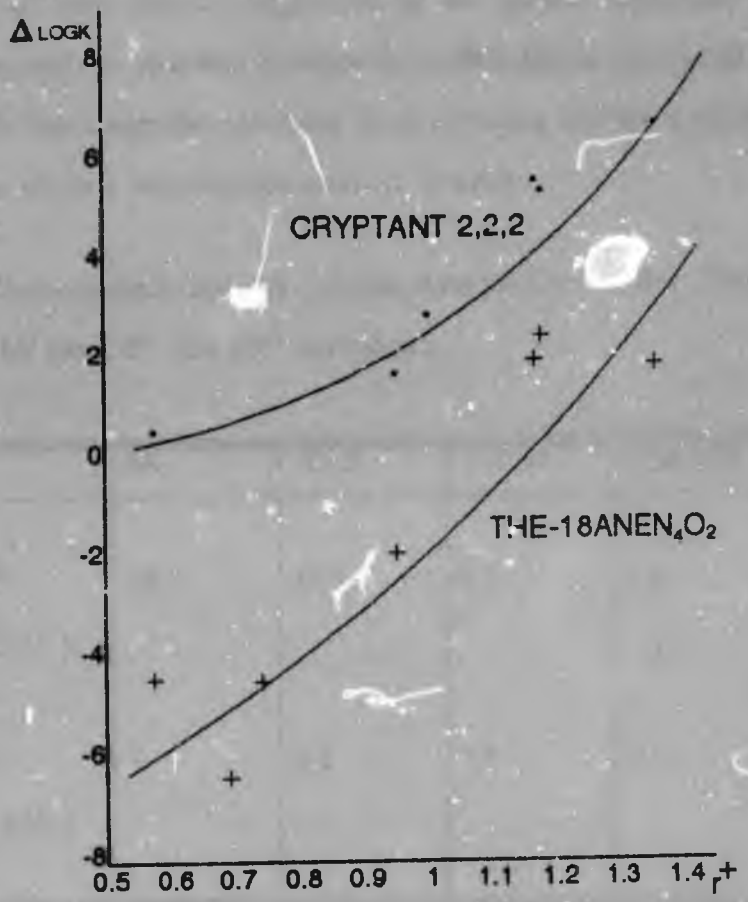


Figure 50 : Change in stability as a function of metal ion radius in passing from K22 to cryptand-2,2,2 and for 18-ane-N_4O_2 to THE-18-ane-N_4O_2

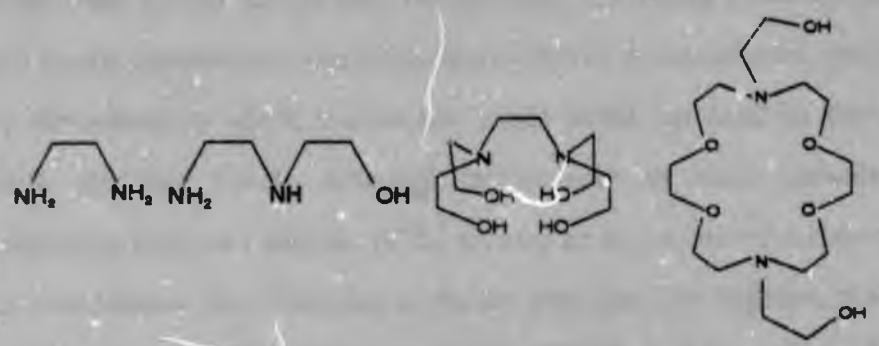


Figure 51 : increased denticities with the introduction of pendant donors.

The denticities of these ligands, as a result of the additional oxygen donors, exceed the coordination numbers of the metals.

This point of view may be supported by the ligand BHE-K22, which is octadentate, and the observed decrease in the stability of the copper complex undoubtedly has a contribution from steric crowding and the inability of the Cu^{2+} ion to attain a coordination number of eight.

TABLE 1 : thermodynamic stability constant data for EN, HEEN, THEEN and BHE-K22 for the Cu^{2+} and Pb^{2+} complexes.

	EN	HEEN	THEEN	BHE-K22
$logK_1$ Cu^{2+} (radius 0.57Å)	10.5	10.1	8.5	6.6
$logK_1$ Pb^{2+} (radius 1.18Å)	5	5.6	7.6	9.2

Passing from EN to HEEN sees the denticity increasing from two to three which hardly exhausts the coordination numbers of the metal ions., and clearly here the selectivity which favours the larger metal ion must be due to the chelate ring size effects. Although factors such as steric crowding and coordination number (Bhavan 1990) do play an important role, they are not as predominant as the effect due to chelate ring size. The addition of a single neutral oxygen donor to EN, to produce HEEN and its enhanced metal selectivity for the larger metal ions, is the most fundamental and elementary example that bears testimony of the importance of chelate ring size.

Selectivity is an important thermodynamic criterion in ligand design but it is

extremely important that the stability of the complexes themselves are not compromised. High selectivity without sufficient complex stability will not be adequate for fruitful applications.

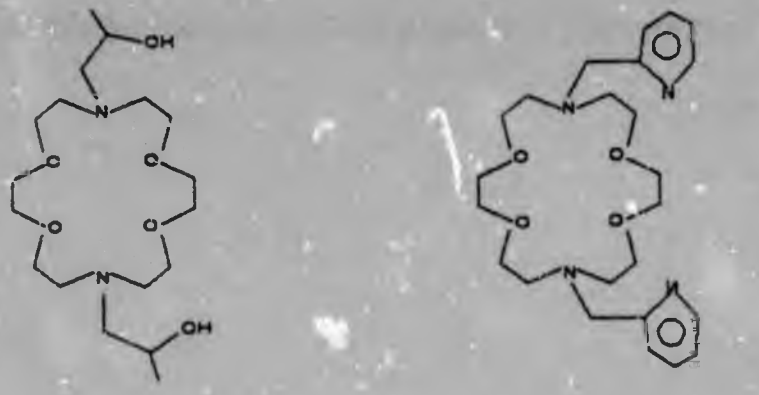


Figure 52 : ligands BHP-K22 and $(Py)_2$-K22 tabulated below

TABLE 2 : Stability constant data for BHP-K22 and $(Py)_2$-K22

	BHP-K22[a]	$(Py)_2$-K22[b]
log K_1 Pb	8.57	11.67
(1.19 Å)		
log K_1 Zn	3.0	6.96
(0.74 Å)		
Pb\Zn	5.6	4.7

[a] Hancock et al (1986)

[b] Damu et al (1986)

The Pb\Zn selectivities of BHP-K22 and $(Py)_2$-K22 are both reasonably good, in the order of 5 log units; however, in the case of BHP-K22 the complex stability may be somewhat compromised in the eventual treatment for lead poisoning. $(Py)_2$-K22 has an acceptable, although poorer, Pb\Zn selectivity but its sufficiently strong complexing of the Pb^{2+} ion would make it a better candidate for treatment of lead poisoning (Hancock et al 1986).

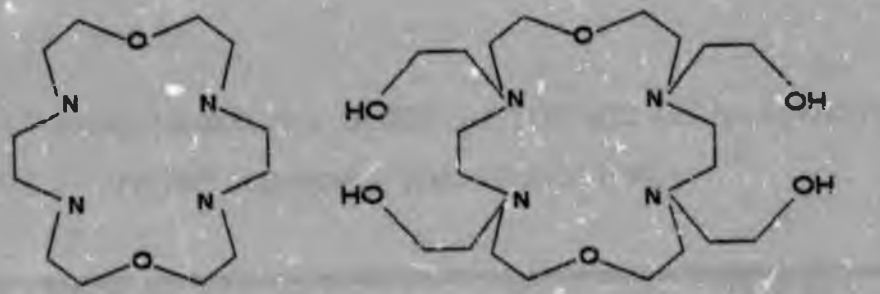


Figure 53 : ligands K22 (18-ane-N_2O_4)and THE-K22 (tetrahydroxyethyl 18-ane-N_2O_4)

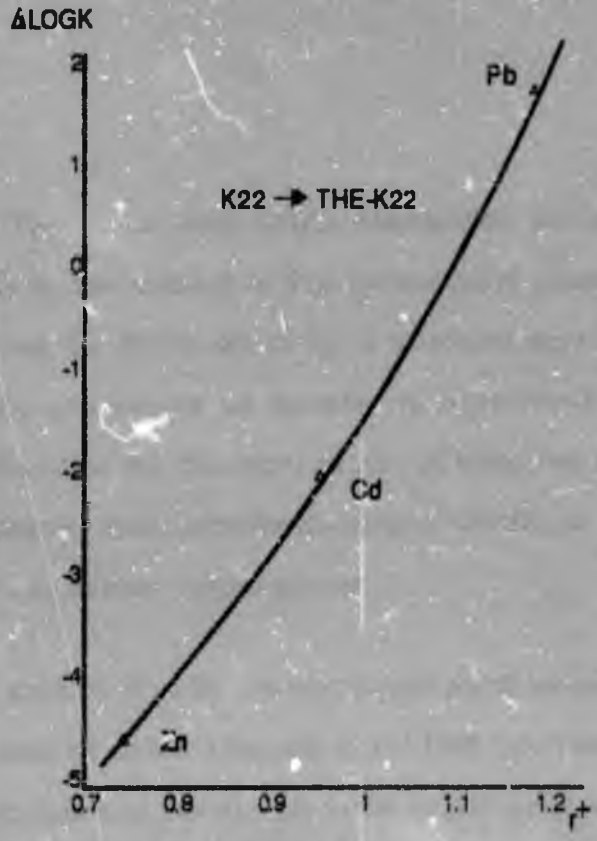


Figure 54 : $\Delta logK_1$ as a function of metal ion radius in passing from K22 to THE-K22

TABLE 3 : Stability constant data for K22 and THE-K22 and the selectivities for Zn^{2+}, Cd^{2+} and Pb^{2+} complexes (Hancock et al 1989).

METAL RADIUS	PARAMETER	K22	THE-K22
0.74	log K_1 Zn^{2+}	10.51	5.90
0.95	log K_1 Cd^{2+}	10.90	8.84
1.19	log K_1 Pb^{2+}	9.01	10.72
selectivities	[a]**Pb\Zn**	-1.50	+4.82
selectivities	[b]**Cd\Zn**	+0.39	+2.94

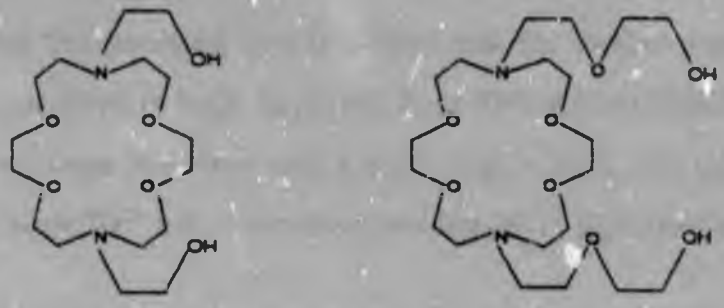
[a] Pb\Zn selectivity = log K_1 Pb^{2+} - log K_1 Zn^{2+}

[b] Cd\Zn selectivity = log K_1 Cd^{2+} - log K_1 Zn^{2+}

Likewise the selectivity of Pb^{2+} and Cd^{2+} ions for K22 over the small Zn^{2+} ion

is inadequate. The Pb\Zn and Cd\Zn selectivities are raised to more acceptable levels by the addition of four hydroxyethyl groups to give THE-K22. The fact that the Pb\Zn selectivity is increased approximately 6 fold while the CD\Zn experiences an increase of approximately 3 orders of magnitude is related to the difference in size of these two metal ions. The larger Pb^{2+} ion shows greater increase in complex stability, as is expected with the addition of four neutral oxygen donors.

To suppress the stability of all but the very largest metal ions sufficient neutral oxygen donors must be added. Hancock et al (1989) pursued this viewpoint and attempted to limit complex stability to the largest metal ions such as Ba^{2+}, Sr^{2+} or Pb^{2+} by adding an extra neutral oxygen donor to each pendant donor group of BHE-K22 to give BHEE-K22. Each pendant arm in this ligand posseses both an alcoholic and ethereal oxygen.



BHE-K22 BHEE-K22

Figure 55 : ligands BHE-K22 and BHEE-K22

TABLE 4 : comparison of stability constant data for BHE-K22 and BHEE-K22 (Hancock et al 1989).

METAL ION	IONIC RADIUS	[a]BHE-K22 LOG K_1	[a]BHEE-K22 LOG K_1	ΔlogK
Cu^{2+}	0.57	6.6	[b]NEC	>5
Cd^{2+}	0.95	8.0	3.3	4.7
Ca^{2+}	1.00	4.1	[b]NEC	>3
Sr^{2+}	1.18	4.7	3.3	1.6
Pb^{2+}	1.19	9.2	7.2	2.0
Ba^{2+}	1.35	5.3	4.9	0.4

[a] Formation constants from Hancock et al (1989)

[b] No evidence of complexation

From the tabulated data it is clear that the smaller metal ions suffer the largest drops in $logK_1$ in passing from BHE-K22 to BHEE-K22, while Ba^{2+}, a very large ion, shows only a slight drop in $logK_1$. this reflects the ability of the large Ba^{2+} ion to accommodate ligands of high denticity.

Hancock et al (1989) report the crystal structures of [K(BHEE-K22)]I and [K(BHE-K22)]Cl which elucidate the coordination that occurs in both compounds and how it may relate to denticity. [K(BHEE-K22)]I appears to be sterically crowded with the pendant donor groups adopting the trans orientation with at leat two of the oxygen donors on the pendant groups left uncoordinated. The $[K(BHEE)]^+$ cation is reported as to different structures

of site occupancy 0.75 and 0.25 in which the latter structure indicates that only one of the oxygens in the pendant groups is coordinated.

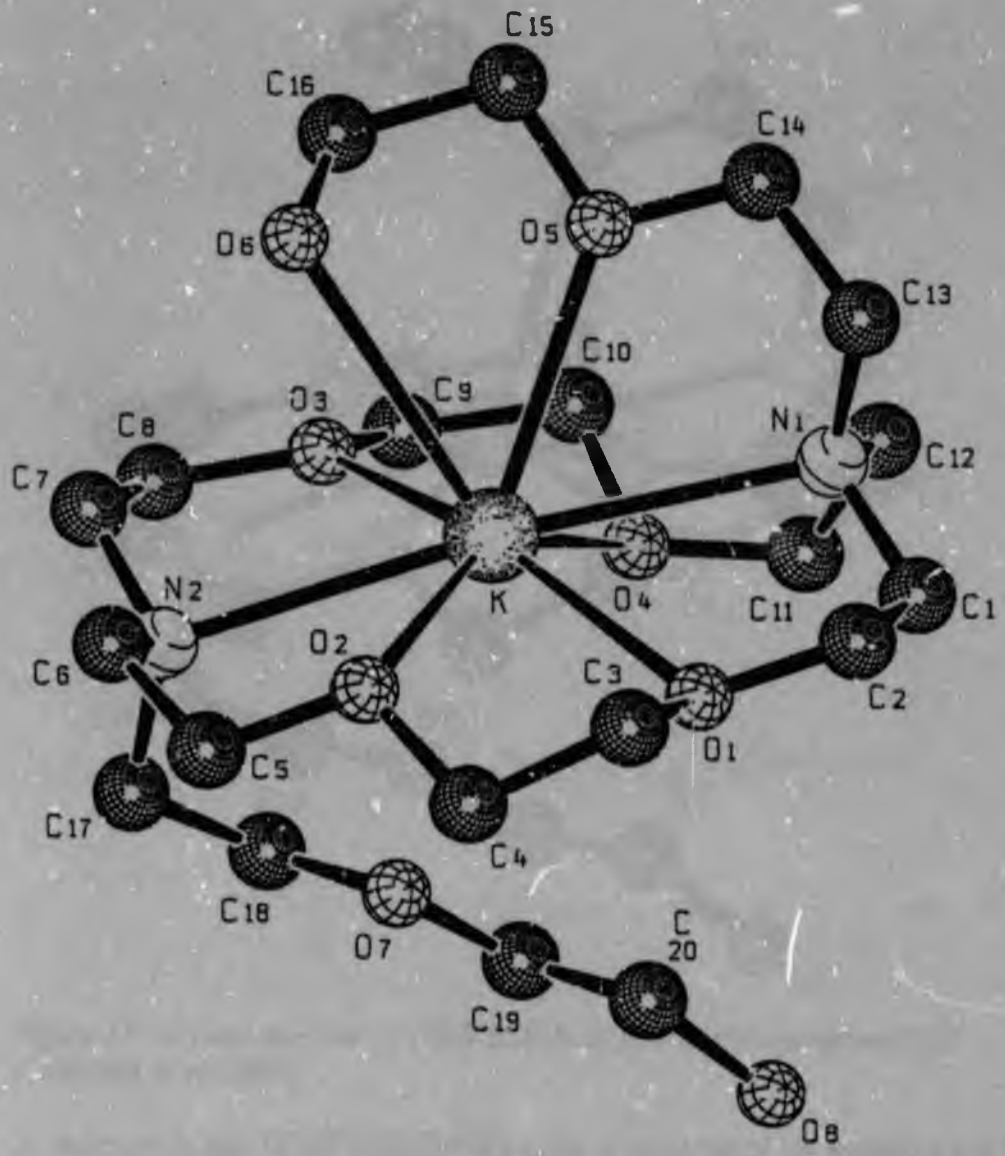


Figure 56 : crystal structure of [K(BHEE-K22)]I with site occupancy 0.75 (Hancock et al 1989)

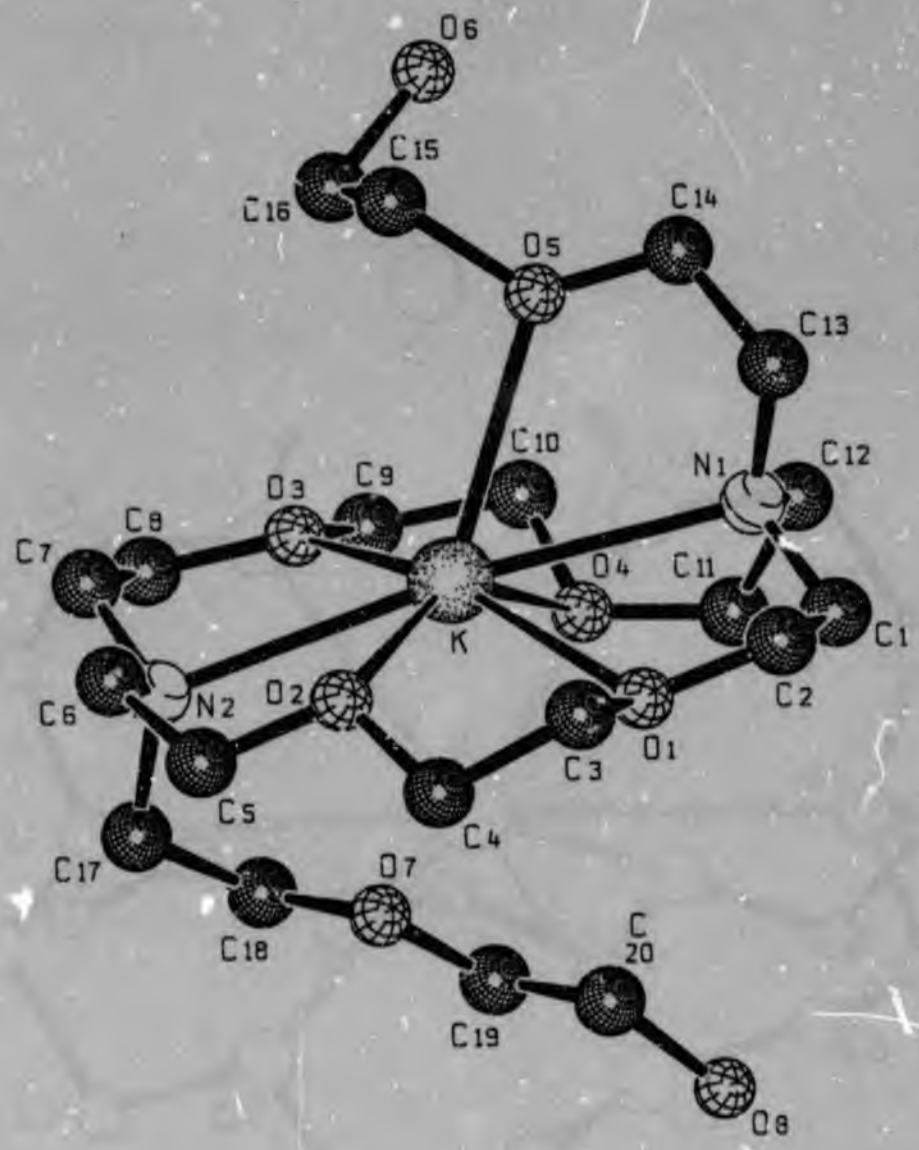


***Figure 57** : crystal structure of [K(BHEE-K22)]I with site occupancy 0.25 (Hancock et al 1989)*

In contrast to this [K(BHE-K22)]Cl adopts a more usual cis arrangement of the pendant donor groups and appears not to be sterically crowded. This crystallographic study (Hancock et al 1989) illustrates the inability of the K^+ ion to accommodate the ligand BHEE-K22 and its higher denticity.

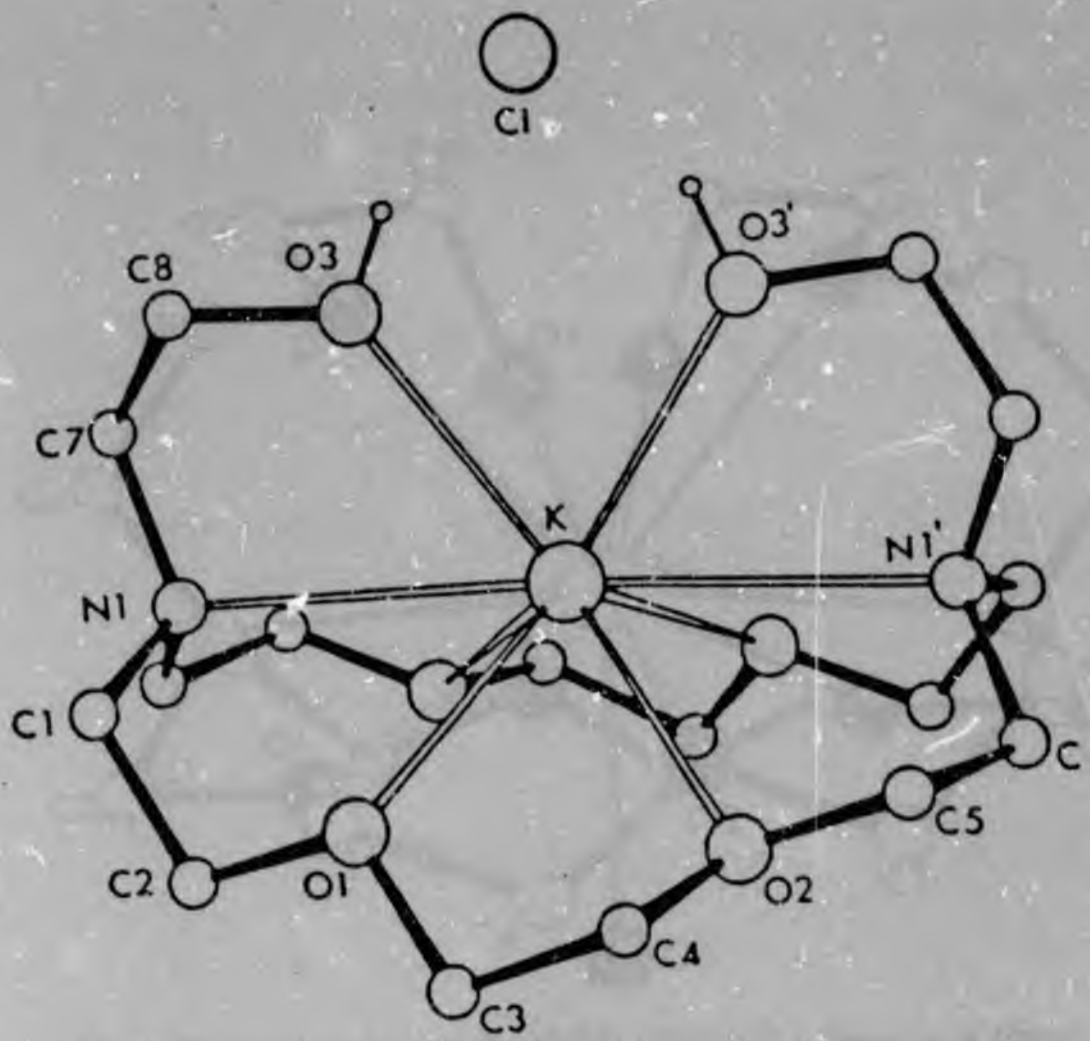


*Figure 58 : crystal structure of [K(BHE-K22)]Cl showing the more sterically favourable cis arrangement of pendant groups (**Hancock et al 1989**)*

The crystal structure of $[Ba(BHEE\text{-}K22)H_2O]^{2+}$ (Bhavan et al 1990) indicates that the Ba^{2+} is sufficiently large to accommodate all of the donor atoms of

BHEE-K22 with ease, and further substantiates the fact by coordinating a water molecule to achieve a coordination number of eleven.

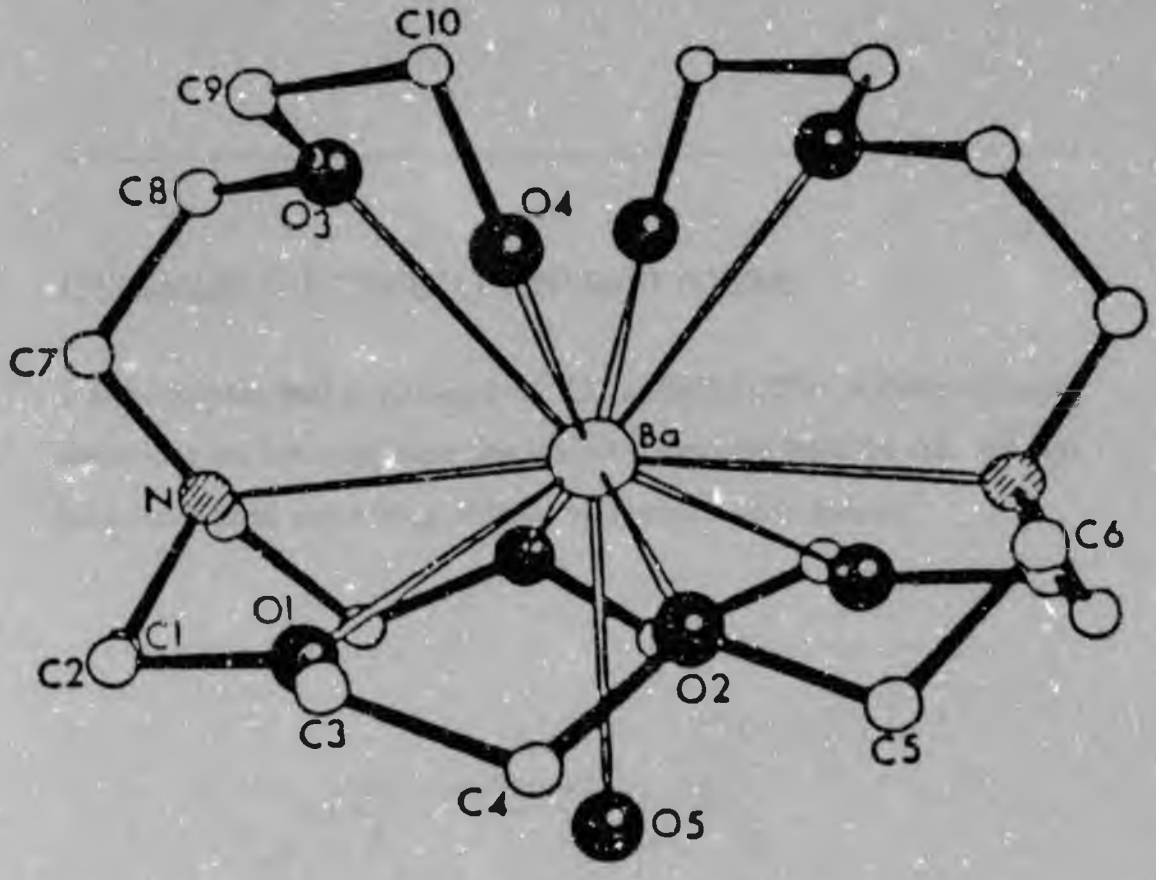


*Figure 59 : crystal structure of $[Ba(BHEE\text{-}K22)H_2O]^{2+}$ (**Bhavan et al 1990**)*

Unlike $[K(BHEE\text{-}K22)]^{+}$ complex that has the trans conformation with the pendant groups on opposite sides of the macrocyclic ring, the $[Ba(BHEE\text{-}K22)H_2O]^{2+}$ complex has a cis conformation in which both of the pendant

groups are on the same side as the macrocyclic ring suggesting that this is a less sterically crowded situation (Hancock et al 1989b). Observations of this fashion demonstrate convincingly that addition of neutral oxygen groups is an important tool in the design of ligands favouring selectivity for large metal ions. Lindoy et al (1983 & 1985) observed similar behaviour when increasing the number of oxygen donors in the macrocyclic ring of mixed nitrogen--oxygen donor macrocycles.

INCREASING THE RIGIDITY OF PENDANT DONORS

It is no surprise that in passing from K22 to BHE-K22 the stability of larger metal ions are favoured, since this is what is expected from the rule that has been established concerning addition of neutral oxygen donors.

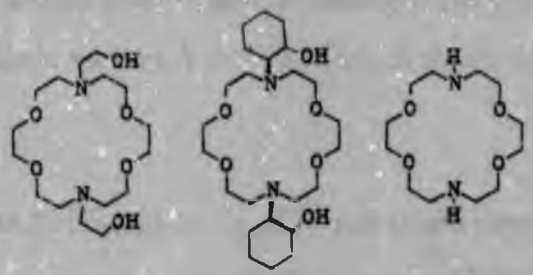


Figure 60 : illustration of ligands K22, BHE-K22 and Cy_2-K22 discussed in this section.

TABLE 5 : Formation constants ($logK_1$) of K22 and its derivatives having pendant oxygen donor groups with a simple ethylene bridge (BHE-K22) and a trans-cyclohexyl group (Cy_2-K22) (de Sousa et al 1991).

LEWIS ACID	IONIC RADIUS	$logK_1$		
		K22	BHE-K22	Cy_2-K22
H+		9.08	8.70	8.88
		7.94	7.47	8.04
Zn^{2+}	0.74	3.1	3.0[a]	4.77
Cu^{2+}	0.75	6.1	6.60	7.63
Cd^{2+}	0.95	5.28	7.96	8.64
Ca^{2+}	1.00	1.74	4.08	4.72
La^{2+}	1.03		3.24[a]	4.08
Sr^{2+}	1.17	2.65	4.05[a]	4.13
Pb^{2+}	1.18	6.8	9.20	8.59
Ba^{2+}	1.36	2.97	5.3	4.59

[a] for the very similar 2-hydroypropyl analogue Hancock et al 1986

[b] Octahedral ionic radii in Å from Martell & Smith 1974-1989

In passing from BHE-K22 to Cy_2-K22 one would expect the effect of adding neutral oxygen donors to be further enhanced due to inductive effects contributed by the electron releasing cyclohexyl groups. In the figure is shown the relationship between ΔlogK and the octahedral ionic radius of the metal ions for Cy_2-K22 relative to BHE-K22.

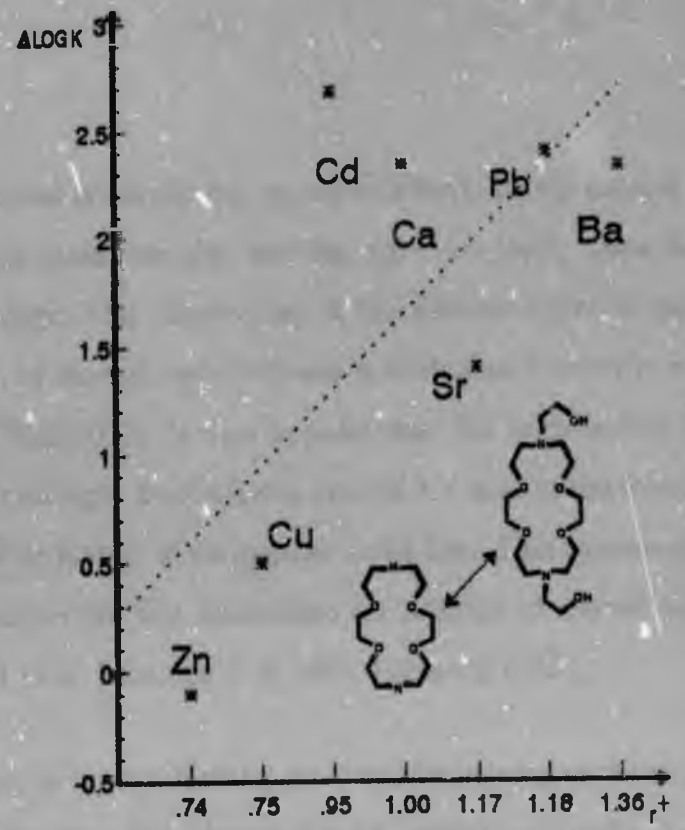


Figure 61 : change in stability constant in passing from K22 to BHE-K22 (de Sousa et al 1991)

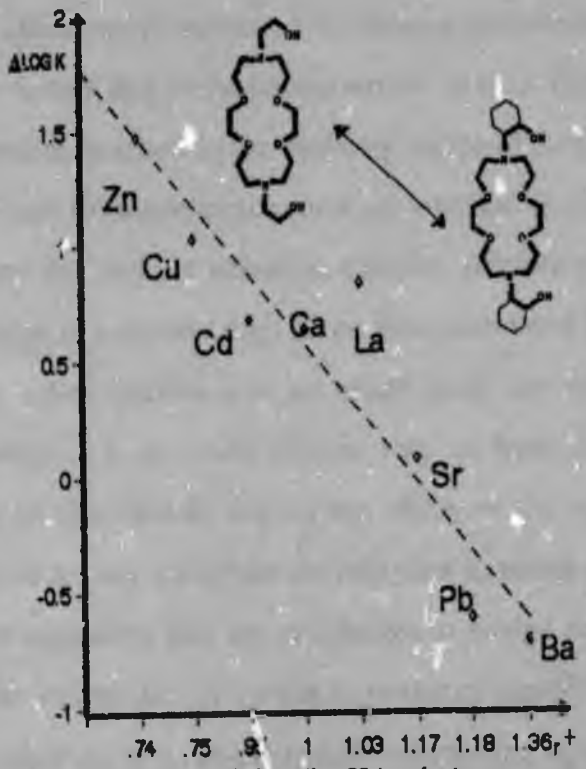


Figure 62 : change in stability ($logK_1$) relating to metal ion size in passing from BHE-K22 to Cy_2-K22 (de Sousa et al 1991)

What is observed is exactly the opposite; a fairly strong inverse relationship exists between metal ion size and the effect on $logK_1$ when introducing a cyclohexyl bridge. This observation of the adverse effect on metal ion size with addition of neutral oxygen donors is analogous to what is observed with the ligand THEDACH. It now appears that the introduction of a neutral oxygen donor strongly discriminates against the large metal ions and reverses the selectivity in favour of the smaller metal ions. This appears contradictory when we consider the rule established for addition of neutral oxygen donors (Thom et al 1986, Hancock et al 1989, Hancock 1986).

The favouring of the small metal ions must be related to the introduction of the cyclohexane ring. The change in $logK_1$ versus ionic radius is very similar in passing from THEEN to THEDACH and BHE-K22 to Cy_2-K22 which suggests that the effect can be produced by fusing a cyclohexane structure to the bridge of the chelate ring in the parent amine, as with THEDACH, or by fusing the cyclohexane structure to the chelating bridge of the pendant donors. Ligands BHEAC and triethanolamine show an identical inverse relationship between metal ion size and the effect on complex stability of introducing a cyclohexylene bridge to a chelate ring. It was first postulated (de Sousa et al 1991) that the effect derives not so much from the presence of the cyclohexylene bridge in a particular chelate ring, as from the effect of the increased rigidity of this chelate ring on the ability of the remaining donor groups of the ligand to be oriented for coordination to metal ions of differing sizes. There is an indication that the cyclohexylene bridge could be a useful tool in altering the selectivities of ligands in favour of smaller metal ions and possibly for the synthesis of more powerfully complexing agents.

CRYSTAL STRUCTURE OF $[Sr(Cy_2\text{-}K22)H_2O](NO_3)_2$

Cy_2-K22 is synthesized by the reaction of cyclohexene oxide with K22 and a mixture of diastereomeric pairs is to be expected. In the light of the strong diastereoselectivity observed in syntheses involving cyclohexene oxide (de Sousa et al 1994) it seems a feasible suggestion that the synthesis of Cy_2-K22 is itself diastereoselective. The synthesis of the complex of $Sr(NO_3)_2$ with Cy_2-K22 provided a means of identifying the stereoisomers that are present. The R,R and S,S forms are the only forms observed, with no indication of the meso-R,S form and $[Sr(Cy_2\text{-}K22)H_2O](NO_3)_2$ crystallises in the optically active space group PNNN with crystals being those of the R,R and S,S forms of the complex.

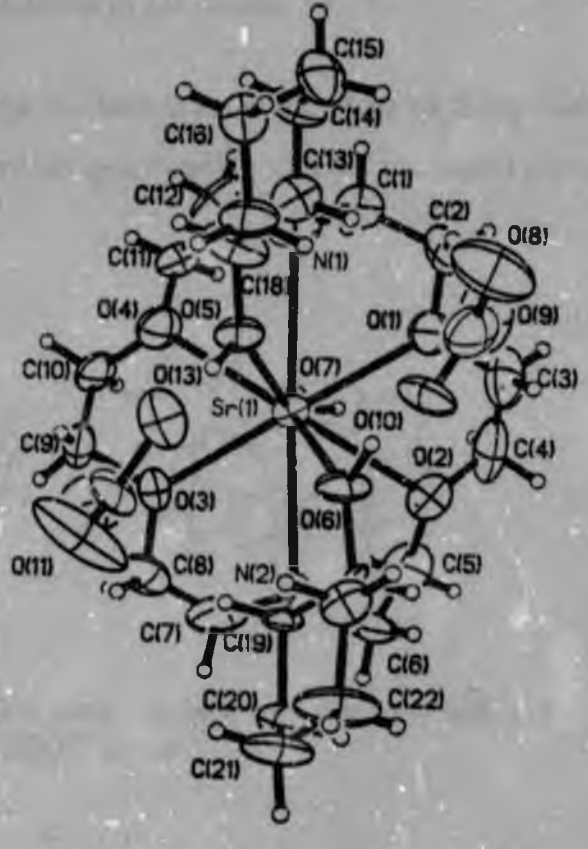


Figure 63 : crystal structure of $[(Cy_2\text{-}K22)H_2O](NO_3)_2$

The complex adopts the cis arrangement which implies that this is not a sterically crowded situation that would have resulted in the trans conformation being observed (Hancock et al 1989b). The bulkier cyclohexyl groups may be more sterically demanding than the hydroxyethyl but the denticity in the latter case is increased by four while only by two in the case of the hydroxycyclohexyl groups. The Sr^{2+} is sufficiently large to further accommodate a coordinated water to attain a coordination number of nine in the complex. It may well be that the Sr^{2+} in fact has a coordination number of 10 if one considers the possible bond between the Sr^{2+} and the oxygen of the nitro group. This can be realised when considering the hydrogen bonding that takes place between the axially coordinated water and the nitro groups of the adjacent cation in the lattice.

The nitro groups are held trans to the plane of the cyclohexyl pendants and are involved in hydrogen bonding with the cyclohexyl groups.

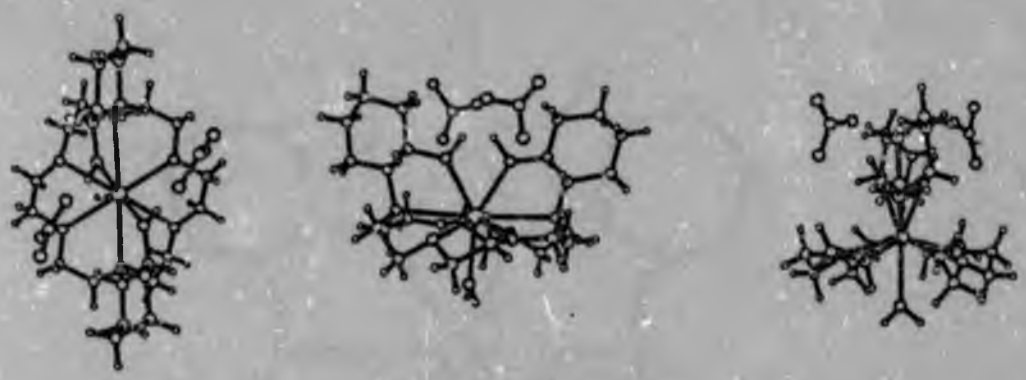


***Figure 64** : top view, side view and side view with a 90° rotation of the $[Sr(Cy_2K22)H_2O]^{+}$ cation.*

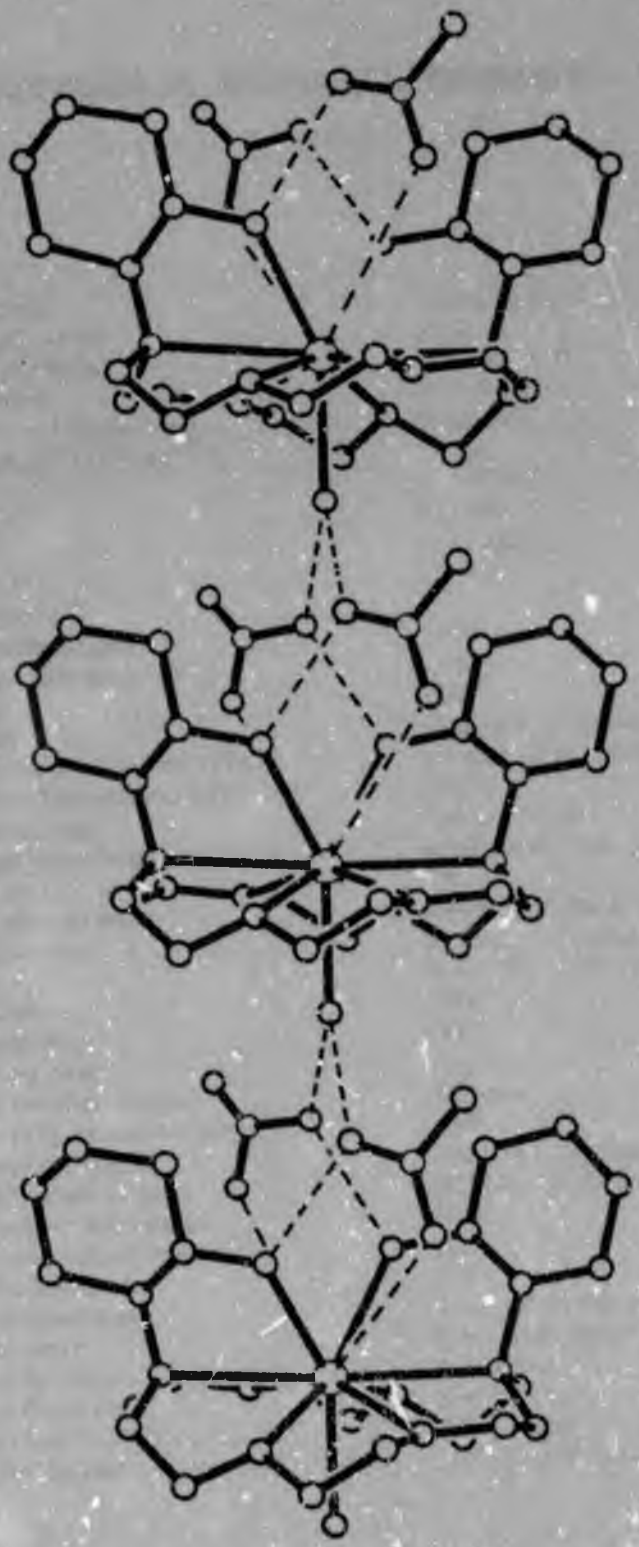


Figure 65 : illustration of hydrogen bonding involved in the lattice

TABLE OF CRYSTAL DATA AND STRUCTURE REFINEMENT

Empirical Formula	$C_{24}\ H_{48}\ N_4\ O_{13}\ Sr$
Formula Weight (AMU)	688.3
Crystal Color and Habit	colorless, plate
Crystal Size (mm)	0.5 x 0.4 x 0.3
Crystal System and Space Group	Monoclinic, C c
Cell Dimensions :: (Å and deg.)	a : 16.809(6) b : 8.889(2) β : 101.47(3) c : 21.232(6)
Cell Volume ($Å^3$)	3109(2)
Z (formula units/cell)	4.
Density (calculated) (g/ml)	1.470
Absorption Coefficient (μ, mm^{-1})	1.802
F(000)	1448.
Diffractometer	Siemens R3m diffractometer
Radiation Source and Wavelength (A)	Mo Ka lambda .7107
Data Collection Temperature (degK)	293(2)
Two-theta range (deg)	5.00 to 50.00
Scan Type and Speed (deg/min)	ω (Wyckoff) : 2.0
Scan width (deg)	1.0
Background Measurements	stationary crystal & counter method
Standard Reflections	3 every 97 reflections
Index ranges	0<h< 19 ; 0<k< 10 ; -25<l< 24
Reflection Collected	2842
Observed Reflections	2435
Observation criterion	I>2σ(I)
Absorption Correction Method	Psi-scans
Max. and Min. Transmission Factors	.960 to .851
Structure Solution Program	SHELXS (Sheldrick, 1982)
Structure Refinement Program	SHELXL-93 (Sheldrick, 1993)
Absolute Configuration Method	Flack
Absolute Configuration Parameter	0(13)
Number of l.s. Parameters	379
Residuals (observed data)	R = .0314 : wR = .0771
Residuals (all data)	R = .0405 : wR = .0863
Goodness-of-fit (observed data)	S = 1.2260
Goodness-of-fit (all data)	S = 1.1960
Largest and Mean l.s. shifts (Δ/sig)	.392 : .055
Largest e- Density Peak and Hole ($e/Å^3$)	.232 : -.229

TABLE OF ATOMIC COORDINATES [$\times 10^4$] AND EQUIVALENT ISOTROPIC DISPLACEMENT PARAMETERS [$(\text{Å}^2 \times 10^3$]

atom	x	y	z	U(eq)
Sr(1)	636(1)	1905(1)	7287(1)	31(1)
O(1)	1453(6)	1290(10)	6367(4)	58(3)
O(2)	2265(5)	1050(10)	7609(4)	49(2)
O(3)	-149(5)	1250(10)	8201(4)	48(2)
O(4)	-912(6)	1060(10)	6965(4)	56(2)
O(5)	-122(5)	4276(8)	6866(3)	41(2)
O(6)	1417(5)	4290(10)	7715(3)	48(2)
O(7)	658(8)	-954(3)	7259(6)	50(1)
O(8)	6570(10)	2630(10)	5970(5)	104(4)
O(9)	6761(8)	130(10)	6200(6)	99(4)
O(10)	6620(7)	1760(10)	6920(3)	56(2)
O(11)	4590(10)	2390(20)	8563(5)	138(6)
O(12)	4505(8)	220(10)	8368(5)	88(3)
O(13)	4696(6)	1730(10)	7627(4)	58(3)
N(1)	-205(6)	1983(8)	5932(4)	42(3)
N(2)	1553(5)	2070(10)	8641(4)	42(2)
N(3)	6679(7)	1440(20)	6385(6)	68(3)
N(4)	4631(6)	1530(10)	8231(4)	49(3)
C(1)	219(7)	1081(8)	5565(5)	47(3)
C(2)	1149(7)	1450(20)	5712(5)	68(4)
C(3)	2320(10)	1350(20)	6527(8)	73(4)
C(4)	2568(8)	480(20)	7098(8)	76(5)
C(5)	2430(10)	350(20)	8231(7)	74(4)
C(6)	2392(7)	1360(10)	8727(4)	58(3)
C(7)	1010(10)	1160(20)	8998(5)	87(5)
C(8)	179(7)	1450(10)	8862(5)	56(3)
C(9)	-1023(7)	1200(20)	8045(6)	64(4)
C(10)	-1284(7)	310(20)	7445(5)	52(3)
C(11)	-1126(7)	210(10)	6384(5)	44(3)
C(12)	-1043(6)	1360(10)	5866(6)	57(3)
C(13)	-315(8)	3680(10)	5745(5)	50(3)
C(14)	-720(10)	3940(10)	5088(5)	53(3)
C(15)	-620(8)	5610(10)	4926(6)	63(3)
C(16)	-1009(6)	6610(10)	5422(5)	48(2)
C(17)	-530(10)	6240(10)	6077(5)	52(3)
C(18)	-573(8)	4570(10)	6240(5)	58(4)
C(19)	1549(7)	3610(10)	8814(4)	32(2)
C(20)	2013(8)	4060(20)	9525(5)	53(3)
C(21)	2050(10)	5690(20)	9658(5)	72(4)
C(22)	2300(10)	6550(20)	9206(5)	86(5)
C(23)	1912(8)	6260(10)	8492(6)	47(3)
C(24)	1905(4)	4600(10)	8340(4)	35(2)

U(eq) is defined as 1/3 the trace of the orthoganlized Uij tensor.

TABLE OF BOND LENGTHS [Å] AND BOND ANGLES [°]

Sr(1)-O(5)	2.533(7)	Sr(1)-O(7)	2.542(3)
Sr(1)-O(6)	2.562(8)	Sr(1)-O(3)	2.618(8)
Sr(1)-O(4)	2.664(9)	Sr(1)-O(1)	2.658(9)
Sr(1)-O(2)	2.793(9)	Sr(1)-N(1)	2.944(9)
Sr(1)-N(2)	2.98(1)	O(1)-C(2)	1.39(2)
O(1)-C(3)	1.42(2)	O(2)-C(4)	1.38(2)
O(2)-C(5)	1.44(2)	O(3)-C(8)	1.41(1)
O(3)-C(9)	1.44(1)	O(4)-C(11)	1.43(1)
O(4)-C(10)	1.46(2)	O(5)-C(18)	1.42(1)
O(6)-C(24)	1.44(1)	O(8)-N(3)	1.36(2)
O(9)-N(3)	1.25(2)	O(10)-N(3)	1.19(2)
O(11)-N(4)	1.05(2)	O(12)-N(4)	1.23(1)
O(13)-N(4)	1.32(1)	N(1)-C(1)	1.40(1)
N(1)-C(12)	1.49(1)	N(1)-C(13)	1.56(1)
N(2)-C(19)	1.42(1)	N(2)-C(6)	1.52(1)
N(2)-C(7)	1.53(1)	C(1)-C(2)	1.57(2)
C(3)-C(4)	1.43(2)	C(5)-C(6)	1.40(2)
C(7)-C(8)	1.38(2)	C(9)-C(10)	1.49(2)
C(11)-C(12)	1.53(2)	C(13)-C(18)	1.45(2)
C(13)-C(14)	1.44(2)	C(14)-C(15)	1.54(2)
C(15)-C(16)	1.61(2)	C(16)-C(17)	1.50(2)
C(17)-C(18)	1.53(1)	C(19)-C(24)	1.54(1)
C(19)-C(20)	1.61(1)	C(20)-C(21)	1.48(2)
C(21)-C(22)	1.36(2)	C(22)-C(23)	1.55(2)
C(23)-C(24)	1.51(1)		

O(5)-Sr(1)-O(7)	146.3(4)	O(5)-Sr(1)-O(6)	67.9(1)
O(7)-Sr(1)-O(6)	145.7(4)	O(5)-Sr(1)-O(3)	98.8(3)
O(7)-Sr(1)-O(3)	78.9(4)	O(6)-Sr(1)-O(3)	102.6(3)
O(5)-Sr(1)-O(4)	75.4(3)	O(7)-Sr(1)-O(4)	74.3(4)
O(6)-Sr(1)-O(4)	136.9(3)	O(3)-Sr(1)-O(4)	61.1(3)
O(5)-Sr(1)-O(1)	102.0(3)	O(7)-Sr(1)-O(1)	76.5(4)
O(6)-Sr(1)-O(1)	97.3(3)	O(3)-Sr(1)-O(1)	155.4(1)
O(4)-Sr(1)-O(1)	112.0(3)	O(5)-Sr(1)-O(2)	135.5(3)
O(7)-Sr(1)-O(2)	73.5(3)	O(6)-Sr(1)-O(2)	74.3(3)
O(3)-Sr(1)-O(2)	111.9(3)	O(4)-Sr(1)-O(2)	147.8(1)
O(1)-Sr(1)-O(2)	60.0(3)	O(5)-Sr(1)-N(1)	61.6(2)
O(7)-Sr(1)-N(1)	90.4(3)	O(6)-Sr(1)-N(1)	116.1(2)
O(3)-Sr(1)-N(1)	121.0(3)	O(4)-Sr(1)-N(1)	60.1(3)
O(1)-Sr(1)-N(1)	60.3(3)	O(2)-Sr(1)-N(1)	120.2(3)
O(5)-Sr(1)-N(2)	115.3(2)	O(7)-Sr(1)-N(2)	93.7(3)
O(6)-Sr(1)-N(2)	59.2(2)	O(3)-Sr(1)-N(2)	62.4(2)
O(4)-Sr(1)-N(2)	123.5(3)	O(1)-Sr(1)-N(2)	118.3(3)
O(2)-Sr(1)-N(2)	58.9(2)	N(1)-Sr(1)-N(2)	175.2(2)
C(2)-O(1)-C(3)	113(1)	C(2)-O(1)-Sr(1)	125.0(7)
C(3)-O(1)-Sr(1)	118(1)	C(4)-O(2)-C(5)	122(1)
C(4)-O(2)-Sr(1)	113.9(8)	C(5)-O(2)-Sr(1)	110.2(8)
C(8)-O(3)-C(9)	114(1)	C(8)-O(3)-Sr(1)	123.6(7)
C(9)-O(3)-Sr(1)	118.5(7)	C(11)-O(4)-C(10)	107(1)
C(11)-O(4)-Sr(1)	115.8(7)	C(10)-O(4)-Sr(1)	118.8(6)

C(18)-O(5)-Sr(1)	128.6(6)	C(24)-O(6)-Sr(1)	130.0(5)
C(1)-N(1)-C(12)	108.1(8)	C(1)-N(1)-C(13)	117(1)
C(12)-N(1)-C(13)	106(1)	C(1)-N(1)-Sr(1)	109.3(7)
C(12)-N(1)-Sr(1)	110.1(7)	C(13)-N(1)-Sr(1)	106.3(6)
C(19)-N(2)-C(6)	115(1)	C(19)-N(2)-C(7)	110(1)
C(6)-N(2)-C(7)	111(1)	C(19)-N(2)-Sr(1)	105.7(6)
C(6)-N(2)-Sr(1)	112.6(6)	C(7)-N(2)-Sr(1)	101.8(6)
O(10)-N(3)-O(9)	124(1)	O(10)-N(3)-O(8)	114(1)
O(9)-N(3)-O(8)	122(1)	O(11)-N(4)-O(12)	120(1)
O(11)-N(4)-O(13)	126(1)	O(12)-N(4)-O(13)	114(1)
N(1)-C(1)-C(2)	111.4(8)	O(1)-C(2)-C(1)	109(1)
O(1)-C(3)-C(4)	107(1)	O(2)-C(4)-C(3)	112(1)
C(6)-C(5)-O(2)	113(1)	C(5)-C(6)-N(2)	111(1)
C(8)-C(7)-N(2)	118(1)	C(7)-C(8)-O(3)	111(1)
O(3)-C(9)-C(10)	109(1)	O(4)-C(10)-C(9)	105(1)
O(4)-C(11)-C(12)	103(1)	N(1)-C(12)-C(11)	113.5(8)
C(18)-C(13)-C(14)	117(1)	C(18)-C(13)-N(1)	113(1)
C(14)-C(13)-N(1)	114(1)	C(13)-C(14)-C(15)	108(1)
C(14)-C(15)-C(16)	108(1)	C(17)-C(16)-C(15)	106(1)
C(16)-C(17)-C(18)	113(1)	O(5)-C(18)-C(13)	113(1)
O(5)-C(18)-C(17)	110.7(8)	C(13)-C(18)-C(17)	110(1)
N(2)-C(19)-C(24)	111.0(8)	N(2)-C(19)-C(20)	117.4(8)
C(24)-C(19)-C(20)	107(1)	C(21)-C(20)-C(19)	115(1)
C(22)-C(21)-C(20)	115(1)	C(21)-C(22)-C(23)	118(1)
C(24)-C(23)-C(22)	111(1)	O(6)-C(24)-C(23)	111.3(8)
O(6)-C(24)-C(19)	105.6(7)	C(23)-C(24)-C(19)	114.0(8)

TABLE OF ANISOTROPIC DISPLACEMENT PARAMETERS

atom	U11	U22	U33	U23	U13	U12
Sr(1)	33(1)	27(1)	33(1)	-2(1)	3(1)	0(1)
O(1)	49(6)	73(6)	51(5)	-3(5)	11(5)	14(5)
O(2)	48(5)	32(4)	66(6)	0(4)	5(4)	0(3)
O(3)	40(5)	60(5)	47(5)	-2(4)	20(4)	6(4)
O(4)	47(5)	63(6)	55(5)	2(4)	2(4)	-21(4)
O(5)	53(5)	31(4)	35(4)	9(3)	-4(4)	10(4)
O(6)	65(6)	42(4)	28(3)	16(3)	-9(4)	-14(4)
O(7)	51(2)	30(1)	73(2)	6(5)	25(2)	2(5)
O(8)	178(9)	70(5)	66(5)	20(4)	28(6)	1(6)
O(9)	84(7)	80(6)	140(9)	-65(6)	44(6)	-23(5)
O(10)	83(7)	60(5)	25(3)	-9(3)	13(4)	11(5)
O(11)	270(20)	106(8)	60(5)	-13(5)	82(8)	-37(9)
O(12)	96(7)	77(6)	86(6)	31(5)	3(5)	-35(6)
O(13)	71(6)	38(4)	72(6)	-5(4)	32(5)	-1(4)
N(1)	57(6)	23(4)	38(5)	-5(4)	-12(4)	-11(4)
N(2)	35(4)	47(6)	45(5)	10(4)	11(4)	-18(4)
N(3)	57(6)	69(7)	72(8)	9(6)	-2(5)	-21(5)
N(4)	64(6)	55(5)	35(5)	13(4)	27(4)	-14(5)
C(1)	63(6)	24(3)	53(5)	-2(3)	8(4)	1(4)
C(2)	56(8)	105(9)	53(6)	-36(6)	32(6)	3(7)
C(3)	57(8)	66(7)	100(10)	23(7)	33(7)	0(6)
C(4)	44(7)	68(8)	130(10)	-29(8)	39(7)	-5(6)
C(5)	64(9)	52(7)	100(10)	24(7)	5(7)	29(6)
C(6)	67(7)	79(8)	24(4)	-1(4)	0(4)	30(6)
C(7)	86(9)	120(10)	43(5)	53(6)	-16(5)	-47(7)
C(8)	77(9)	49(5)	43(6)	-18(5)	14(6)	-18(6)
C(9)	31(6)	110(10)	58(7)	20(6)	18(5)	10(6)
C(10)	33(5)	68(7)	52(5)	4(4)	0(4)	-21(5)
C(11)	41(6)	40(5)	45(5)	5(4)	-6(4)	-1(4)
C(12)	34(5)	25(4)	99(8)	-12(5)	-21(5)	7(4)
C(13)	56(7)	31(5)	61(6)	6(4)	5(5)	-6(5)
C(14)	87(9)	38(5)	34(5)	4(4)	10(5)	-3(6)
C(15)	69(6)	60(7)	66(7)	15(6)	28(5)	-7(5)
C(16)	53(5)	36(5)	56(6)	3(4)	13(4)	2(4)
C(17)	71(8)	39(7)	38(6)	6(5)	-5(5)	19(5)
C(18)	118(9)	17(4)	40(5)	0(4)	15(5)	-4(4)
C(19)	39(5)	41(5)	13(3)	8(3)	-3(3)	-10(4)
C(20)	60(7)	68(7)	27(4)	3(4)	3(5)	-1(6)
C(21)	110(9)	68(8)	27(5)	-14(5)	-10(5)	-16(6)
C(22)	140(10)	54(7)	43(6)	-18(5)	-19(7)	-18(8)
C(23)	48(6)	36(6)	54(7)	4(5)	2(5)	7(5)
C(24)	11(3)	64(6)	27(4)	2(4)	-4(3)	-10(3)

The anisotropic dispacement factor exponent takes the form
2 pi^2 [h^2a*^2U(11) +...+ 2hka*b*U(12)]

TABLE OF HYDROGEN COORDINATES AND ISOTROPIC DISPLACEMENT PARAMETERS

atom	x	y	z	U(eq)
H(1O5)	-180(5)	5189(8)	7167(3)	50
H(1O6)	1424(5)	5310(10)	7356(3)	50
H(1O7)	1044(8)	-1610(3)	7137(6)	50
H(2O7)	443(8)	-1602(3)	7481(6)	50
H(1A)	-50(7)	1115(8)	5122(5)	80
H(1B)	211(7)	68(8)	5720(5)	80
H(2A)	1462(7)	950(20)	5442(5)	80
H(2B)	1167(7)	2520(20)	5654(5)	80
H(3A)	2580(10)	2310(20)	6562(8)	80
H(3B)	2520(10)	780(20)	6212(8)	80
H(4A)	2404(8)	-550(20)	7042(8)	80
H(4B)	3149(8)	500(20)	7228(8)	80
H(5A)	2980(10)	-40(20)	8283(7)	80
H(5B)	2070(10)	-470(20)	8269(7)	80
H(6A)	2584(7)	950(10)	9149(4)	80
H(6C)	2746(7)	2170(10)	8667(4)	80
H(7A)	1170(10)	1360(20)	9449(5)	80
H(7B)	1120(10)	120(20)	8938(5)	80
H(8A)	-64(7)	680(10)	9079(5)	80
H(8B)	41(7)	2400(10)	9024(5)	80
H(9A)	-1202(7)	2230(20)	7983(6)	80
H(9B)	-1213(7)	780(20)	8404(6)	80
H(10A)	-1070(7)	-690(20)	7503(5)	80
H(10B)	-1865(7)	260(20)	7331(5)	80
H(11A)	-1655(7)	-240(10)	6320(5)	80
H(11B)	-728(7)	-570(10)	6385(5)	80
H(12A)	-1119(6)	780(10)	5477(6)	80
H(12B)	-1460(6)	2120(10)	5819(6)	80
H(13A)	237(8)	4010(10)	5785(5)	80
H(14A)	-1270(10)	3570(10)	4995(5)	80
H(14B)	-430(10)	3420(10)	4812(5)	80
H(15A)	-923(8)	5760(10)	4498(6)	80
H(15B)	-69(8)	5890(10)	4924(6)	80
H(16A)	-1590(6)	6550(10)	5360(5)	80
H(16B)	-865(6)	7630(10)	5335(5)	80
H(17A)	-800(10)	6770(10)	6374(5)	80
H(17B)	20(10)	6560(10)	6159(5)	80
H(18A)	-1134(8)	4310(10)	6206(5)	80
H(19A)	1000(7)	3900(10)	8813(4)	80
H(20A)	2573(8)	3850(20)	9524(5)	80
H(20B)	1845(8)	3430(20)	9840(5)	80
H(21A)	2360(10)	5910(20)	10077(5)	80
H(21B)	1490(10)	5940(20)	9649(5)	80
H(22A)	2850(10)	6260(20)	9222(5)	80
H(22B)	2290(10)	7610(20)	9288(5)	80
H(23A)	2125(8)	6850(10)	8184(6)	80
H(23B)	1361(8)	6570(10)	8474(6)	80
H(24A)	2445(4)	4290(10)	8315(4)	80

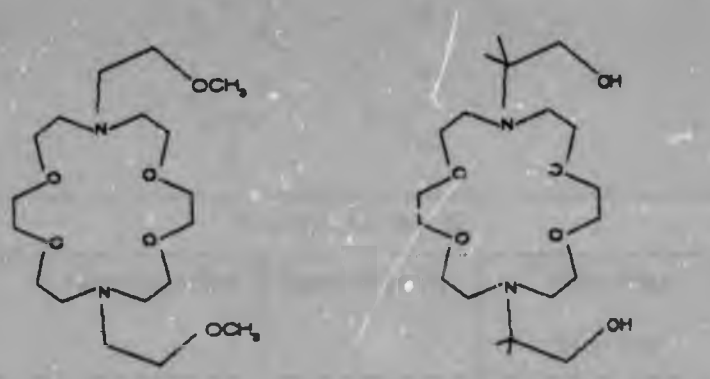
The conformation of the $[Sr(Cy_2\text{-}K22)H_2O]^{2+}$ cation is analogous to that reported (Hancock et al 1989b) for $[K(BHE\text{-}K22)]^{+}$ with the exception of the coordinated water because of the larger Sr^{2+} being able to attain a higher coordination number. The trend observed in the hydroxyethyl derivative should only be further enforced with the fusion of cyclohexylene groups on the pendant moieties, nevertheless what is apparent is that they are complete opposites in terms of their stabilities with complexed metal ions when adding the neutral oxygen donors.

STERICALLY AND STRUCTURALLY MORE COMPLEX PENDANT DONOR GROUPS WITH NEUTRAL OXYGEN DONORS

The examples given to us by nature highlight the need for investigating other pendant groups. *eg* Monensin with oxygen donors that are part of pendant tetrahydrofurfuryl groups.

It is necessary that other types of pendant groups be evaluated over and above the pendant donor groups containing neutral oxygens that are connected by simple ethylene bridges. More sterically demanding ligands based on K22 were initially synthesized by Gatto & Gokel (1984) and later by Damu et al (1991).

In both of the ligands below the simple hydroxyethyl group was modified structurally by the addition of methyl groups which resulted in interesting and novel effects on complex stability and selectivity towards metal ions.

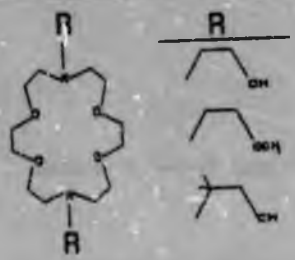


BME-K22 BDME-K22

Figure 66 : modifying the hydroxyethyl pendant group by the introduction of methyl groups

In the case of BME-K22 the methoxyethyl groups were brought about by the addition of methyl groups to the neutral oxygen donor of the pendant donor group. The ligand BDME-K22 has two methyl groups added to the carbon backbone of the ethylene bridge in the hydroxyethyl pendant donor. ie. the methyl groups are added as C-methyl groups.

TABLE 6 : formation constants for derivatives of K22 with metal ions of differing size.



	Pendant Group R			
	[a]hydroxyethyl	[b]methoxyethyl	[b]dimethyl hydroxy	[c]Ionic radius
$\log K_1$ Cu^{2+}	6.6	5.40	-	0.75
$\log K_1$ Cd^{2+}	7.96	3.93	6.12	0.95
$\log K_1$ Ca^{2+}	4.08	-	2.97	1.00
$\log K_1$ Sr^{2+}	4.05	3.23	2.69	1.17
$\log K_1$ Pb^{2+}	9.20	7.54	6.95	1.18
$\log K_1$ Ba^{2+}	5.3	3.72	2.73	1.36

[a] de Sousa et al 1991

[b] Damu et al 1991

[c] Shanon 1976

The two different ways of adding methyl groups to the ligand K22 produced effects on complex stability with respect to metal ion size that are remarkably opposite. Hancock & Martell (1989) in their review established as a general

rule that : ***addition of methyl groups to donor atoms, be they nitrogen or oxygen donors, of the ligand results in a drop in complex stability which is more pronounced for small than for large metal ions.***

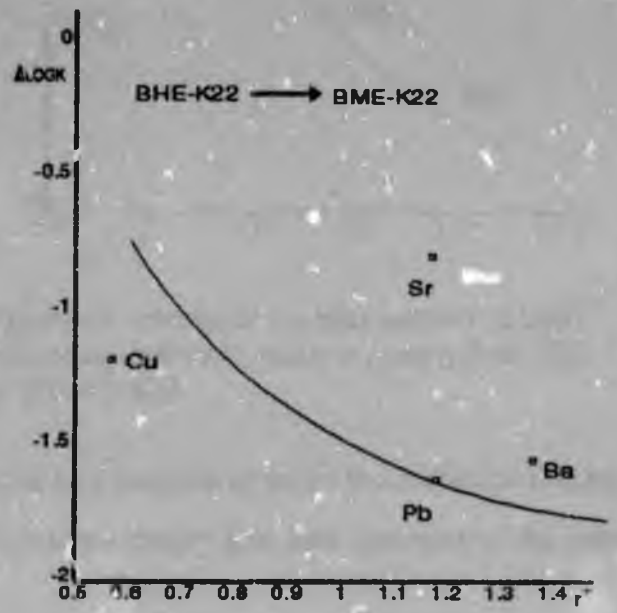


***Figure 67** : change in complex stability (ΔlogK) plotted against ionic radius in passing from BHE-K22 to BME-K22*

The plot of ΔlogK versus ionic radius in passing from BHE-K22 to BME-K22 shows the largest decrease in $LogK_1$ for the smaller metal ions (alkyl groups added to the donor atoms). The same plot for BHE-K22 through to BDME-K22 indicates the opposite effect and an inverse relationship exists between complex stability and metal ion size. A greater decrease in complex stability is observed for the larger metal ions with addition of C-methyl groups.

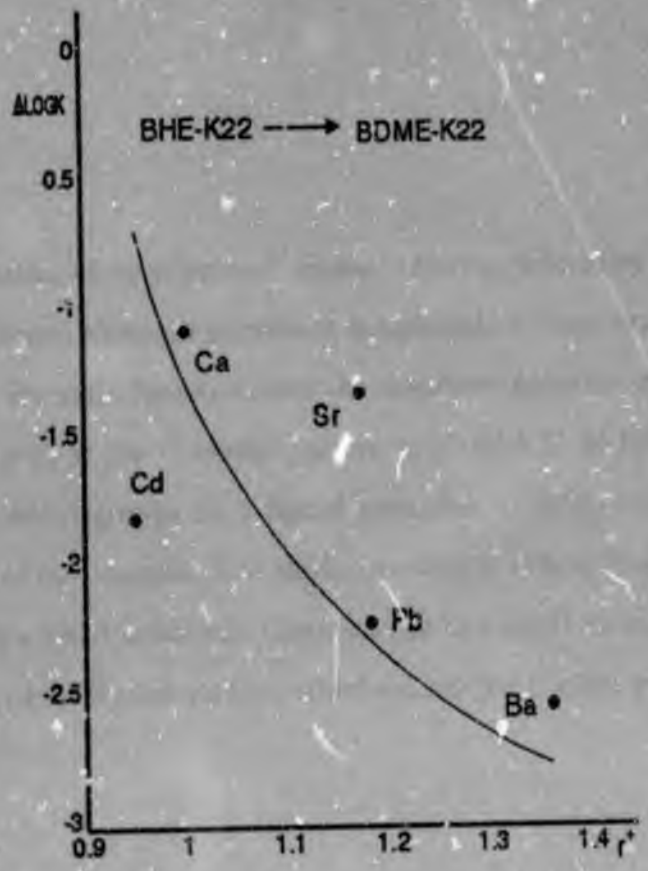


Figure 68 : change in complex stability (ΔlogK) plotted against ionic radius in passing from K22 to BDME-K22

ΔlogK when plotted as a function of metal ion radius for passing from EDTA to DMEDTA gives some insight into how quantitative the relationship is.

table 8 : Stability constants for EDTA and DMEDTA (Martell & Smith 1974-1989)

metal ion	Dmedta	Edta	ΔlogK
Cu	20.33	18.78	+1.55
Zn	17.02	16.45	+0.57
Cd	17.92	16.5	+1.42
Pb	17.42	18.0	-0.58
Sr	8.40	8.74	-0.34
La	15.43	1546	-0.03
Ba	6.98	7.84	-0.86

The phenomenon of cyclohexenyl groups altering selectivity in favour of smaller metal ions , although somewhat inexplicable at first, can be viewed as deriving from the same factors as does the selectivity patterns produced by C-alkyl groups; such as the C-methyl groups on BME-K22 or DMEDTA. The presence of C-alkyl groups on a ligand gives rise to steric crowding on the outer surface of the complex. The steric crowding is relieved when the ligand coordinates to a small metal ion. Coordination to a small metal ion increases the curvature of the ligand surface, which causes the C-alkyl groups to move further apart.

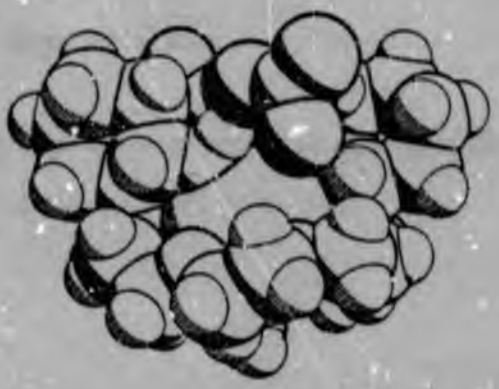


Figure 69 : spacefill diagram of Sr(Cy$_2$-K22) (de Sousa et al to be published)

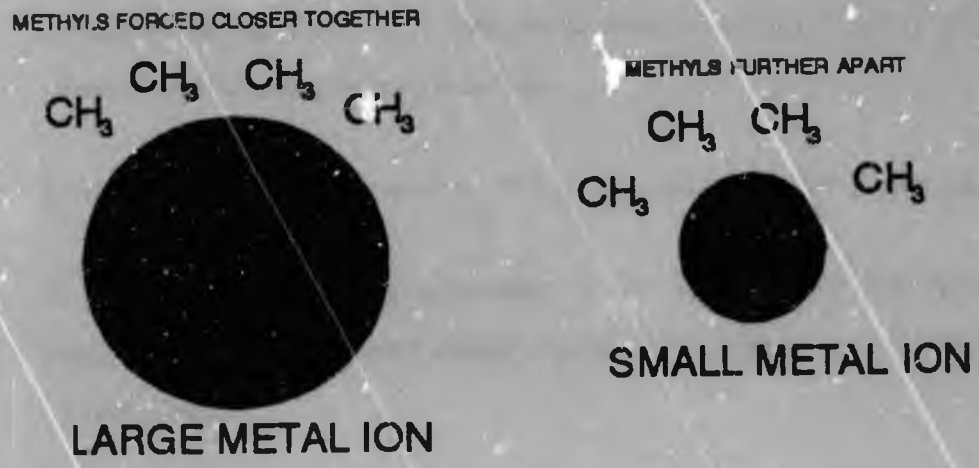


Figure 70 : increased curvature on complexation of small metal ions

The methyl groups are forced closer together on the outside of the complex of the larger metal ion by the smaller curvature of the ligand which leads to greater van der Waals repulsion between these methyl groups, and therefore for the complexes of the larger metal ions greater steric destabilisation.

Two additional rules may now be considered for ligand design :

1) addition of C-alkyl groups to ligands tends to increase the ligand selectivity for small relative to large metal ions

2) addition of alkyl groups to donor atoms of ligands tends to increase ligand selectivity for large relative to small metal ions.

These two rules can be viewed as additional tools to control selectivity for metal ions as a function of size. Ideally the addition of alkyl groups should also lead to an increase in the stability of the complexes; this situation

demands that the effects that tend to increase complex stability are not overshadowed by the overall increase in steric crowding. The increase of complex stability may be promoted by :

1) inductive effects of the added alkyl groups; increase atom donor basicity

2) preorganisation or pre-orientation of the free ligand; free ligand is constrained to be in a conformation required for complexation of metal ions (Cram 1983).

The concept of preorganisation is evident in the relationship between EDTA and DMEDTA. The syn conformer is more easily attained due to the steric repulsion of the C-methyl groups destabilising the anti conformation (Hancock 1995) . The effect of the two C-methyl groups on the ethylene bridge of DMEDTA is a lowering of the energy barrier between the anti conformer, preferred by the free ligand, and the syn conformer required to form the metal complex.

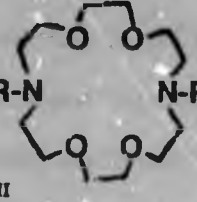
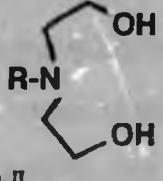
BALANCE BETWEEN INDUCTIVE AND STERIC EFFECTS ON THE THERMODYNAMIC STABILITY OF COMPLEXES

The inductive effect can contribute in a favourable manner if the steric conditions arising from the bulky electron releasing groups is accommodated. Neither of these effects can lead to a favourable contribution to complex stability by compromising the other. The introduction of N-alkyl groups to

existing ligands shows favourable effects on complex stability under sterically favourable conditions. Addition of C- alkyl groups to K22 to give DiMe-K22 (Damu & Maumela 1991) produces a slight increase in $\log K_1$ for the large Pb^{2+} ion, however, for the larger isopropyl group in Di-isoPr-K22 there is a drop in complex stability.

Small ligands do not show this trend. For small ligands of the nature R-$N(CH_2CHCH_3OH)_2$ there is a continuous steady increase in complex stability as R is increased in size along the series (Damu & Maumela et al 1991) :

$$CH_3- < (CH_3)_2CH- < (CH_3)_3C-$$

ligand, 	R = H	R= CH_3	R = $CH(CH_3)_2$	R = $C(CH_3)_3$
$\log K_1$ Pb^{II}	6.8	7.79	6.19	-
ligand 				
$\log K_1$ Pb^{II}	3.4	3.70	4.14	4.33

For the larger ligands based on K-22 there is a drop in complex stability of the large Pb^{2+} ion as R becomes increasingly more bulky than a methyl group. This indicates that the steric effects have completely outweighed the

inductive effects of the methyl groups.

In contrast to this the sterically favourable small R-N(CH_2CHCH_3OH)$_2$ ligands result in a steady increase in logK_1 even when R is the bulky tert-butyl group. This demonstrates that there exists a delicate balance between the steric destabilisation of the complex, and stabilisation due to inductive effects as R is simultaneously varied in size and inductive strength along the series (Hancock 1980, Hancock, Nakani, Marsicano 1983)

METHYL < ETHYL < ISO-PROPYL < TERT-BUTYL

Large metal ions tolerate placement of alkyl groups directly on the donor atoms rather better than on the carbon backbone because for these very large metal ions the donor atoms are further apart. This reduces the steric implications associated with C-alkyl groups. The alkyl groups on small ligands are better tolerated by large metal ions, because the issue of curvature of the ligand surface becomes less important, and an important consideration here is to avoid steric crowding with coordinated solvent molecules. Where steric interactions are with coordinated solvent molecules the most important factor is how far apart the donor atoms are, and as the metal ion gets larger so the donor atoms should get further apart. The unidentate ligands t-butylamine and triethylamine which are sterically crowded ligands appear to form no complexes with smaller metal ions, but do complex very large metal ions such as Ag^+ and Pb^{2+} (Hancock 1980, Hancock, Nakani Marsicano 1983 & Hancock and Martell 1995)

MOLECULAR MECHANICS STUDIES OF Cy_2-K22

Molecular mechanics calculations were done using the SYBYL program with the TAFF force field (Clark et al 1989) on an Iris work station. The atom coordinates were taken from the crystal structure of the strontium complex, $[Sr(Cy_2\text{-}K22)H_2O]$ (NO_3), and introduced in the force field for minimisations as a function of metal to nitrogen distance. The metal to oxygen distances were made 0.06Å smaller, characteristic of metal to oxygen bonds. The conformation adopted by the crystal structure was reproduced on each minimisation allowing for no change of conformation of the ligand. The parameters that were allowed to vary were the bond lengths between donors and the metal centre. From the fact that the coordination sphere of the strontium complex incorporates a coordinated water molecule, arises the question of steric crowding for the smaller metal ions. A plot in change of internal energy ΔU against the metal to nitrogen distance was obtained for the cationic complex species of $(Cy_2\text{-}K22)H_2O$ and $(Cy_2\text{-}K22)$. As would be expected from steric implications the smaller metal ions prefer the Cy_2-K22 cationic species with no coordinated water molecule, whereas the larger metal ions appear to be more stable by fuifilling their coordination number with a solvent water molecule. The point of intersection , r M-N=2.64Å although both parabolic curves have similar minima , suggests that metal ions with a radius of 1.18Å or larger will accommodate the coordination of a solvent water molecule. The metal ions such as Ba^{2+} and Pb^{2+} would in all likelihood be nine or ever ten coordinate, while Cu^{2+}, Ni^{2+} and Zn^{2+} would have great difficulty in coordinating water.

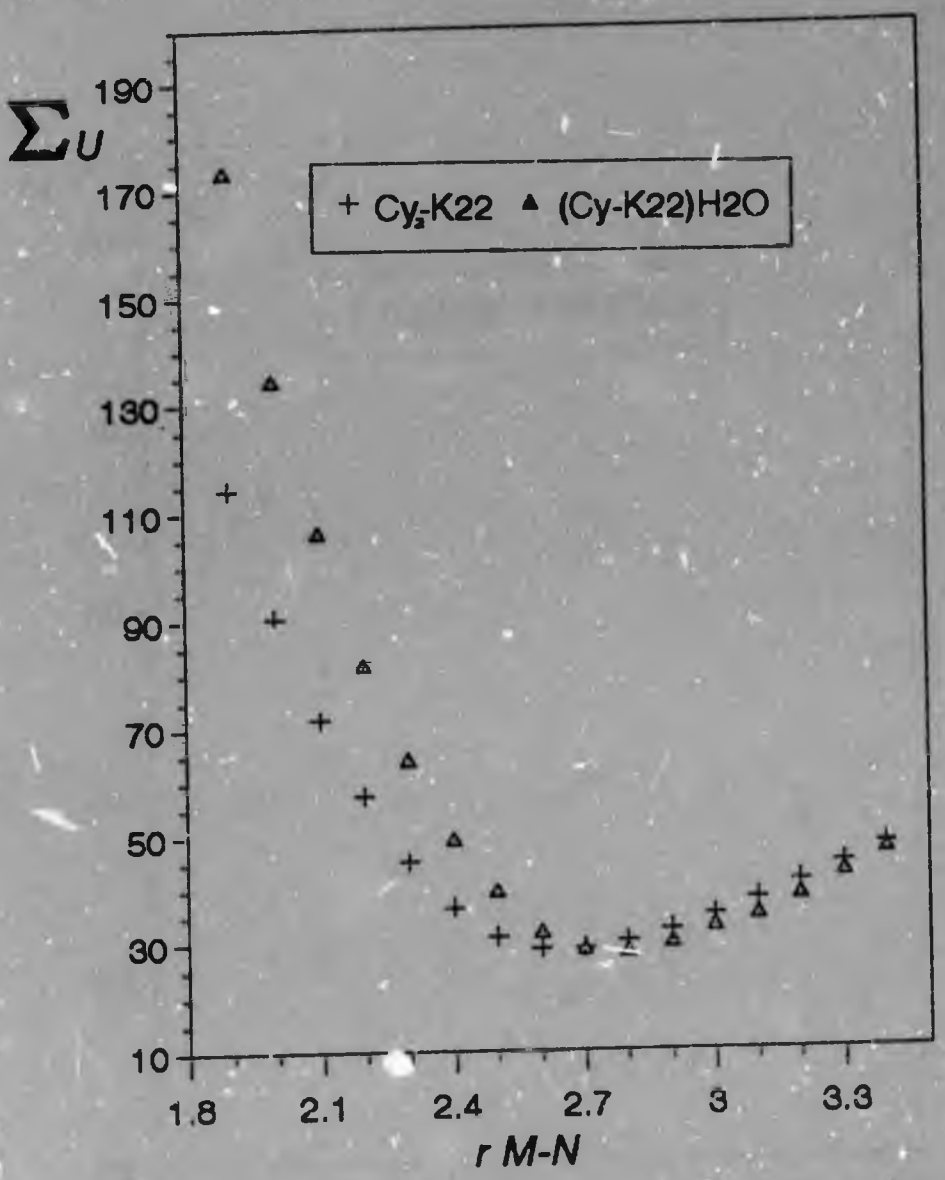


Figure 71 : change in internal energy as a function of M-N bond distance for Cy_2-K22 in comparison with $(Cy_2$-K22$)H_2O$.

A similar study is undertaken for Cy_2-K22 and its hydroxyethyl analogue. A plot is obtained that illustrates the difference in internal energy between the Cy_2-K22 and BHEK22.

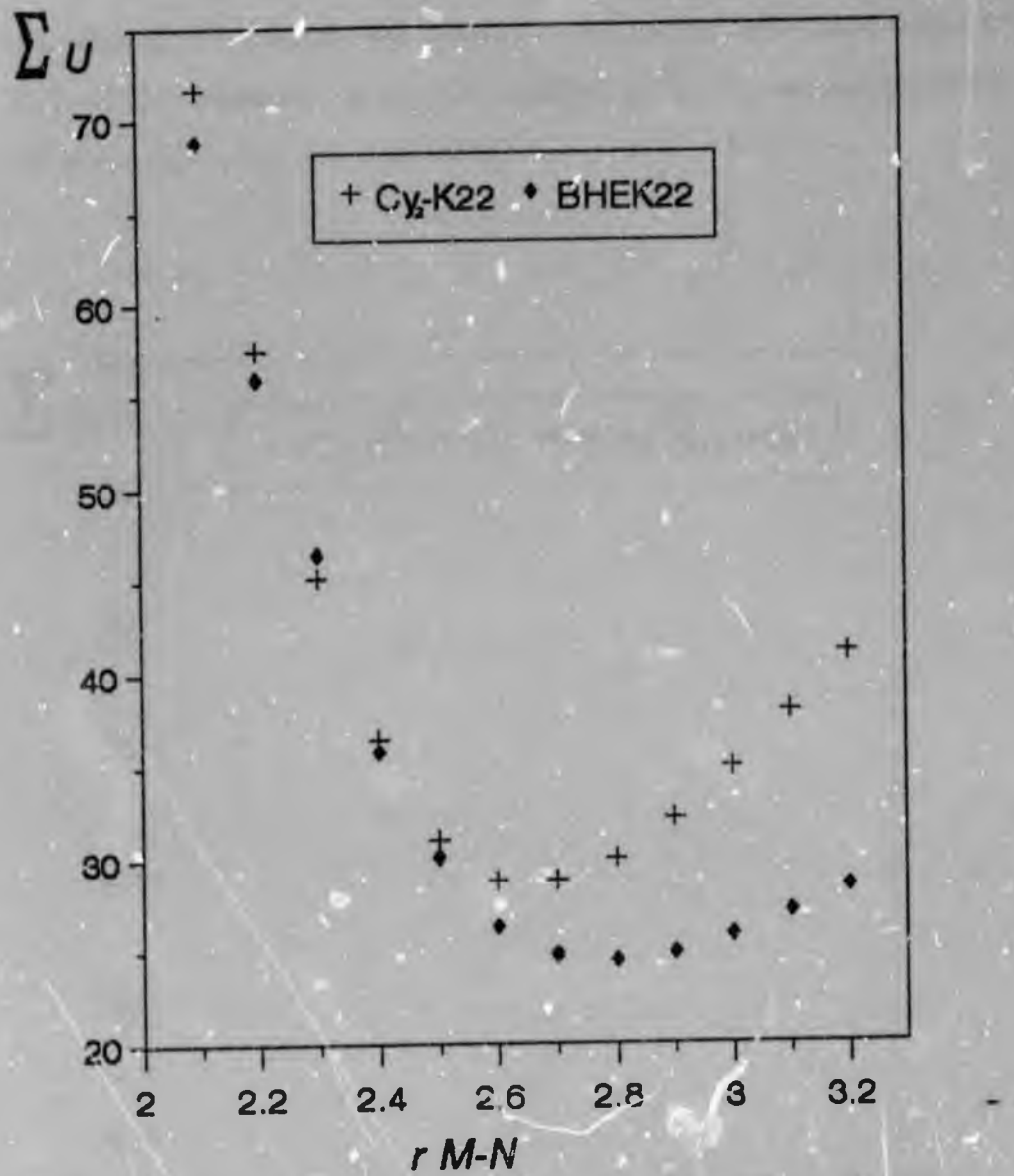


Figure 72 : change in internal energy as a function of M-N distance for Cy_2-K22 in comparison to BHEK22.

Arguably the complexes for the small metal (short M-N distances)ions are comparable in energy, what is immediately evident is the strong disfavouring of the cyclohexyl groups towards the large metal ions. From *r* M-N=2.5 Å (metal ions with ionic radius >1Å) the cyclohexyl bridged derivative becomes increasingly less stable than its ethylene bridged analogue. This is the

characteristic observed for the $\Delta \log K_1$ plot versus the metal ionic radius fro BHE-K22 in comparison to Cy_2-K22 reported earlier. A more accurate study will involve the solvation of the complex.

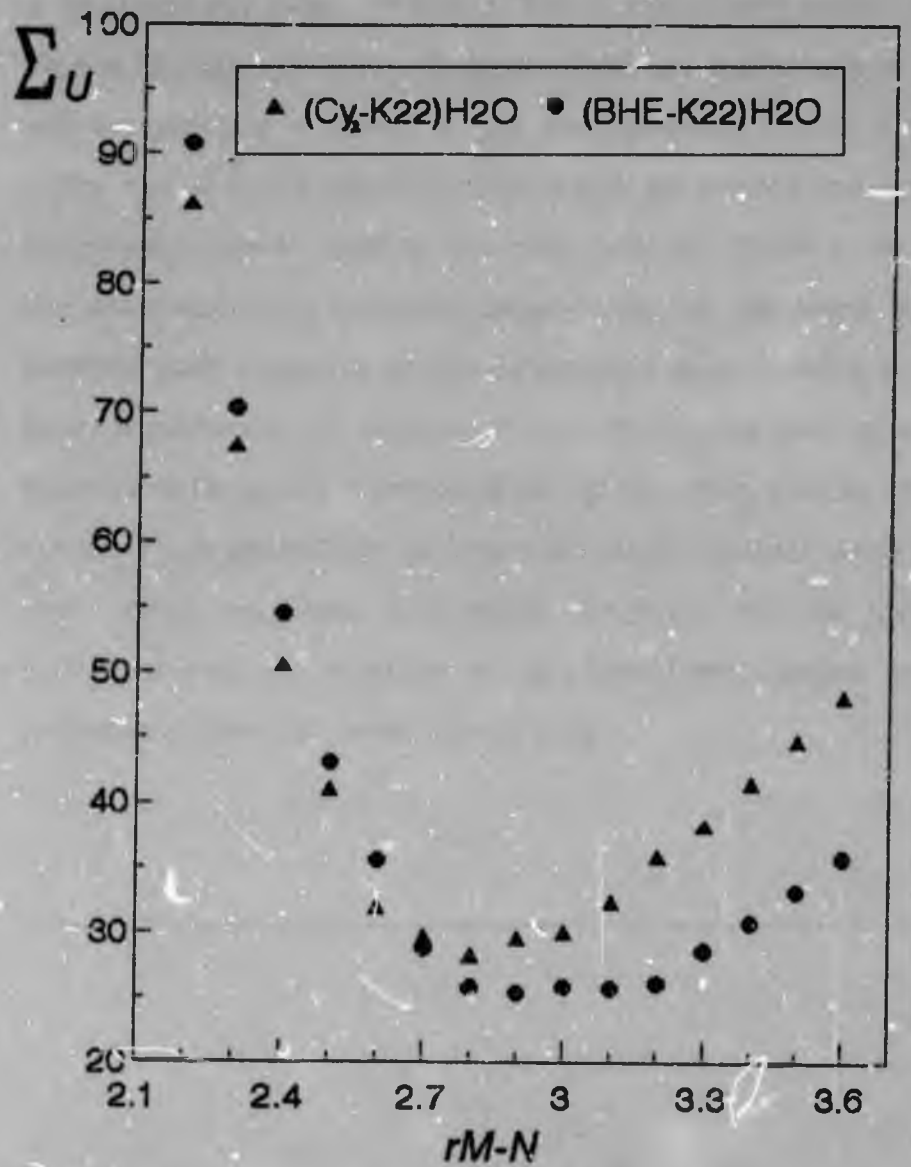


Figure 73 : changes in internal energy as a function of M-N bond distance for $(Cy_2\text{-}K22)H_2O$ in comparison with $(BHE\text{-}K22)H_2O$

Repeating the study with solvation of the coordination sphere by introducing a coordinated water molecule as was observed for the strontium complex reproduces the dissatisfaction of the hydroxycyclohexyl groups towards the large metal ions. The plot of internal energy versus M-N distance for the (Cy_2-K22)H_2O complex shows a minimum at r M-N=2.86 Å which corresponds to a metal of ionic radius r=1.40 Å. This is substantially smaller than that observed for the hydroxyethyl derivative which has its minimum at r=3.02 Å and can therefore be viewed as best accommodating a metal ion of ionic radius r=1.56 Å. It is noteworthy that in both the solvated and non-solvated coordination spheres used in the study with the TAFF force field the discrimination of the cyclohexyl moieties towards the larger metal ions manifests itself, suggesting that the unfavourable steric crowding at the metal centre is relieved by the decrease in the overwhelming steric crowding that results from the greater curvature of the ligand surface allowing for reduced van der Waals interactions. As is viewed from the internal energy plots the larger metal ions form more stable complexes with the hydroxyethyl derivatives were the crowding on the ligand outer surface is not the predominant factor for metal ion selectivity.

CHAPTER 5

PENDANT OXYGEN DONORS OF OPEN-CHAIN AMINES

The addition of pendant donors to existing ligands and/or the alterations made to the backbone of such ligands goes hand in hand with attempts to enhance complex stability and improve kinetic inertness by reducing demetallation. The replacement of the ethylene bridge between the nitrogen donors of EDTA by the cyclohexylene bridge to form CDTA is an elementary example of how complex stabilities and metal ion selectivities can be enhanced (Schwarzenbach et al 1954). The complexes of CDTA have formation constants that are up to five log units greater than their EDTA analogues, yet alarmingly the cyclohexylene bridge has not been used to any great extent in designing new ligands. Introduction of a more rigid cyclohexylene bridge results in a more highly preorganised ligand that can more easily adopt the conformation required for the complexation of metal ions. Brechiel and Jansow (1992) have reported DTPA (diethylenetriaminetetraacetic acid) analogues in which a trans cyclohexyl moiety is introduced, for the complexation of ^{212}Bi on cancer therapy applications. The reason for fusing a trans-cyclohexyl moiety into DTPA was to increase the steric rigidity in the complex and to improve the orientation of the chelating groups (de Sousa et al 1991), which greatly reduced the rate of loss of the ^{212}Bi in vivo.

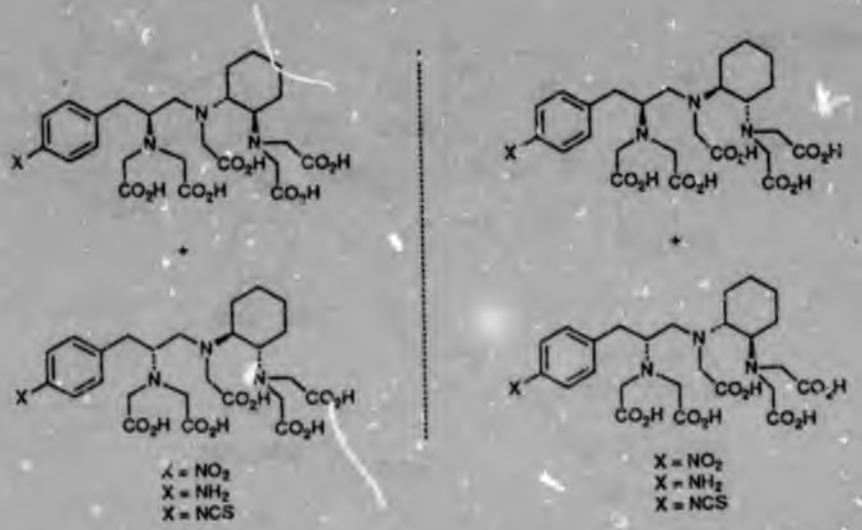
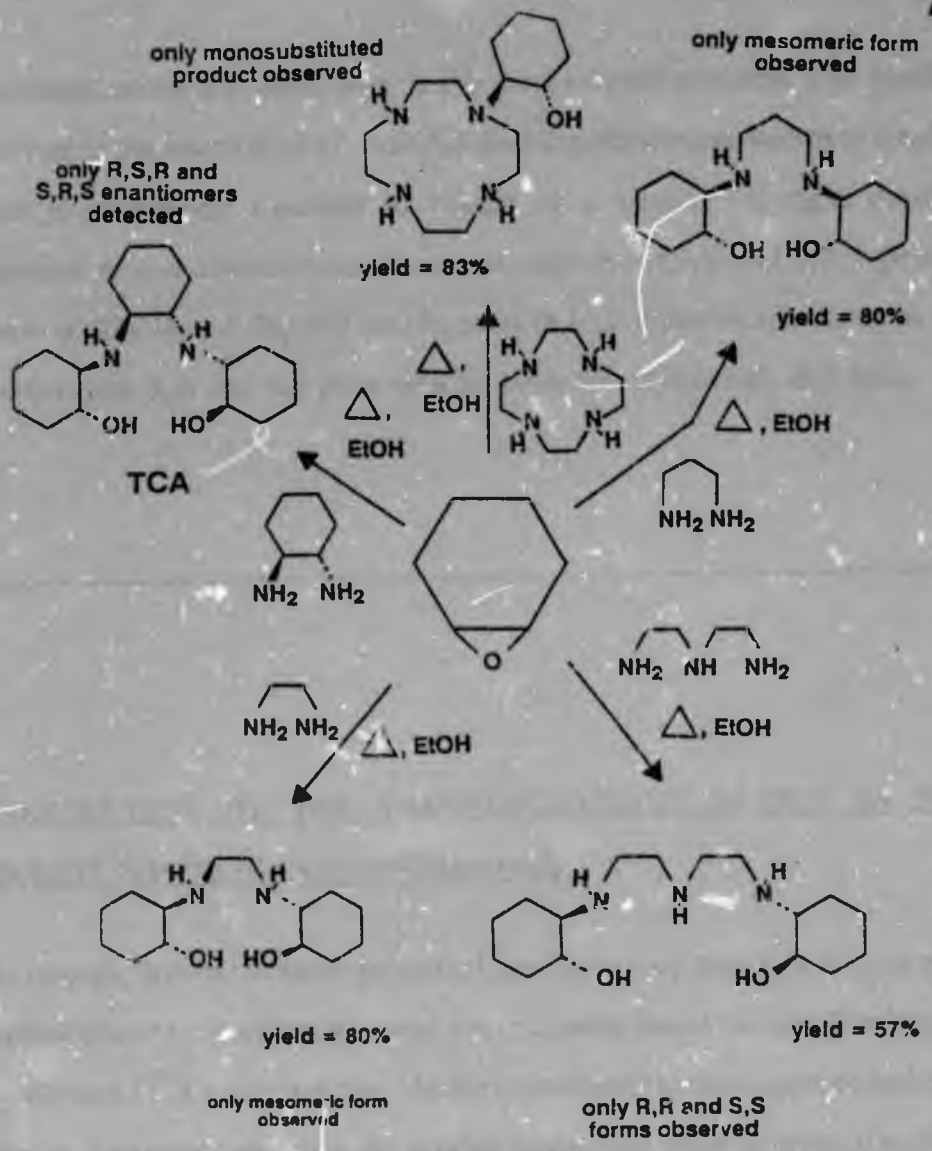


Figure 74 : C-functionalised cyclohexyldiethylenetriaminepenta-acid derivatives (Brechiel & Gansow 1992)

Recently de Sousa et al (1991) reported on the chemistry of ligands containing the cyclohexylene bridge. The ligands showed increased selectivity for the smaller metal ions as compared to their ethylene bridged analogues, and greater thermodynamic complex stability. The utility of cyclohexene oxide has been demonstrated in the synthesis of ligands containing 2-hydroxycyclohexyl pendant donor groups (Hancock & de Sousa 1995). The use of cyclohexene oxide in the synthesis of ligands produces pendant donor groups that are highly rigid and preorganised with a degree of diastereomeric selectivity.

Of particular importance in ligand synthesis using cyclohexene oxide and polyamines is the strong diastereoselectivity that prevails.



Reaction of cyclohexene oxide with diamines and triamines yield a single substitution product, that is crystalline, consisting only of a single enantiomer and its corresponding mirror image. When cyclohexene oxide is reacted with ethylenediamine only the N, N' disubstituted product is obtained; likewise only two cyclohexene oxide molecules react with trans-1,2-diaminocyclohexane to give the N, N' - Bis(2-hydroxycyclohexyl) product. Prolonged reactions with large excesses of the cyclohexene oxide still produces a disubstituted product and no trisubstitution or tetrasubstitution is observed. The reaction's strong

enantioselectivity is present even in the disubstituted products. The product spectrum in the reaction of *d,l*-trans-1,2-diaminocyclohexane with cyclohexene oxide is statistically expected to consist of a mixture of eight possible enantiomers and diastereomers, however, only the R,S,R and S,R,S pairs is observed. The ligand Cy_2-K22 also forms with high diastereoselectivity as the enantiomeric R,R and S,S pairs with no evidence of the *meso*-R,S form.

INTRODUCTION OF THE TRANS-CYCLOHEXYL MOIETY IN THE PENDANT DONOR GROUPS OF DIAMINES

The introduction of the trans-cyclohexyl pendant group results in a more rigid pendant donor that influences metal ion selectivity based on size. The ligands Cy_2-EN and TCA each have two 2-hydroxycyclohexyl pendant groups and both show an increased selectivity for smaller metal ions when compared to their analogues having only ethylene bridges. The constants for the ligand Cy_2-EN and its analogue is compared in the table below were $\log K_1$ values for complexes of Cy_2-EN and DHEEN are shown.

TABLE 1 : protonation and formation constants of Cy_2-EN and DHEEN showing the effect of cyclohexyl bridges on complex stability in relation to metal ion size.

metal ion	ionic radius	DHEEN $logK_1$	Cy_2-EN $logK_1$	$\Delta logK_1$
pK_1	-	9.24	9.66	-
pK_2	-	6.26	6.62	-
Cu^{2+}	.57	9.68	11.47	+1.78
Ni^{2+}	.69	6.67	7.77	+1.10.
Zn^{2+}	.74	4.79	6.18	+1.39
Cd^{2+}	.95	5.07	5.69	+0.62
Pb^{2+}	1.18	6.12	6.56	+0.44

[a] from Martell & Smith 1974-1989

[b] at 25°C and 0.1M ionic strength

The introduction of the cyclohexylene bridges on the pendant arms resulted in an increase in complex stability for all the metal ions studied. This increase in stability as observed from the $logK_1$ values was not uniform, but an influence on metal ion selectivity becomes apparent. The smaller metal ions such as Cu^{2+}, Ni^{2+} and Zn^{2+} are favoured by the more rigid bridging over the larger Cd^{2+} and Pb^{2+} ions.

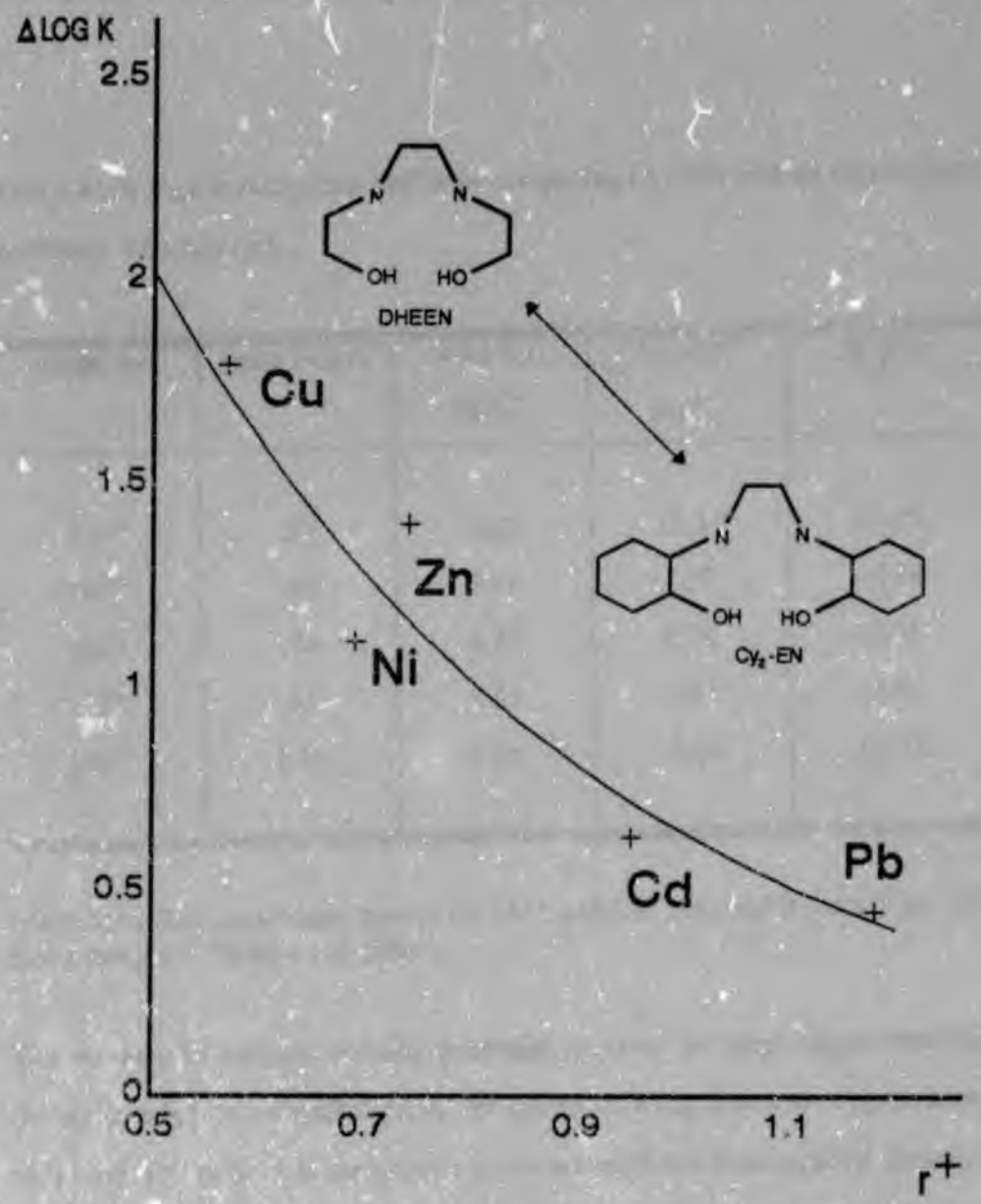


Figure 75 · change in complex stability when comparing DHEEN and Cy_2-EN

The effect is more pronounced when comparing the constants of Cy_2-EN with another of its analogues containing only ethylene bridges between donor atoms. The macrocycle 12-ane-N_2O_2 can be considered as an analogue of Cy_2-EN, despite its macrocyclic character, since it consists of the same number and

type of donor atoms linked together by ethylene bridges only.

TABLE 2 : change in complex stability in comparing Cy_2-EN with its macrocyclic analogue 12-ane-N_2O_2 .

metal ion	ionic radius	12-ane-N_2O_2 $\log K_1$ *	Cy_2-EN $\log K_1$	$\Delta \log K_1$
Cu^{2+}	.57	8.66	11.47	+2.81
Ni^{2+}	.69	5.91	7.77	+1.86
Zn^{2+}	.74	6.22	6.18	-0.04
Cd^{2+}	.95	6.55	5.69	-0.86
Pb^{2+}	1.18	6.34	6.56	+0.22

* data for 1,7-dioxa isomer, except for Pb^{2+} and Cu^{2+} for which data is for 1,4-dioxa isomer (Thom et al 1986)

The increase in complex stability generally observed for large metal ions with the addition of hydroxyalkyl groups or groups bearing ethereal oxygens is not observed. The benefit of the greater donor strength of a hydroxyalkyl chelating group appears to have been neglected for the large metal ions, and the high strain resulting from steric crowding around the small metal ion (Thom et al 1986) seems to be overcome by a favourable energy of complexation. The cause of this novel size-selective behaviour that arises when ethylene bridges are replaced with cyclohexenyl bridges seems to be the greater curvature of the ligand when it is coordinated to a small metal ion, which relieves steric

crowding on the outer side of the ligand caused by the bulky cyclohexenyl bridges.

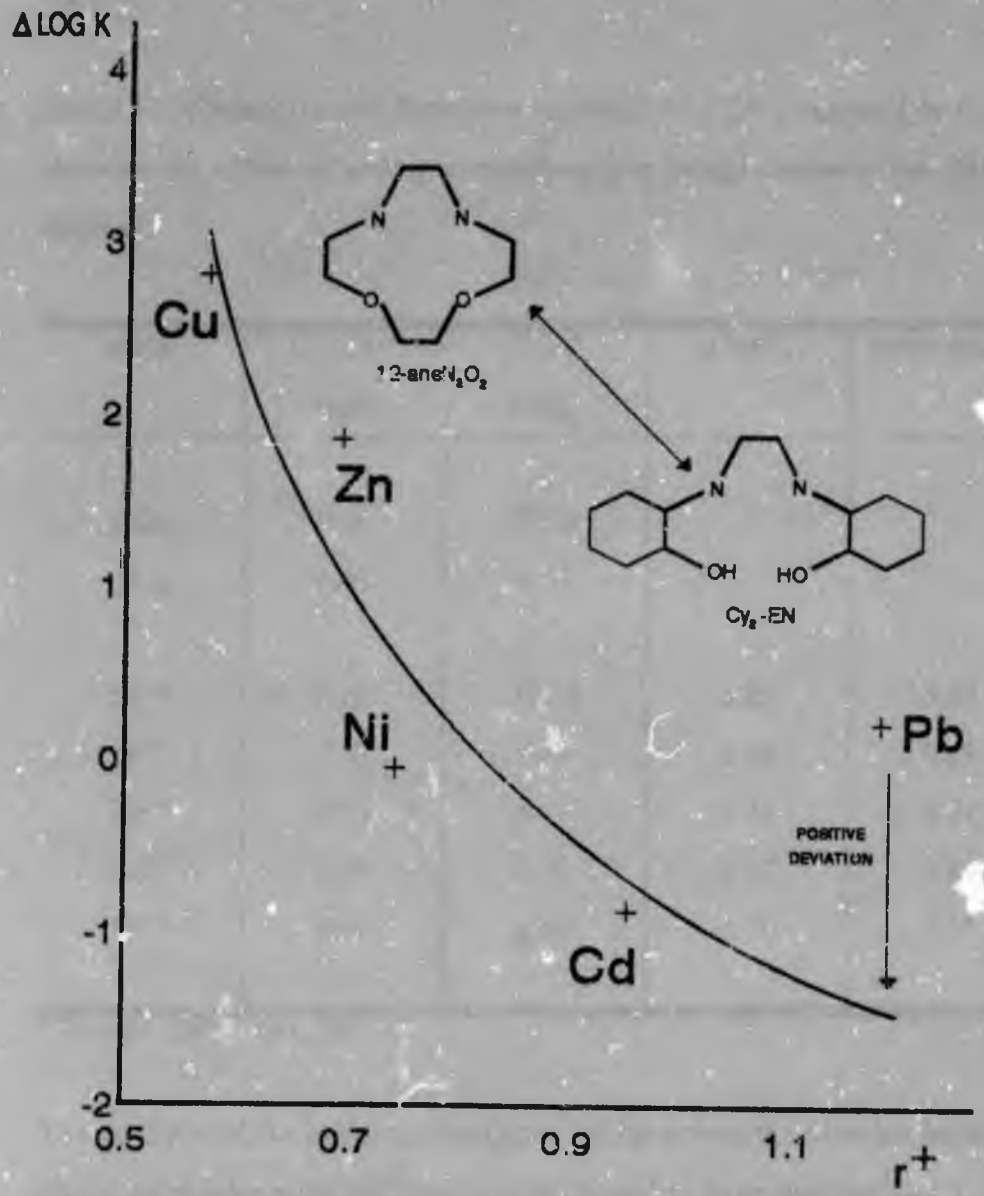


Figure 76 : plot of change in complex stability relating to metal ion size when passing from 12-ane-N_2O_2 to Cy_2-EN

By analogy to EDTA and CDTA the ligand pairs of Cy_2-EN and TCA should display a similar level of preorganisation since both pairs of ligands have a cyclohexylene bridge fused to the diamine backbone. In addition to this the

change in complex stability in passing from Cy_2-EN to TCA should have a similar trend to that observed for EDTA through to CDTA (de Sousa et al 1991).

TABLE 3 : protonation and formation constants of TCA compared to Cy_2-EN showing the effect of adding a cyclohexylene bridge between the nitrogen donors.

metal	Cy_2-EN[a] $\log K_1$	TCA[a] $\log K_1$	$\Delta \log K_1$	ionic radius
pKa_1	9.66	9.54	-	-
pKa_2	6.62	4.52	-	-
Cu^{2+}	11.47	11.50	0.03	0.57
Ni^{2+}	7.77	6.84	-0.93	0.69
Zn^{2+}	6.18	4.77	-1.41	0.74
Cd^{2+}	5.69	4.08	-1.61	0.95
Pb^{2+}	6.56	4.80	-1.76	1.18

[a] Temp= 25°C I=0.1M

The addition of the bulky cyclohexylene bridge across the diamine backbone places emphasis on the preference of the ligand to wrap itself around a metal ion that is smaller so as to relieve the steric strain caused by the cyclohexylene bridges pushed against each other. Repulsive van der Waals interactions brought about by crowding on the outer surface of the ligand are responsible for the decrease in complex stability with increasing metal ion

size. The smaller curvature of the ligand when complexing a large metal ion causes the carbon backbone of the cyclohexylene bridges to be brought closer together resulting in an unfavourable steric strain.

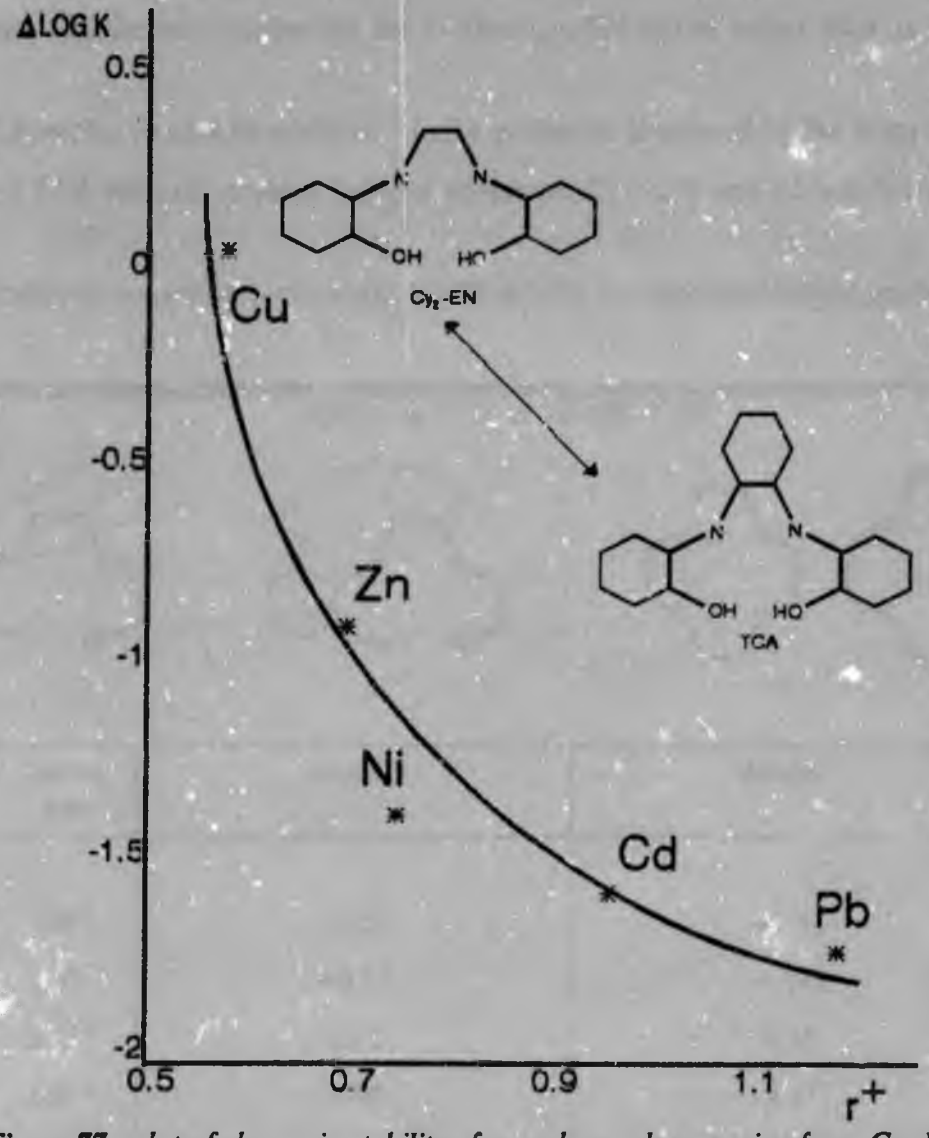


Figure 77 : plot of change in stability of complexes when passing from Cy_2-EN to TCA

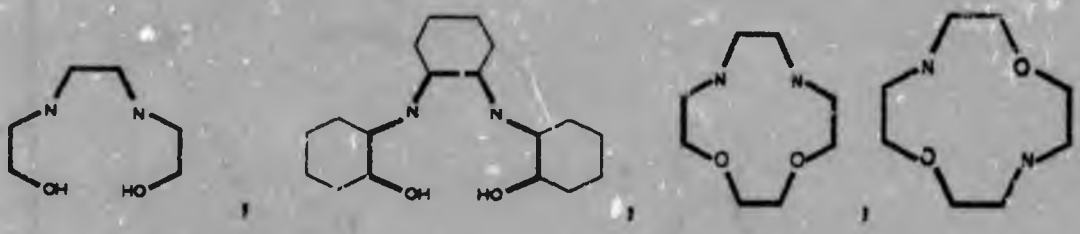
The fact that large metal ions are unable to tolerate placement of alkyl groups on the carbon backbone is clearly illustrated in the relationship between Cy_2-EN and TCA. Complexes of the large metal ions have reduced stabilities of

approximately 2 log units with only the Cu^{2+} complex showing a small enhancement of 0.03 log units. The issue of curvature is more important in the larger, more bulky, TCA ligand and the larger metal ions are able to tolerate the cyclohexenyl bridges on the smaller Cy_2-EN ligand better than on TCA.

Crowding caused by additional bulky groups is illustrated by the comparison of TCA with its ethylene bridged analogues DHEEN and 12-ane-N_2O_2.

TABLE 4 : comparison of $\Delta logK_1$ for TCA with the ethylene bridged analogues.

DHEEN TCA 12-ANE-N_2O_2



metal ion	$\Delta logK^a$	$\Delta logK^b$
Cu^{2+}	+1.82	+2.84
Ni^{2+}	+0.17	+0.93
Zn^{2+}	-0.02	-1.45
Cd^{2+}	-0.99	-2.47
Pb^{2+}	-1.32	-1.54

[a] $logK_1$(TCA)-$logK_1$(DHEEN) [b] $logK_1$(TCA)-$logK_1$(12-ane-N_2O_2)

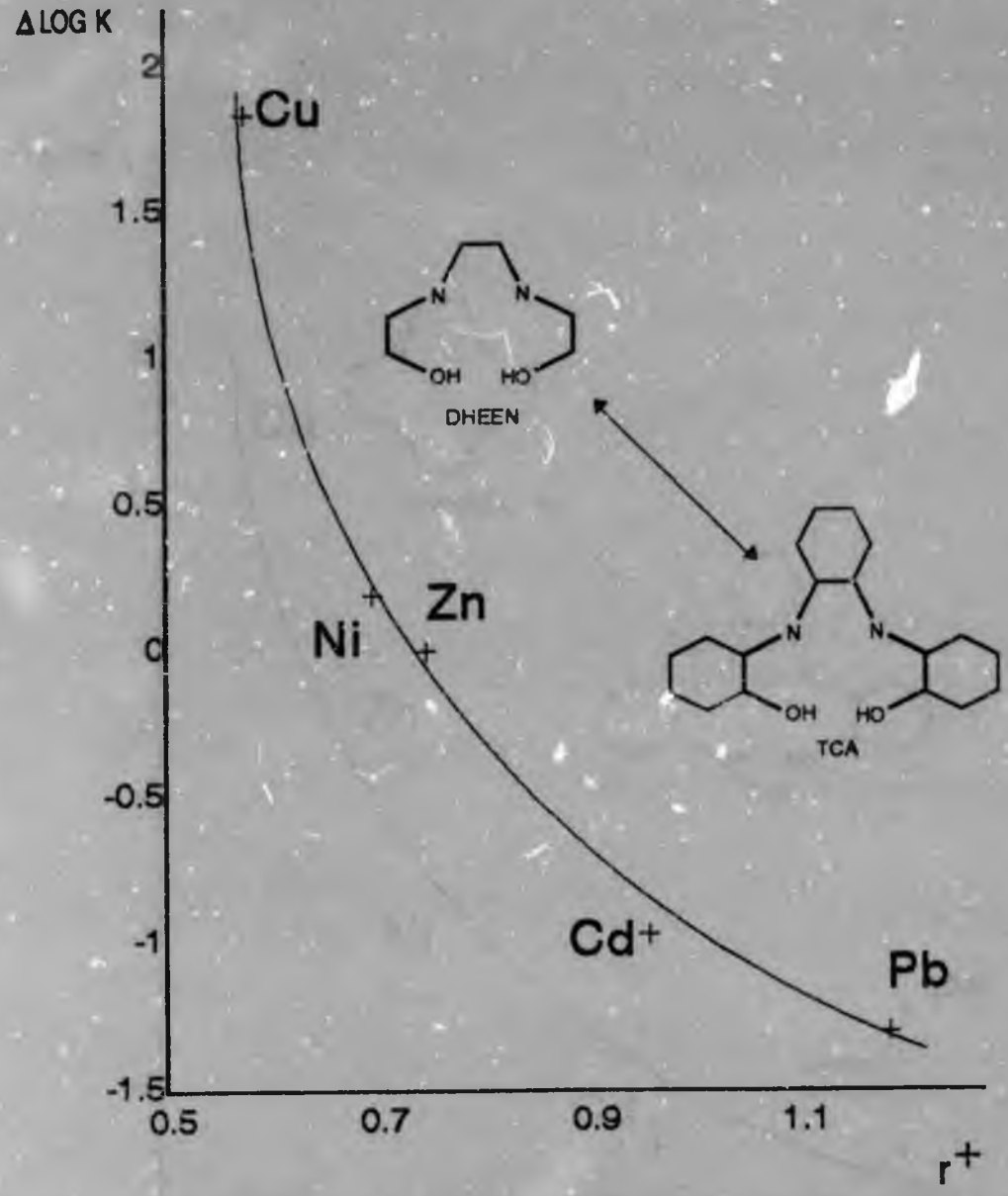


Figure 78 · plot of ΔlogK for DHEEN passing through to TCA

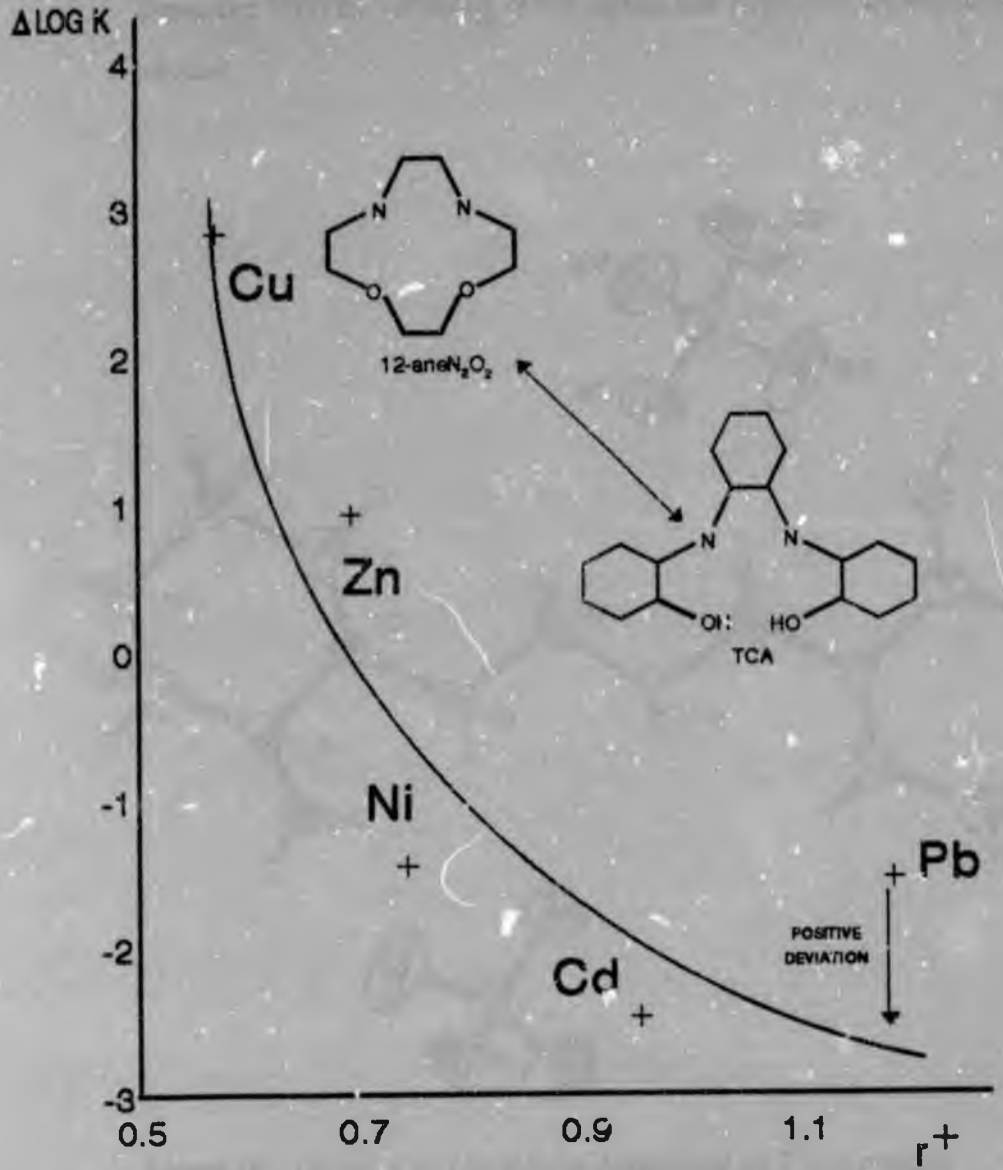


Figure 79 : plot of ΔlogK for 12-ane-N_2O_2 through to TCA

STRUCTURE OF Cy_2-EN

To facilitate the crystallisation of the free ligand Cy_2-EN it was necessary to synthetically convert it to a diperchlorate salt. The perchlorate counter ions were chosen due to the relative ease by which crystallise when compared to the other ions in the literature, such as nitrates or chlorides. The figure below shows the ORTEP drawing of the ligand and indicates the atomic numbering scheme.

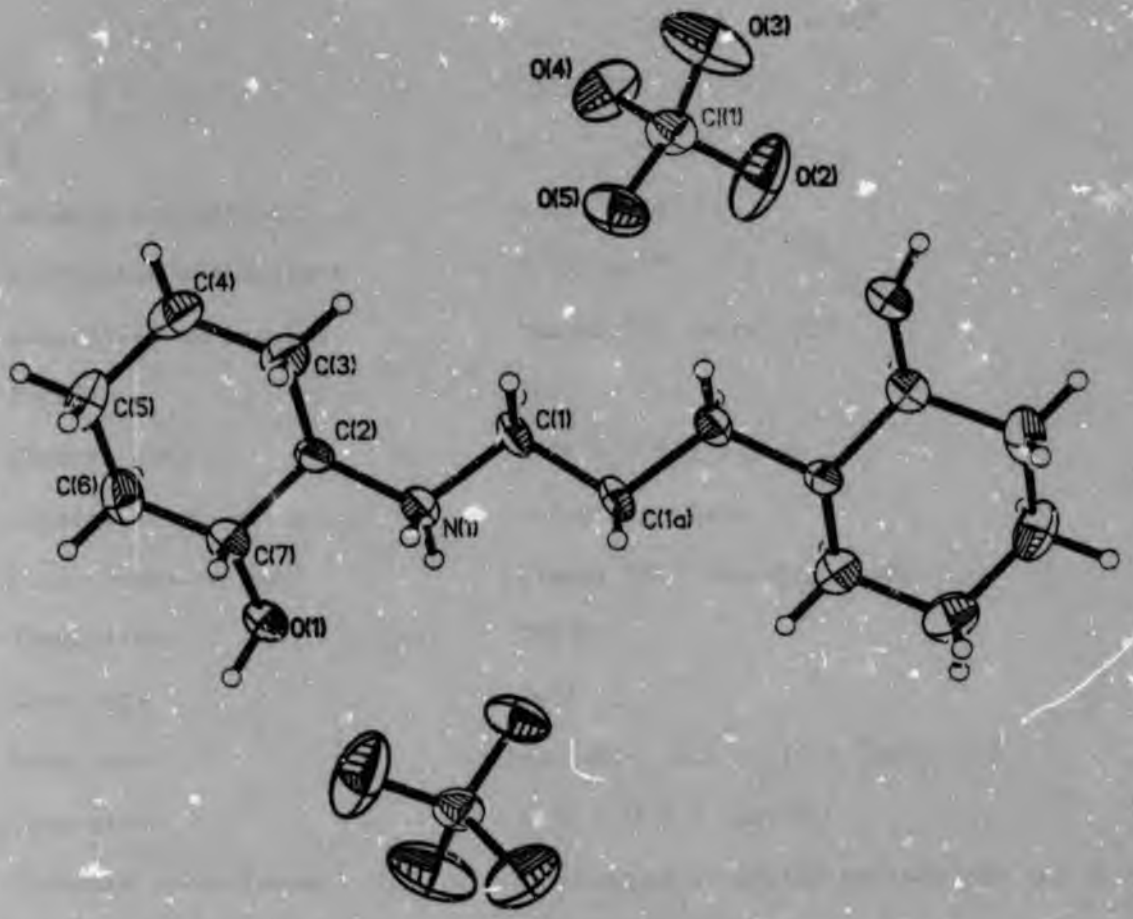


Figure 80 : structure of Cy_2-EN as determined by X-ray analysis

TABLE OF CRYSTAL DATA AND STRUCTURE REFINEMENT

Empirical formula	$C_4H_{5.25}Cl_{0.25}NO_{3.25}$
Formula weight	129.21
Temperature	293(2) K
Wavelength	0.71073 Å
Crystal system	Monoclinic
Space group	$P\ 2_1/n$
Unit cell dimensions	a = 7.034(3) Å α = 90° b = 20.276(6) Å β = 105.80(2)° c = 7.475(2) Å γ = 90°
Volume	1025.8(6) $Å^3$
Z	4
Density (calculated)	0.837 Mg/m^3
Absorption coefficient	0.134 mm^{-1}
Absorption correction	Tmax=0.999 Tmin=0.958
F(000)	270
Crystal size	0.04 x 0.2 x 0.2 mm
Crystal color and habit	colorless plate
Diffractometer used	Rigaku AFC5 rotating anode
Temperature	298°K
Scan type	θ-2θ
Scan speed	variable; 4.0 to 16.0 °/min
Scan width	1.78 + 0.3 x tan(θ)
Standard reflections	3 measured every 150 reflections (no decay)
θ range for data collection	2.01 to 25.03°
Index ranges	$0 \le h \le 8$, $0 \le k \le 24$, $-8 \le \ell \le 8$
Reflections collected	1965
Independent reflections	1815 (R_{int} = 0.0972)

Refinement method	Full-matrix least-squares on F^2 SHELXL-93 (Cray-FPS 500, MicroVaxII)
Data / restraints / parameters	1799 / 0 / 127
Goodness-of-fit on F^2	1.005
Final R indices [$I>2\sigma(I)$]	R1 = 0.0707, wR2 = 0.1415
R indices (all data)	R1 = 0.1796, wR2 = 0.2107
Largest and mean Δ/σ	0.0001, 0.0001
Largest diff. peak and hole	0.526 and -0.356 $eÅ^{-3}$

The excellent diastereomeric selectivity of the reaction between ethylenediamine and cyclohexene oxide is emphasized by X-ray analysis of the crystals revealing the disubstituted product to be the *meso* form. The free ligand adopts the skew arrangement, as did EDTA, that is unsuitable for complexation with the OH groups of the hydroxycyclohexyl groups lying on opposite sides of the plane define by the ethylenediamine bridge.

TABLE OF ATOMIC COORDINATES [$\times 10^4$] AND EQUIVALENT ISOTROPIC DISPLACEMENT PARAMETERS [$(\text{Å})^2 \times 10^3$]

	x	y	z	U(eq)
Cl(1)	2353(2)	748(1)	5403(2)	35(1)
O(1)	-5504(5)	517(2)	11583(5)	32(1)
O(2)	2520(10)	80(3)	4930(8)	84(2)
O(3)	4155(7)	1083(3)	5498(7)	78(2)
O(4)	819(7)	1047(2)	3994(6)	60(2)
O(5)	1975(7)	786(3)	7157(5)	54(1)
N(1)	-1887(6)	469(2)	10854(6)	26(1)
C(1)	-499(8)	326(3)	9723(8)	27(1)
C(2)	-3237(8)	1054(3)	10223(7)	24(1)
C(3)	-2076(9)	1672(3)	10106(9)	41(2)
C(4)	-3492(11)	2255(3)	9596(11)	53(2)
C(5)	-4735(11)	2327(3)	10976(10)	49(2)
C(6)	-5870(9)	1705(3)	11084(9)	40(2)
C(7)	-4459(8)	1127(3)	11600(7)	29(1)

Hydrogen bonding occurs between the perchlorate and the nitrogens in the ethylenediamine bridge accounting for the lack of disorder associated with perchlorates.

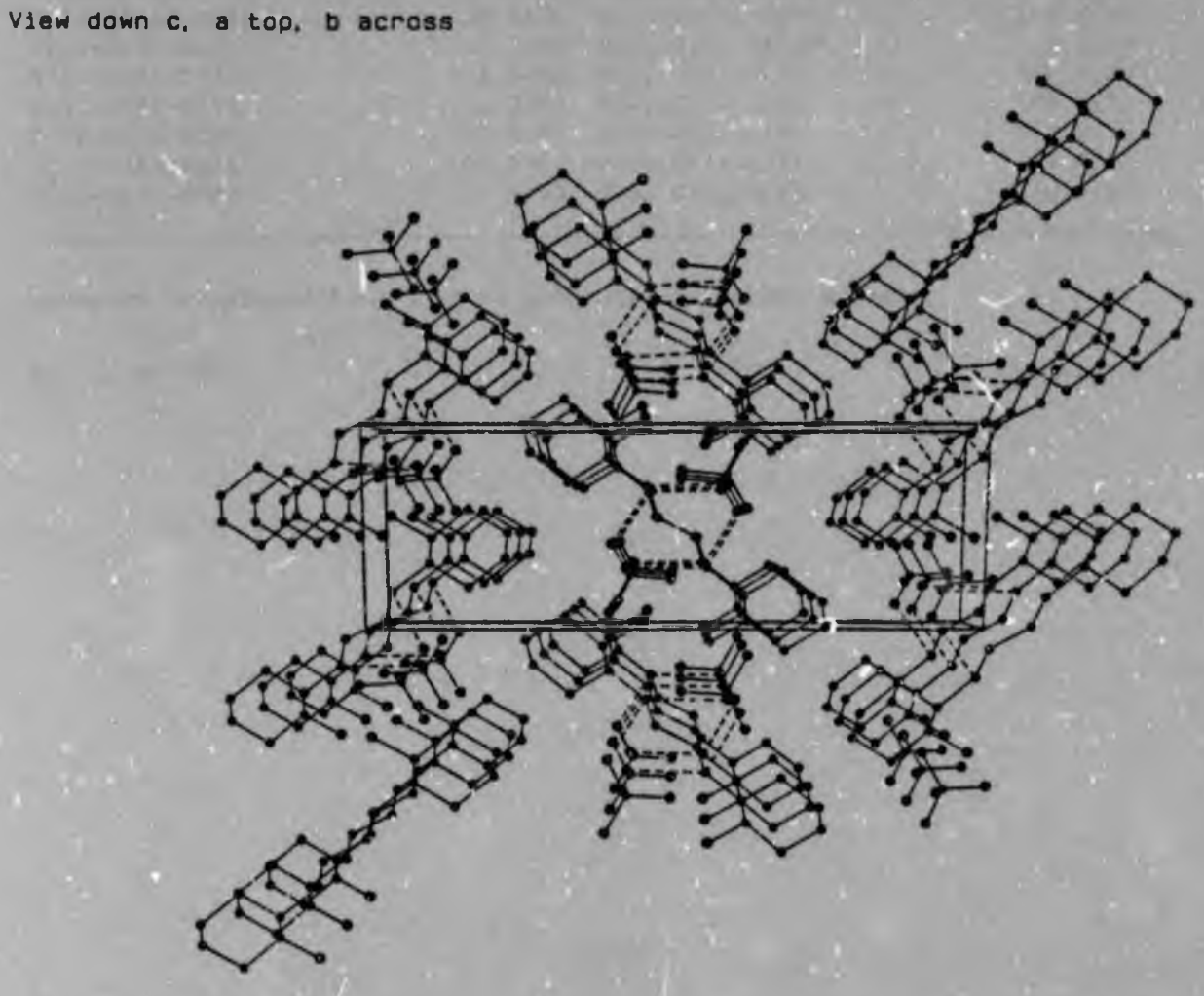


Figure 81 : three dimensional view illustrating hydrogen-bonding between the molecules packed in the lattice

TABLE OF BOND LENGTHS [Å] AND ANGLES [°]

Cl(1)-O(5)	1.411(4)	Cl(1)-O(2)	1.412(5)
Cl(1)-O(3)	1.419(5)	Cl(1)-O(4)	1.424(5)
O(1)-C(7)	1.437(7)	N(1)-C(1)	1.484(6)
N(1)-C(2)	1.513(7)	C(1)-C(1)#1	1.500(11)
C(2)-C(3)	1.511(8)	C(2)-C(7)	1.518(7)
C(3)-C(4)	1.526(9)	C(4)-C(5)	1.530(9)
C(5)-C(6)	1.507(9)	C(6)-C(7)	1.515(8)

O(5)-Cl(1)-O(2)	109.5(3)	O(5)-Cl(1)-O(3)	108.7(3)
O(2)-Cl(1)-O(3)	109.9(4)	O(5)-Cl(1)-O(4)	111.4(3)
O(2)-Cl(1)-O(4)	108.6(3)	O(3)-Cl(1)-O(4)	108.7(3)
C(1)-N(1)-C(2)	115.5(4)	N(1)-C(1)-C(1)#1	110.2(6)
N(1)-C(2)-C(3)	111.4(4)	N(1)-C(2)-C(7)	106.8(4)
C(3)-C(2)-C(7)	111.9(5)	C(2)-C(3)-C(4)	109.3(5)
C(3)-C(4)-C(5)	111.0(6)	C(6)-C(5)-C(4)	111.4(5)
C(5)-C(6)-C(7)	109.9(5)	O(1)-C(7)-C(6)	111.4(5)
O(1)-C(7)-C(2)	107.0(4)	C(6)-C(7)-C(2)	110.8(5)

Symmetry transformations used to generate equivalent atoms:

#1 -x,-y,-z+2

TABLE OF ANISOTROPIC DISPLACEMENT PARAMETERS

The anisotropic displacement factor exponent takes the form:
$-2\pi^2 [(ha^*)^2 U_{11} + \ldots + 2hka^*b^*U_{12}]$

	U11	U22	U33	U23	U13	U12
Cl(1)	37(1)	44(1)	20(1)	3(1)	4(1)	1(1)
O(1)	29(2)	37(3)	33(2)	0(2)	15(2)	-3(2)
O(2)	120(5)	50(4)	67(4)	-17(3)	-1(4)	34(4)
O(3)	50(3)	137(6)	49(3)	4(3)	15(3)	-34(4)
O(4)	60(3)	58(4)	45(3)	13(2)	-15(3)	1(3)
O(5)	70(3)	70(4)	29(2)	0(2)	24(2)	-5(3)
N(1)	24(3)	33(3)	22(2)	0(2)	9(2)	3(2)
C(1)	20(3)	32(4)	34(3)	-7(3)	15(3)	-2(3)
C(2)	23(3)	28(3)	25(3)	5(2)	10(3)	2(3)
C(3)	41(4)	38(4)	48(4)	10(3)	17(3)	6(3)
C(4)	61(5)	30(5)	73(5)	10(4)	28(4)	-1(4)
C(5)	55(5)	26(4)	61(5)	-3(3)	12(4)	10(4)
C(6)	35(4)	47(5)	39(4)	-3(3)	9(3)	11(3)
C(7)	27(3)	33(4)	25(3)	-3(3)	7(3)	-3(3)

TABLE OF HYDROGEN COORDINATES [$\times 10^4$] AND ISOTROPIC DISPLACEMENT PARAMETERS

	x	y	z	U(eq)
H(1E)	-5900(5)	486(2)	12557(5)	80
H(1C)	-1179(6)	539(2)	12037(6)	80
H(1D)	-2635(6)	108(2)	10843(6)	80
H(1A)	485(8)	666(3)	9916(8)	80
H(1B)	-1205(8)	320(3)	8428(8)	80
H(3A)	-1352(9)	1616(3)	9197(9)	80
H(3E)	-1147(9)	1754(3)	11288(9)	80
H(4A)	-4350(11)	2190(3)	8369(11)	80
H(4B)	-2753(11)	2653(3)	9592(11)	80
H(5A)	-5644(11)	2687(3)	10618(10)	80
H(5B)	-3874(11)	2423(3)	12183(10)	80
H(6A)	-6794(9)	1620(3)	9901(9)	80
H(6B)	-6598(9)	1757(3)	11991(9)	80
H(7A)	-3597(8)	1197(3)	12823(7)	80

STRUCTURE OF TCA

The ligand was dissolved in acetone with mild heating to render a very dilute solution. Crystals were obtained on cooling and evaporation. No counter ions were included as the free ligand was not converted to any mineral acid salt, hence the search for heavy atoms in the refinement process would prove futile. The Patterson search for assigning heavy atoms was not necessary and the structure was solved using direct methods of refinement. Great difficulty was encountered in collecting a feasible data set that would allow for sufficient parameterisation for solving the structure. The data set limited a more accurate structure determination because of the small number of measured reflections. The unique reflections used in the solution proved to be insufficient for a more precise refinement as is elucidated by the high value of the R-factor and the exceptional standard deviations associated with bond parameters especially with bond angles. The structure obtained is adequate for the purpose of indicating the orientation of the two hydroxycyclohexyl groups relative to Cy_2-EN and $[Cu(TCA)]^{2+}$.

The ORTEP diagram of the free ligand with the numbering scheme clearly illustrates that the hydroxycyclohexyl groups are orientated in a more trans conformation in comparison to the Cy_2-EN skew orientation.

TABLE OF CRYSTAL DATA AND STRUCTURE REFINEMENT

formula	$C_{18}H_{34}N_2O_2$
mol. wt	310.98
crystal colour	white
crystal system	monoclinic
space group	$C2/_c$
a	12.027(2)
b	17.789(4)
c	10.414(2)
α	90.01(1)
β	122.82(2)
γ	89.99(2)
z	4
V	1872.42
ρ	1.103 (calc)
	1.092 (measured)
abs. coeff	0.4
radiation	.71073
F(000)	690
scan mode	ω -2θ
scan speed	0.60-2.75
ω -scan angle	0.60+0.35tanθ
theta range	10.43<θ<23.30
range h,k,l	32,26,15
crystal dimensions	0.43×0.39×0.28
reflections measured	609
unique reflections	471
used reflections	471
parameters refined	101
final R	0.1301

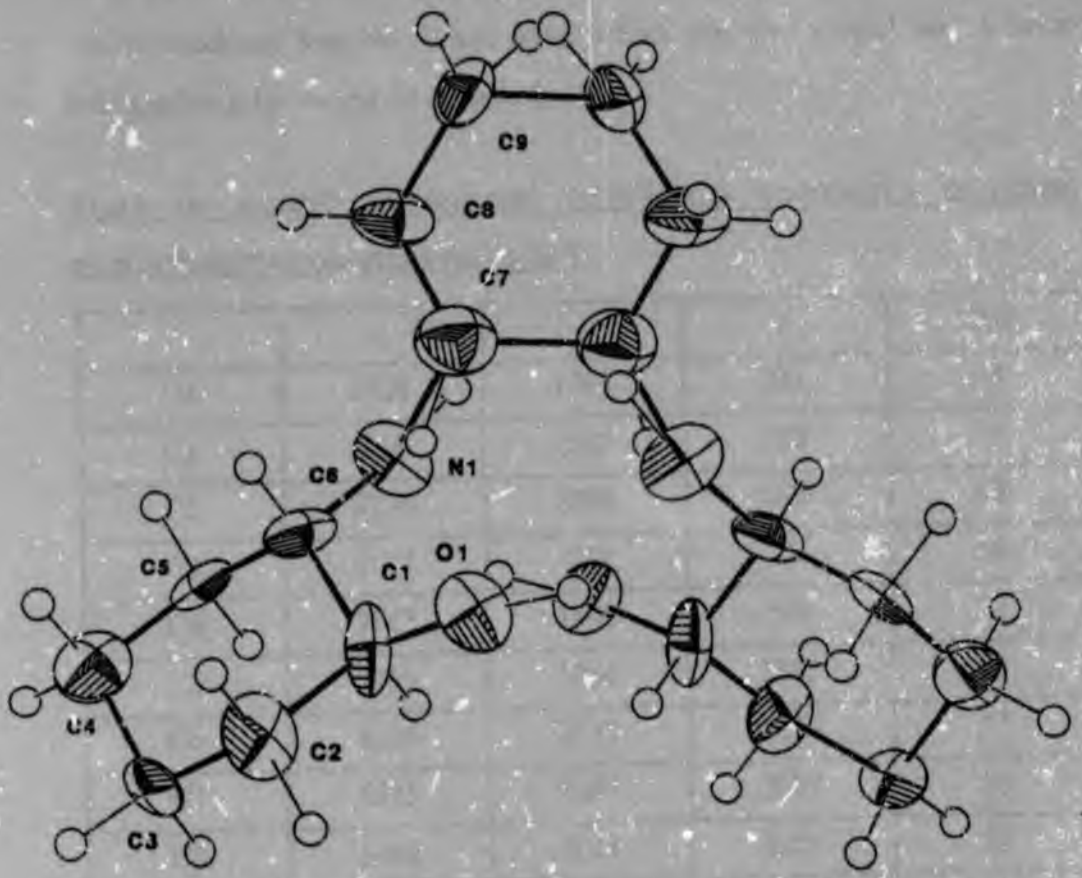


Figure 82 : ORTEP diagram of free TCA ligand in the trans conformation

The ligand crystallises in the C2/c space group and the asymmetric unit consists of only half the molecule (through the C_2 axis of symmetry) with the symmetry related atoms being generated by the symmetry transformations.

The TCA ligand is analogous to CDTA concerning the conformation which the free ligand adopts. The crystal structure clearly shows the choice of a trans arrangement which is the conformer ideal for metal ion complexation. The bulky hydroxycyclohexyl groups that preferred the skew arrangement in Cy_2-EN to minimise van der Waals interactions are now forced into a trans conformation by the cyclohexylene bridge.

TABLE OF ATOMIC COORDINATES [$\times 10^4$] AND EQUIVALENT ISOTROPIC DISPLACEMENT PARAMETERS [$(Å)^2 \times 10^3$]

	x	y	z	Ueq
O1	3926	1785	267	58
C1	5209	1545	783	70
C2	5134	1088	-529	60
C3	6507	770	-3	66
C4	7547	1402	590	72
C5	7565	1864	1862	64
C6	6205	2177	1297	52
C7	5323	3297	2017	52
C8	6080	4014	2229	72
C9	5284	4698	1953	60
N1	6303	2613	2568	47

TABLE OF BOND LENGTHS [Å] AND ANGLES [°]

O1-C1	1.396(19)	C2-C1-O1	107.2(1.5)
C1-C2	1.551 (23)	C6-C1-O1	114.0(1.6)
C1-C6	1.513(23)	C6-C1-C2	111.0(1.5)
C2-C3	1.538(22)	C3-C2-C1	109.9(1.5)
C3-C4	1.540(23)	C4-C3-C2	110.8(1.5)
C5-C4	1.550(24)	C5-C4-C3	111.3(1.6)
C6-C5	1.513(21)	C6-C5-C4	110.6(1.6)
N1-C6	1.483(22)	N1-C6-C1	111.7(1.6)
N1-C7	1.569(19)	N1-C6-C5	107.4(1.5)
C7-C8	1.513(23)	C9-C8-C7	113.1(1.5)
C7-C7*	1.570(34)	C5-C6-C1	110.2(1.4)
C8-C9	1.477(23)		
C9-C9*	1.615(33)		

TABLE OF ANISOTROPIC DISPLACEMENT PARAMETERS

	u11	u22	u33	u23	u13	u12
O1	36(6)	57(2)	42(9)	6(7)	9(6)	3(6)
C1	49(9)	79(8)	40(6)	12(5)	28(8)	6(3)
C2	53(7)	57(2)	64(4)	-1(0)	52(2)	7(2)
C3	89(8)	36(7)	64(9)	-10(2)	52(2)	7(2)
C4	54(2)	46(5)	77(5)	16(2)	34(1)	6(3)
C5	53(9)	37(8)	76(1)	0(6)	40(4)	7(4)
C6	49(5)	34(1)	62(1)	14(7)	29(8)	-3(0)
N1	36(8)	67(0)	34(9)	-14(2)	15(3)	6(0)
C7	35(0)	47(9)	59(1)	6(6)	15(2)	8(8)
C8	62(9)	52(0)	65(3)	-9(7)	32(5)	-6(6)
C9	89(0)	40(7)	65(3)	4(0)	55(6)	8(5)

TABLE OF HYDROGEN COORDINATES AND ISOTROPIC DISPLACEMENT PARAMETERS

H	Xa	Yb	Zc	Ueq
1	3319	1524	616	71.6
2	5564	1206	1793	
3	4804	1450	-1503	
4	4442	630	-845	
5	6793	368	901	
6	6460	494	-955	
7	8512	1156	1045	
8	7315	1771	-346	
9	8258	2323	2197	
10	7870	1505	2835	
11	5868	2539	321	
12	6297	3029	3319	
13	4557	2717	3193	
14	3597	4010	3558	
15	3067	4031	1614	
16	4632	5043	2145	
17	5162	5022	4089	

STRUCTURE OF $[Cu(TCA)](ClO_4)_2$

The copper complex was synthesized as described in the section on synthesis in the chapter on experimental procedure. $[Cu(TCA)]^{2+}$ crystallises in the space group C2/c as did the free ligand.

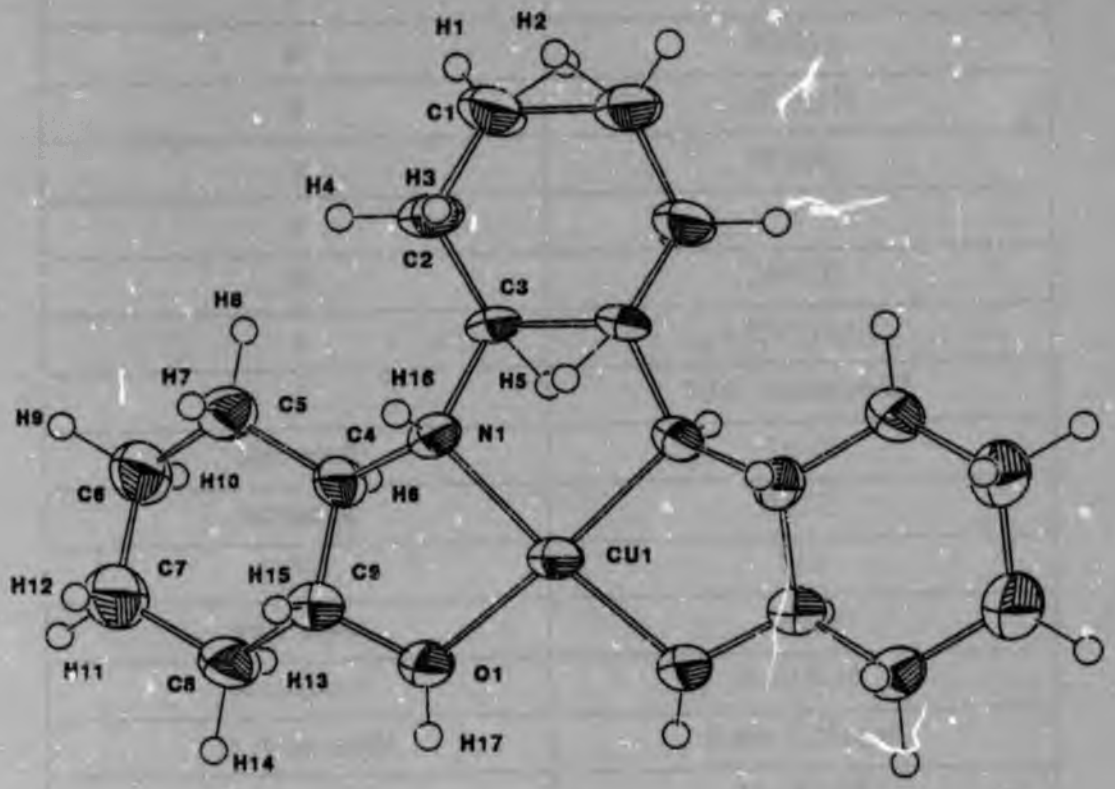


Figure 83 : ORTEP diagram of $[Cu(TCA)]^{2+}(ClO_4)_2$

TABLE OF CRYSTAL DATA AND STRUCTURE REFINEMENT

formula	$C_{18}H_{34}N_2O_{10}CL_2Cu$
mol. wt	572.93
crystal colour	blue
crystal system	monoclinic
space group	$C2/_c$
a	14.175(1)
b	19.249(2)
c	9.214(1)
α	90.0(0)
β	103.86(1)
γ	90.0(0)
z	4
V	2440.95
ρ	1.559 (calc)
	1.543 (measured)
abs. coeff	11.75
radiation	.71073
F(000)	715
scan mode	ω -2θ
scan speed	0.60-5.49
ω -scan angle	0.60+0.35tanθ
theta range	11<θ<20
range h,k,l	26,34,9
crystal dimensions	0.22×0.15×0.09
reflections measured	5306
unique reflections	1150
used reflections	985
parameters refined	153
final R	0.0563

The asymmetric unit solves for half of the structure; the symmetry transformations generate the symmetry related atoms. The copper centre occupies a special position and is given a site occupancy of 0.5.

TABLE OF ATOMIC COORDINATES [$\times 10^4$] AND EQUIVALENT ISOTROPIC DISPLACEMENT PARAMETERS [$(Å)^2 \times 10^3$]

	x	y	z	Ueq
CL	1225	-1419	1453	54
O1	601	-2012	1167	73
O2	733	-847	525	67
O3	1439	-1231	2988	94
O4	2103	-1567	1021	94
CU	0000	1010	2500	46
C1	548	3706	2406	68
C2	732	3050	1577	52
C3	564	2422	2512	41
N1	769	1739	1781	39
C4	1784	1465	2245	40
C5	2529	1880	1627	49
C6	3532	1522	2095	64
C7	3465	755	1498	67
C8	2710	359	2113	58
C9	1721	712	1608	45
O5	1008	369	2236	48

TABLE OF BOND LENGTHS [Å] AND ANGLES [°]

O1-CL	1.428(7)	O2-CL-O1	107(4)
O2-CL	1.464(7)	O3-CL-O1	111.2(5)
O3-CL	1.421(8)	O4-CL-O2	110.3(5)
O4-CL	1.422(8)	O4-CL-O1	109.55(5)
N1-CU	1.985(7)	O4-CL-O2	108.3(5)
O5-CU	1.947(6)	O4-CL-O3	109.7(6)
C2-C1	1.530(4)	O5-CU-N1	885.9(3)
C1-C1*	1.603(2)	C3-C2-C1	107.5(9)
C3-C2	1.537(1)	N1-C3-C2	110.9(8)
N1-C3	1.536(1)	C3-N1-CU	106.3(5)
C3-C3*	1.593(7)	C4-N1-C3	116.6(7)
C4-N1	1.496(1)	O5-CU-O5	101.3(4)
C5-C4	1.538(1)	N1-CU-N1	90.1(4)
C4-C9	1.557(2)	C5-C4-N1	114.2(7)
C6-C5	1.545(1)	C9-C4-N1	104.8(7)
C7-C6	1.570(4)	C9-C4-C5	109.1(8)
C8-C7	1.529(3)	C6-C5-C4	109.4(8)
C9-C8	1.527(3)	C7-C6-C5	110.3(8)
O5-C9	1.439(1)	C8-C7-C6	109.1(9)
		C9-C8-C7	109.8(8)
		C8-C9-C4	109.4(8)
		O5-C9-C4	105.0(7)
		O5-C9-C8	110.8(8)
		C9-O5-CU	111.5(5)

The Cu-N bond lengths are 1.985 Å which is approximately 0.02 Å shorter than the characteristic Cu-N bond length. The Cu-O bond length of 1.947 Å is shorter and defines the plane of the metal centre that includes all of the donor atoms i.e. the nitrogen and oxygen donors lie in a plane in which the metal ion is contained. The oxygen labelled O_2, associated with the perchlorate is a distance 2.750 Å away from the metal centre and may be viewed as being coordinated to the copper forming an octahedral geometry

around the metal . If this is the interpretation chosen , the octahedron appears to be completely distorted with the axially coordinated perchlorates occupying positions that are very near the plane of the nitrogen and oxygen donors. The O_2 oxygen of the perchlorate however, is 2.797 Å away from the coordinated oxygen of the hydroxycyclohexyl pendant. The correct interpretation therefore includes the possibility of hydrogen bonding between the O_2 and O_5 on the pendant group.

The complex is therefore square planar with the copper having a coordination number of four. The ligand wraps itself around the copper encapsulating the metal with the use of the pendant donor groups.

The N_1 - Cu - N_1 angle is 90.1°, and the O_5 - Cu - N_1 angle is 85.9° showing little deviation from a square planar geometry. The shorter bond of Cu-O (0.04 Å shorter than the Cu-N bond) together with the C_4 - N_1 - C_3 angle of 116.6° suggests movement of the cyclohexyl groups away from each other to minimise van der Waals repulsive interactions.

Comparing the structure of the complex with that of the free ligand we notice that the cyclohexyl groups are forced closer together as they coordinate the copper ion. This will occur even more for the larger metal ions, which explains the stability and selectivity trends observed. It is understandable why there is only a slight increase in stability of the copper complex, as this already shows the cyclohexyl groups being forced together.

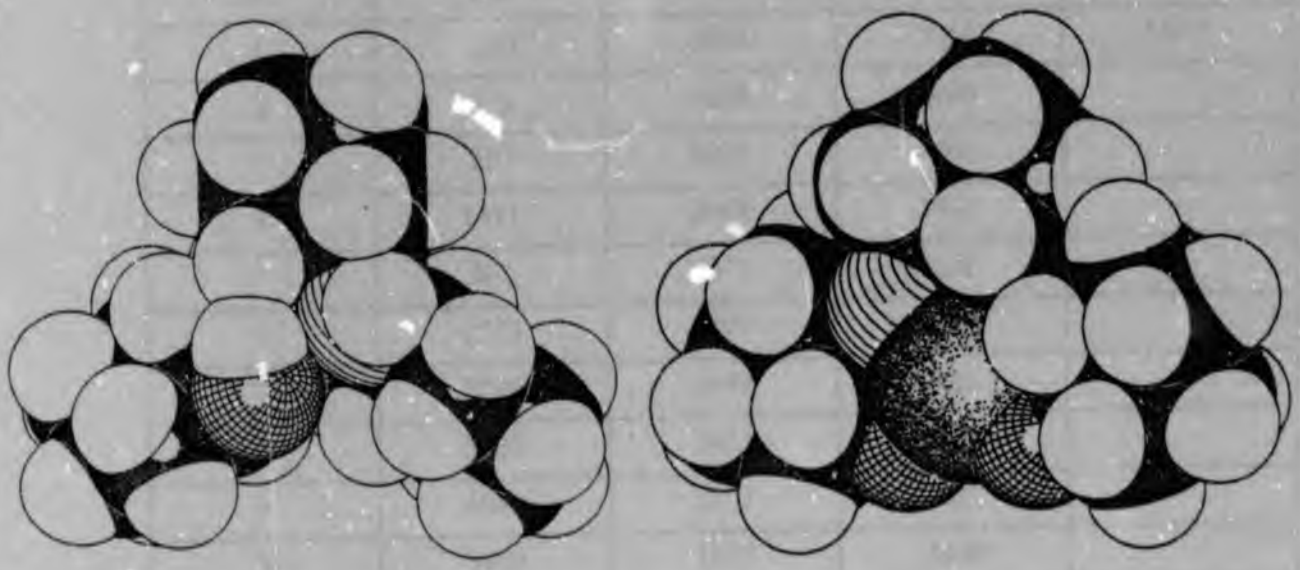


Figure 84: spacefill diagram of $[Cu(TCA)]^{2+}$ and TCA indicating the movement of the cyclohexyl groups on complexation

TABLE OF ANISOTROPIC DISPLACEMENT PARAMETERS

	u11	u22	u33	u23	u13	u12
CU	42(3)	23(6)	88(5)	0.0	22(4)	0.0
C1	52(6)	29(7)	146(8)	-11(6)	29(5)	O(6)
C2	57(5)	26(2)	90(5)	9(0)	18(8)	-1(2)
C3	46(0)	17(6)	76(1)	-1(3)	23(0)	-6(5)
N1	35(1)	28(1)	56(1)	3(2)	13(1)	-4(4)
C4	26(3)	37(6)	60(6)	-1(3)	6(0)	3(5)
C5	42(1)	39(2)	76(6)	-6(9)	13(1)	-7(7)
C6	42(2)	58(9)	101(3)	-14(6)	21(5)	-3(8)
C7	44(5)	59(2)	116(4)	-7(0)	24(3)	0(7)
C8	42(0)	37(2)	109(0)	0(8)	20(4)	6(6)
C9	49(6)	31(3)	63(2)	-3(7)	19(1)	-1(7)
O5	42(0)	28(3)	91(3)	6(9)	25(2)	4(5)

TABLE OF HYDROGEN COORDINATES AND ISOTROPIC DISPLACEMENT PARAMETERS

H	Xa	Yb	Zc	Ueq
1	1123	4025	3054	115.1
2	-111	4008	2086	
3	237	3031	486	
4	1471	3048	1454	
5	392	2071	3328	
6	2036	1497	3445	
7	2299	1899	422	
8	2581	2401	2071	
9	4049	1807	1637	
10	3769	1517	3300	
11	4165	506	1864	
12	3252	758	292	
13	2928	356	3319	
14	1659	-168	1702	
15	1522	698	401	
16	607	1848	598	
17	677	-45	1496	

PREORGANISATION

Preorganisation is a term that refers to the extent to which a free ligand is fixed in the conformation that is most suitable for complexing a desired metal ion (Cram et al 1985). This idea provides a means of enhancing complex

stability that does not involve increasing the covalent nature of the M-L bonds in the complex. Hancock & Martell (1988) associate enhanced complex stability, due to chelate and macrocyclic effects, with the concept of preorganisation. Macrocyclic ligands are often thought of as being preorganised by virtue of the rigidity that is inherent of its structure. This is on certain occasions incorrect due to unexpected flexibility and solvation effects. Ligands such as 18-crown-6 are known to fold in on themselves in solvents of low dielectric constant so as to minimise dipole-dipole repulsions. Solvation may weaken the dipole-dipole repulsions and the D_3d conformer may be stable in aqueous solution.

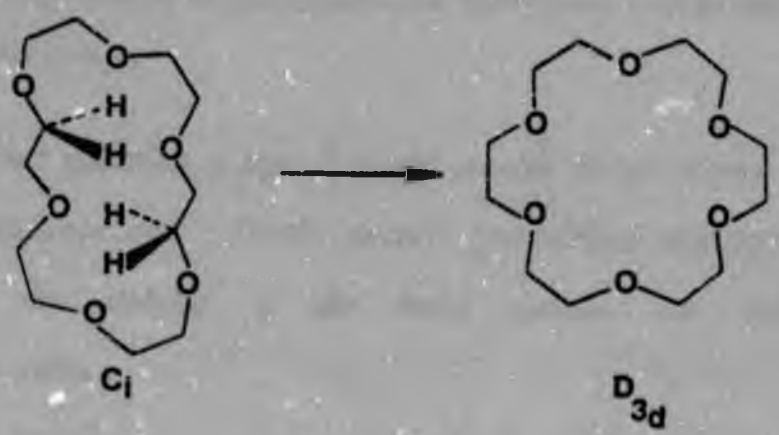


Figure 85 : stabilisation of D3d conformer of 18-crown-6 in aqueous solution (Martell et al 1994)

The macrocyclic ligand, cryptand-2,2,2 , is another example of a ligand with limited preorganisation

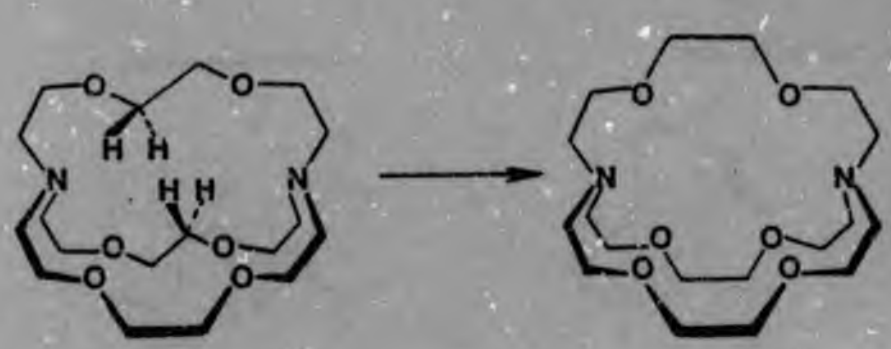


Figure 86 : conformers of cryptand-2,2,2 (Martell et al 1994)

In polar solvents the conformer correct for complex formation collapses to maximise the solvation of polar groups and hydrophobic interactions of the hydrocarbon groups.

In a perfect situation a ligand would provide donor atoms at the correct distance and with the correct geometrical orientation to optimise the stability of the metal complex i.e. complete preorganisation .

Preorganisation is also an important idea when considering open-chain ligands. The EDTA and CDTA example quoted by Hancock & Martell (1989) is an illustration of how open-chain ligands may show enhanced stability by forcing the donor groups to adopt a conformation that is more suitable for complex formation.

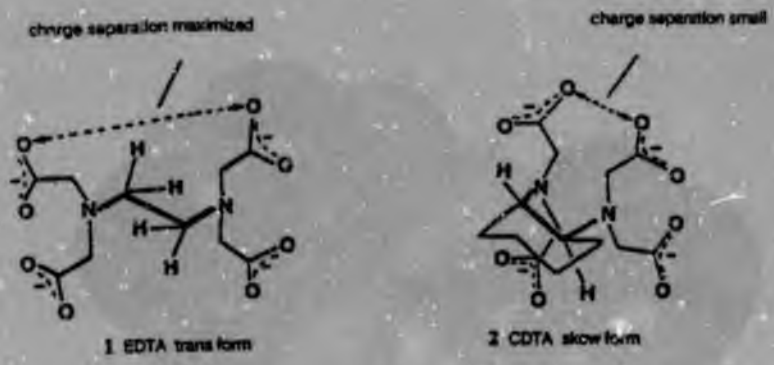


***Figure 87** : Conformations of EDTA and CDTA indicating degrees of preorganisation for open-chain ligands (**Martell et al 1994**)*

The donor groups in Trans-CDTA are forced closer together by the ligand synthesis partially overcoming the mutual repulsions of the charged groups on complex formation. The entropy loss in forming CDTA complexes is reduced because of the restricted movement of the donor groups. The complexes of CDTA therefore have greater stability than those of EDTA. Analogous to this are the set of ligands THEEN and THEDACH (de Sousa et al 1991). The pair of ligands Cy_2-EN and TCA reveal the concept of preorganisation, in which the ligand TCA has a conformation more nearly like the conformation of the metal complex. The loss of entropy in forming complexes of TCA is much less than for Cy_2-EN since the pendant hydroxycyclohexyl donor groups are not as free to move. In the TCA ligand the bulky hydroxycyclohexyl groups are brought much closer together and the repulsive van der Waals interactions, that must be overcome on complexation, are in part overcome by the synthesis of the ligand.

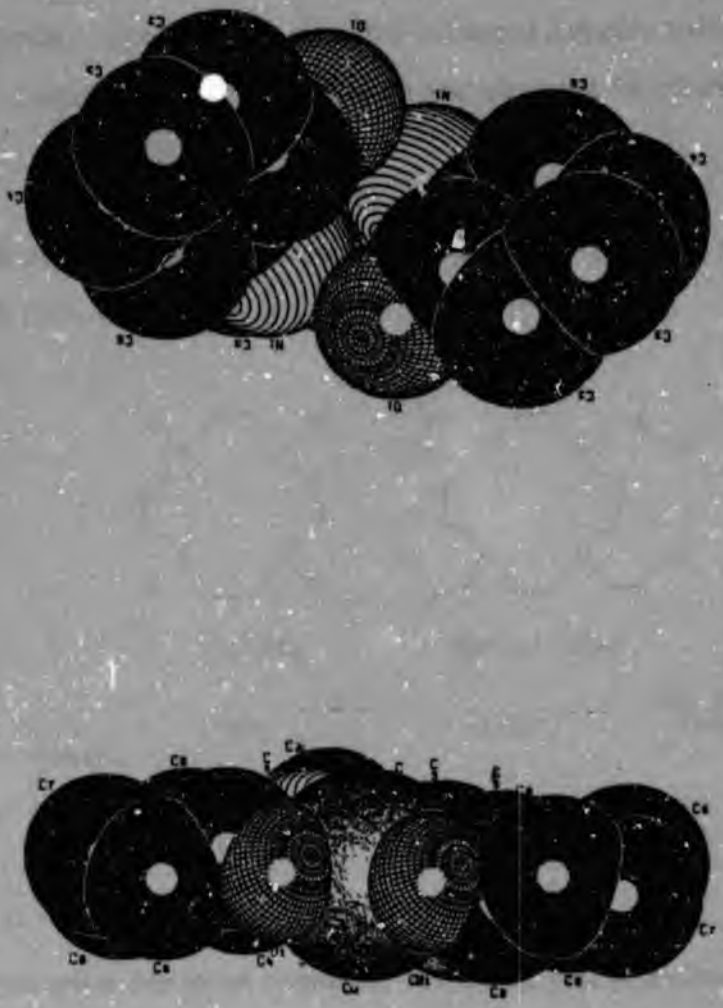
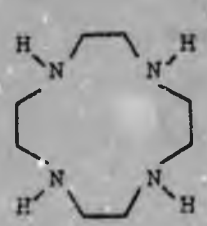


Figure 88 : comparison of the conformations of TCA, and $[Cu(TCA)]^{2+}$

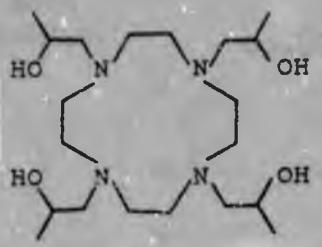
THE LONE PAIR ON Pb^{2+} ION

The behaviour of the Pb^{2+} ion in complexation to various ligands may vary from that which is expected. The expected enhanced complex stability of Pb^{2+} with THP-12-aneN$_4$ does not compare with that observed for other large ions such as Cd^{2+} and Ca^{2+}.

TABLE 5 : formation constants of metal ions with THP-12-aneN$_4$ (Martell& Smith 1974-1989, Hancock et al 1988[b], Hancock 1993)



12-aneN$_4$



THP-12-aneN

	ionic radius(Å)	logK$_1$	logK$_1$	change in logK$_1$
Cd(II)	0.95	14.3	17.46	+3.1
Pb(II)	1.18	15.9	15.07	-0.8
Ca(II)	1.00	3.1	5 68	+2.6
Zn(II)	0.74	16.2	13.45	-2.7
Cu(II)	0.57	23.3	19.48	-3.8

This problem arises due to the behaviour of the lone pair of electrons on Pb^{2+} ion (Hancock et al 1988[b]). The lone pair may occupy the symmetric 6s orbital in its valence shell and become stereochemically inactive. The stereochemically inactive form causes long ionic metal-ligand bonds by the delocalised lone pair repelling the donor electrons of the ligand. The donor electrons of the incoming ligand are not repelled by the lone pair if it is stereochemically active and resides in the localised s p^x d^y hybrid orbital. The result is a better overlap of the metal and ligand orbitals that produce shorter

metal-ligand bonds of greater covalent character. The bonds furthest away from the active lone pair will be shortened by approximately 0.3 Å (Hancock 1993) while those in the vicinity of the lone pair will remain long as they still experience some repulsion.

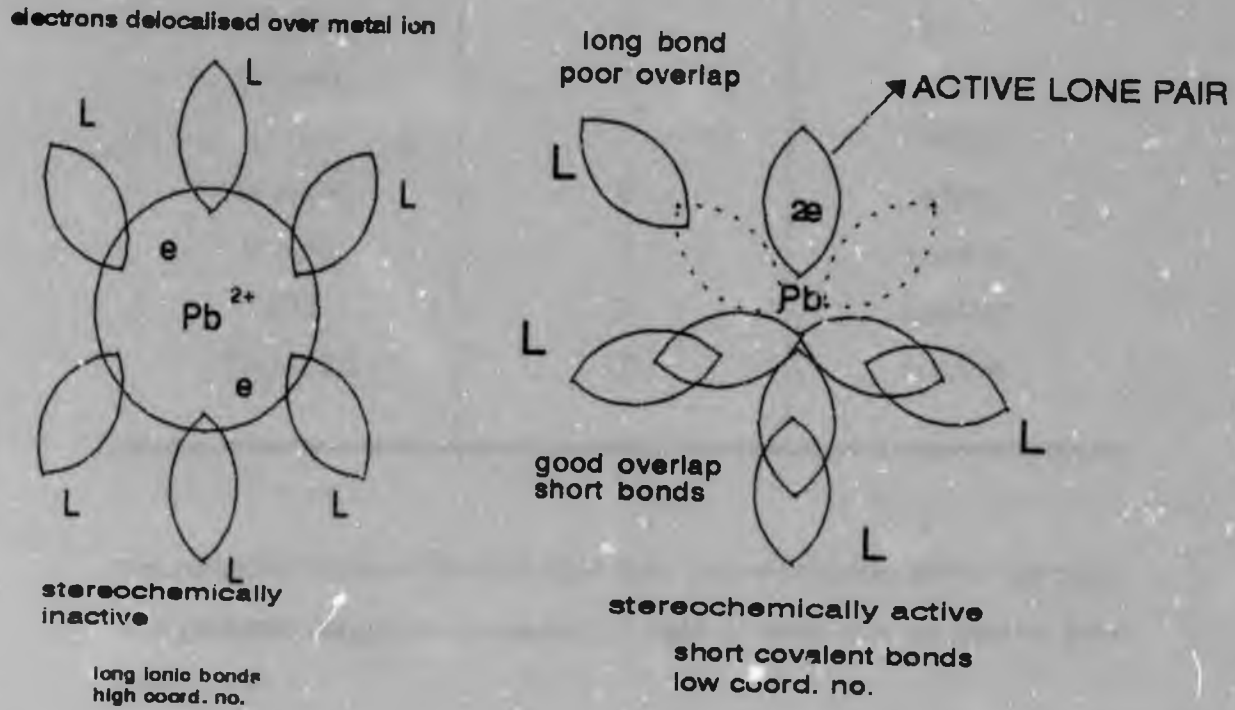


Figure 89 : the active and inactive forms of the lone pair of electrons on Pb^{2+} complexes (Shaikjee 1987)

Shaikjee (1987) tabulated a number of Pb^{2+} complexes of ligands with nitrogen and/or oxygen donors arranged in order of their coordination number. He commented on the fact that the stereochemical form of the lone

pair is related to coordination number.

TABLE 6 : stereochemical form of Pb^{2+} complexes and their coordination number.

LIGAND	COORDINATION NO.	LONE PAIR FORM
porphyrin	4	active
9-aneN_3	6	active
PyN_5	6	active
16-aneN_4	7	active
EDTA	7	active
14-aneN_4	8	active
PyN_3O_3	8	inactive
K22	8	inactive
Cryp-2,2,2	10	inactive

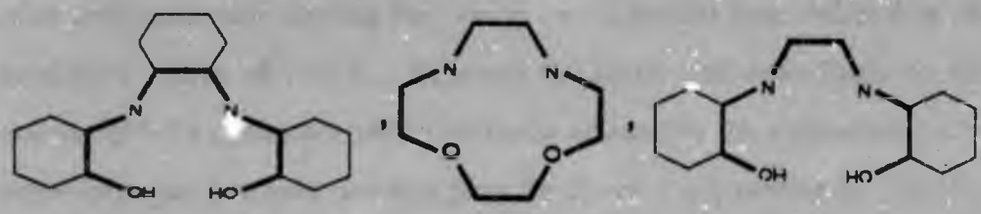
Coordination numbers less than eight have stereochemically active lone pairs and generally coordination numbers of eight or more have an inactive lone pair.

In lead complexes in which Pb^{2+} has a stereochemically active lone pair we are dealing with a metal ion that is much smaller than its suggested octahedral radius. The tendency for the lone pair on Pb^{2+} to become stereochemically active becomes stronger as the donor atoms on the ligand form metal-ligand bonds that are increasingly more covalent.

Comparing the changes in $\log K_1$ of TCA and CY_2-EN relative to 12-aneN_2O_2 for Pb^{2+}, Cd^{2+} and Zn^{2+} a positive deviation is observed from the trend as a function of ionic radius.

TABLE 7 : $\Delta\log K_1$ as a function of ionic radius for TCA and Cy_2-EN relative to 12-aneN_2O_2.

TCA ← 12-aneN_2O_2 → Cy_2-EN



metal	$\Delta\log K_1$	$\Delta\log K_1$	radius
Zn^{2+}	-1.45	-0.04	0.74
Cd^{2+}	-2.47	-0.86	0.95
Pb^{2+}	**-1.54**	**+0.22**	1.18

In both the TCA and Cy_2-EN lead complexes the change in stability of the complex deviates from the trend observed for the metal ions Zn^{2+} and Cd^{2+}. The plots of change in $\log K_1$ against metal ion radius for passing from 12-ane N_2O_2 to TCA and Cy_2-EN both clearly indicate the deviation of the Pb^{2+} ion from inverse relationship observed. The value of $\Delta\log K_1$ for the Pb^{2+} for the 12-ane N_2O_2 to TCA relation is only -1.54 in comparison to -2.47 for the Cd^{2+} ion that is the next largest metal. The prediction would be that Pb^{2+} should show a drop in stability greater than -2.50 . For the 12-ane N_2O_2 to Cy_2-EN

relation the lead complex achieves enhanced stability while the Zn^{2+} and Cd^{2+} show a decrease in stability.

In light of this observation and the tendency of ligands containing hydroxycyclohexyl groups to form stable complexes with smaller metal ions that are covalently bonded; we suggest that the lead complexes of TCA and Cy_2-EN have a stereochemically active lone pair. The apparent anomaly concerning the stability of these complexes can be attributed to the possibility of an active lone pair allowing Pb^{2+} ion to have a smaller ionic radius than its octahedral radius of 1.19 Å . Adjusting the metal size accordingly by an amount of 0.3 Å (Hancock 1993) for bonds affected by the stereochemically active lone pair produces two new plots for 12-ane N_2O_2 passing to Cy_2-EN and TCA that better include the points for Pb^{2+}.

An important assumption is being made in terms of the coordination number of the Pb^{2+} ion in the complexes of 12-ane N_2O_2 and Cy_2-EN. In the plots reflecting the change in stability the metal ion is assumed to be octahedral. It must be noted that the Pb^{2+} may have a coordination number greater than six.

If the coordination of the Pb^{2+} ion reaches nine or ten coordinate then the rationalisation of the observed results is not valid, but it may well be that the stability of the Pb^{2+} complexes will then reflect the same trend as the other large metal ions.

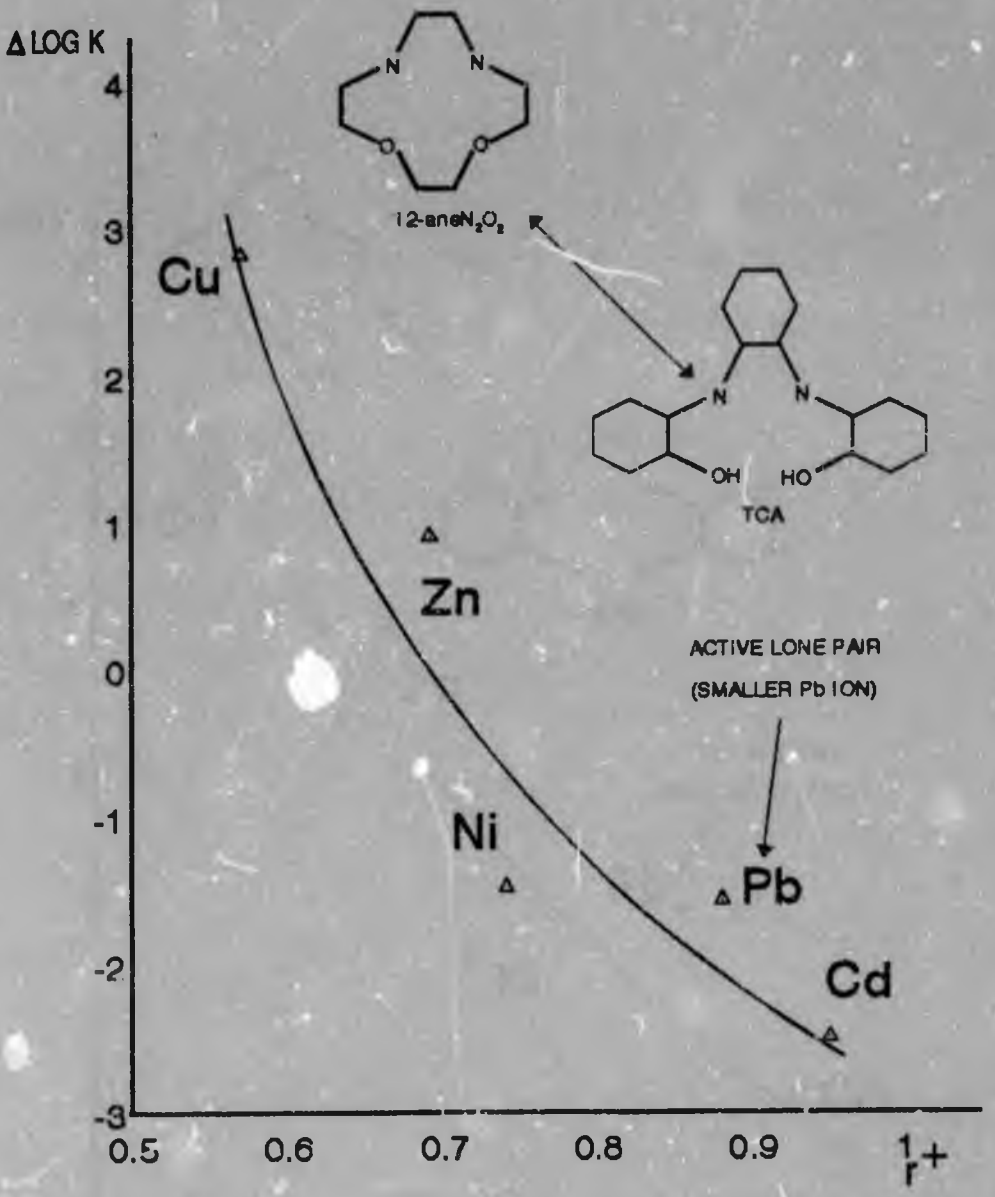


Figure 90 : change in stability in passing from 12-ane N_2O_2 to TCA for active lone pair on Pb^{2+}

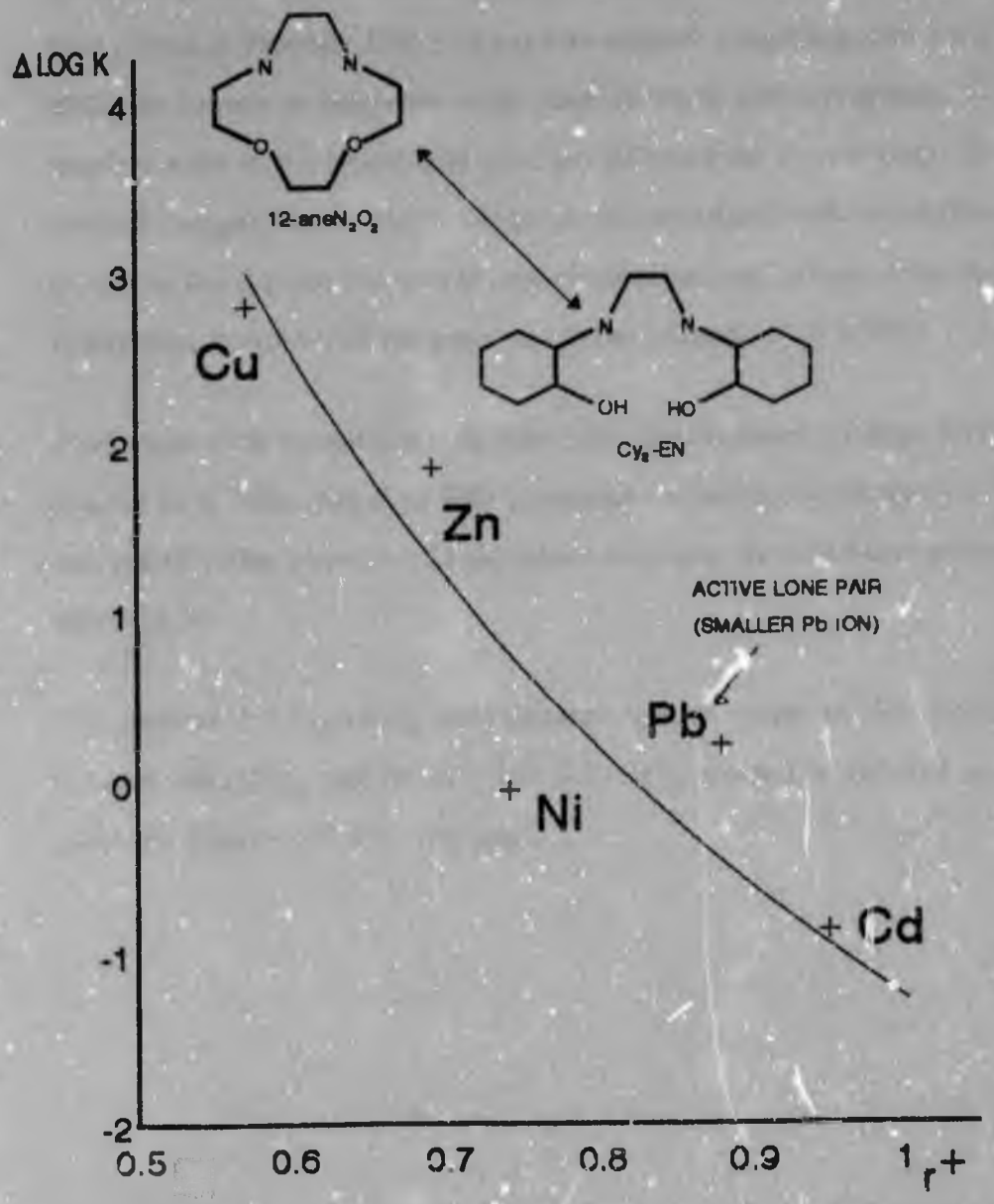


Figure 91 : change in stability for passing from 12-ane N_2O_2 to Cy_2-EN with stereochemically active lone pair on Pb^{2+}

SOLUTION STUDIES

Potentiometric and spectroscopic studies have indicated the existence of hydrolytic products for metal complexes of aminoalcohols (Hall & Dean 1960, Hall , Dean & Pacofsky 1960). In aqueous solution complex species have the ability to behave as polyprotic acids when alcoholic hydroxyl groups, in the pendant arms of the ligand molecule, are able to form chelate rings via the alcoholic oxygen atoms. The acidic properties associated with the chelates is related to the deprotonation of the coordinated hydroxyl groups of the ligand rather than hydrolysis of the aqua complexes (Orama et al 1979[a]).

Evaluation of the potentiometric data with the computer package ESTA (Murray et al 1984, may et al 1985) postulates a model for the species ML and MLH^{a}. The respective LogK values may then be calculated assuming pKw=13.78 .

The method for expressing deprotonated species varies in the literature between $ML(OH)_a$ and MLH^{a}. The $ML(OH)_a$ method is selected in the tabulated data on the following page.

TABLE 8 : stability constants of Cy_2-EN including the deprotonated species.

METAL ION	EQUILIBRIUM	logK
	$H+L \rightleftharpoons HL$	9.66
	$HL+H \rightleftharpoons H_2L$	6.62
Cu^{2+}	$M+L \rightleftharpoons ML$	11.47
	$ML+OH \rightleftharpoons MLOH$	6.64
	$MLOH+OH \rightleftharpoons ML(OH)_2$	4.59
Zn^{2+}	$M+L \rightleftharpoons ML$	6.18
	$ML+OH \rightleftharpoons MLOH$	5.29
	$MLOH+OH \rightleftharpoons ML(OH)_2$	4.17
Ni^{2+}	$M+L \rightleftharpoons ML$	7.77
Cd^{2+}	$M+L \rightleftharpoons ML$	5.69
	$ML+OH \rightleftharpoons MLOH$	4.02
Pb^{2+}	$M+L \rightleftharpoons ML$	6.56
	$ML+OH \rightleftharpoons MLOH$	5.37

STABILITY CONSTANTS FOR CU AND NI COMPLEXES OF TCA

The deprotonation of hydroxyalkyl pendant arms rather than the deprotonation of coordinated water molecules is supported by crystallographic evidence (Hay et al 1987 , Orama & Orama 11979 and de Sousa et al 1995 to be published). The titrations for TCA were not determined potentiometrically because of the lack of solubility of the free ligand. An out-of-cell technique was used, and a series of solutions containing equal amounts of ligand and metal ion were prepared at different pH values. The visible spectrum of each of these solutions was recorded, taking note of the pH of the solution, and used to determine the stability constants.

TABLE 9 : Absorbance of $[Cu(TCA)]^{2+}$ at wavelength 650 nm

$A_o = 0.0$ $A_\infty = 0.288$

pH	Abs
2.27	0.040
2.42	0.077
2.75	0.146
2.97	0.182
3.52	0.251
4.28	0.282
4.81	0.288

The calculation involves the following equilibrium :

$$Cu^{2+} + L \rightleftharpoons CuL$$

$$K = \frac{[CuL]}{[L][Cu^{2+}]}$$

Cu^{2+} - free copper in solution

CuL - complex

L - free ligand in solution

Ka_1 & Ka_2 - protonation constants of ligand.

$$[CuL] = \bar{n}[Cu_{tot}]$$

Cu_{tot} - total Cu in solution

$\bar{n}$ - fraction of metal complexed is calculated from the spectrum

$$\bar{n} = \frac{A_n - A_o}{A_\infty - A_o}$$

A_o - absorbance when no complex is formed

A_∞ - absorbance when all the metal is complexed

A_n - absorbance of the n^{th} solution

$[Cu^{2+}]$ is calculated from the mass balance equations :

$$[Cu_{tot}] = [Cu^{2+}]+[CuL]$$

$$[Cu^{2+}] = [Cu_{tot}] - [CuL]$$

Calculation of the free ligand concentration, [L], requires the experimentally determined pH of the solutions in the mass balance equations :

$$[L_{tot}] = [L] + Ka_1[H^+][L] + Ka_1Ka_2[H^+]^2[L] + [CuL]$$

which rearranges to

$$[L_{tot}] - [CuL] = [L](1+Ka_1[H^+]+Ka_1Ka_2[H^+]^2$$

substitution of each of these calculated parameters into the expression for K gives the result LogK = 11.50 .

Recording the spectrum at higher pH produces a new spectrum that shows a shift in the band at 650 nm. Formation of deprotonated species is generally accompanied by changes in the visible spectrum.

Recording the absorbance at smaller intervals of pH generated the data in table 10.

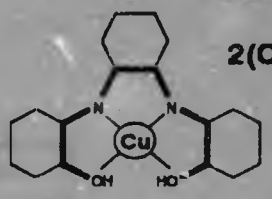


Figure 94 : visible spectrum at higher pH for [Cu(TCA)]

TABLE 10 : Absorbance of $[Cu(TCA)]^{2+}$ at λ = 598 nm

pH	Abs	pH	Abs
11.73	0.1659	8.17	0.1553
11.45	0.1657	7.85	0.1530
10.80	0.1652	7.42	0.1479
10.46	0.1647	6.78	0.1435
9.94	0.1640	6.41	0.1337
9.43	0.1639	5.92	0.1269
8.95	0.1624	5.51	0.1204
8.64	0.1598	5.15	0.1190

A plot of absorbance versus pH allows for the calculation of pK_1 and pK_2 for the deprotonated species MLOH and $ML(OH)_2$. A curve was fitted to the above data using a computer program NLFIT that minimises the deviations via simplex calculations.

A single deprotonation step model (MLOH species) did not accommodate the data accurately and the model that best suited the acquired data made provision for the deprotonation of both pendant arms. The parameters as calculated by the simplex minimisation shows the pK values of MLOH and $ML(OH)_2$ to be :

$pK_1 = -\log K_1 = -\log (5.67 \times 10^{-7}) = 6.25$

$pK_2 = -\log K_2 = -\log (6.96 \times 10^{-9}) = 8.16$

```
Curve fitting using the Simplex method

Cu-TCA

FUNCTION:
(b3/(10^x)^2+(b1*b2)/10^x+b1*b4*b5)/(1/(10^x)^2+b1/10^x+b1*b5)

                    Convergence = 1.000E-0005
          Reflection factor: alpha = 1.000E+0000
          Contraction factor: beta = 5.000E-0001
          Expansion factor:  gamma = 2.000E+0000
                    Step length = 1.000E-0003
 Maximum number of function calls = 1000
            Number of data points =   16
       Total number of parameters =    5
Number of parameters to be varied =    5

Initial estimates:
 b 1 = 5.67000000E-0007    b 2 = 1.46400000E-0001    b 3 = 1.19000000E-0001
 b 4 = 1.65500000E-0001    b 5 = 6.96000000E-0009

SSE = 2.7736668E-0005      1 calls
  5.67000000E-0007    1.46400000E-0001    1.19000000E-0001    1.65500000E-0001
  6.96000000E-0009

SSE = 2.7736668E-0005     24 calls
  5.67000000E-0007    1.46400000E-0001    1.19000000E-0001    1.65500000E-0001
  6.96000000E-0009

SSE = 2.7736668E-0005     51 calls
  5.67000000E-0007    1.46400000E-0001    1.19000000E-0001    1.65500000E-0001
  6.96000000E-0009

SSE = 2.7736668E-0005     78 calls
  5.67000000E-0007    1.46400000E-0001    1.19000000E-0001    1.65500000E-0001
  6.96000000E-0009

SSE = 2.7736668E-0005     99 calls
  5.67000000E-0007    1.46400000E-0001    1.19000000E-0001    1.65500000E-0001
  6.96000000E-0009

SSE = 2.7736668E-0005    120 calls
  5.67000000E-0007    1.46400000E-0001    1.19000000E-0001    1.65500000E-0001
  6.96000000E-0009

     Number of function evaluations =  125
                       Convergence = 9.288E-0006
             Number of data points =   16
          Sum of squares of errors = 2.773666775E-0005
        Total number of parameters =    5
       Number of parameters varied =    5
     Estimated standard deviation = 1.587927974E-0003

Minimum obtained - normal termination


Final set of parameters:

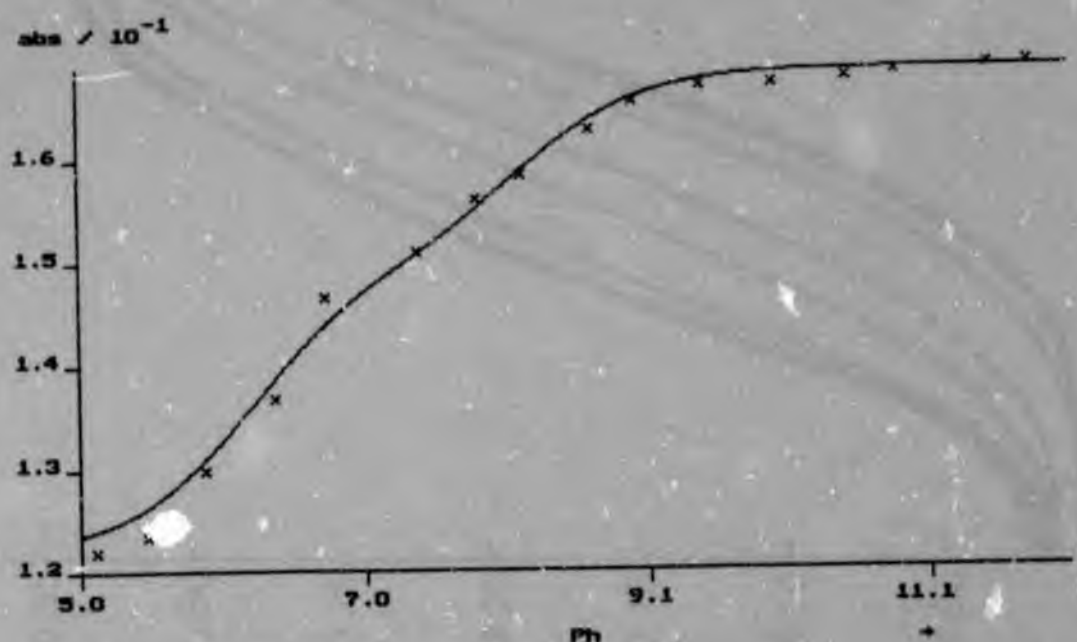
 b 1 = 5.6700000E-0007                  b 2 = 1.4640000E-0001
 b 3 = 1.1900000E-0001                  b 4 = 1.6550000E-0001
```

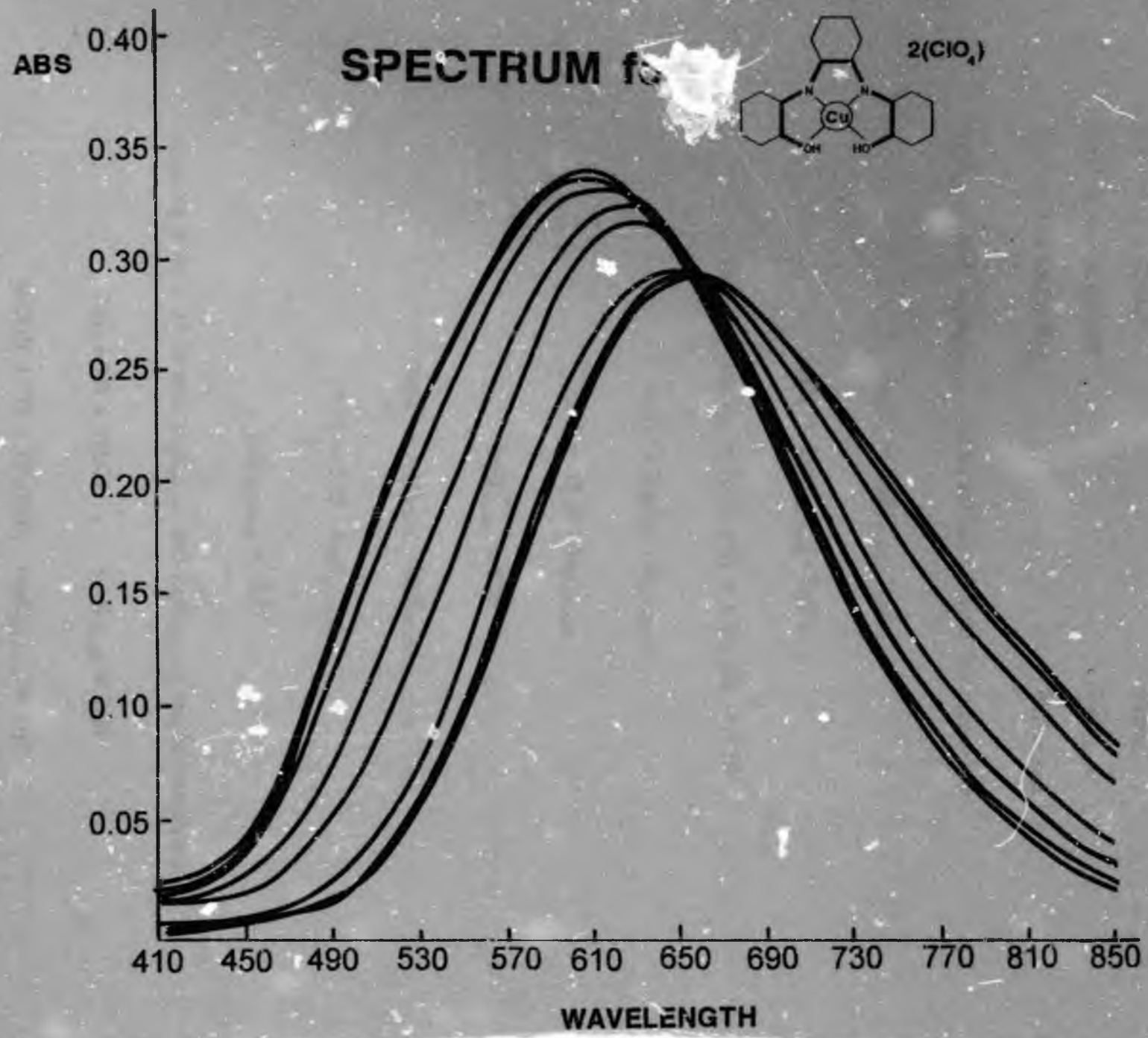
b 5 = 6.9600000E-0009

	Ph	abs obs	calc	obs - calc
1	1.1730000E+0001	1.6590000E-0001	1.6549489E-0001	4.0510871E-0004
2	1.1450000E+0001	1.6570000E-0001	1.6549027E-0001	2.0973216E-0004
3	1.0800000E+0001	1.6520000E-0001	1.6545660E-0001	-2.5660239E-0004
4	1.0460000E+0001	1.6470000E-0001	1.6540530E-0001	-7.0530426E-0004
5	9.9400000E+0000	1.6400000E-0001	1.6518988E-0001	-1.1898792E-0003
6	9.4300000E+0000	1.6390000E-0001	1.6453057E-0001	-6.3057037E-0004
7	8.9500000E+0000	1.6240000E-0001	1.6283632E-0001	-4.3632340E-0004
8	8.6400000E+0000	1.5980000E-0001	1.6072836E-0001	-9.2836064E-0004
9	8.1700000E+0000	1.5530000E-0001	1.5587199E-0001	-5.7198963E-0004
10	7.8500000E+0000	1.5300000E-0001	1.5215138E-0001	8.4861602E-0004
11	7.4200000E+0000	1.4790000E-0001	1.4772733E-0001	1.7266585E-0004
12	6.7800000E+0000	1.4350000E-0001	1.4099114E-0001	2.5088636E-0003
13	6.4100000E+0000	1.3370000E-0001	1.3556765E-0001	-1.8676506E-0003
14	5.9200000E+0000	1.2690000E-0001	1.2785079E-0001	-9.5078550E-0004
15	5.5100000E+0000	1.2040000E-0001	1.2326264E-0001	-2.8626410E-0003
16	5.1500000E+0000	1.1900000E-0001	1.2103501E-0001	-2.0350058E-0003

Cu-TCA

(b3/(10^x)^2+(b1*b2)/10^x+b1*b4*b5)/(1/(10^x)^2+b1/10^x+b1*b5)




SPECTRUM fo
2(ClO4)
Cu
OH
HO
ABS
0.40
0.35
0.30
0.25
0.20
0.15
0.10
0.05
410
450
490
530
570
610
650
690
730
770
810
850
WAVELENGTH

The model considered the following equilibria :

$Cu^{2+} + L \rightleftharpoons (CuL)^{2+}$ $\log\beta_{ML}$

$Cu^{2+} + L \rightleftharpoons (CuLOH)^{+}$ $\log\beta_{MLOH}$

$Cu^{2+} + L \rightleftharpoons CuL(OH)_2$ $\log\beta_{ML(OH)2}$

$\log\beta_{MLOH}$ and $\log\beta_{ML(OH)2}$ can be calculated from the expressions :

$$\log K_1 = \log\beta_{MLOH} - \log\beta_{ML}$$

$$\log K_2 = \log\beta_{ML(OH)2} - \log\beta_{MLOH}$$

$$\log K_{ML} = \log\beta_{ML} = 11.50,\ pK_1 = 6.25,\ pK_2 = 8.16$$

$$-\log K_1 = \log\beta_{ML} - \log\beta_{MLOH}$$

$$6.25 = 11.50 - \log\beta_{MLOH}$$

$$\therefore \log\beta_{MLOH} = 5.25$$

$$-\log K_2 = \log\beta_{MLOH} - \log\beta_{ML(OH)2}$$

$$8.16 = 5.25 - \log\beta_{ML(OH)2}$$

$$\therefore \log\beta_{ML(OH)2} = -2.91$$

assuming pKw = 13.78 then $\log K_{MLOH}$ and $\log K_{ML(OH)2}$ can be calculated:

$ML + OH \rightleftharpoons MLOH$ $\log K_{MLOH} = 7.53$

$MLOH + OH \rightleftharpoons ML(OH)_2$ $\log K_{ML(OH)2} = 5.62$

The spectrum for the nickel complex (HIGH SPIN) was recorded to as high a pH as possible before precipitation occurred.

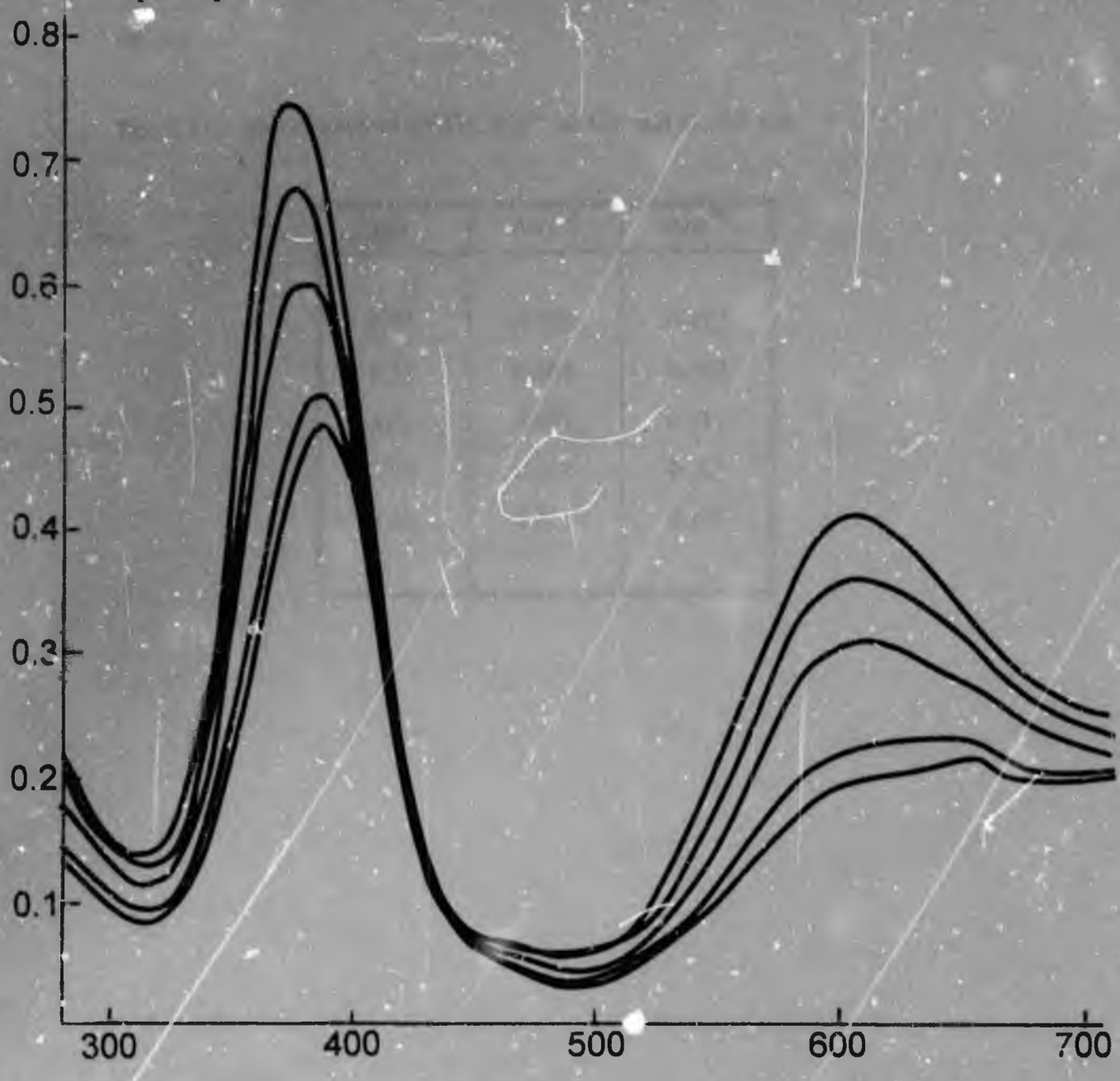


Figure 95 : spectrum of $[Ni(TCA)]^{2+}$ (HIGH SPIN)

Recording the absorbance of the band at 604 nm and 395 nm gave the tabulated data that was used in calculations similar to those employed for copper.

TABLE 11 : Absorbance of $[Ni(TCA)]^{2+}$ at 604 nm & 395 nm

pH	Abs^{604}	Abs^{395}
5.97	0.750	0.412
5.17	0.680	0.362
4.33	0.595	0.311
3.59	0.458	0.221
2.40	0.415	0.198

```
Curve fitting using the Simplex method

Bi-TCA

FUNCTION:
(b3/(10^x)^2+(b1*b2)/10^x+b1*b4*b5)/(1/(10^x)^2+b1/10^x+b1*b5)

                    Convergence = 1.000E-0005
          Reflection factor: alpha = 1.000E+0000
          Contraction factor: beta = 5.000E-0001
          Expansion factor:  gamma = 2.000E+0000
                     Step length = 1.000E-0005
 Maximum number of function calls = 1000
            Number of data points =    5
       Total number of parameters =    5
Number of parameters to be varied =    2

Initial estimates:
 b 1 = 1.00000000E-0004    *b 2 = 5.95000000E-0001    *b 3 = 4.15000000E-0001
*b 4 = 7.50000000E-0001     b 5 = 1.00000000E-0005

SSE = 1.2864821E-0003       1 calls
  1.00000000E-0004  * 5.95000000E-0001  * 4.15000000E-0001  * 7.50000000E-0001
  1.00000000E-0005

     Number of function evaluations =   16
                        Convergence = 9.667E-0006
              Number of data points =    5
          Sum of squares of errors = 8.872524677E-0004
         Total number of parameters =    5
         Number of parameters varied =    2
       Estimated standard deviation = 1.719740744E-0002

Minimum obtained - normal termination

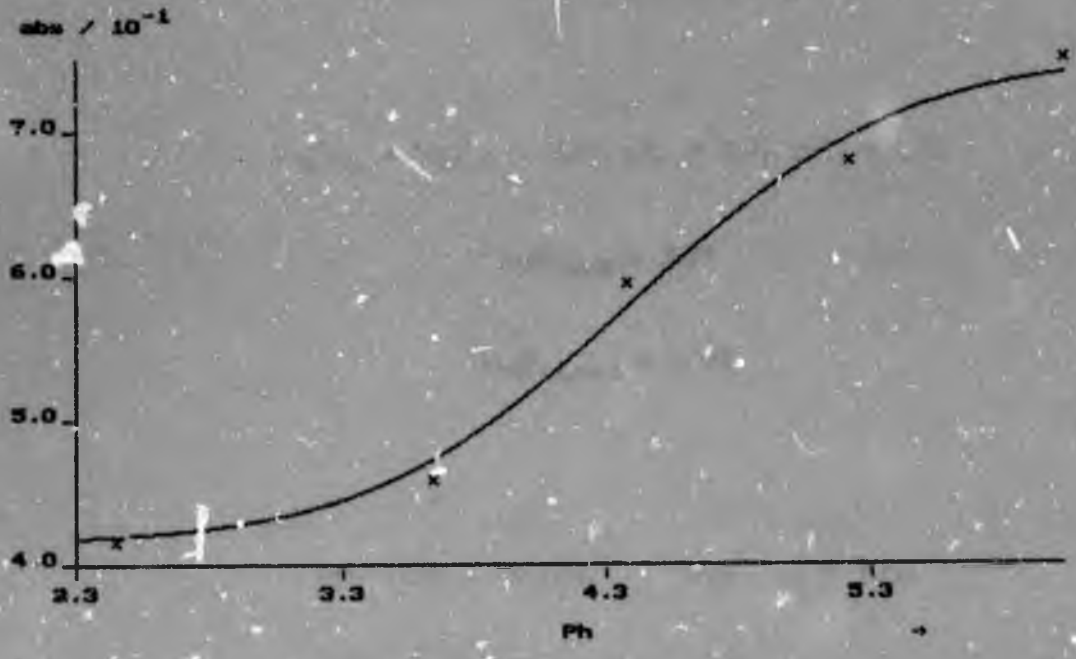

Final set of parameters:

 b 1 = 1.07500000E-0004                  *b 2 = 5.95000000E-0001
*b 3 = 4.15000000E-0001                  *b 4 = 7.50000000E-0001
 b 5 = 1.49999970E-0005
```

	Ph	abs obs	calc	obs - calc
1	5.97000000E+0000	7.50000000E-0001	7.39450230E-0001	1.05497690E-0002
2	5.17000000E+0000	6.80000000E-0001	6.96345950E-0001	-1.63459540E-0002
3	4.33000000E+0000	5.95000000E-0001	5.78704930E-0001	1.62950690E-0002
4	3.59000000E+0000	4.58000000E-0001	4.72850120E-0001	-1.48501230E-0002
5	2.40000000E+0000	4.15000000E-0001	4.19765420E-0001	-4.76541960E-0003

Ni-TCA

(b3/(10^x)^2+(b1*b2)/10^x+b1*b4*b5)/(1/(10^x)^2+b1/10^x+b1*b5)



As with the copper study the data was best fitted to a model that postulated the existence of the MLOH and $ML(OH)_2$ species.

$$\log K_{ML} = \log\beta_{ML} = 6.84,\ pK_1 = 3.97,\ pK_2 = 4.82$$

$$\log\beta_{MLOH} = 2.87$$

$$\log\beta_{ML(OH)2} = -1.95$$

$$ML + OH \rightleftharpoons MLOH \qquad \log K_{MLOH} = 9.81$$

$$MLOH + OH \rightleftharpoons ML(OH)_2 \qquad \log K_{ML(OH)2} = 8.96$$

An interesting aspect of the stability of TCA complexes is the greater acidity of the coordinated hydroxyl group, as illustrated by the complex with Cu^{2+}

$$[Cu(TCA)]^{2+} + OH^- \rightleftharpoons [Cu(TCA)OH]^+ \qquad \log K = 7.53$$

$$[Cu(DHEEN)]^{2+} + OH^- \rightleftharpoons [Cu(DHEEN)OH]^+ \qquad \log K = 6.63$$

MODEL SUBMITTED FOR CURVE FITTING BY SIMPLEX METHOD

The model consisted of the two deprotonation steps :

$$AH_2 \rightleftharpoons AH + H \quad K_1$$

$$AH \rightleftharpoons A + H \quad K_2$$

$$K_1 = \frac{[AH][H]}{[AH_2]} \qquad K_2 = \frac{[A][H]}{[AH]}$$

rearranging in terms of [A], [AH_2]

$$[A] = \frac{K_2[AH]}{[H]} \qquad [AH_2] = \frac{[AH][H]}{K_1}$$

$$[L_{tot}] = [AH_2] + [AH] + [A]$$

$$\therefore \text{Abs}_{tot} = \int AH_2 \cdot \text{Abs}_{AH2} + \int AH \cdot \text{Abs}_{AH} + \int A \cdot \text{Abs}_{A}$$

$$\int AH_2 = \frac{1}{1 + \frac{[AH]}{[AH_2]} + \frac{[A]}{[AH_2]}} = \frac{1}{1 + \frac{K_1}{[H]} + \frac{K_1K_2}{[H]^2}} = \frac{[H]^2}{[H]^2 + K_1[H] + K_1K_2}$$

similarly

$$\int AH = \frac{[AH]}{[AH_2]+[AH]+[A]} = \frac{K_1[H]}{[H]^2+K_1[H]+K_1K_2}$$

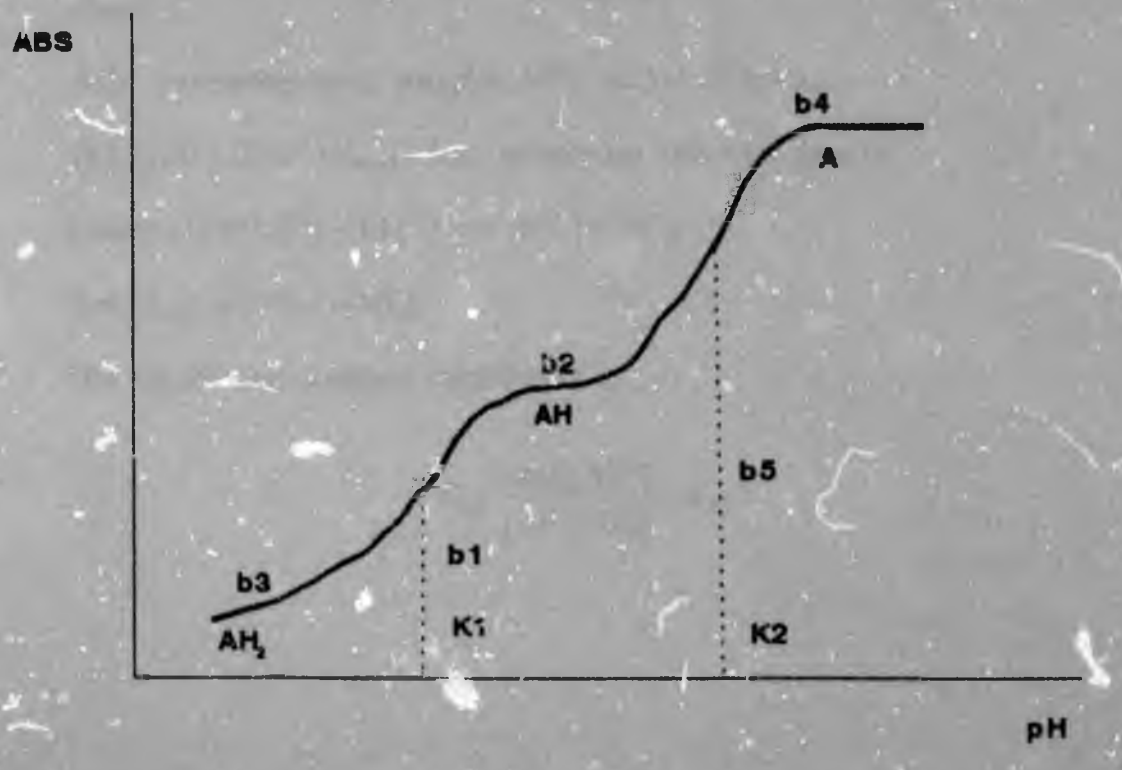
$$\int A = \frac{[A]}{[AH_2]+[AH]+[A]} = \frac{K_1K_2}{[H]^2+K_1[H]+K_1K_2}$$

therefore

$$Abs_{tot} = \frac{[H]^2 Abs_{AH_2}+K_1[H]Abs_{AH}+K_1K_2 Abs_A}{[H]^2+K_1[H]+K_1K_2}$$

Five parameters in this equation are submitted as b_1 to b_5 and all are allowed to vary in the simplex calculation until it has reached a minimum.

b_1 - K_1, b_2 - Abs_{AH}, b_3 - Abs_{AH2}, b_4 - Abs_{AH2}, b_5 - K_2



SPECTROSCOPIC STUDY OF COMPETITION TITRATIONS

The determination of the stability constants of Zn, Cd and Pb could not be done potentiometrically because of precipitation of the ligand. The titrations could be done however, using an out-of-cell technique. The metals were done in competition with Ni, and measurements were performed on the UV-VIS spectrophotometer at 25°C and 0.1M ionic strength. Solutions were prepared containing the same amounts of nickel (1.04×10^{-2}M), ligand (1.04×10^{-2}M) and acid (pH=4.8), and competing amounts (3.4×10^{-2}) of Cd, Zn and Pb were added to them.

The nickel complex was used as the study probe since the stability of the copper complex was large; not allowing the Cd, Zn and Pb to displace it from the ligand. The metals could however compete favourably with the weaker nickel complex. Calculations used the following mass balance equations:

$$[L_{tot}] = [NiL]+[ML]+[L]+[LH^{+}]+[LH^{2+}]$$

where

ML - competing metal complex, NiL - nickel complex,

$[L]$, $[LH^{+}]$, $[LH^{2+}]$,$[L_{tot}]$ - free, protonated and total ligands

assume $[L]+[LH^{+}]+[LH^{2+}] << [NiL]+[ML]$

then $[L_{tot}] = [NiL]+[ML]$

The equilibrium equation simplifies to :

$$K_M = \frac{[ML][Ni^{2+}]}{[M^{2+}][NiL]} \times K_{Ni}$$

The concentrations of ML, Ni^{2+}, M^{2+}, NiL were calculated in the following manner :

$[NiL] = \bar{n} \times Ni_{tot}$

$[Ni^{2+}] = [Ni_{tot}]-[NiL]$

$[ML] = [L_{tot}] - [NiL]$

$[M^{2+}] = [M_{tot}]-[ML]$

Solutions were allowed to stand until equilibrium had been reached (10 to 12 days) and the visible spectrum was then recorded.

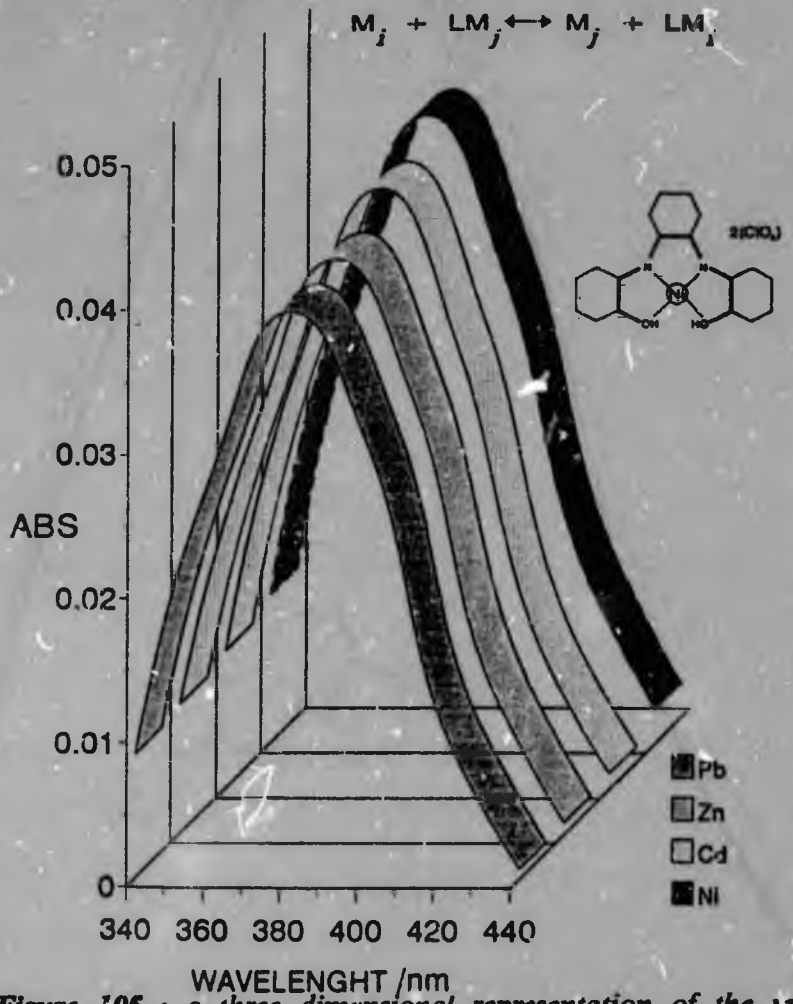


Figure 105 : a three dimensional representation of the recorded spectrum for the competition of Zn, Cd & Pb with NiL.

Competition of NiL with Zn, Pb & Cd

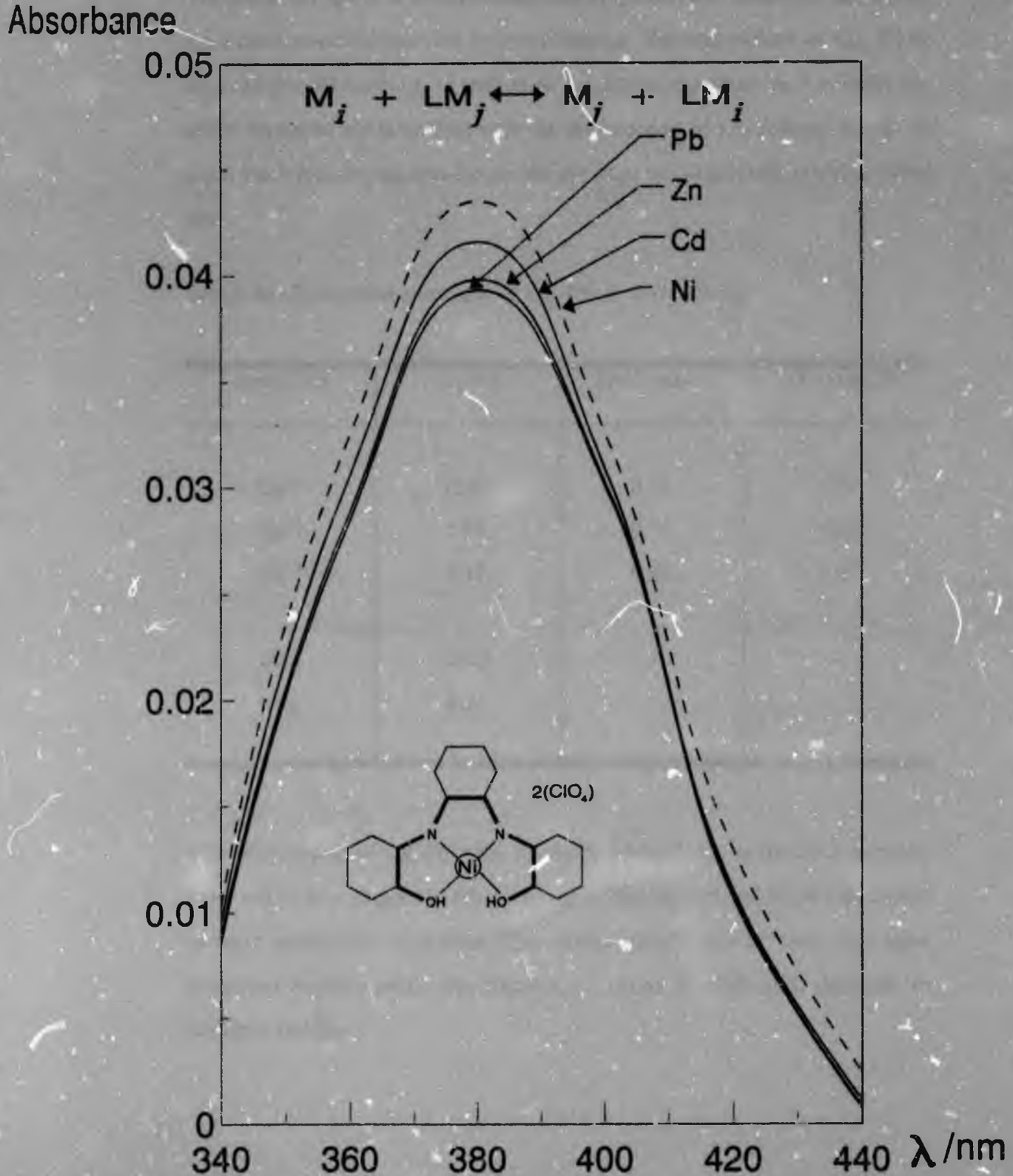


Figure 106 : recorded visible spectrum of Ni complex in competition with Zn, Cd & Pb

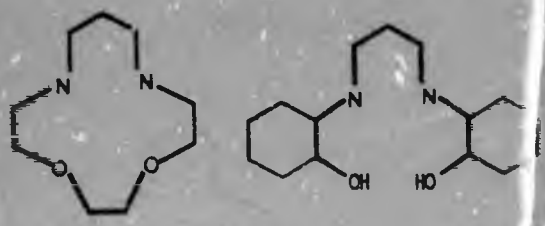
The study of Cy_2-PN is of importance due to the diamine backbone that forms a six-membered chelate ring on complexation. The comparison of Cy_2-PN to its analogue 13-aneN_2O_2 as well as to Cy_2-EN is important as it reflects the effect on metal ion selectivity with the introduction of a cyclohexyl groups in a structure forming six-membered chelate rings on complexation with a metal ion.

TABLE 12 : Formation constants of Cy_2-PN & 13-aneN_2O_2.

metal ion	Cy_2-PN	ionic radius	13-aneN_2O_2
Cu^{2+}	12.67	0.57	8.39
Zn^{2+}	5.04	0.74	4.89
Cd^{2+}	4.15	0.95	5.40
pK_{a1}	10.12	-	-
pK_{a2}	8.21	-	-

The relationship of Cy_2-PN with regard to 13-aneN_2O_2 as function of metal ionic radius is analogous to what is observed for Cy_2-EN and TCA with regard to their macrocyclic analogues. The smaller metal ions Cu^{2+} and Zn^{2+} have enhanced stability while the larger Cd^{2+} shows a substantial decrease in complex stability.

TABLE 13 : change in complex stability in passing from 13-a N_2O_2 to Cy_2-PN

13-aneN_2O_2 ⇌ Cy_2-PN		
		
metal ion	ionic radius	ΔlogK
Cu^{2+}	0.57	+4.28
Zn^{2+}	0.74	+0.15
Cd^{2+}	0.95	-1.25

Changing ethylene bridges to cyclohexylene bridges produces the surprising result of a five-membered chelate ring promoting complex stability for small metal ions (de Sousa et al 1991). It is therefore interesting to compare Cy_2-PN with Cy_2-EN since both contain the same number of donor atoms and cyclohexyl pendant groups. A difference arises only in the parent amine backbone that forms a five-membered and six-membered chelate ring respectively.

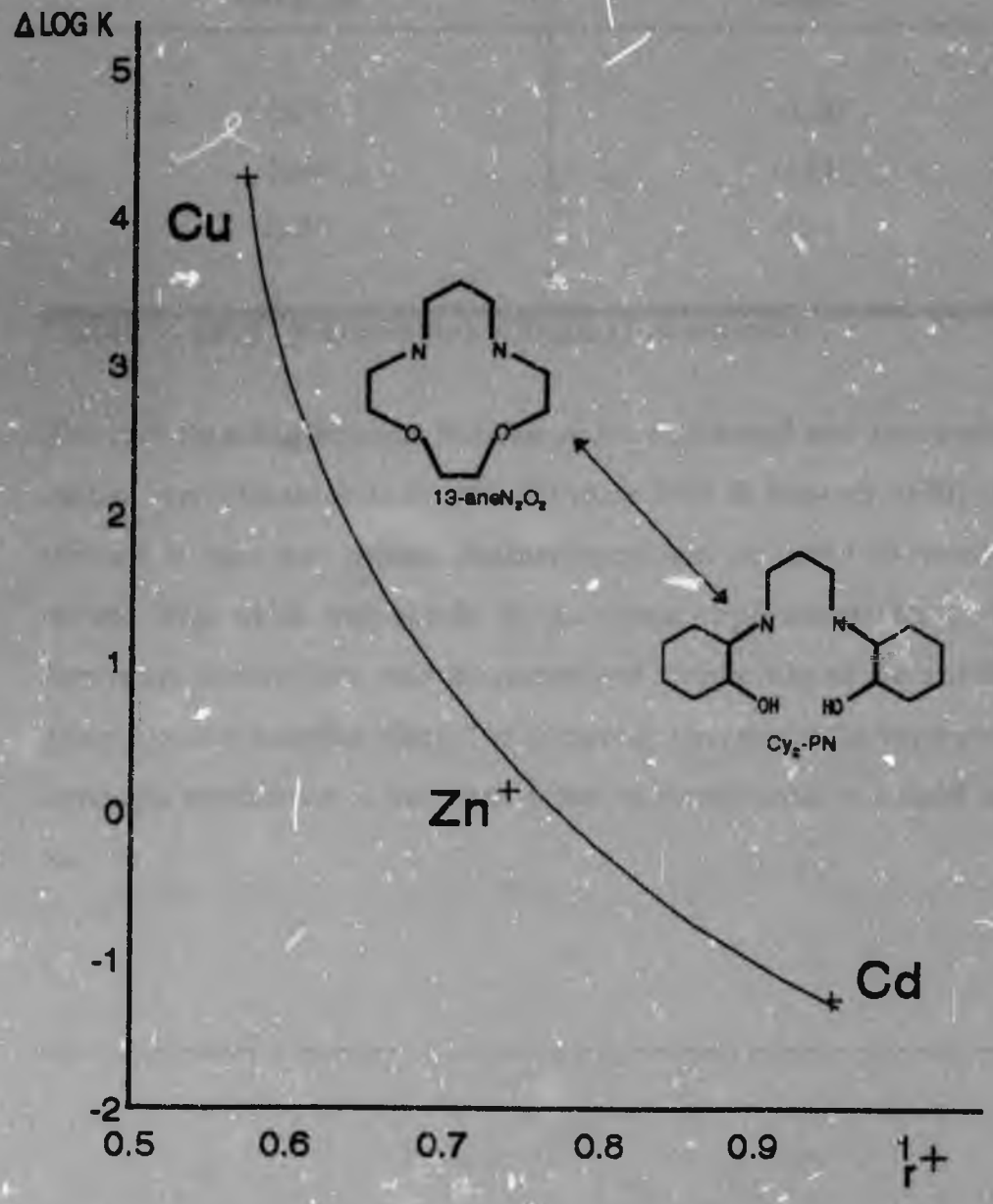


Figure 107 : Change in stability in comparing 13-aneN_2O_2 and Cy_2-PN

TABLE 14 : change in complex stability on altering chelate ring size by parent amine in passing from Cy_2-EN to Cy_2-PN.

metal ion	ΔlogK*
Cu^{2+}	+1.20
Zn^{2+}	-1.14
Cd^{2+}	-1.54

* ΔlogK = ΔlogK (6-membered) - ΔlogK (5-membered)

The rule regarding complex stability of five-membered and six-membered chelate rings (Hancock et al 1990, Hancock 1989 & Hancock 1990) is not violated in these two systems. Smaller metal ions do prefer six-membered chelate rings which best satisfy the geometric requirements for complex formation, however, the rigid five-membered chelate ring of the cyclohexyl group produces a similar effect. The steric crowding, due to the bulky groups, outweighs steric strain at the metal centre in coordination to a small metal ion.

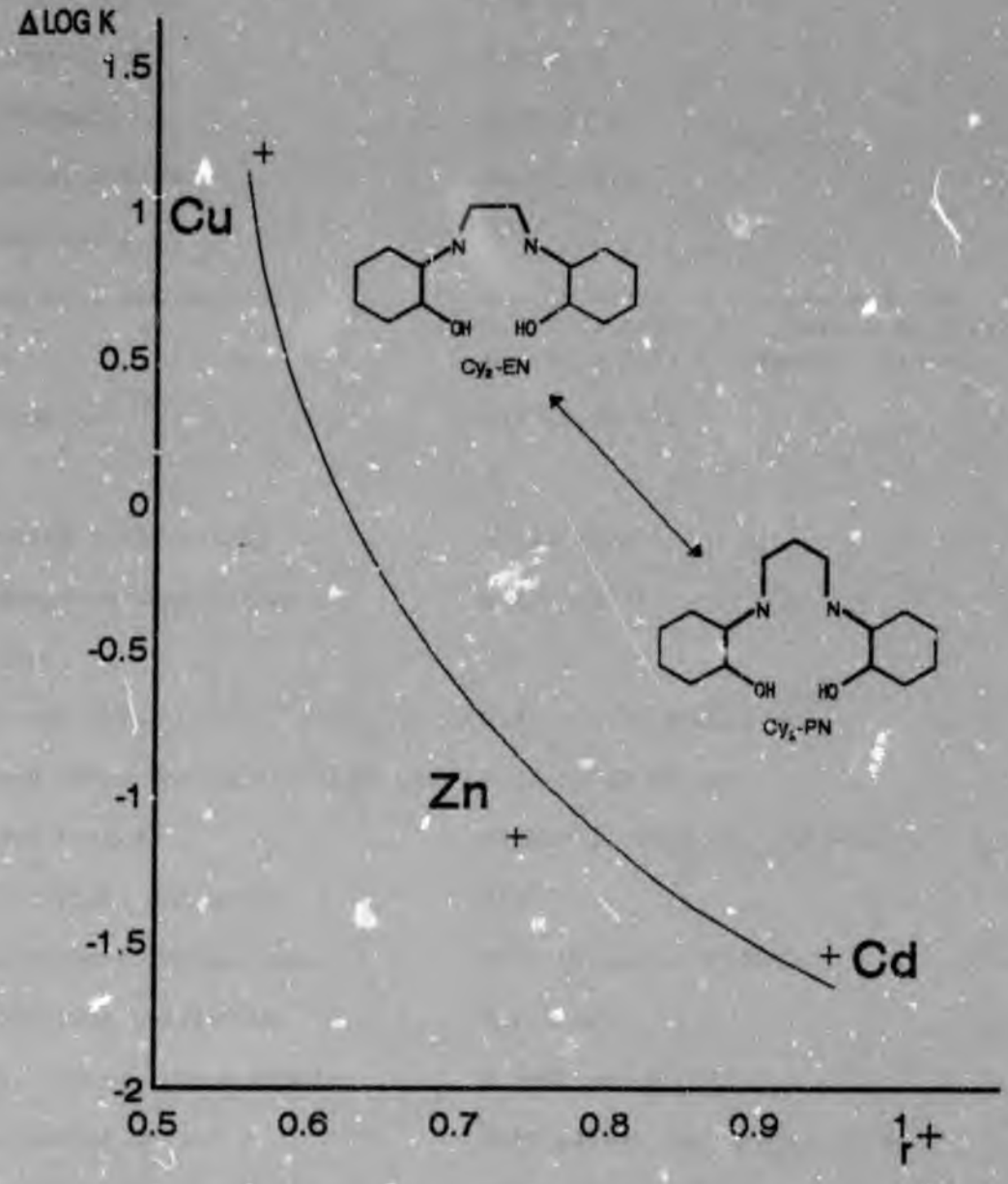


Figure 108 : relating Cy_2-EN and Cy_2-PN with their five and six-membered chelate rings in the parent amine

STRUCTURE OF $[Cu(Cy,-PN)H_2O]^{2+}(ClO_4^-)_2$

TABLE OF CRYSTAL DATA AND STRUCTURE REFINEMENT

Empirical formula	C15 H32 Cl2 Cu N2 O11
Formula weight	550.87
Temperature	163(2) K
Wavelength	0.71073 A
Crystal system	Monoclinic
Space group	P n
Unit cell dimensions	a = 11.627(2) A alpha = 90 deg. b = 7.8950(10) A beta = 98.15(3) deg. c = 12.737(8) A gamma = 90 deg.
Volume	1157.4(8) A^3
Z	2
Density (calculated)	1.581 Mg/m^3
Absorption coefficient	1.231 mm^-1
F(000)	574
Crystal size	0.41 x 0.33 x 0.12 mm
Theta range for data collection	2.22 to 25.06 deg.
Index ranges	0<=h<=13, 0<=k<=9, -15<=l<=15
Reflections collected	2161
Independent reflections	2161 [R(int) = 0.0000]
Absorption correction	Psi-scans
Max. and min. transmission	0.9999 and 0.8513
Refinement method	Full-matrix least-squares on F^2
Data / restraints / parameters	2130 / 63 / 308
Goodness-of-fit on F^2	1.062
Final R indices [I>2sigma(I)]	R1 = 0.0524, wR2 = 0.1359
R indices (all data)	R1 = 0.0619, wR2 = 0.1594
Absolute structure parameter	-0.02(3)
Largest diff. peak and hole	1.616 and -0.655 e.A^-3

The X-ray analysis of the crystal of the copper complex proved only the mesomeric form is observed.

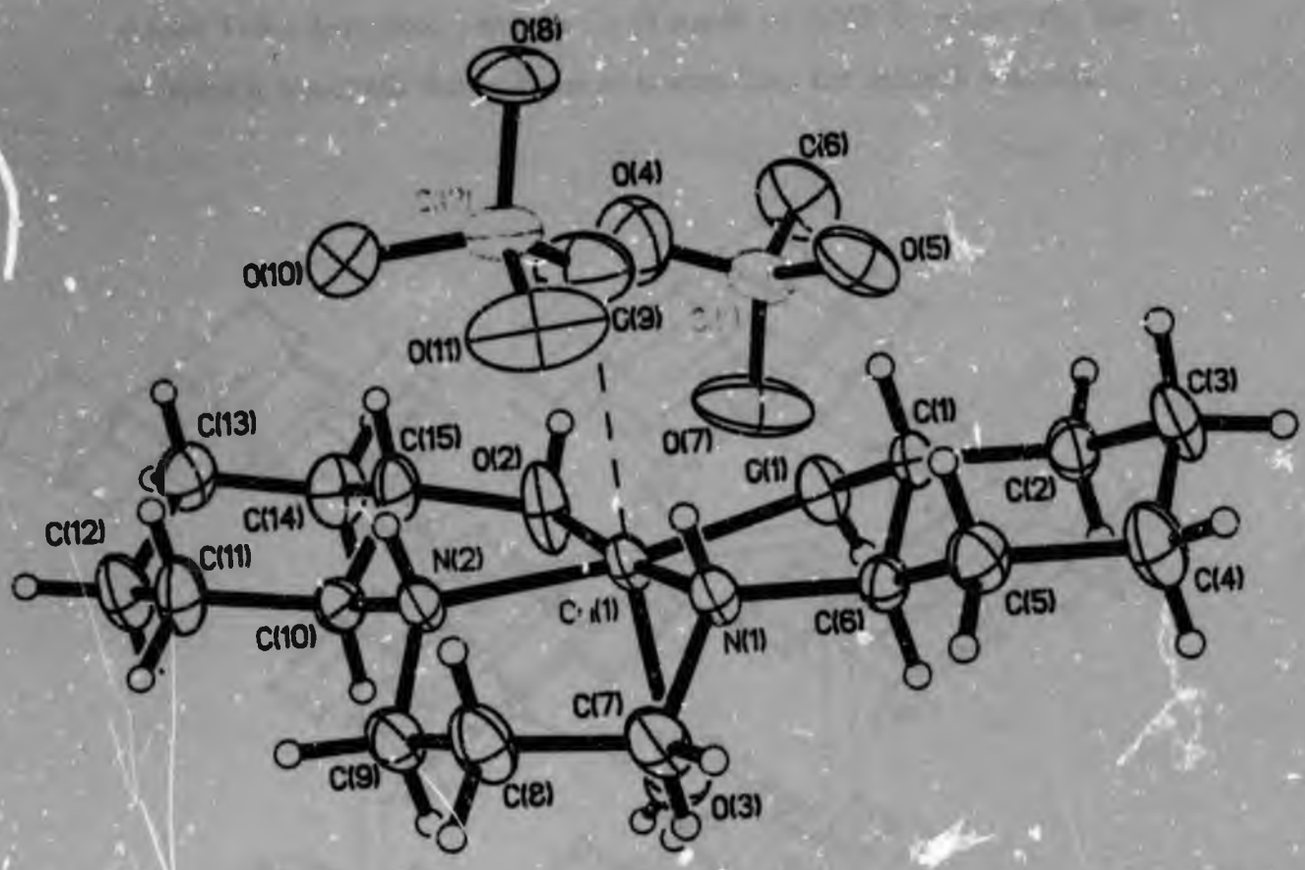


Figure 109 : ORTEP diagram of the structure of $[Cu(Cy_2\text{-}PN)H_2O]^{2+}(ClO^-)_2$

The copper complex is octahedral with the perchlorate and a coordinated water occupying the axial sites. The nitrogen and oxygen donors of the ligand define an irregular equatorial plane with Cu-N and Cu-O being of the order of 2 Å . The axial bonds are typically longer than the equatorial counterparts (Jahn Teller distortions) and the Cu-O bonds are 2.263 Å respectively. The complex is essentially flat or linear as is seen from the spacefill diagram.

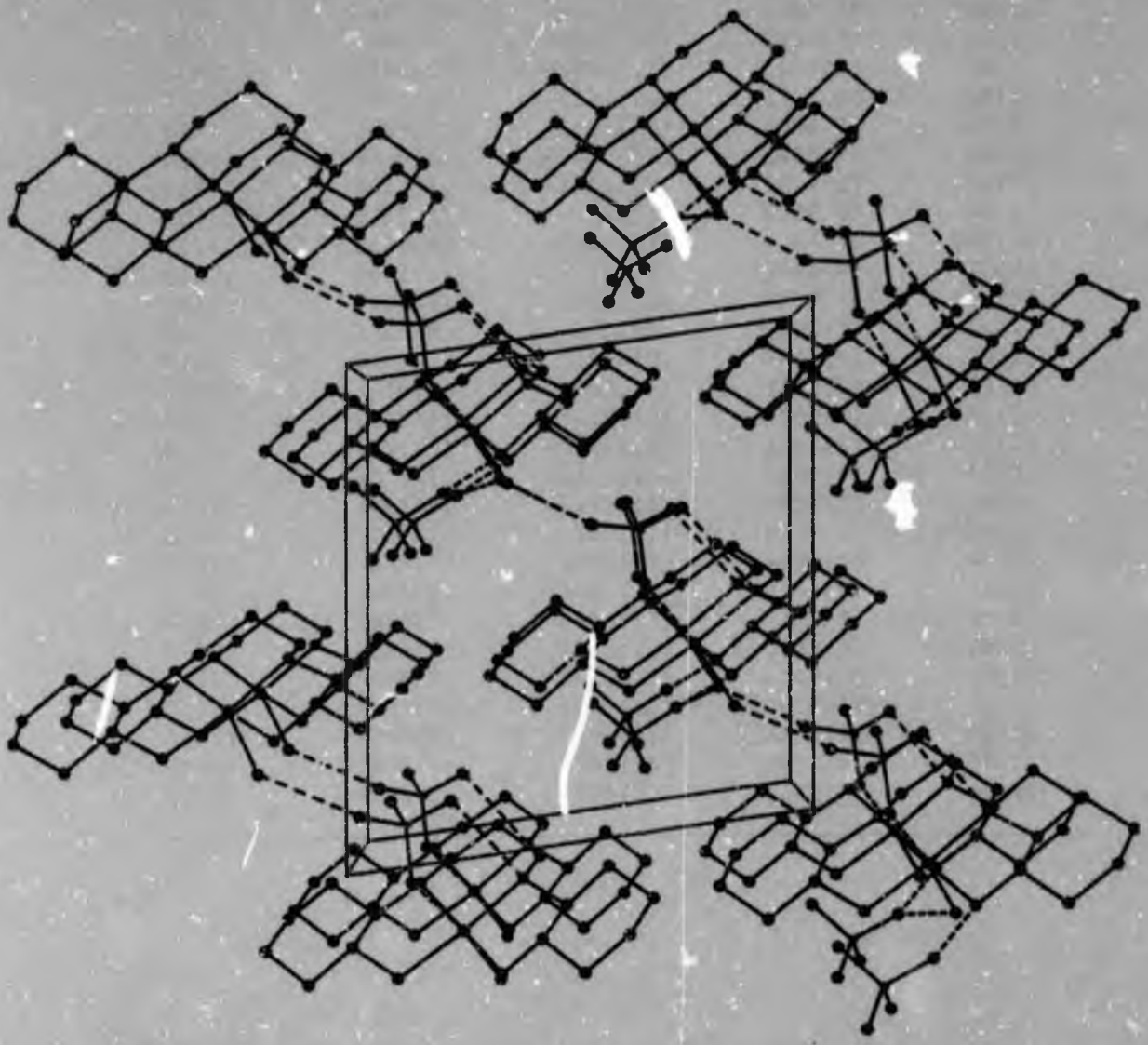


Figure 110 : representation of the unit cell in 3-D lattice

TABLE OF ATOMIC COORDINATES [$\times 10^4$] AND EQUIVALENT ISOTROPIC DISPLACEMENT PARAMETERS [$(\text{Å})^2 \times 10^3$]

	x	y	z	U(eq)
Cu(1)	2508(1)	486(1)	3538(1)	25(1)
Cl(1)	3800(2)	-3793(3)	1717(2)	38(1)
Cl(2)	3656(2)	-1875(3)	5914(2)	41(1)
O(1)	1647(6)	-1425(8)	2759(5)	30(1)
O(2)	3899(8)	278(12)	2796(7)	46(2)
O(3)	1725(8)	2381(12)	2308(8)	53(2)
O(4)	4668(10)	-3303(14)	2527(10)	81(3)
O(5)	2770(8)	-4320(10)	2151(8)	57(2)
O(6)	4194(10)	-5099(13)	1107(8)	66(3)
O(7)	3515(12)	-2337(14)	1115(10)	88(4)
O(8)	3899(15)	-3354(10)	6496(7)	47(5)
O(8')	4430(15)	-3060(19)	6450(8)	59(3)
O(9)	3513(8)	-2144(10)	4814(3)	64(3)
O(11)	2717(11)	-986(23)	6220(9)	86(8)
O(11')	2536(8)	-2164(33)	6247(10)	108(10)
O(10)	4672(12)	-778(20)	6142(9)	71(7)
O(10')	3998(21)	-218(10)	6177(10)	100(9)
N(1)	1213(8)	470(9)	4398(7)	24(2)
N(2)	3477(7)	2119(10)	4482(6)	25(2)
C(1)	774(7)	-2082(11)	3372(7)	25(2)
C(2)	-125(8)	-3139(12)	2699(8)	31(2)
C(3)	-1056(9)	-3724(12)	3362(9)	37(2)
C(4)	-1577(9)	-2247(14)	3860(9)	41(2)
C(5)	-645(8)	-1165(13)	4527(8)	32(2)
C(6)	247(7)	-584(11)	3837(7)	24(2)
C(7)	859(9)	2205(13)	4683(10)	40(2)
C(8)	1811(9)	3147(14)	5363(9)	41(2)
C(9)	2853(9)	3604(13)	4785(9)	34(2)
C(10)	4504(3)	2575(11)	3948(7)	26(2)
C(11)	5496(9)	3426(15)	4647(9)	39(2)
C(12)	6497(10)	3751(15)	4018(10)	46(3)
C(13)	6895(8)	2104(15)	3553(9)	42(2)
C(14)	5896(9)	1308(15)	2821(8)	39(2)
C(15)	4916(8)	976(13)	3482(8)	33(2)

TABLE OF BOND LENGTHS [Å] AND ANGLES [°]

Cu(1)-N(1)	1.977(9)
Cu(1)-O(2)	1.992(9)
Cu(1)-O(1)	1.996(6)
Cu(1)-N(2)	1.998(7)
Cu(1)-O(3)	2.263(9)
Cl(1)-O(4)	1.392(11)
Cl(1)-O(7)	1.395(10)
Cl(1)-O(6)	1.406(9)
Cl(1)-O(5)	1.449(9)
Cl(2)-O(8)	1.390(5)
Cl(2)-O(10')	1.395(5)
Cl(2)-O(11)	1.400(5)
Cl(2)-O(9)	1.404(4)
Cl(2)-O(8')	1.405(5)
Cl(2)-O(11')	1.444(5)
Cl(2)-O(10)	1.460(5)
O(1)-C(1)	1.460(11)
O(2)-C(15)	1.474(12)
O(8)-O(8')	0.67(2)
O(11)-O(11')	0.95(2)
O(11)-O(10')	1.62(2)
O(10)-O(10')	0.91(2)
N(1)-C(7)	1.492(12)
N(1)-C(6)	1.501(12)
N(2)-C(9)	1.459(12)
N(2)-C(10)	1.499(12)
C(1)-C(6)	1.492(13)
C(1)-C(2)	1.507(12)
C(2)-C(3)	1.535(13)
C(3)-C(4)	1.50(2)
C(4)-C(5)	1.538(14)
C(5)-C(6)	1.522(12)
C(7)-C(8)	1.50(2)
C(8)-C(9)	1.547(14)
C(10)-C(15)	1.503(14)
C(10)-C(11)	1.511(13)
C(11)-C(12)	1.53(2)
C(12)-C(13)	1.53(2)
C(13)-C(14)	1.519(14)
C(14)-C(15)	1.531(13)

N(1)-Cu(1)-O(2)	172.8(4)
N(1)-Cu(1)-O(1)	84.5(3)
O(2)-Cu(1)-O(1)	94.9(3)
N(1)-Cu(1)-N(2)	94.5(3)
O(2)-Cu(1)-N(2)	85.0(3)
O(1)-Cu(1)-N(2)	170.9(3)
N(1)-Cu(1)-O(3)	97.2(4)
O(2)-Cu(1)-O(3)	90.0(4)
O(1)-Cu(1)-O(3)	91.8(3)
N(2)-Cu(1)-O(3)	97.3(3)
O(4)-Cl(1)-O(7)	105.6(8)
O(4)-Cl(1)-O(6)	110.8(7)
O(7)-Cl(1)-O(6)	111.8(7)
O(4)-Cl(1)-O(5)	110.4(7)
O(7)-Cl(1)-O(5)	107.5(6)

O(6)-Cl(1)-O(5)	110.6(6)
O(8)-Cl(2)-O(10')	129.1(7)
O(8)-Cl(2)-O(11)	112.3(5)
O(10')-Cl(2)-O(11)	70.7(9)
O(8)-Cl(2)-O(9)	113.0(4)
O(10')-Cl(2)-O(9)	111.8(5)
O(11)-Cl(2)-O(9)	111.6(4)
O(8)-Cl(2)-O(8')	27.7(7)
O(10')-Cl(2)-O(8')	111.6(5)
O(11)-Cl(2)-O(8')	132.0(7)
O(9)-Cl(2)-O(8')	111.2(4)
O(8)-Cl(2)-O(11')	80.5(8)
O(10')-Cl(2)-O(11')	108.4(5)
O(11)-Cl(2)-O(11')	39.2(9)
O(9)-Cl(2)-O(11')	106.5(5)
O(8')-Cl(2)-O(11')	107.1(5)
O(8)-Cl(2)-O(10)	107.2(4)
O(10')-Cl(2)-O(10)	36.9(9)
O(11)-Cl(2)-O(10)	106.7(4)
O(9)-Cl(2)-O(10)	105.5(4)
O(8')-Cl(2)-O(10)	81.7(7)
O(11')-Cl(2)-O(10)	140.6(8)
C(1)-O(1)-Cu(1)	109.9(5)
C(15)-O(2)-Cu(1)	109.0(6)
O(8')-O(8)-Cl(2)	77.4(7)
O(8)-O(8')-Cl(2)	74.9(6)
O(11')-O(11)-Cl(2)	72.9(6)
O(11')-O(11)-O(10')	125.1(8)
Cl(2)-O(11)-O(10')	54.5(5)
O(11)-O(11')-Cl(2)	67.9(6)
O(10')-O(10)-Cl(2)	67.6(6)
O(10)-O(10')-Cl(2)	75.5(6)
O(10)-O(10')-O(11)	128.8(7)
Cl(2)-O(10')-O(11)	54.8(5)
C(7)-N(1)-C(6)	114.0(8)
C(7)-N(1)-Cu(1)	113.0(6)
C(6)-N(1)-Cu(1)	108.6(6)
C(9)-N(2)-C(10)	112.6(7)
C(9)-N(2)-Cu(1)	114.8(6)
C(10)-N(2)-Cu(1)	107.4(5)
O(1)-C(1)-C(6)	106.6(7)
O(1)-C(1)-C(2)	111.8(7)
C(6)-C(1)-C(2)	111.9(7)
C(1)-C(2)-C(3)	10[illegible].9(8)
C(4)-C(3)-C(2)	111.0(8)
C(3)-C(4)-C(5)	111.8(8)
C(6)-C(5)-C(4)	109.5(8)
C(1)-C(6)-N(1)	107.7(7)
C(1)-C(6)-C(5)	110.0(7)
N(1)-C(6)-C(5)	114.9(7)
N(1)-C(7)-C(8)	112.7(9)
C(7)-C(8)-C(9)	113.8(9)
N(2)-C(9)-C(8)	113.0(8)
N(2)-C(10)-C(15)	107.3(7)
N(2)-C(10)-C(11)	115.5(8)
C(15)-C(10)-C(11)	110.3(8)
C(10)-C(11)-C(12)	110.0(8)
C(11)-C(12)-C(13)	110.8(9)
C(14)-C(13)-C(12)	110.1(9)
C(13)-C(14)-C(15)	107.3(8)

O(2)-C(15)-C(10)	105.9(8)
O(2)-C(15)-C(14)	109.6(8)
C(10)-C(15)-C(14)	112.2(8)

Symmetry transformations used to generate equivalent atoms:

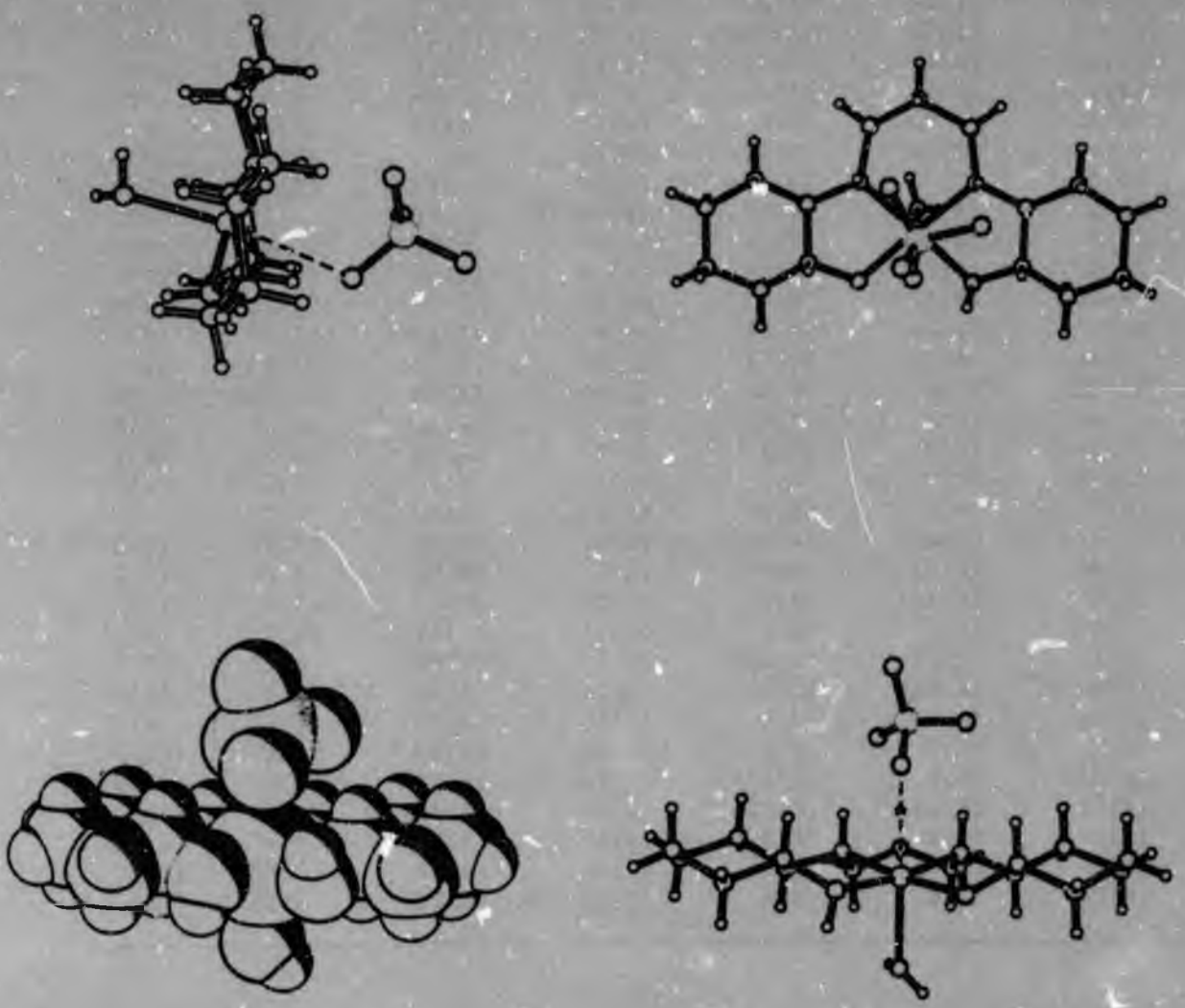


***Figure 111** : top view, side view, side view through 90°, spacefill diagrams for* $[Cu(Cy_2\text{-}PN)H_2O]^{2+}(ClO^-_4)_2$

TABLE OF HYDROGEN COORDINATES AND ISOTROPIC DISPLACEMENT PARAMETERS

	x	y	z	U(eq)
H(1D)	1309(6)	-1071(8)	2164(5)	80
H(2C)	3763	1554	3077	80
H(2C)	4124	-738	2941	50
H(3C)	2014(8)	3039(12)	1899(8)	50
H(3D)	1322(8)	3028(12)	2646(8)	80
H(1A)	1473(8)	-67(9)	5010(7)	80
H(1B)	1167(7)	-2764(11)	3936(7)	80
H(2A)	-472(8)	-2493(12)	2098(8)	80
H(2B)	236(8)	-4118(12)	2441(8)	80
H(3A)	-1656(9)	-4311(12)	2908(9)	80
H(3B)	-726(9)	-4499(12)	3904(9)	80
H(4A)	-2005(9)	-1552(14)	3317(9)	80
H(4B)	-2113(9)	-2660(14)	4309(9)	80
H(5A)	-1008(8)	-198(13)	4798(8)	80
H(5B)	-268(8)	-1806(13)	5117(8)	80
H(6A)	-147(7)	79(11)	3264(7)	80
H(7A)	619(9)	2841(13)	4047(10)	30
H(7B)	204(9)	2103(13)	5060(10)	80
H(8A)	1499(9)	4161(14)	5628(9)	80
H(8B)	2098(9)	2452(14)	5962(9)	80
H(9A)	3377(9)	4322(13)	5235(9)	80
H(9B)	2561(9)	4242(13)	4162(9)	80
H(10A)	4238(8)	3340(11)	3379(7)	80
H(11A)	5239(9)	4488(15)	4898(9)	80
H(11B)	5757(9)	2725(15)	5250(9)	80
H(12A)	6236(10)	4502(15)	3441(10)	80
H(12B)	7132(10)	4290(15)	4458(10)	80
H(13A)	7526(8)	2333(15)	3163(9)	80
H(13B)	7164(8)	1340(15)	4122(9)	80
H(14A)	5637(9)	2069(15)	2248(8)	80
H(14B)	6136(9)	270(15)	2526(8)	80
H(15A)	5182(8)	190(13)	4039(8)	80

TABLE OF ANISOTROPIC DISPLACEMENT PARAMETERS

The anisotropic displacement factor exponent takes the form:
$-2\pi^2 [h^2 a^{*2} U11 + ... + 2 h k a^* b^* U12]$

	U11	U22	U33	U23	U13	U12
Cu(1)	22(1)	22(1)	32(1)	-6(1)	9(1)	-5(1)
Cl(1)	44(1)	30(1)	44(1)	2(1)	22(1)	5(1)
Cl(2)	61(2)	31(1)	29(1)	1(1)	-2(1)	15(1)
O(1)	30(3)	32(3)	32(3)	-8(3)	13(3)	-7(3)
O(2)	36(5)	55(5)	50(5)	-27(4)	17(4)	-25(4)
O(3)	43(5)	43(5)	68(5)	20(4)	-8(4)	-7(4)
O(4)	70(7)	69(7)	100(9)	-24(6)	1(6)	1(6)
O(5)	62(6)	35(4)	82(6)	4(4)	40(5)	7(4)
O(6)	75(6)	54(5)	75(6)	-22(5)	32(5)	7(5)
O(7)	117(9)	62(6)	99(8)	48(6)	55(7)	31(6)
O(8)	56(9)	39(7)	47(8)	25(6)	9(6)	4(7)
O(8')	56(10)	39(8)	75(10)	12(7)	-20(8)	-1(7)
O(9)	95(7)	50(5)	44(5)	-5(4)	3(5)	18(5)
O(11)	103(12)	91(12)	70(10)	28(8)	35(8)	47(9)
O(11')	92(13)	111(14)	129(14)	3(10)	44(10)	16(10)
O(10)	66(10)	50(9)	84(10)	11(7)	-32(8)	-6(8)
O(10')	125(14)	62(11)	100(12)	-4(9)	-30(10)	22(10)
N(1)	22(4)	21(4)	31(4)	-6(3)	9(3)	-4(3)
N(2)	27(4)	20(3)	29(4)	-1(3)	2(3)	-6(3)
C(1)	20(4)	24(4)	32(4)	1(4)	2(3)	-7(3)
C(2)	27(5)	28(5)	38(5)	-6(4)	3(4)	-5(4)
C(3)	34(5)	28(5)	50(6)	-10(4)	14(4)	-16(4)
C(4)	35(5)	39(5)	52(6)	-9(5)	19(5)	-14(5)
C(5)	27(5)	33(5)	38(5)	-3(4)	11(4)	-3(4)
C(6)	19(4)	25(4)	27(4)	-3(3)	4(3)	-2(3)
C(7)	25(5)	28(5)	72(7)	-14(5)	20(5)	-1(4)
C(8)	38(6)	34(5)	53(6)	-15(5)	17(5)	-6(4)
C(9)	29(5)	27(4)	47(5)	-8(4)	8(4)	-2(4)
C(10)	23(4)	26(4)	30(4)	5(4)	4(4)	-5(4)
C(11)	25(5)	45(6)	49(6)	-16(5)	8(4)	-10(4)
C(12)	37(6)	41(6)	62(7)	-12(5)	12(5)	-15(5)
C(13)	26(5)	47(6)	55(6)	-8(5)	8(5)	0(5)
C(14)	29(5)	51(6)	40(5)	-6(5)	17(4)	-8(5)
C(15)	22(4)	37(5)	43(5)	-8(4)	8(4)	-9(4)

In Magnetic resonance imaging (MRI) successful relaxation agents consist of metal complexes, paramagnetic metal complexes of lanthanides, which can be limited by the number of coordinated water molecules. Relaxation agents serve to decrease the relaxation times of nearby water protons and in so doing enhance the image contrast. For this purpose it is best to increase the number of coordinated water molecules (Annie Bligh et al 1992). The coordinated water molecule on $[Cu(Cy2\text{-}PN)H_2O]^{2+}$ suggests such an application with lanthanide complexes, such as gadolinium, of this type of compound.

INTRODUCING TRANS HYDROXYCYCLOHEXYL GROUPS ON DIETHYLENETRIAMINE

The ability of the hydroxycyclohexyl pendant groups to enhance metal ion selectivity for the smaller metal ions applies to the to the diamines at large as illustrated in the previous sections. In all the cases studied with diamines coordination of the hydroxycyclohexyl pendant arm took place along a equatorial plane. This means that van der Waals interactions between the bulky cyclohexyl bridges and the carbon backbone of the parent amine were emphasized and played an important role in the pattern observed for the metal ion selectivity. Extending the study to triamines allows for investigation of changes in metal ion selectivity should the hydroxycyclohexyl pendant arm coordinate in an axial position. Axial coordination, which results in longer bonds, and the new positioning of the bulky cyclohexyl groups may have a pronounced effect on the selectivity pattern. The idea is to investigate if the effect of the hydroxycyclohexyl group is reproducible no matter what its

orientation. For this reason Cy_2-DIEN was studied. The ligand contains three N-donors and two O-donors; if all are involved in the coordination to a metal ion then occupation of an axial site is inevitable. A suitable analogue for an appropriate comparison with Cy_2-DIEN is the macrocycle 15-aneN_3O_2 since it contains the same number of donors and only has ethylene bridges connecting the donor atoms.

TABLE 15 : Protonation and formation constants of Cy_2-DIEN compared to those of 15-aneN_3O_2 in terms of metal ionic radius.

metal ion	ionic radius	Cy_2-DIEN	15-aneN_3O_2[a]	ΔlogK
Cu^{2+}	0.57	16.74	15.27	+1.47
Zn^{2+}	0.74	9.57	8.85	+0.72
Cd^{2+}	0.95	9.34	10.05	-0.71
Pb^{2+}	1.18	9.01	10.07	-1.06
pKa_1		9.85	9.20	-
pKa_2		8.76	8.50	-
pKa_3		3.84	2.12	-

[a] Hancock et al (1989)

The effect of the hydroxycyclohexyl pendant group on metal ion selectivity for triamines appears identical to that observed in the studies of diamine derivatives in earlier sections.

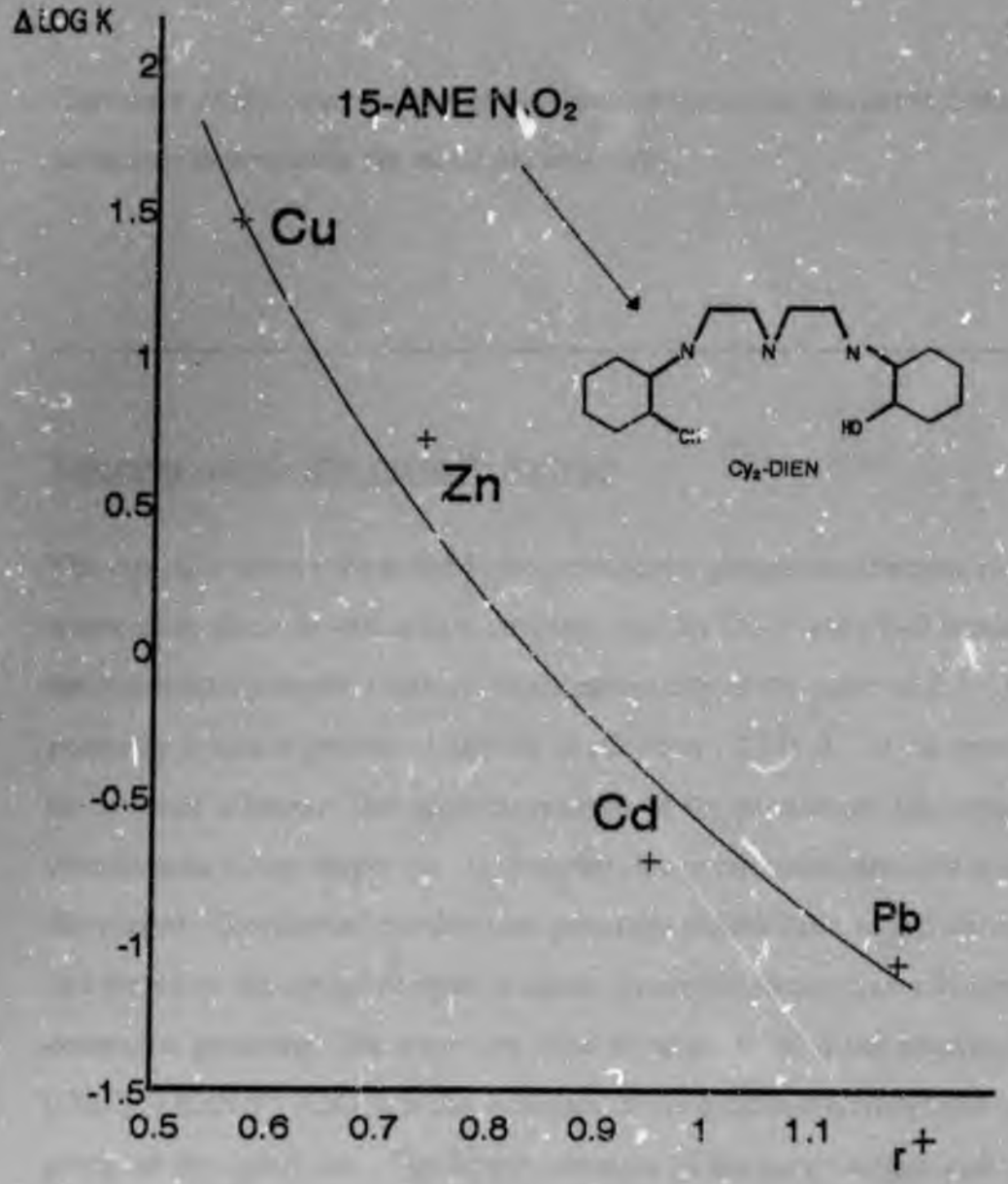


Figure 112 : change in stability in relation to metal ionic radius in comparing Cy_2-DIEN with 15-aneN_3O_2

The expectation of relaxed selectivity for the smaller metal ions is proven incorrect as is evident from the steepness of the slope in plotting ΔlogK versus ionic radius when passing from 15-aneN_3O_2 to Cy_2-DIEN. The positioning of the bulky cyclohexyl pendant group, so as to coordinate at an axial site, does not appear to decrease the repulsive van der Waals interactions between the cyclohexyl group and the carbon backbone of diethylenetriamine (DIEN).

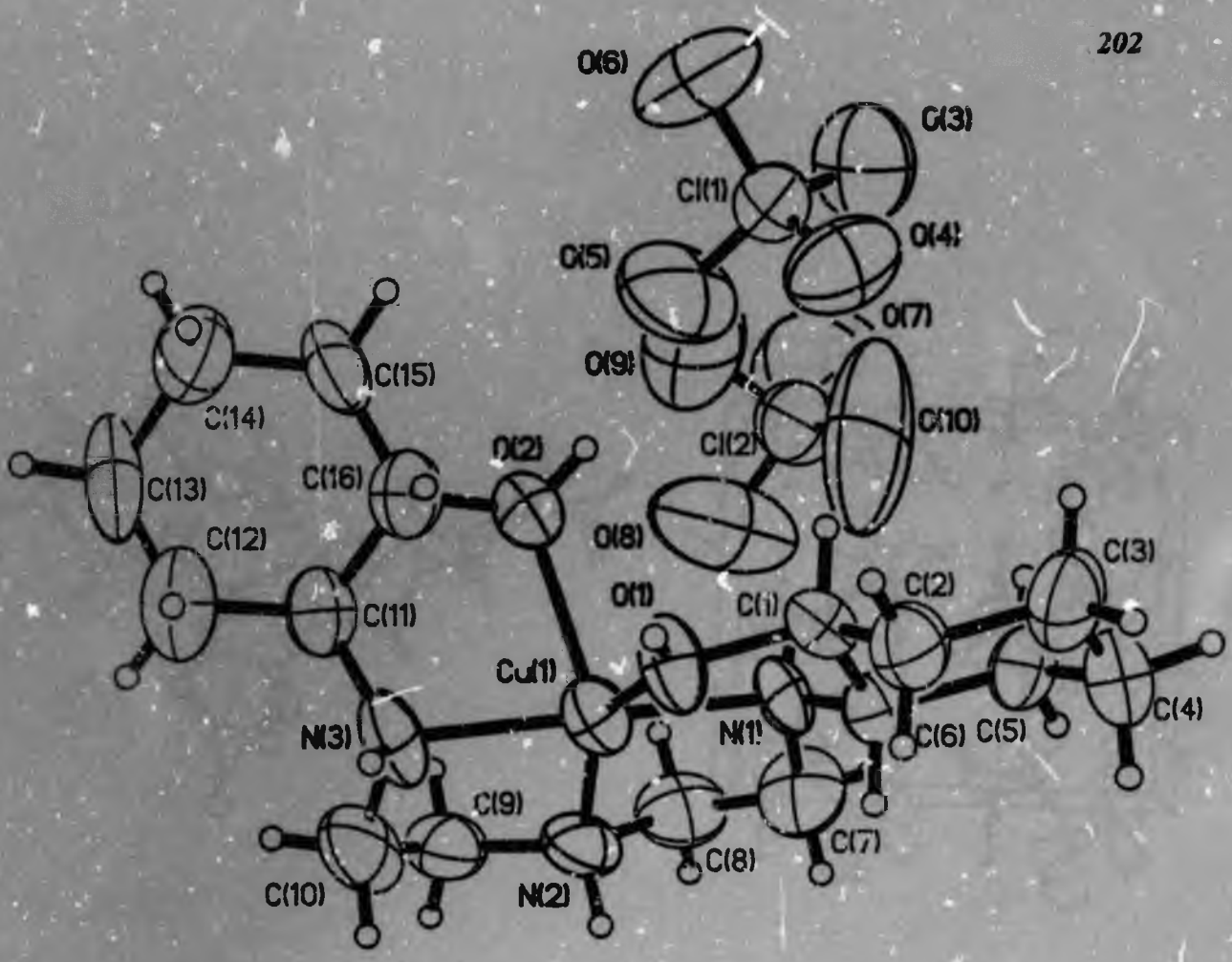


Figure 113 : ORTEP diagram of $[Cu(Cy_2\text{-}DIEN]^{2+}(ClO_4^-)_2$



Figure 114 : spacefill diagram of $[Cu(Cy_2\text{-}DIEN)]^{2+}(ClO_4^-)_2$

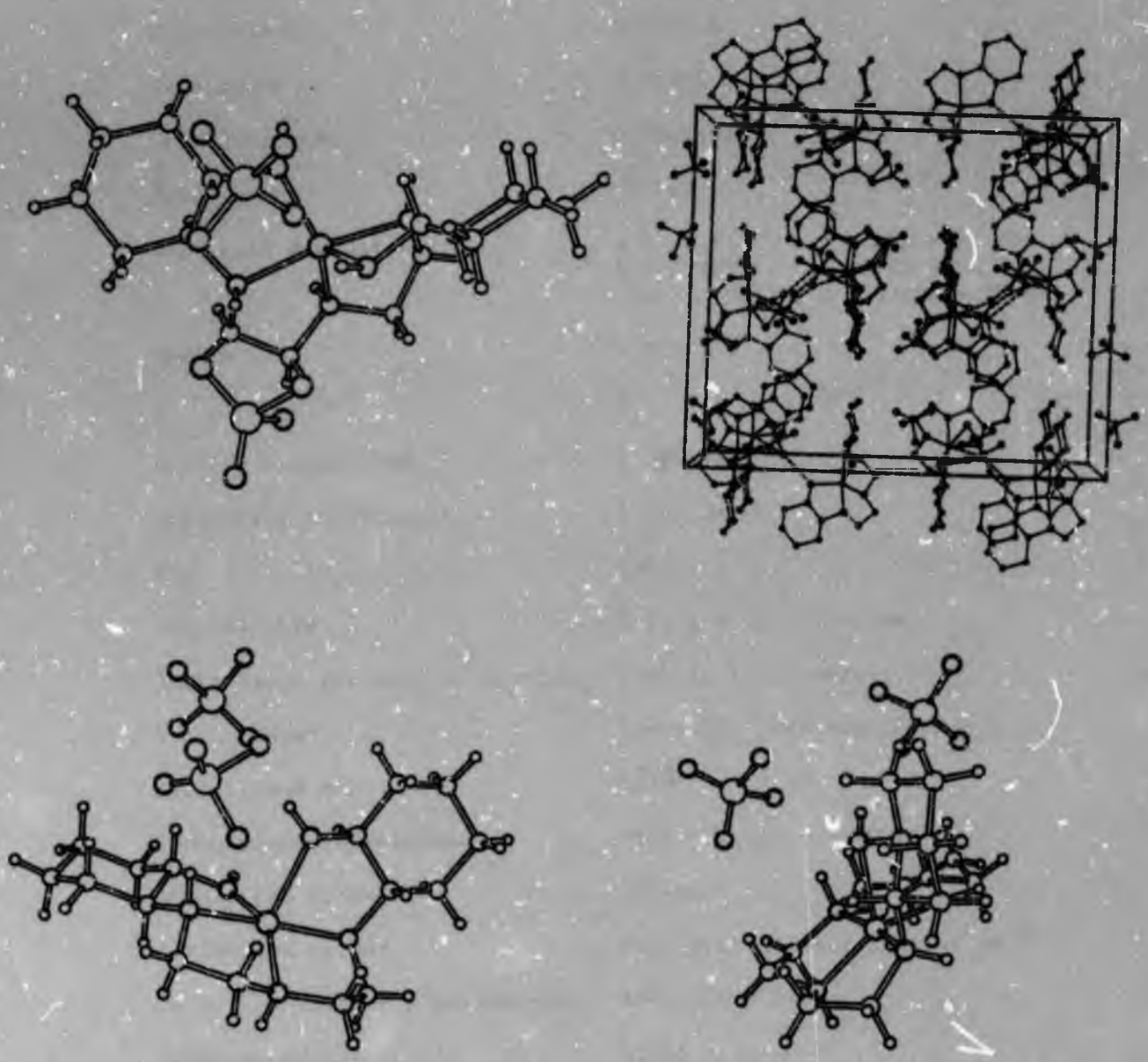


Figure 115 : diagram of unit cell in 3-D lattice, side, top and side with 90° rotation drawings

TABLE OF CRYSTAL DATA AND STRUCTURE REFINEMENT

Empirical formula	C16 H33 Cl2 Cu N3 O10
Formula weight	561.89
Temperature	293(2) K
Wavelength	0.71073 A
Crystal system	Orthorhombic
Space group	P bca
Unit cell dimensions	a = 21.82(2) A alpha = 90 deg. b = 8.525(7) A beta = 90 deg. c = 25.404(14) A gamma = 90 deg.
Volume	4725(6) A^3
Z	8
Density (calculated)	1.580 Mg/m^3
Absorption coefficient	1.206 mm^-1
F(000)	2344
Crystal size	0.25 x 0.22 x 0.10 mm
Theta range for data collection	2.69 to 25.07 deg.
Index ranges	0<=h<=25, 0<=k<=10, 0<=l<=30
Reflections collected	4715
Independent reflections	4104 [R(int) = 0.0000]
Absorption correction	Difabs
Refinement method	Full-matrix least-squares on F^2
Data / restraints / parameters	4072 / 6 / 289
Goodness-of-fit on F^2	1.041
Final R indices [I>2sigma(I)]	R1 = 0.0821, wR2 = 0.2058
R indices (all data)	R1 = 0.2302, wR2 = 0.3743
Largest diff. peak and hole	0.819 and -0.447 e.A^-3

TABLE OF ATOMIC COORDINATES [$\times 10^4$] AND EQUIVALENT ISOTROPIC DISPLACEMENT PARAMETERS [$(Å)^2 \times 10^3$]

	x	y	z	U(eq)
Cu(1)	5550(1)	1024(3)	3694(1)	58(1)
Cl(1)	5616(1)	-4966(3)	2934(1)	58(1)
Cl(2)	6467(2)	-3325(5)	4646(2)	92(1)
O(1)	5636(3)	369(8)	2945(3)	60(2)
O(2)	5083(3)	-1213(8)	3926(3)	73(2)
O(3)	6073(5)	-5858(12)	3196(4)	115(3)
O(4)	5855(4)	-4224(10)	2490(3)	96(3)
O(5)	5381(5)	-3881(12)	3291(4)	135(4)
O(6)	5135(4)	-6023(11)	2786(3)	108(3)
O(7)	6671(10)	-4130(28)	5010(9)	275(10)
O(8)	6273(9)	-1880(16)	4835(6)	203(7)
O(9)	5838(8)	-3943(21)	4526(8)	227(8)
O(10)	6697(6)	-3179(28)	4173(5)	249(10)
N(1)	6417(3)	286(10)	3750(3)	54(2)
N(2)	5761(4)	2528(10)	4250(4)	68(3)
N(3)	4672(4)	1800(12)	3756(3)	68(3)
C(1)	6217(4)	-435(11)	2847(4)	49(3)
C(2)	6426(5)	-282(14)	2285(4)	65(3)
C(3)	7030(5)	-1151(15)	2217(5)	83(4)
C(4)	7499(6)	-559(16)	2601(5)	84(4)
C(5)	7291(4)	-563(14)	3166(5)	68(3)
C(6)	6679(4)	279(12)	3222(4)	56(3)
C(7)	6733(6)	1310(16)	4143(5)	84(4)
C(8)	6286(6)	1831(15)	4539(5)	78(4)
C(9)	5190(6)	2896(14)	4530(5)	77(3)
C(10)	4712(6)	3138(15)	4126(5)	91(4)
C(11)	4251(5)	518(13)	3955(4)	61(3)
C(12)	3594(5)	828(17)	3814(5)	85(4)
C(13)	3194(5)	-454(18)	4020(5)	101(5)
C(14)	3399(5)	-2036(17)	3827(6)	101(5)
C(15)	4065(5)	-2345(14)	3955(5)	79(4)
C(16)	4478(5)	-1016(14)	3753(4)	67(3)

TABLE OF BOND LENGTHS [Å] AND ANGLES [°]

Cu(1)-N(2)	1.963(9)
Cu(1)-O(1)	1.991(6)
Cu(1)-N(1)	1.997(7)
Cu(1)-N(3)	2.033(8)
Cu(1)-O(2)	2.241(7)
Cl(1)-O(5)	1.392(10)
Cl(1)-O(4)	1.395(8)
Cl(1)-O(3)	1.420(10)
Cl(1)-O(6)	1.434(8)
Cl(2)-O(7)	1.23(2)
Cl(2)-O(10)	1.309(13)
Cl(2)-O(8)	1.388(14)
Cl(2)-O(9)	1.50(2)
O(1)-C(1)	1.462(10)
O(2)-C(16)	1.400(12)
N(1)-C(6)	1.457(12)
N(1)-C(7)	1.495(13)
N(2)-C(9)	1.468(13)
N(2)-C(8)	1.484(13)
N(3)-C(10)	1.48(2)
N(3)-C(11)	1.514(14)
C(1)-C(2)	1.504(12)
C(1)-C(6)	1.514(13)
C(2)-C(3)	1.52(2)
C(3)-C(4)	1.50(2)
C(4)-C(5)	1.50(2)
C(5)-C(6)	1.523(13)
C(7)-C(8)	1.47(2)
C(9)-C(10)	1.48(2)
C(11)-C(16)	1.49(2)
C(11)-C(12)	1.501(14)
C(12)-C(13)	1.49(2)
C(13)-C(14)	1.50(2)
C(14)-C(15)	1.51(2)
C(15)-C(16)	1.54(2)

N(2)-Cu(1)-O(1)	148.1(3)
N(2)-Cu(1)-N(1)	86.1(4)
O(1)-Cu(1)-N(1)	83.7(3)
N(2)-Cu(1)-N(3)	87.3(4)
O(1)-Cu(1)-N(3)	104.7(3)
N(1)-Cu(1)-N(3)	171.5(3)
N(2)-Cu(1)-O(2)	118.2(3)
O(1)-Cu(1)-O(2)	93.2(3)
N(1)-Cu(1)-O(2)	98.3(3)
N(3)-Cu(1)-O(2)	80.1(3)
O(5)-Cl(1)-O(4)	111.3(6)
O(5)-Cl(1)-O(3)	108.0(7)
O(4)-Cl(1)-O(3)	111.0(6)
O(5)-Cl(1)-O(6)	108.6(7)
O(4)-Cl(1)-O(6)	110.3(5)
O(3)-Cl(1)-O(6)	107.5(6)
O(7)-Cl(2)-O(10)	127.0(13)
O(7)-Cl(2)-O(8)	110.1(12)
O(10)-Cl(2)-O(8)	110.5(12)
O(7)-Cl(2)-O(9)	106.7(13)

O(10)-Cl(2)-O(9)	101.3(10)
O(8)-Cl(2)-O(9)	96.0(10)
C(1)-O(1)-Cu(1)	112.1(5)
C(16)-O(2)-Cu(1)	104.1(7)
C(6)-N(1)-C(7)	115.9(9)
C(6)-N(1)-Cu(1)	107.9(6)
C(7)-N(1)-Cu(1)	107.4(7)
C(9)-N(2)-C(8)	120.0(9)
C(9)-N(2)-Cu(1)	106.8(7)
C(8)-N(2)-Cu(1)	106.0(6)
C(10)-N(3)-C(11)	112.3(8)
C(10)-N(3)-Cu(1)	104.2(8)
C(11)-N(3)-Cu(1)	111.3(6)
O(1)-C(1)-C(2)	112.6(8)
O(1)-C(1)-C(6)	106.3(7)
C(2)-C(1)-C(6)	111.1(9)
C(1)-C(2)-C(3)	109.2(9)
C(4)-C(3)-C(2)	110.6(10)
C(3)-C(4)-C(5)	114.5(10)
C(4)-C(5)-C(6)	110.7(9)
N(1)-C(6)-C(1)	108.6(8)
N(1)-C(6)-C(5)	115.6(8)
C(1)-C(6)-C(5)	109.6(8)
C(8)-C(7)-N(1)	109.2(9)
C(7)-C(8)-N(2)	107.0(9)
N(2)-C(9)-C(10)	107.1(10)
C(9)-C(10)-N(3)	112.0(10)
C(16)-C(11)-C(12)	113.0(10)
C(16)-C(11)-N(3)	108.5(8)
C(12)-C(11)-N(3)	111.9(10)
C(13)-C(12)-C(11)	110.2(10)
C(12)-C(13)-C(14)	111.5(11)
C(13)-C(14)-C(15)	111.9(10)
C(14)-C(15)-C(16)	111.4(11)
O(2)-C(16)-C(11)	108.1(10)
O(2)-C(16)-C(15)	111.1(9)
C(11)-C(16)-C(15)	109.7(8)

Symmetry transformations used to generate equivalent atoms:

TABLE OF ANISOTROPIC DISPLACEMENT PARAMETERS

The anisotropic displacement factor exponent takes the form:
-2 pi^2 [h^2 a*^2 U11 + ... + 2 h k a* b* U12]

	U11	U22	U33	U23	U13	U12
Cu(1)	60(1)	59(1)	55(1)	-5(1)	6(1)	11(1)
Cl(1)	58(2)	59(2)	57(2)	5(1)	-3(2)	0(2)
Cl(2)	106(3)	85(3)	84(2)	7(2)	28(2)	2(2)
O(1)	52(4)	85(5)	44(4)	-14(4)	-1(3)	23(4)
O(2)	60(5)	57(5)	102(6)	4(5)	11(4)	11(4)
O(3)	104(7)	134(8)	108(7)	15(7)	-10(6)	16(7)
O(4)	117(7)	102(6)	69(5)	10(6)	9(5)	-36(6)
O(5)	184(11)	100(8)	121(8)	-32(7)	67(8)	0(8)
O(6)	102(7)	103(7)	120(7)	45(6)	-43(6)	-49(6)
O(7)	276(10)	275(10)	275(10)	2(2)	-2(2)	3(2)
O(8)	311(21)	102(10)	196(14)	-7(10)	24(13)	4(13)
O(9)	144(12)	239(18)	298(22)	-53(16)	76(13)	-24(13)
O(10)	130(11)	477(31)	141(11)	-62(16)	64(9)	23(15)
N(1)	42(4)	58(5)	62(5)	0(5)	-9(4)	24(4)
N(2)	88(7)	43(5)	72(6)	-9(5)	30(6)	2(5)
N(3)	69(6)	82(6)	53(5)	6(5)	16(5)	37(5)
C(1)	56(6)	40(6)	51(6)	-2(5)	1(5)	9(5)
C(2)	63(7)	69(8)	63(7)	-7(6)	11(6)	1(7)
C(3)	67(8)	99(10)	82(8)	0(8)	26(7)	-6(8)
C(4)	55(7)	84(9)	113(10)	-8(8)	19(8)	18(7)
C(5)	38(6)	75(8)	92(9)	0(7)	-2(6)	-1(6)
C(6)	48(6)	52(6)	67(7)	0(6)	-1(6)	5(5)
C(7)	76(9)	98(10)	76(8)	-21(8)	-20(7)	-11(8)
C(8)	96(10)	71(8)	67(7)	-18(7)	-8(8)	-13(8)
C(9)	86(9)	51(7)	93(9)	-11(7)	19(8)	-5(7)
C(10)	104(11)	74(9)	95(10)	8(8)	49(9)	23(9)
C(11)	59(7)	82(8)	43(6)	-4(6)	8(5)	9(6)
C(12)	64(8)	130(12)	61(7)	-1(8)	0(6)	16(9)
C(13)	45(7)	169(16)	89(10)	-47(11)	-11(7)	38(9)
C(14)	64(8)	111(12)	127(12)	-32(10)	3(8)	-5(8)
C(15)	64(8)	86(9)	85(8)	-30(8)	-1(7)	31(7)
C(16)	60(7)	81(8)	50(7)	0(7)	7(6)	5(7)

TABLE OF HYDROGEN COORDINATES AND ISOTROPIC DISPLACEMENT PARAMETERS

	x	y	z	U(eq)
H(1C)	5449(3)	186(8)	2658(3)	50
H(2C)	5253(3)	-2057(8)	3825(3)	50
H(1)	6415(3)	-715(10)	3874(3)	80
H(2)	5894(4)	3426(10)	4094(4)	80
H(3)	4539(4)	2142(12)	3436(3)	80
H(1A)	6176(4)	-1524(11)	2936(4)	80
H(2A)	6453(5)	802(14)	2185(4)	80
H(2B)	6127(5)	-785(14)	2066(4)	80
H(3A)	7177(5)	-972(16)	1866(5)	80
H(3B)	6980(5)	-2262(16)	2262(5)	80
H(4A)	7598(6)	505(16)	2512(5)	80
H(4B)	7865(6)	-1170(16)	2559(5)	80
H(5A)	7598(4)	-51(14)	3375(5)	80
H(5B)	7257(4)	-1631(14)	3282(5)	80
H(6A)	6727(4)	1360(12)	3125(4)	80
H(7A)	6848(6)	2235(16)	3952(5)	80
H(7B)	7097(6)	855(16)	4289(5)	80
H(8A)	6150(6)	924(15)	4731(5)	80
H(8B)	6470(6)	2563(15)	4779(5)	80
H(9A)	5239(6)	3795(14)	4753(5)	80
H(9B)	5089(6)	2003(14)	4743(5)	80
H(10A)	4322(6)	3247(15)	4297(5)	80
H(10B)	4799(6)	4107(15)	3949(5)	80
H(11A)	4288(5)	498(13)	4331(4)	80
H(12A)	3524(5)	923(17)	3442(5)	80
H(12B)	3457(5)	1776(17)	3980(5)	80
H(13A)	2773(5)	-331(18)	3918(5)	80
H(13B)	3208(5)	-403(18)	4398(5)	80
H(14A)	3316(5)	-2173(17)	3459(6)	80
H(14B)	3164(5)	-2801(17)	4017(6)	80
H(15A)	4183(5)	-3301(14)	3783(5)	80
H(15B)	4131(5)	-2479(14)	4326(5)	80
H(16A)	4483(5)	-1036(14)	3375(4)	80

INTRODUCTION OF HYDROXYCYCLOHEXYL PENDANT GROUPS TO TETRAAZAMACROCYCLES

Over the years macrocyclic ligands have attracted much attention in an attempt to encapsulate metal ions. There have been many strategies involved in obtaining metal complexes of macrocyclic ligands. With multidentate cyclic ligands metal ions are trapped by inserting the metal within the macromonocycle (Lindoy & Busch 1971), inserting the metal ion within the cavity of a macrobicyclic ligand (Sargeson 1979) and more recently much emphasis has been placed on using macrocycles that have pendant arms which carry suitable donor groups to compliment those in the macrocycle.

It is the latter strategy that has led to a class of compounds termed *"scorpiands"* by Pallavicini et al (1987). These macrocycles have potentially coordinating pendants that may bind metal ions at axial sites in addition to the coordination of the macrocyclic donors that surround the metal ion encapsulated in the macrocyclic ring. Such compounds are synthesized as either N-functionalised or C-functionalised derivatives and the number of pendant donors that are attached varies from one to as many as four. The aim is to encapsulate the metal ion as effectively as possible. Ultimately the ideal encapsulation, that is the most effective, is when the axial sites are occupied by the pendant donors. The mode of complexation for these compounds are similar to that observed for macrobicyclic compounds except that they are more prone to dissociation due to the pendant arms.

Curvature of the outer surface of the ligand remains the dominant factor in ultimately determining the metal ion selectivity.

STRUCTURE OF $[Cu(Cy_2\text{-}DIEN)]^{2+}$ $(ClO^-_4)_2$

The crystal structure shows the hydroxycyclohexyl groups coordinating in the donor atom plane as well as in a axial fashion. The Cu-N and Cu-O bonds in the distorted equatorial plane are characteristically of the order of 2 Å . The geometry is square pyramidal and the Cu-O bond (2.241 Å) at the apex of the pyramid is longer. The apparent position of the perchlorate ion suggests coordination to the copper via O_8 , however, the perchlorates are both highly disordered. Coordinated perchlorates generally exhibit little or no disorder and therefore the copper complex is square pyramidal rather than a distorted octahedral geometry. The important issue to be made from the structure of $[Cu(Cy_2\text{-}DIEN)]^{2+}$ $(ClO^-_4)_2$ is the influence of the hydroxycyclohexyl pendant group on the apical site. The ligand curvature of the outer surface appears as crowded as the planar molecule of $Cu(Cy_2\text{-}PN)H_2O]^{2+}$ $(ClO^-_4)_2$ and hence the rationalisation for the retention of selectivity favouring the smaller metal ions.

Table 16 : Stability constants of Cy-12aneN$_4$ \ Cy-cyclen at 25°C and 0.1M ionic strength.

metal ion	ionic radius	logK
Pb2+	1.18	11.40
Cd2+	0.95	14.58
Zn2+	0.75	13.85
pKa_1	-	10.65
pKa_2	-	9.51
pKa_3	-	4.03

An increase in the stability of cadmium is observed when compared to the parent macrocycle. Cadmium appears to be the exception when considering Zn and Pb that are on opposite sides in terms of size. A molecular mechanics investigation with the SYBYL molecular mechanics package (Clarke et al 1989) revealed Cadmium to have the ideal size for efficient encapsulation in the cavity of Cy-12-aneN$_4$. The plots for ML and ML(H_2O) complex species as a function of metal-nitrogen distance revealed two minima. The curve for the ML species exhibits a minimum at 2.12 Å which is equivalent to a metal ion of radius 0.66 Å. The ML(H_2O) species has a minimum at a metal-nitrogen distance of 2.38 Å which corresponds to a metal ion with radius 0.92 Å. The nitrogen radius was taken to be 1.46 Å (Shanon et al 1976). This suggests that metals with an ionic radius smaller than 0.92 Å would not be able to incorporate a coordinate water molecule and would be most stable with a coordination number of five, while the larger metal ions with ionic radii $\geq$ 0.92

Å would accommodate a coordinated water.

The minimum for the $ML(H_2O)$ species is also at a lower internal energy than that for the ML species implying that metal ions with radius ≥ 0.92 Å would form more stable complexes. This is of a comparable size to Gd^{3+} and the introduction of hydroxycyclohexyl pendant groups may prove to be advantageous in the design of Gd^{3+} complexes to act as imaging agents .

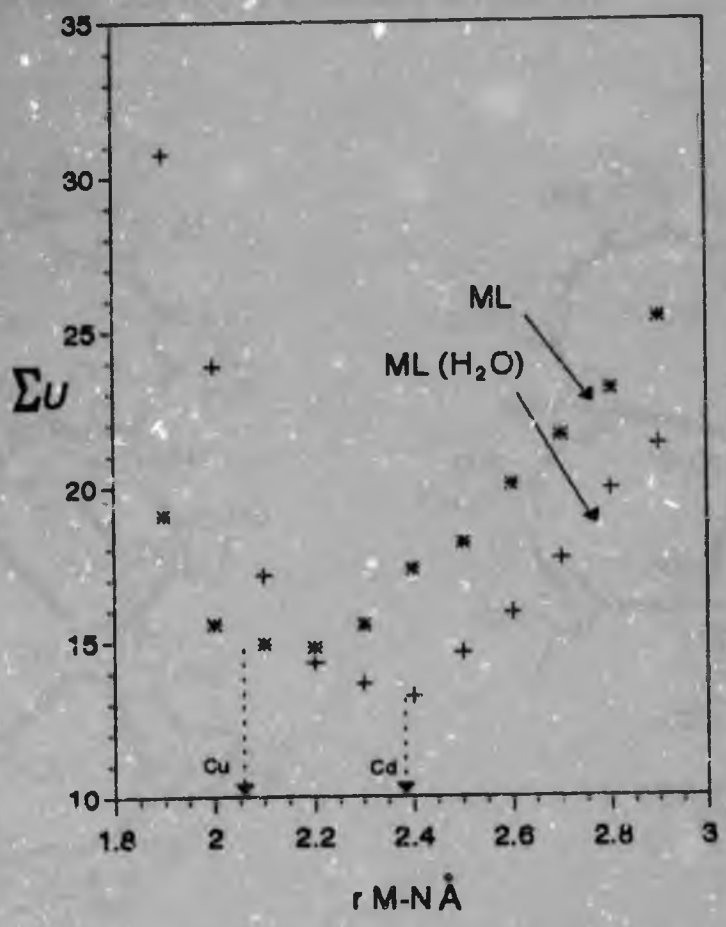


Figure 116 : Plot of change in internal energy for Cy-12-aneN$_4$ as a function metal-nitrogen distance

STRUCTURE OF $[Cu(Cy\text{-}12aneN_4)](ClO_4)_2$

On complexation the macrocycle adopts the transI conformation with the hydroxycyclohexyl pendant arm coordinating at the axial site. The structure solution shows the complex and its mirror image. The short axial bonds (2.197Å & 2.130Å) reflect the need of the bulky cyclohexyl groups to reduce steric strain on the outer surface of the ligand by increasing the ligand curvature. In coordinating the smaller Cu^{2+} ion is brought closer towards the macrocyclic cavity, decreasing interactions between the bulky cyclohexenyl group and the backbone of the macrocycle. This may be appreciated in figure 119

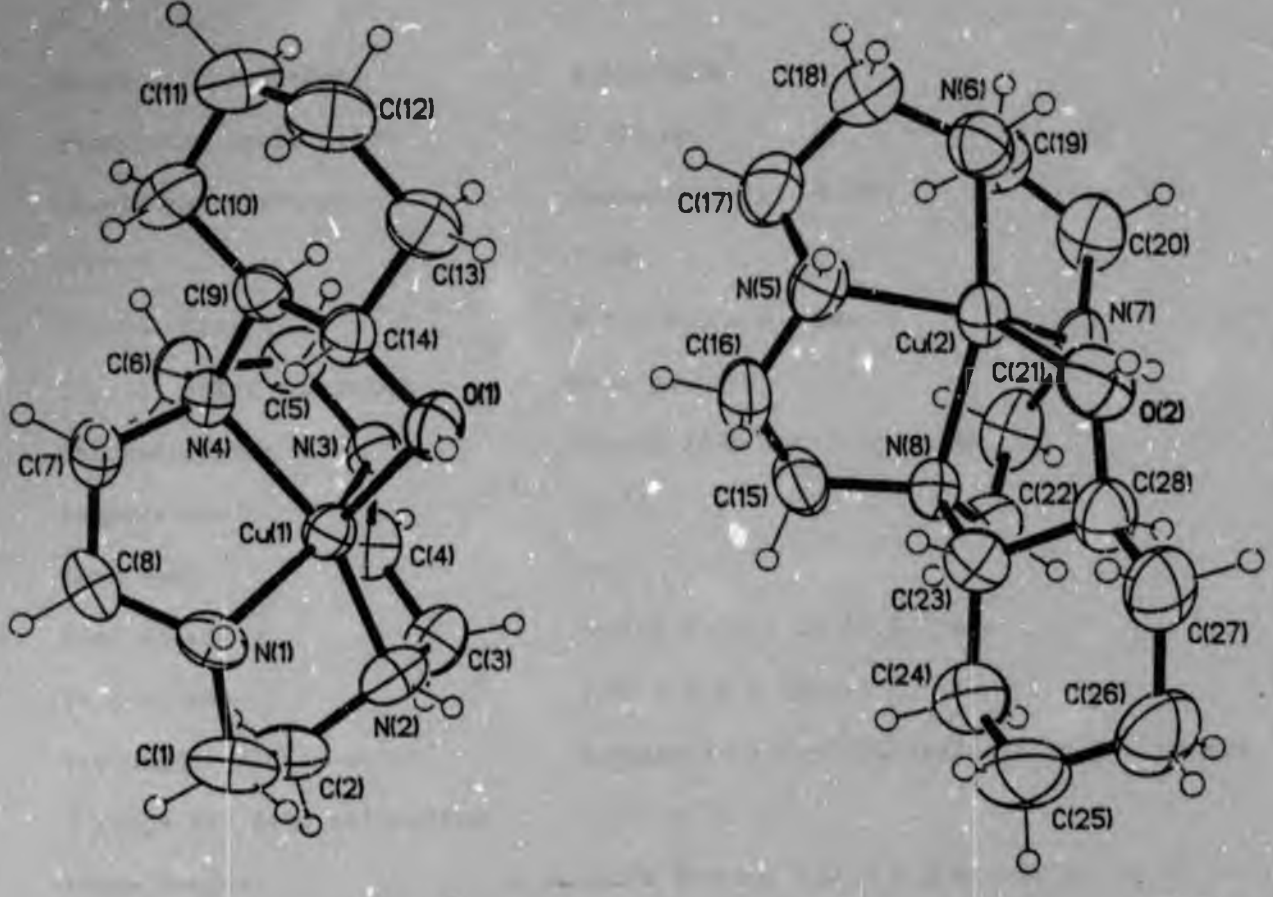


Figure 117 : ORTEP diagram of $[Cu(Cy\text{-}12aneN_4)]^{2+}$ and its mirror image

TABLE OF CRYSTAL DATA AND STRUCTURE REFINEMENT

Empirical formula	$C_{14}H_{30}Cl_2CuN_4O_9$
Formula weight	532.86
Temperature	293(2) K
Wavelength	0.71073 Å
Crystal system	Triclinic
Space group	$P\bar{1}$
Unit cell dimensions	a = 8.6320(10) Å α = 86.80(2)° b = 14.677(2) Å β = 78.71(2)° c = 17.797(4) Å γ = 83.320(10)°
Volume	2194.8(6) $Å^3$
Z	4
Density (calculated)	1.613 Mg/m^3
Absorption coefficient	1.292 mm^{-1}
Absorption correction	Tmax=0.999 Tmin=0.802
F(000)	1108
Crystal size	0.1 x 0.4 x 0.4 mm
Crystal color and habit	blue plate
Diffractometer used	Rigaku AFC5 rotating anode
Temperature	298°K
Scan type	θ-2θ
Scan speed	variable; 4.0 to 16.0 °/min
Scan width	1.68 + 0.3 x tan(θ)
Standard reflections	3 measured every 150 reflections (no decay)
θ range for data collection	1.79 to 25.05°
Index ranges	$-10 \le h \le 10$, $-17 \le k \le 0$, $-21 \le l \le 21$
Reflections collected	8115
Independent reflections	7779 (R_{int} = 0.0345)

Refinement method	Full-matrix least-squares on F^2 SHELXL-93 (Cray-FPS 500, MicroVaxII)
Data / restraints / parameters	7731 / 0 / 541
Goodness-of-fit on F^2	1.007
Final R indices [$I>2\sigma(I)$]	R1 = 0.0606, wR2 = 0.1386
R indices (all data)	R1 = 0.1445, wR2 = 0.3217
Largest and mean Δ/σ	0.002, 0.0001
Largest diff. peak and hole	0.783 and -0.506 $eÅ^{-3}$

TABLE OF ATOMIC COORDINATES [$\times 10^4$] AND EQUIVALENT ISOTROPIC DISPLACEMENT PARAMETERS [$(Å)^2 \times 10^3$]

	x	y	z	U(eq)
Cu(1)	3477(1)	9036(1)	8096(1)	38(1)
Cu(2)	7403(1)	4290(1)	6859(1)	43(1)
Cl(1)	6473(2)	7448(1)	9398(1)	55(1)
Cl(2)	1765(3)	6223(2)	6647(2)	77(1)
Cl(3)	11449(3)	2500(2)	5926(1)	67(1)
Cl(4)	2055(2)	8889(1)	1693(1)	49(1)
O(1)	5823(5)	8440(3)	7508(3)	48(1)
O(2)	9369(6)	3904(4)	7412(3)	64(2)
O(3)	6836(12)	7445(9)	10099(5)	171(4)
O(4)	6544(13)	8295(6)	9044(7)	199(6)
O(5)	7671(10)	6859(8)	8990(7)	186(5)
O(6)	4983(7)	7134(4)	9401(5)	101(2)
O(7)	799(14)	6326(8)	7329(6)	201(6)
O(8)	2832(9)	6884(6)	6498(7)	155(4)
O(9)	2652(9)	5348(5)	6568(5)	125(3)
O(10)	810(10)	6260(7)	6100(6)	150(4)
O(11)	10302(12)	1872(8)	5939(6)	163(4)
O(12)	10823(10)	3324(6)	5653(5)	145(4)
O(13)	12867(8)	2160(5)	5469(4)	109(2)
O(14)	11641(9)	2529(5)	6706(4)	112(3)
O(15)	3271(8)	8294(5)	1281(6)	134(3)
O(16)	603(6)	8762(5)	1493(4)	86(2)
O(17)	2013(9)	8684(6)	2473(4)	118(3)
O(18)	2474(7)	9788(4)	1490(4)	77(2)
N(1)	3907(7)	9979(4)	8783(3)	48(1)
N(2)	2290(7)	8443(4)	9039(3)	52(2)
N(3)	2001(6)	8519(4)	7520(3)	46(1)
N(4)	3824(6)	9985(3)	7229(3)	37(1)
N(5)	7442(7)	5643(4)	6685(4)	51(2)
N(6)	7518(8)	4224(4)	5729(4)	60(2)
N(7)	6223(7)	3174(4)	6976(4)	54(2)
N(8)	6311(6)	4567(3)	7953(3)	40(1)
C(1)	3058(10)	9771(7)	9573(4)	71(2)
C(2)	1701(10)	9241(6)	9520(4)	65(2)
C(3)	1052(9)	7949(5)	8808(5)	60(2)
C(4)	560(8)	8422(5)	8111(5)	56(2)
C(5)	1802(9)	9142(5)	6863(4)	57(2)
C(6)	2278(8)	10079(5)	6964(4)	51(2)
C(7)	4067(9)	10847(4)	7587(4)	48(2)
C(8)	3321(8)	10846(5)	8407(4)	48(2)
C(9)	5188(7)	9649(4)	6621(4)	39(2)
C(10)	5842(9)	10385(5)	6049(4)	57(2)
C(11)	7125(9)	9959(6)	5422(4)	65(2)
C(12)	8452(9)	9412(6)	5760(5)	66(2)
C(13)	7782(8)	8689(5)	6356(4)	54(2)
C(14)	6523(8)	9137(4)	6970(4)	39(2)
C(15)	5481(9)	5503(5)	7868(4)	57(2)

C(16)	6552(10)	6115(5)	7361(5)	62(2)
C(17)	6735(10)	5838(5)	5991(5)	67(2)
C(18)	7564(11)	5167(6)	5400(5)	74(2)
C(19)	6103(11)	3772(6)	5672(5)	73(2)
C(20)	6069(11)	2940(6)	6187(5)	72(2)
C(21)	4751(9)	3482(5)	7504(5)	65(2)
C(22)	5156(9)	3872(6)	8180(5)	61(2)
C(23)	7510(8)	4530(5)	8445(4)	49(2)
C(24)	6861(10)	4516(6)	9303(5)	72(2)
C(25)	8165(12)	4455(8)	9760(5)	90(3)
C(26)	9430(13)	3688(7)	9529(6)	88(3)
C(27)	10099(10)	3737(6)	8684(5)	68(2)
C(28)	8825(9)	3778(5)	8209(5)	55(2)

TABLE OF BOND LENGTHS [Å] AND ANGLES [°]

Cu(1)-N(2)	1.999(5)	Cu(1)-N(1)	2.009(5)
Cu(1)-N(3)	2.018(5)	Cu(1)-N(4)	2.022(5)
Cu(1)-O(1)	2.197(5)	Cu(2)-N(5)	1.996(5)
Cu(2)-N(6)	2.002(6)	Cu(2)-N(7)	2.008(6)
Cu(2)-N(8)	2.031(5)	Cu(2)-O(2)	2.130(5)
Cl(1)-O(3)	1.343(8)	Cl(1)-O(4)	1.364(7)
Cl(1)-O(5)	1.383(8)	Cl(1)-O(6)	1.415(6)
Cl(2)-O(7)	1.336(9)	Cl(2)-O(10)	1.389(8)
Cl(2)-O(8)	1.393(7)	Cl(2)-O(9)	1.415(7)
Cl(3)-O(12)	1.369(7)	Cl(3)-O(13)	1.387(6)
Cl(3)-O(11)	1.425(9)	Cl(3)-O(14)	1.434(7)
Cl(4)-O(17)	1.398(6)	Cl(4)-O(15)	1.400(7)
Cl(4)-O(16)	1.402(5)	Cl(4)-O(18)	1.419(5)
O(1)-C(14)	1.460(7)	O(1)-O(4)	2.911(12)
O(2)-C(28)	1.413(9)	O(2)-O(14)	2.809(8)
N(1)-C(1)	1.485(9)	N(1)-C(8)	1.487(9)
N(2)-C(2)	1.472(10)	N(2)-C(3)	1.491(9)
N(3)-C(5)	1.469(9)	N(3)-C(4)	1.479(9)
N(4)-C(6)	1.489(8)	N(4)-C(9)	1.491(8)
N(4)-C(7)	1.502(8)	N(5)-C(16)	1.458(9)
N(5)-C(17)	1.481(10)	N(6)-C(18)	1.474(10)
N(6)-C(19)	1.478(10)	N(7)-C(21)	1.465(10)
N(7)-C(20)	1.499(9)	N(8)-C(23)	1.476(8)
N(8)-C(15)	1.489(8)	N(8)-C(22)	1.493(9)
C(1)-C(2)	1.501(11)	C(3)-C(4)	1.496(10)
C(5)-C(6)	1.509(10)	C(7)-C(8)	1.476(9)
C(9)-C(14)	1.519(8)	C(9)-C(10)	1.521(9)
C(10)-C(11)	1.516(10)	C(11)-C(12)	1.523(11)
C(12)-C(13)	1.537(10)	C(13)-C(14)	1.502(9)
C(15)-C(16)	1.500(10)	C(17)-C(18)	1.500(11)
C(19)-C(20)	1.484(11)	C(21)-C(22)	1.478(10)
C(23)-C(28)	1.502(10)	C(23)-C(24)	1.519(10)
C(24)-C(25)	1.506(11)	C(25)-C(26)	1.490(13)
C(26)-C(27)	1.503(12)	C(27)-C(28)	1.507(10)

N(2)-Cu(1)-N(1)	87.0(2)	N(2)-Cu(1)-N(3)	86.8(2)
N(1)-Cu(1)-N(3)	150.4(2)	N(2)-Cu(1)-N(4)	156.0(2)
N(1)-Cu(1)-N(4)	87.3(2)	N(3)-Cu(1)-N(4)	86.9(2)
N(2)-Cu(1)-O(1)	122.0(2)	N(1)-Cu(1)-O(1)	105.5(2)
N(3)-Cu(1)-O(1)	102.3(2)	N(4)-Cu(1)-O(1)	81.9(2)
N(5)-Cu(2)-N(6)	86.9(3)	N(5)-Cu(2)-N(7)	150.2(2)
N(6)-Cu(2)-N(7)	86.8(3)	N(5)-Cu(2)-N(8)	86.7(2)
N(6)-Cu(2)-N(8)	154.9(2)	N(7)-Cu(2)-N(8)	86.7(2)
N(5)-Cu(2)-O(2)	103.1(2)	N(6)-Cu(2)-O(2)	123.8(2)
N(7)-Cu(2)-O(2)	104.5(2)	N(8)-Cu(2)-O(2)	81.3(2)
O(3)-Cl(1)-O(4)	111.3(7)	O(3)-Cl(1)-O(5)	104.4(7)
O(4)-Cl(1)-O(5)	107.4(8)	O(3)-Cl(1)-O(6)	113.5(6)
O(4)-Cl(1)-O(6)	110.2(5)	O(5)-Cl(1)-O(6)	109.6(5)
O(7)-Cl(2)-O(10)	107.1(7)	O(7)-Cl(2)-O(8)	112.0(6)
O(10)-Cl(2)-O(8)	111.9(7)	O(7)-Cl(2)-O(9)	113.3(7)
O(10)-Cl(2)-O(9)	104.4(6)	O(8)-Cl(2)-O(9)	108.0(5)
O(12)-Cl(3)-O(13)	112.9(5)	O(12)-Cl(3)-O(11)	106.5(7)
O(13)-Cl(3)-O(11)	108.9(6)	O(12)-Cl(3)-C(14)	112.8(5)
O(13)-Cl(3)-O(14)	110.2(4)	O(11)-Cl(3)-O(14)	105.2(6)

O(17)-Cl(4)-O(15)	107.6(6)	O(17)-Cl(4)-O(16)	110.8(4)
O(15)-Cl(4)-O(16)	109.5(5)	O(17)-Cl(4)-O(18)	111.3(4)
O(15)-Cl(4)-O(18)	106.0(4)	O(16)-Cl(4)-O(18)	111.5(4)
C(14)-O(1)-Cu(1)	108.0(3)	C(14)-O(1)-O(4)	118.5(4)
Cu(1)-O(1)-O(4)	83.8(3)	C(28)-O(2)-Cu(2)	109.9(4)
C(28)-O(2)-O(14)	116.1(4)	Cu(2)-O(2)-O(14)	115.8(3)
Cl(1)-O(4)-O(1)	115.5(6)	Cl(3)-O(14)-O(2)	107.3(3)
C(1)-N(1)-C(8)	116.3(6)	C(1)-N(1)-Cu(1)	107.7(5)
C(8)-N(1)-Cu(1)	101.5(4)	C(2)-N(2)-C(3)	115.9(6)
C(2)-N(2)-Cu(1)	101.4(4)	C(3)-N(2)-Cu(1)	107.8(4)
C(5)-N(3)-C(4)	116.4(6)	C(5)-N(3)-Cu(1)	108.2(4)
C(4)-N(3)-Cu(1)	103.4(4)	C(6)-N(4)-C(9)	112.7(5)
C(6)-N(4)-C(7)	111.3(5)	C(9)-N(4)-C(7)	113.5(5)
C(6)-N(4)-Cu(1)	102.2(4)	C(9)-N(4)-Cu(1)	110.4(4)
C(7)-N(4)-Cu(1)	105.9(4)	C(16)-N(5)-C(17)	114.1(6)
C(16)-N(5)-Cu(2)	109.6(4)	C(17)-N(5)-Cu(2)	103.3(4)
C(18)-N(6)-C(19)	115.9(7)	C(18)-N(6)-Cu(2)	107.4(5)
C(19)-N(6)-Cu(2)	103.8(5)	C(21)-N(7)-C(20)	116.8(6)
C(21)-N(7)-Cu(2)	102.1(4)	C(20)-N(7)-Cu(2)	106.8(5)
C(23)-N(8)-C(15)	113.2(5)	C(23)-N(8)-C(22)	113.5(5)
C(15)-N(8)-C(22)	111.4(5)	C(23)-N(8)-Cu(2)	109.7(4)
C(15)-N(8)-Cu(2)	102.5(4)	C(22)-N(8)-Cu(2)	105.7(4)
N(1)-C(1)-C(2)	108.4(6)	N(2)-C(2)-C(1)	109.6(6)
N(2)-C(3)-C(4)	109.3(6)	N(3)-C(4)-C(3)	108.6(6)
N(3)-C(5)-C(6)	111.5(6)	N(4)-C(6)-C(5)	110.0(5)
C(8)-C(7)-N(4)	110.7(5)	C([illegible]C(8)-N(1)	108.7(5)
N(4)-C(9)-C(14)	111.1(5)	N(4)-C(9)-C(10)	115.0(5)
C(14)-C(9)-C(10)	109.7(5)	C(11)-C(10)-C(9)	110.6(6)
C(10)-C(11)-C(12)	110.8(6)	C(11)-C(12)-C(13)	110.7(6)
C(14)-C(13)-C(12)	110.4(6)	O(1)-C(14)-C(13)	110.1(5)
O(1)-C(14)-C(9)	107.1(5)	C(13)-C(14)-C(9)	110.4(6)
N(8)-C(15)-C(16)	111.1(6)	N(5)-C(16)-C(15)	111.5(6)
N(5)-C(17)-C(18)	107.8(7)	N(6)-C(18)-C(17)	109.8(7)
N(6)-C(19)-C(20)	108.2(7)	C(19)-C(20)-N(7)	110.5(6)
N(7)-C(21)-C(22)	109.0(6)	C(21)-C(22)-N(8)	111.7(6)
N(8)-C(23)-C(28)	110.7(6)	N(8)-C(23)-C(24)	115.5(6)
C(28)-C(23)-C(24)	113.1(6)	C(25)-C(24)-C(23)	111.9(7)
C(26)-C(25)-C(24)	112.8(8)	C(25)-C(26)-C(27)	111.6(8)
C(26)-C(27)-C(28)	112.2(7)	O(2)-C(28)-C(23)	107.0(6)
O(2)-C(28)-C(27)	114.6(7)	C(23)-C(28)-C(27)	112.2(6)

Symmetry transformations used to generate equivalent atoms

C(16)	73(5)	33(4)	79(6)	-5(4)	-20(5)	3(4)
C(17)	78(6)	50(5)	74(6)	11(4)	-14(5)	-10(4)
C(18)	86(6)	69(6)	61(6)	13(5)	-4(5)	-4(5)
C(19)	83(6)	83(6)	61(6)	-11(5)	-30(5)	7(5)
C(20)	93(7)	56(5)	81(6)	-14(5)	-45(5)	-13(5)
C(21)	56(5)	51(5)	96(7)	8(5)	-31(5)	-19(4)
C(22)	55(5)	67(5)	62(5)	8(4)	-13(4)	-15(4)
C(23)	47(4)	52(4)	50(5)	-5(3)	-10(3)	-6(3)
C(24)	77(6)	76(6)	63(6)	-3(5)	-15(5)	-1(5)
C(25)	106(8)	115(9)	57(6)	-11(6)	-35(5)	-4(7)
C(26)	111(8)	86(7)	82(7)	3(6)	-56(6)	-3(6)
C(27)	65(5)	69(6)	76(6)	-3(5)	-33(5)	4(4)
C(28)	56(5)	50(4)	63(5)	-4(4)	-23(4)	0(4)

HYDROGEN COORDINATES AND ISOTROPIC DISPLACEMENT PARAMETERS

	x	y	z	U(eq)
H(1O1)	6696(5)	8457(3)	7688(3)	80
H(1O2)	10274(6)	3870(4)	7334(3)	80
H(1C)	4957(7)	9959(4)	8773(3)	80
H(2C)	2955(7)	8049(4)	9264(3)	80
H(3C)	2431(6)	7962(4)	7349(3)	80
H(5C)	8451(7)	5783(4)	6587(4)	80
H(6C)	8402(8)	3869(4)	5520(4)	80
H(7C)	6763(7)	2703(4)	7192(4)	80
H(1A)	2662(10)	10339(7)	9821(4)	80
H(1B)	3755(10)	9423(7)	9868(4)	80
H(2A)	1203(10)	9032(5)	10021(4)	80
H(2B)	920(10)	9623(6)	9296(4)	80
H(3A)	152(9)	7965(5)	9222(5)	80
H(3B)	1443(9)	7318(5)	8713(5)	80
H(4A)	-127(8)	8059(5)	7922(5)	80
H(4B)	1(8)	9017(5)	8226(5)	80
H(5A)	710(9)	9198(5)	6808(4)	80
H(5B)	2440(9)	8887(5)	6403(4)	80
H(6A)	2383(8)	10424(5)	6486(4)	80
H(6B)	1474(8)	10406(5)	7332(4)	80
H(7A)	3616(9)	11369(4)	7324(4)	80
H(7B)	5186(9)	10887(4)	7533(4)	80
H(8A)	3581(8)	11365(5)	8645(4)	80
H(8B)	2187(8)	10887(5)	8461(4)	80
H(9A)	4802(7)	9206(4)	6330(4)	80
H(10C)	6276(9)	10821(5)	6309(4)	80
H(10D)	4998(9)	10703(5)	5825(4)	80
H(11A)	7542(9)	10425(6)	5064(4)	80
H(11B)	6671(9)	9546(6)	5148(4)	80
H(12A)	8947(9)	9827(6)	6012(5)	80
H(12B)	9240(9)	9130(6)	5359(5)	80
H(13A)	8618(8)	8353(5)	6575(4)	80
H(13B)	7306(8)	8265(5)	6103(4)	80
H(14A)	6991(8)	9565(4)	7241(4)	80
H(15A)	5129(9)	5754(5)	8367(4)	80
H(15B)	4564(9)	5465(5)	7646(4)	80
H(16A)	5938(10)	6653(5)	7203(5)	80
H(16B)	7278(10)	6306(5)	7651(5)	80
H(17A)	6870(10)	6457(5)	5808(5)	80
H(17B)	5620(10)	5770(5)	6113(5)	80
H(18A)	7083(11)	5234(6)	4954(5)	80
H(18B)	8654(11)	5284(6)	5247(5)	80
H(19A)	6118(11)	3630(6)	5151(5)	80
H(19B)	5179(11)	4192(6)	5845(5)	80
H(20A)	5083(11)	2684(6)	6217(5)	80
H(20B)	6922(11)	2493(6)	5975(5)	80
H(21A)	4154(9)	2970(5)	7665(5)	80
H(21B)	4122(9)	3930(5)	7244(5)	80

The monosubstituted macrocycles have been of some interest since these are ideal ligands for investigating changes in structure and stability when donor groups are added as pendant arms (Studer et al 1990). Kimura et al (1986) found that adding a single phenol pendant to triamines increased complex stability. The pendant phenolate also stabilised higher oxidation states of the metal through axial coordination in substituted polyamines (Kimura et al 1986).

The effect for addition of a hydroxycyclohexyl pendant on 12-aneN_4 (1,4,7,10-tetraazacyclo-dodecane) was studied to determine how the stability would change. Selective complexation of metal ions for biological applications is of major scientific interest such as the synthesis of ligands for complexation of Gd^{3+} in magnetic resonance imaging. Such ligands should give complexes with Gd^{3+} that are neutral overall and require addition of a single neutral pendant donor in addition to the three acetates usually added when based on the macrocycle 12-aneN_4 . The cyclohexene oxide reacts with 12-aneN_4 to give a single substitution product with only one pendant group, requiring no synthetic steps for the protection of the other three nitrogens.

Determination of the stability constants for Pb, Cd and Zn employed the out-of-cell technique. Equal amounts of metal and ligand were made up in solutions containing differing amounts of acid.

ANISOTROPIC DISPLACEMENT PARAMETERS

The anisotropic displacement factor exponent takes the form:

$-2\pi^2 [(ha^*)^2 U_{11} + \ldots + 2hka^*b^* U_{12}]$

	U11	U22	U33	U23	U13	U12
Cu(1)	37(1)	38(1)	40(1)	1(1)	-10(1)	-3(1)
Cu(2)	45(1)	35(1)	52(1)	-5(1)	-16(1)	0(1)
Cl(1)	58(1)	54(1)	56(1)	1(1)	-15(1)	-7(1)
Cl(2)	57(1)	81(2)	93(2)	-35(1)	-13(1)	1(1)
Cl(3)	70(1)	65(1)	60(1)	-1(1)	-14(1)	19(1)
Cl(4)	41(1)	48(1)	58(1)	6(1)	-14(1)	-5(1)
O(1)	45(3)	43(3)	54(3)	5(2)	-9(2)	1(2)
O(2)	42(3)	86(4)	64(4)	-15(3)	-17(3)	11(3)
O(3)	156(8)	286(13)	83(6)	21(7)	-57(6)	-30(8)
O(4)	195(10)	131(8)	321(15)	150(9)	-166(10)	-99(7)
O(5)	96(6)	237(12)	224(11)	-162(10)	24(6)	-40(7)
O(6)	51(4)	88(5)	163(7)	15(4)	-21(4)	-12(3)
O(7)	214(11)	199(11)	167(10)	-112(8)	81(9)	-75(9)
O(8)	82(5)	102(6)	274(12)	-88(7)	20(6)	-29(5)
O(9)	121(6)	79(5)	174(8)	-27(5)	-42(6)	20(4)
O(10)	111(6)	185(9)	170(9)	10(7)	-75(6)	-11(6)
O(11)	161(9)	194(10)	153(9)	7(7)	-39(7)	-90(8)
O(12)	143(7)	117(6)	140(7)	67(6)	-1(6)	54(5)
O(13)	91(5)	141(7)	86(5)	-40(5)	-12(4)	36(5)
O(14)	137(6)	119(6)	76(5)	-32(4)	-40(4)	57(5)
O(15)	75(5)	68(4)	234(10)	-25(5)	19(5)	16(4)
O(16)	50(3)	129(6)	89(5)	-5(4)	-30(3)	-22(3)
O(17)	125(6)	169(7)	80(5)	58(5)	-50(4)	-71(6)
O(18)	96(5)	47(3)	96(5)	7(3)	-31(4)	-15(3)
N(1)	42(3)	62(4)	41(3)	-13(3)	-10(3)	-8(3)
N(2)	46(3)	63(4)	46(4)	16(3)	-9(3)	-7(3)
N(3)	48(3)	41(3)	50(4)	-1(3)	-10(3)	-12(3)
N(4)	35(3)	36(3)	41(3)	-1(2)	-13(2)	-5(2)
N(5)	55(4)	39(3)	61(4)	6(3)	-15(3)	-12(3)
N(6)	60(4)	63(4)	56(4)	-8(3)	16(3)	4(3)
N(7)	65(4)	35(3)	67(4)	-1(3)	-27(3)	-3(3)
N(8)	39(3)	34(3)	48(3)	1(2)	-8(3)	-3(2)
C(1)	70(6)	106(7)	39(5)	-12(4)	-8(4)	-18(5)
C(2)	62(5)	89(6)	40(4)	-4(4)	3(4)	-11(5)
C(3)	49(5)	60(5)	73(6)	15(4)	-12(4)	-16(4)
C(4)	41(4)	56(5)	77(6)	-1(4)	-17(4)	-12(4)
C(5)	55(5)	63(5)	60(5)	5(4)	-28(4)	-17(4)
C(6)	46(4)	48(4)	61(5)	4(4)	-22(4)	-2(3)
C(7)	56(4)	33(4)	58(5)	-3(3)	-16(4)	-7(3)
C(8)	42(4)	41(4)	62(5)	-18(4)	-8(4)	-1(3)
C(9)	41(4)	41(4)	38(4)	-5(3)	-11(3)	-4(3)
C(10)	64(5)	62(5)	48(5)	14(4)	-19(4)	-15(4)
C(11)	58(5)	90(6)	44(5)	10(4)	-7(4)	-10(5)
C(12)	51(5)	88(6)	55(5)	-6(4)	1(4)	-11(4)
C(13)	43(4)	64(5)	54(5)	-10(4)	-7(4)	-3(4)
C(14)	42(4)	35(4)	42(4)	-1(3)	-11(3)	-5(3)
C(15)	61(5)	47(4)	61(5)	-13(4)	-11(4)	11(4)

H(22A)	4203(9)	4163(6)	8485(5)	80
H(22B)	5595(9)	3392(6)	8491(5)	80
H(23A)	8000(8)	5104(5)	8332(4)	80
H(24A)	6242(10)	4007(6)	9436(5)	80
H(24B)	6169(10)	5071(6)	9422(5)	80
H(25A)	7112(12)	4363(8)	10293(5)	80
H(25B)	8547(12)	5019(8)	9704(5)	80
H(26A)	8967(13)	3119(7)	9636(6)	80
H(26B)	10258(13)	3679(7)	9821(6)	80
H(27A)	10854(10)	3213(5)	8542(5)	80
H(27B)	10644(10)	4278(6)	8579(5)	80
H(28A)	8362(9)	3193(5)	8292(5)	80

The pechlorates are hydrogen bonded to the hydroxy group in the pendant arm.

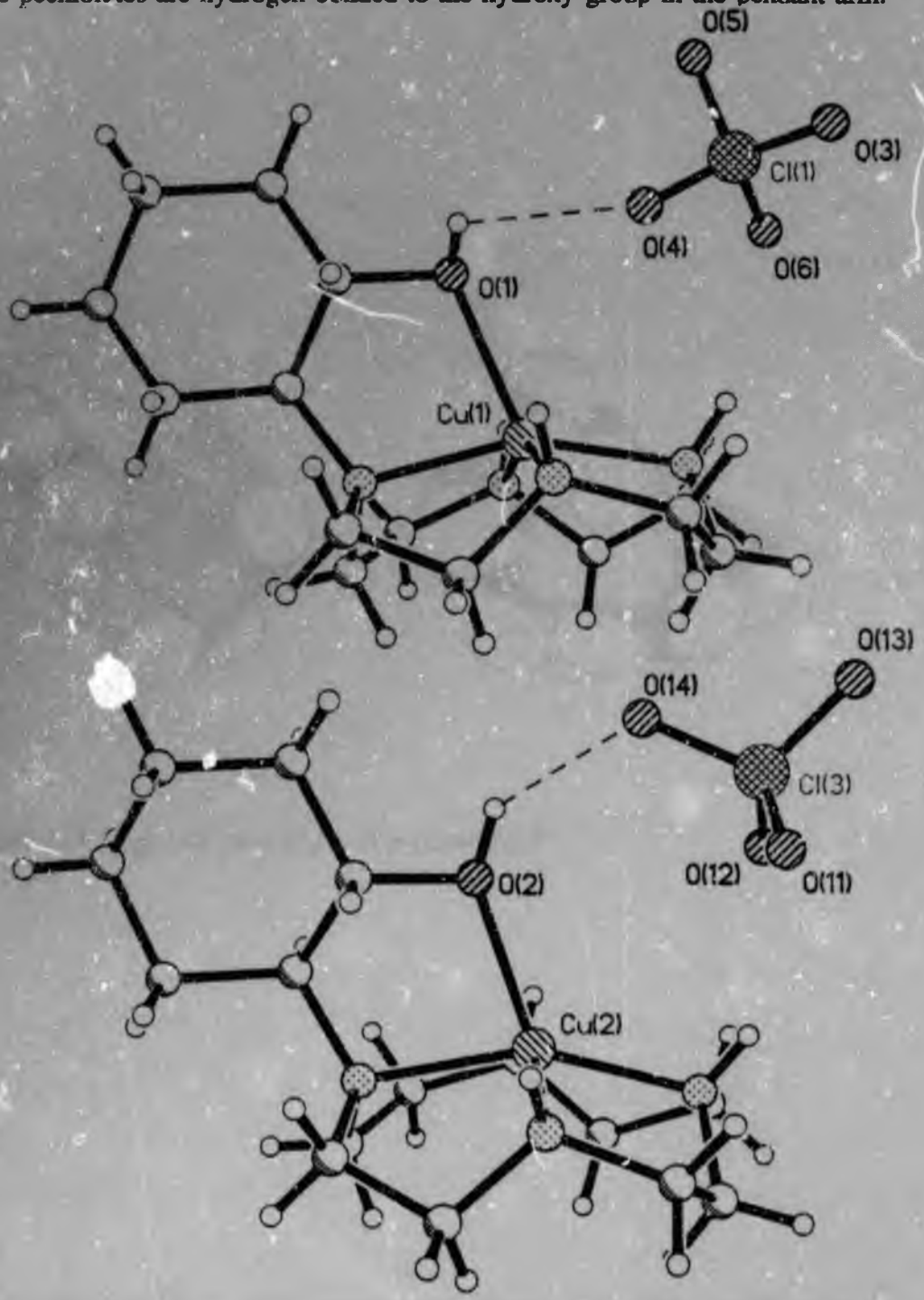


***Figure 118** : hydrogen bonding involving perchlorate counter ions and the hydroxy group on the pendant side arm*

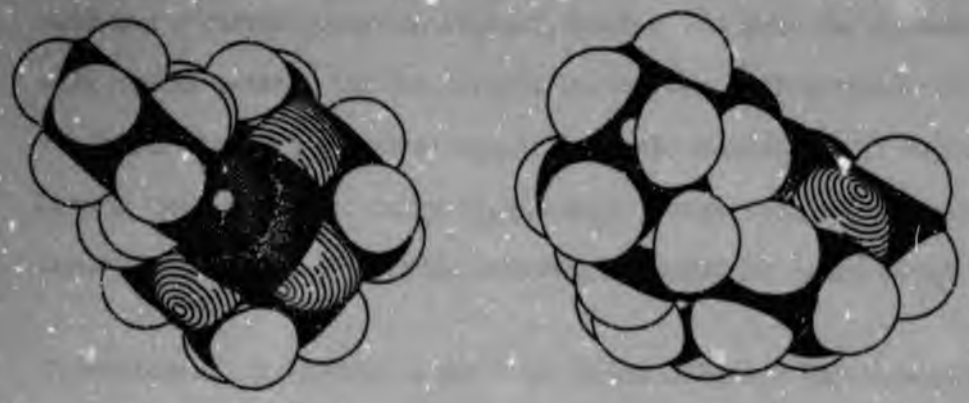


Figure 119 : top; side view of [Cu(Cy-12aneN4)]$^{2+}$

CHAPTER 6

CONCLUSION

The design approach in manipulating selectivity is to add neutral oxygen donors until a required selectivity has been attained. With addition of neutral oxygen donors the stability of all but the very largest metal ions is suppressed. Addition of methyl groups to a ligand , however has quite the opposite effect with respect to metal ion size. Despite the fact that hydroxycyclohexyl groups are in effect adding a neutral oxygen donor the stability of the larger metal ions is decreased. The bulky cyclohexenyl groups reverses the metal ion selectivity which leads us to the following two rules for ligand design :

1) addition of alkyl groups to the donor atoms of ligands improves selectivity for large metal ions

2) addition of C-alkyl groups to ligands improves selectivity for small metal ions.

The effectiveness of the cyclohexenyl bridge in, ligands favouring selectivities for small metal ions relies on the degree of preorganisation achieved during synthesis. The selectivity is increased towards the smaller metal ions as the number of cyclohexyl groups on the ligand increases. The idea is that the presence of bulky C-alkyl groups on the ligand leads to steric crowding on the outer surface of the complex. Complexation to a large metal ion would force the methyl groups closer together increasing the unfavourable van der Waals repulsions and resulting in destabilisation of the complex. The steric crowding is relieved on complexation to a small metal ion which will allow the bulky

bulky groups to move further apart. The idea of "ligand curvature" relating to steric crowding on the outer surface of the ligand must be considered when C-alkyl groups are introduced into existing ligands. The inductive effects of the larger, more electron donating cyclohexenyl bridge would favour selectivity for the larger metal ions, however these are overcome by the steric implications resulting from unfavourable interactions between the bulky cyclohexenyl groups and the carbon backbone.

CHAPTER 7

SYNTHETIC METHODS

SYNTHESIS OF MACROCYCLES

Macrocycles have been predominantly synthesized by the direct synthesis approach or by the template approach; both of which result in low yields because of a series of side reactions giving rise to unnecessary by-products. The direct synthesis method relies on high dilution so as to minimise polymerisation and produce the desired macrocyclic ligand (Dietrich et al 1963, Rossa & Vogtle 1983). The available reaction sites results in an broad product spectrum due to the number of competing reactions that take place simultaneously. This requires the use of more diverse techniques for isolation of the macrocyclic compound. Reducing the number of feasible reaction sites; making these more specific, may eliminate competing side reactions and narrow the product spectrum. Koyama et al (1972) proposed the introduction of protecting groups in macrocyclic chemistry. Richmand and Atkins (1974) revised the method of Koyama and suggested the use of tosylates as cyclic precursors which are then combined to produce a macrocycle. Both the starting building blocks (amines and glycols) of the macrocycle are tosylated separately and then combined via a condensation of the glycol tosylate and the disodium salt of the amine tosylate.

With the need to synthesize a broader spectrum of polycyclic ligands, various researchers have either modified the method further, or appended to it.

CHAPTER 7

SYNTHETIC METHODS

SYNTHESIS OF MACROCYCLES

Macrocycles have been predominantly synthesized by the direct synthesis approach or by the template approach; both of which result in low yields because of a series of side reactions giving rise to unnecessary by-products. The direct synthesis method relies on high dilution so as to minimise polymerisation and produce the desired macrocyclic ligand (Dietrich et al 1963, Rossa & Vogtle 1983). The available reaction sites results in an broad product spectrum due to the number of competing reactions that take place simultaneously. This requires the use of more diverse techniques for isolation of the macrocyclic compound. Reducing the number of feasible reaction sites; making these more specific, may eliminate competing side reactions and narrow the product spectrum. Koyama et al (1972) proposed the introduction of protecting groups in macrocyclic chemistry. Richmand and Atkins (1974) revised the method of Koyama and suggested the use of tosylates as cyclic precursors which are then combined to produce a macrocycle. Both the starting building blocks (amines and glycols) of the macrocycle are tosylated separately and then combined via a condensation of the glycol tosylate and the disodium salt of the amine tosylate.

With the need to synthesize a broader spectrum of polycyclic ligands, various researchers have either modified the method further, or appended to it.

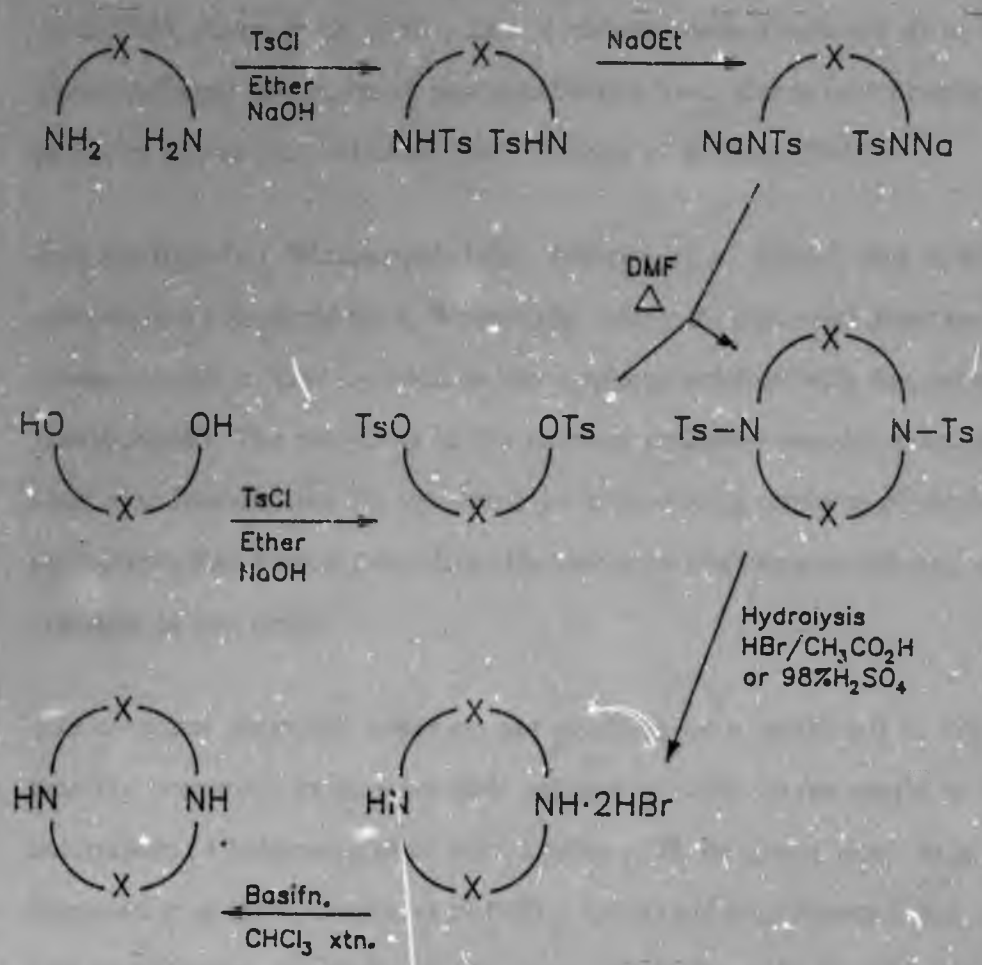


Figure 120 : synthetic scheme for macrocycles using tosylate precursors

These additional methods allow for the preparation of N-functionalised polyazamacrocycles (Hedinger & Kaden 1983, Studer & Kaden 1986) and macrocycles having pendant arms with additional donor groups (Kaden 1984).

Of much interest have been the tetraderivatives of macrocycles. The cyclic tetramines are reacted with an excess of the alkylating agent such as halogencarboxylic acids (Stetter et al 1979), acrylonitrile (Wainwright 1980) , ethylene oxide (Buøen et al 1982), halogenated methylpyridines (Alcock et al 1986, Asato et al 1989) and propylene oxide (Hancock et al 1986). These different categories of functionalisation have also in part been applied to Larial ethers (Gokel et al 1980, Tsubuke et al 1986, 1989).

Bi[illegible] (Wainwright 1980, Alfheim et al 1986) and reinforced ma[illegible]cles (Ramasubbu & Wainwright 1980) are produced using synthetic routes similar to that outlined in the synthetic scheme with the respective modifications. The simplicity of the reaction pathways become relaxed with each modification, and the disadvantage of producing mixtures of products is introduced. Purification procedures that are more elaborate become necessary resulting in low yields.

The template approach relies on the presence of a metal ion to hold the reacting precursors in an acceptable position to facilitate the synthesis of the macrocycle (Christensen et al 1974, Lindoy 1975, de Sousa Healy et al 1978, Sargeson at al 1984, Comba et al 1986). Of critical importance is the nature and coordination geometry of the metal ion to be used as this ultimately determines the fashion in which the coordinated ligands will react to give the sought after macrocycle. Planar geometries are generally useful in synthesizing

tetraaza macrocycles (Busch & Cairns 1987, Gokel & Korzeniowski 1982).

This synthetic route is often used to narrow the product spectrum or eliminate polymer formation that would otherwise occur in a direct synthesis. The metal ion can then removed after cyclisation with an extracting agent such as sodium cyanide (Hertli et al 1975). A disadvantage in this method lies in the fact that the metal ion template is on occasion complexed so strongly by the formed macrocycle that its removal is extremely difficult (Suh et al 1987). Extreme conditions are then necessary to successfully remove the metal ion and this may well place the survival of the macrocyclic ring in jeopardy.

The direct synthetic approach was used for the macrocycles synthesised in this presentation to avoid possible denaturation of the product with the removal of a metal template.

SYNTHESIS OF MONOSUBSTITUTED MACROCYCLES

Functionalised macrocycles have dominated a significant portion of macrocyclic coordination chemistry. This is primarily so because of their potentially many versatile applications (Pilichowski et al 1985). The monosubstituted macrocycles have a reduced number of donors, in comparison to their tetrasubstituted counterparts, which makes for complexing properties that are more readily studied and understood. The synthesis of the monosubstituted macrocycles is however more intricate and may involve a series of steps for complete isolation and characterisation. Inevitably polyalkylated products are formed in conjunction with the mono-derivative.

The syntheses employed generally rely on the introduction of a side chain in the macrocycle precursor (Lotz et al 1977, 1978, Alcock et al 1985). Cyclisation then yields the desired monosubstituted macrocycle. The synthesis of different monosubstituted macrocyclic compounds will necessitate the preparation of new precursors. A more flexible route allows for differentiation of the three N-atoms by protecting these through selective tosylation (Hedinger et al 1983). The fourth N-atom is then the only nitrogen available for the introduction of a side chain. This route is not as time consuming, since it allows for a large variety of pendant groups to be attached to the monosubstituted parent (after cyclisation) and therefore the precursors need not be synthesized for each new derivative. This is still a multi step process and requires much time.

Studer et al (1986) reported a one-step synthesis of mono-N-substituted azamacrocycles. In this preparation the alkylating agent is reacted with a five-fold excess of the macrocycle. The product spectrum consists of unreacted starting material and the mono-alkylated derivative. This method is still extremely laborious involving the separation of the two products by extraction of the unreacted macrocycle from a basic solution with chloroform. Poor recovery yields of the unreacted material may become a factor. Yaouanc et al (1991) and Parker et al (1993) have used chromium and molybdenum tricarbonyl complexes as protecting groups for three of the ring nitrogens. The monoalkylated amine was then isolated by the removal of the metal moiety in aqueous acid. Although this offers a more facile synthesis caution must be taken as the tricarbonyl complex is air sensitive and must remain under argon.

In synthesizing Cy-12-aneN$_4$ no protection was required for the

monoalkylation of the macrocycle. Only one cyclohexene oxide molecule reacts with the tetraazamacrocycle to produce the monosubstituted product. The addition of a single hydroxycyclohexyl group that may be involved in hydrogen bonding and the adopted ligand conformation inhibits the addition of a second hydroxycyclohexyl group. The convenience of the reaction lies in its narrow product spectrum and the high yields that are produced. Isolation of the monosubstituted product is a one-step process involving mere recrystallisation of the obtained product.

LIGAND AND METAL COMPLEX SYNTHESIS

INSTRUMENTATION

Nuclear magnetic resonance spectroscopy (NMR), Infra-red spectroscopy (IR) and microanalysis for carbon ,nitrogen and hydrogen were the techniques used for the characterisation of ligands and their metal complexes. NMR spectra were recorded on a Varian EM 360A spectrophotometer. Infra-red spectra were recorded on a FTIR spectrophotometer.

The microanalysis for carbon, nitrogen and hydrogen were done at CSIR, Division of Energy Technology, Pretoria and Galbraith Laboratories Inc., Knoxville, USA.

CHEMICALS USED IN SYNTHESES

The following chemicals were used in the synthetic preparations of ligands and their metal complexes :

Ethylenediamine (SAARCHEM)

Propylenediamine (Aldrich)

Diethylenetriamine (Riedel-de Haen A G)

cyclohexene oxide (Fluka)

ethylene oxide (BDH)

p-toluenesulphonyl chloride (Merck & SAARCHEM)

ethylene glycol (BDH)

trans-1,2-diaminocyclohexane (Aldrich)

Chromotropic acid (BDH)

bromoethylacetate (Merck)

Kryptofix K22 (Merck)

Tetrahydroxyethyl ethylenediamine (Fluka)

The purity of all of the above-mentioned chemicals was acceptable for synthetic applications and the products obtained with these chemicals , after purification, were of extremely reasonable purity.

SYNTHESIS

N,N'-BIS(2-HYDROXYCYCLOHEXYL)-TRANS-1,2-DIAMINOCYCLOHEXANE

The trans-1,2 diaminocyclohexane (1.0g , 8.76×10^{-3}mol) was dissolved in 60 ml of anhydrous ethanol. Cyclohexene oxide (3.5g , 3.50×10^{-2}mol) was added dropwise with stirring. Solution was refluxed for 12 hours with a condenser attached to a $CaCl_2$ drying tube. Evaporation of the solvent produced a colourless, viscous oil. Drying under reduced pressure rendered a dirty white solid. This residue was dissolved in 20 ml of acetone and cooled in a refrigerator for approximately 12 hours. The white precipitate was collected by filtration.

Mw C_{18} H_{34} N_2 O_2 = 310.48 g mol^{-1}

Mass collected = 1.9g

Yield = 73%

ANALYSIS	EXPECTED	OBSERVED
% C	69.63	69.61
% H	11.04	11.39
% N	9.02	8.99

0000 0000 2735

SYNTHESIS

N,N'-BIS(2-HYDROXYCYCLOHEXYL)-TRANS-1,2-DIAMINOCYCLOHEXANE

The trans-1,2 diaminocyclohexane (1.0g , 8.76×10^{-3}mol) was dissolved in 60 ml of anhydrous ethanol. Cyclohexene oxide (3.5g , 3.50×10^{-2}mol) was added dropwise with stirring. Solution was refluxed for 12 hours with a condenser attached to a $CaCl_2$ drying tube. Evaporation of the solvent produced a colourless, viscous oil. Drying under reduced pressure rendered a dirty white solid. This residue was dissolved in 20 ml of acetone and cooled in a refrigerator for approximately 12 hours. The white precipitate was collected by filtration.

Mw C_{18} H_{34} N_2 O_2 = 310.48 g mol^{-1}

Mass collected = 1.9g

Yield = 73%

ANALYSIS	EXPECTED	OBSERVED
% C	69.63	69.61
% H	11.04	11.39
% N	9.02	8.99

CU(II)-N,N'-BIS(2-HYDROXYCYCLOHEXYL)-TRANS-1,2-DIAMINOCYCLOHEXANE PERCHLORATE

Dissolved the copper perchlorate (**0.6g , 1.61×10^{-3}mol**) in 10 ml of deionised H_2O. To this was added a 10 ml solution of KOH (**0.2g , 3.22×10^{-3}mol**), and allowed to stir in an ice-bath for 30 min. Ligand (**0.5g , 1.61×10^{-3}mol**), in 15 ml of deionised H_2O was added dropwise with stirring and gentle warming i.e. 60 °C. Precipitation occurred and pH was adjusted by adding 1 ml of perchloric acid (12 M). Solution became clear and was allowed to cool down to room temperature. On evaporation purple crystals were obtained. These were filtered and air dried.

MW C_{18} H_{34} N_2 O_{10} Cl_2 Cu = 572.93g mol^{-1}

Mass collected = 0.68g

Yield = 73.7%

ANALYSIS	EXPECTED	OBSERVED
% C	36.59	36.56
% H	6.14	5.85
% N	4.74	4.74

N,N',N''- TRIS(2-HYDROXYCYCLOHEXYL) DIETHYLENETRIAMINE.

The triamine (2 g , 1.94×10^{-2} mol) was dissolved in 60 ml of anhydrous ethanol. To this was added 5 equivalents of cyclohexene oxide (9.5 g , 9.69×10^{-2} mol) and the solution was allowed to reflux for 24 hours with a $CaCl_2$ drying tube. After cooling the solvent was removed to give a pale yellow oil. Under reduced pressure the product solidified to a dirty white solid. This was dissolved in hot acetone at approximately 40 ° C and allowed to cool to room temperature causing a white precipitate to form. This was filtered and air dried to yield the product.

Mw $C_{16}H_{33}N_3O_2$ = 299.46 g mol^{-1}

Mass collected = 3.3g

Yield = 57 %

ANALYSIS	EXPECTED	OBSERVED
% C	69.63	69.61
% H	11.11	11.54
% N	14.03	13.81

Collection Number: A2084

SUZMAN, Helen, Papers, 1944-2009

PUBLISHER:

Publisher:- **Historical Papers Research Archive**
Location:- **Johannesburg**
©2014

LEGAL NOTICES:

Copyright Notice: All materials on the Historical Papers website are protected by South African copyright law and may not be reproduced, distributed, transmitted, displayed, or otherwise published in any format, without the prior written permission of the copyright owner.

Disclaimer and Terms of Use: Provided that you maintain all copyright and other notices contained therein, you may download material (one machine readable copy and one print copy per page) for your personal and/or educational non-commercial use only.

People using these records relating to the archives of Historical Papers, The Library, University of the Witwatersrand, Johannesburg, are reminded that such records sometimes contain material which is uncorroborated, inaccurate, distorted or untrue. While these digital records are true facsimiles of paper documents and the information contained herein is obtained from sources believed to be accurate and reliable, Historical Papers, University of the Witwatersrand has not independently verified their content. Consequently, the University is not responsible for any errors or omissions and excludes any and all liability for any errors in or omissions from the information on the website or any related information on third party websites accessible from this website.

This document forms part of the Helen Suzman Papers, a private collection deposited with the Historical Papers Research Archive at The University of the Witwatersrand, Johannesburg.